CHARLES UNIVERSITY
THIRD FACULTY OF MEDICINE

Division of Cell and Molecular Biology
Department of Biochemistry, Cell and Molecular Biology

PhD THESIS

MECHANISMS OF THE INDUCTION OF TAXANE RESISTANCE IN BREAST CANCER CELLS

MECHANISMY NAVOZENÍ TAXANOVÉ REZISTENCE U NÁDOROVÝCH BUNĚK PRSU

MGR. PETR DANIEL

SUPERVISOR: PROF. RNDR. JAN KOVÁŘ, DRSC

PRAGUE 2023

Identifikační záznam:

DANIEL Petr. *Mechanismy navození taxanové rezistence u nádorových buněk prsu. [Mechanisms of taxane resistance induction in breast cancer cells]*. Praha, 2023. 151 s. Disertační práce Univerzita Karlova v Praze, 3. lékařská fakulta, Ústav biochemie, buněčné a molekulární biologie, Oddělení buněčné a molekulární biologie 3. LF UK. Vedoucí práce prof. RNDr. Jan Kovář, DrSc.

Klíčová slova: taxany, taxanové deriváty, nádory prsu, získaná rezistence, ABC transportéry, TRIP6

Klíčová slova: taxanes, taxane derivatives, breast cancer, acquired resistance, ABC transporters, TRIP6

DECLARATION

I prepared the final thesis independently and I adequately listed and cited all sources and literature. At the same time, I declare that the work has not been used to obtain another or the same title.

I agree to the permanent storage of the electronic version of my thesis in the database of the inter-university systém Theses.cz for the purpose of continuous control of the similarity of qualification theses.

This work was supported by grants 19-03063S (Czech Science Foundation), GA UK 664216 and Cooperation Program MED ONCO 39 (Charles University in Prague, Czech Republic), KONTAKT II LH 14096 (Czech Ministry Of Education, Youth And Sports, Czech Republic), Inter-Excellence LTA-USA, 19032 (Czech Ministry Of Education, Youth And Sports, Czech Republic), NT 13679-4 (Internal Grant Agency, Ministry of Health of the Czech Republic) and by CA 103314 (National Institutes of Health, USA).

Prague, 03. 04. 2023

Mgr. Petr DANIEL

ACKNOWLEDGEMENT

At this place, I would like to thank my supervisor, prof. Jan Kovář for his leadership of my PhD thesis.

I would like to thank my colleagues Honza, Michael, Kamila, Nela, Vlasta, Simona, Jana, Linda, Hanka, Markéta Jarda, Pavel, Radka, Alžběta and Karolína. Special thanks belong to my mom Petra, my sister Silvie and Eva and my little niece Ema.

"Measure what is measurable, and make measurable what is not so."

Galileo Galilei

TABLE OF CONTENTS

LIST OF ABBREVIATIONS

2-D PAGE – two-dimensional polyacrylamide gel electrophoresis
10-DAB – 10deacetyl baccatin III
A – anthracycline (doxorubicin, epirubicin)
ABC – ATP binding cassette
AC – adriamycin, cyclophosphamide
AC/T –adriamycin cyclophosphamide followed by taxane
AI – aromatase inhibitor (for example, exemestane)
AR – androgen receptor
ATP – adenosine 5'-triphosphate
BAC – baccatin
BC – breast cancer
BL – basal like
CEP17 – centromere probe chromosome 17
CMF – cyclophosphamide, methotrexate, 5-fluorouracil
CNA – copy number alteration
CRPC – castration-resistant prostate cancer
CT – chemotherapy
DCIS – ductal carcinoma *in situ*
DNA – deoxyribonucleic acid
ER – estrogen receptor
ET – endocrine therapy
EQTL – expression quantitative trait loci
FAC – 5-fluorouracil, adriamycin, cyclophosphamide
FDA – Food and Drug Administration
FEC – 5-fluorouracil, epirubucin, cyxlophosphamide
G-CSF – granulocyte colony-stimulating factor
GnRH – gonadothropin-releasing hormone agonist
GTP – guanosine 5'-triphosphate
FISH – fluorescence *in situ* hybridization
HER2 – human epithelial receptor 2
IBC – invasive breast carcinoma
IBC-NST – invasive breast carcinoma of no specific type
IDC – invasive ductal carcinoma
IF – inward-facing
IHC – immunohistochemistry
ILC – invasive lobular carcinoma
IntClust – integrative cluster
ISH – *in situ* hybridization
LAR – luminal androgen receptor
LCIS – lobular carcinoma *in situ*
M – mesenchymal
MAP – microtubule associated protein
METABRIC – Molecular Taxonomy of Breast Cancer International Consortium

MTOC – microtubule organizing center
NBD – nucleotide binding domain
NCI – The National Cancer Institute
OF – outward-facing
OFS – ovarian function suppresion
PAM50 – Prediction Analysis of Microarray 50
PARP – poly(ADP-ribose) polymerase
PARPi - poly(ADP-ribose) polymerase inhibitor
PF – protofilamentum
PR – progesterone receptor
REDOR-NMR – rotational-echo, double-resonance nuclear magnetic resonance
ROR – risk of reccurence
RTI – Research Triangle Institute
SAR – structure-activity relationship
SB-T – Stony Brook Taxane
SERM – selective estrogen receptor modulator (for example, tamoxifen)
SLC – solute carrier
SNP – single nucleotide polymorphism
SNV – single nucleotide variant
T – taxane
TAC – taxane, adriamycin, cyclophosphamide
TAM – tamoxifen
Taxoid – taxane derivative
t-BOC – *tert*-butoxycarbonyl group
TNBC – triple negative breast cancer
TCGA – The Cancer Genome Atlas
TDLU – terminal ductal lobular unit
TMD – transmembrane domain
TRIP6 – thyroid hormone receptor interactor 6
WHO – World Health Organization

SUMMARY

About 1 in 3 humans will experience cancer during their lifetime, and about 1 in 6 humans will die of cancer disease. Breast cancer is currently the most diagnosed neoplasm in women, with 2.2 million cases and 685 thousand of deaths worldwide.

Despite significant advances in diagnostics, molecular biology and drug development toward the goal of patient-tailored therapy, the mortality rate stagnates. Patients become unresponsive to treatment due to drug resistance occurs. Generally, cancer can be naturally insensitive to primary treatment (innate resistance) or manifest resistant phenotype after a prolonged period (acquired resistance).

This PhD thesis concerns acquired drug resistance to taxanes in breast cancer cells. We aimed to put light on mechanisms involved in paclitaxel and Stony Brook Taxane 0035 resistance and how we can overcome them.

We found several suspect genes with changed expression at the protein level between taxane-sensitive and taxane-resistant breast cancer cells. Among them, *ABCB1* gene codes for a versatile multidrug transporter P-glycoprotein was pivotal for resistance to paclitaxel and Stony Brook Taxane 0035.

Other genes with altered expression were localized primarily on the q arm of chromosome 7, exemplified by thyroid hormone receptor interactor 6 (*TRIP6*). A combination of active cyclic AMP response element (CRE) motif, hypomethylated *TRIP6* proximal promoter, the lack of *TRIP6*-regulatory miRNA-138-5p and amplification contribute to high TRIP6 expression in taxane-resistant MCF-7 breast cancer cells.

Novel semi-synthetic docetaxel derivatives named second-generation Stony Brook Taxanes, represented by SB-T-1216, efficiently overcome ABCB1-mediated taxane resistance. We hypothesize that C3' and C3'N taxoids poorly interact with residues in the ABCB1 binding pocket in contrast to paclitaxel.

To conclude, ABCB1 transporter has an essential role in taxane resistance *in vitro*. Taxane derivatives, in particular, bearing C3' and C3'N modifications can overcome ABCB1-mediated resistance. Furthermore, when *ABCB1* is ampli-

fied, genes proximal to *ABCB1*, exemplified by CRE-stimulated *TRIP6*, can be co-selected.

SOUHRN

Zhruba jeden ze tří lidí čelí v průběhu života nádorovému onemocnění a zhruba každý šestý člověk nádorovému onemocnění podlehne. Nejčastěji diagnostikovaný typ nádoru u žen v celosvětovém měřítku je nádor prsu, přibližně postihne 2,2 milionů žen a má na svědomí 685 tisíc úmrtí ročně.

Navzdory pokrokům v diagnostice, molekulární biologii a vývoji nový léčiv za účelem personalizované medicíny, úmrtnost způsobená nádory prsu zůstává stejná. Pacienti neodpovídají na léčbu v důsledku rezistence na použitá léčiva. Obecně rozeznáváme mezi nádory již primárně rezistentními vůči léčbě medikamenty (přirozená rezistence) anebo se může rezistence vyvinout u nádoru, který byl na danou léčbu původně odpovídající (získaná rezistence).

Tato dizertační práce se zabývá mechanismy získané rezistence k taxanům u buněk nádorů prsu. Pokusili jsme se objasnit mechanismy účastnící se rezistence k paclitaxelu a derivátu paclitaxelu Stony Brook Taxane 0035 (SB-T-0035) a jak tyto mechanismy můžeme překonat.

Podařilo se nám identifikovat suspektní geny s rozdílnou expresí na úrovni proteinu mezi buňkami nádorů prsu senzitivními a rezistentními k taxanům. Mezi těmito geny jsme objevili univerzální transportér P-glykoprotein (kódovaný genem *ABCB1*) asociovaný s mnohočetnou lékovou rezistencí. P-glykoprotein se ukázal být nezbytný pro rezistenci k paclitaxelu a derivátu SB-T-0035.

Další geny vykazující změnu v expresi na úrovni proteinu byly primárně lokalizovány na chromosomu 7 v blízkosti lokusu genu *ABCB1*. Příkladem je gen kódující protein interagující s hormonem štítné žlázy 6 (*TRIP6*). Zjistili jsme, že v buňkách MCF-7 senzitivních i rezistentních k taxanům je zvýšená exprese genu *TRIP6* dána aktivním elementem responsivním pro cyklický AMP, hypomethylací proximálního promotoru genu *TRIP6*, absencí miRNA-138-5p regulující gen TRIP6 a amplifikace lokusu genu *TRIP6*.

Taxanové deriváty druhé generace reprezentované taxoidem SB-T-1216 jsou schopné překonat rezistenci k taxanům zprostředkovanou transportérem

ABCB1. Domníváme se, že deriváty s modifikacemi na C3' a C3'N pozicích hůře interagují s aminokyselinovými zbytky ve vazebné kapse transportéru ABCB1.

Závěrem lze říct, že transportér ABCB1 má zásadní roli v rezistenci vůči taxanům *in vitro*. Deriváty taxanu nesoucí C3' a C3'N modifikace, mohou překonat rezistenci zprostředkovanou ABCB1. Kromě toho, když je *ABCB1* amplifikován, mohou být společně selektovány geny proximální k *ABCB1*, jejichž příkladem je gen CRE-stimulovaný gen *TRIP6*.

1. LITERATURE REVIEW

1.1 BREAST CANCER

According to the actual release of the Globocan Study, with 2.3 million newly diagnosed cases (11.7% of all cancer cases) in 2019, breast cancer (BC) became the most diagnosed human cancer disease worldwide (**Sung et al., 2021**). In European Union, nearly 400,000 cases and 100,000 deaths account for BC in recent years (**Cardoso et al., 2019**). Furthermore, about 7,000 women were diagnosed with BC, and 1,600 women died of BC in the Czech republic each year in the period 2016–2018 (**Krejčí et al., 2018**)

A hallmark of BC is heterogeneity. It is well established that tumour mass comprises cell subpopulations with genetic and non-genetic divergences. A combination of intrinsic (i.e., epithelial-to-mesenchymal transition, occurrence of stem cells) and extrinsic (i.e., tumour microenvironment) factors drive intratumoural heterogeneity (**Lüönd et al., 2021**). The most studied traits of cancer are metastastic potential and drug resistance. Concerning BC heterogeneity, an exciting study documented HER2-positive metastases in HER2-negative primary tumour patients, delineating the extraordinary plasticity of BC cells (**Lindstrom et al., 2012**).

Intertumoural heterogeneity means the patient-to-patient variations in histopathology, genetic alterations and therapy outcome (**Turashvili & Brogi, 2017**). The basis for intertumoural heterogeneity of BC lies foremost in the structure of the mammary gland. BC originates from a terminal ductal lobular unit (TDLU), a basic mammary gland structure consisting of a lobule and extralobular terminal duct (**Figure 1.01**). Each lobule contains tens of alveoli and ducts resembling a stem with grapes. The branches of ducts converge into large ones that open at the nipple (**Harbeck et al., 2019**).

Two primary cell lineages build a duct: luminal epithelial cells and myoepithelial (basal) cells. The luminal cells can further differentiate into milk-secretory alveolar cells, while the myoepithelial cells contract the duct (**Figure 1.01**) (**Hassiotou & Geddes, 2013**). The luminal cells can be readily distin-

guished by staining for cytokeratins 8/18 in the mammary gland. In comparison, myoepithelial (basal) cells (stained for keratins 5/6 and 14) make the outer layer of the duct.

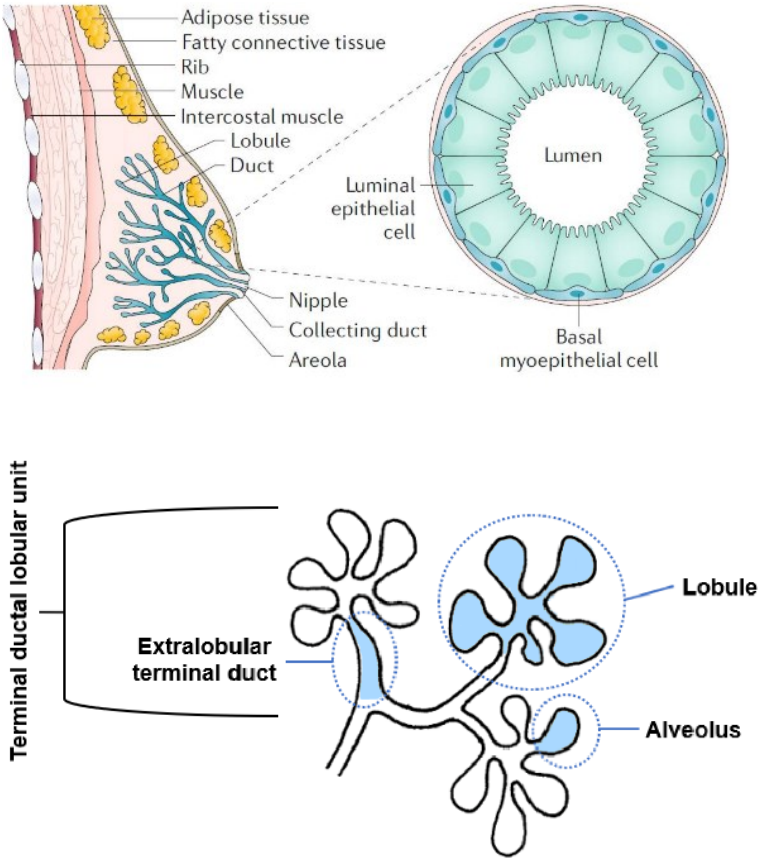

Figure 1.01 Anatomy of the human breast. Breast cancer cells can arise from luminal (milk-producing) and surrounding basal myoepithelial cells in the lobule and duct. *From Harbeck et al., 2019* (top). The terminal ductal lobular unit is formed by the extralobular terminal duct connected with one lobule. Alveoli (individual sacs) are found within each lobule (bottom).

1.1.1 Histological subtypes of breast cancer

The categorisation of primary BC is performed to facilitate the prediction of disease outcomes and guide for patient-tailored treatment modality. From the historical view, BC has been ascribed to histopathological characteristics.

Two types of BC can be distinguished. The non-invasive type (carcinoma *in situ*) is a lesion growing inside the duct. The invasive type, also called infiltrating carcinoma, is a malign disease in that the cancer cells spread beyond the basal membrane (**Figure 1.02**) (**Burstein et al., 2004**).

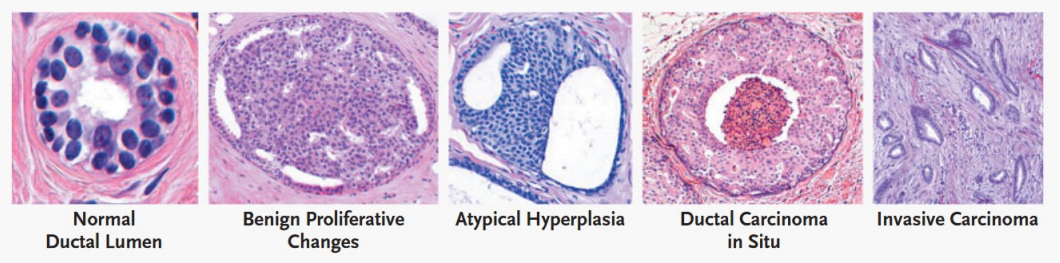

Figure 1.02 Comparison of histologic changes during cancerogenesis in breast tissue. *Taken from Burstein et al., 2004*.

Histopathologic features were the first recognised characteristics of BC that simplified clinicians in managing the most suitable follow-up therapy. The histological classification of BC by WHO tentatively recognises epithelial, fibroepithelial, mesenchymal, haematolymphoid BC, tumours of the nipple and very rare male BC (**WHO Classification of Tumours Editorial Board, 2019**).

Epithelial tumours further comprise hyperplasia, adenoma, adenosis and benign sclerosis lesions, papilloma, epithelial-myoepithelial tumours, salivary gland tumours, neuroendocrine neoplasms, non-invasive lobular neoplasia (lobular carcinoma *in situ*, LCIS), ductal carcinoma *in situ* (DCIS) and the most common invasive breast carcinoma (IBC) (**WHO Classification of Tumours Editorial Board, 2019**).

In particular, IBC is of significant concern as it represents a progressive state of disease. Nevertheless, 80 % of cases account for IBC of no specific type (IBC-NST), an artificious subgroup with promiscuous histopathologic characteristics. The second common type of BC is invasive lobular carcinoma (ILC) which also encompasses morphologically distinct subtypes (**McCart Reed et al., 2015**). Frame-shift mutations and deep deletion of *CDH1* (cadherin 1, 16q22.1) are frefrequently found in ILC, suggesting CDH1 loss as an early event in this type of cancer (**Ciriello et al., 2015; McCart Reed et al., 2015**). Rare invasive carcinomas are also distinguished in clinics, as shown in **Figure 1.03**.

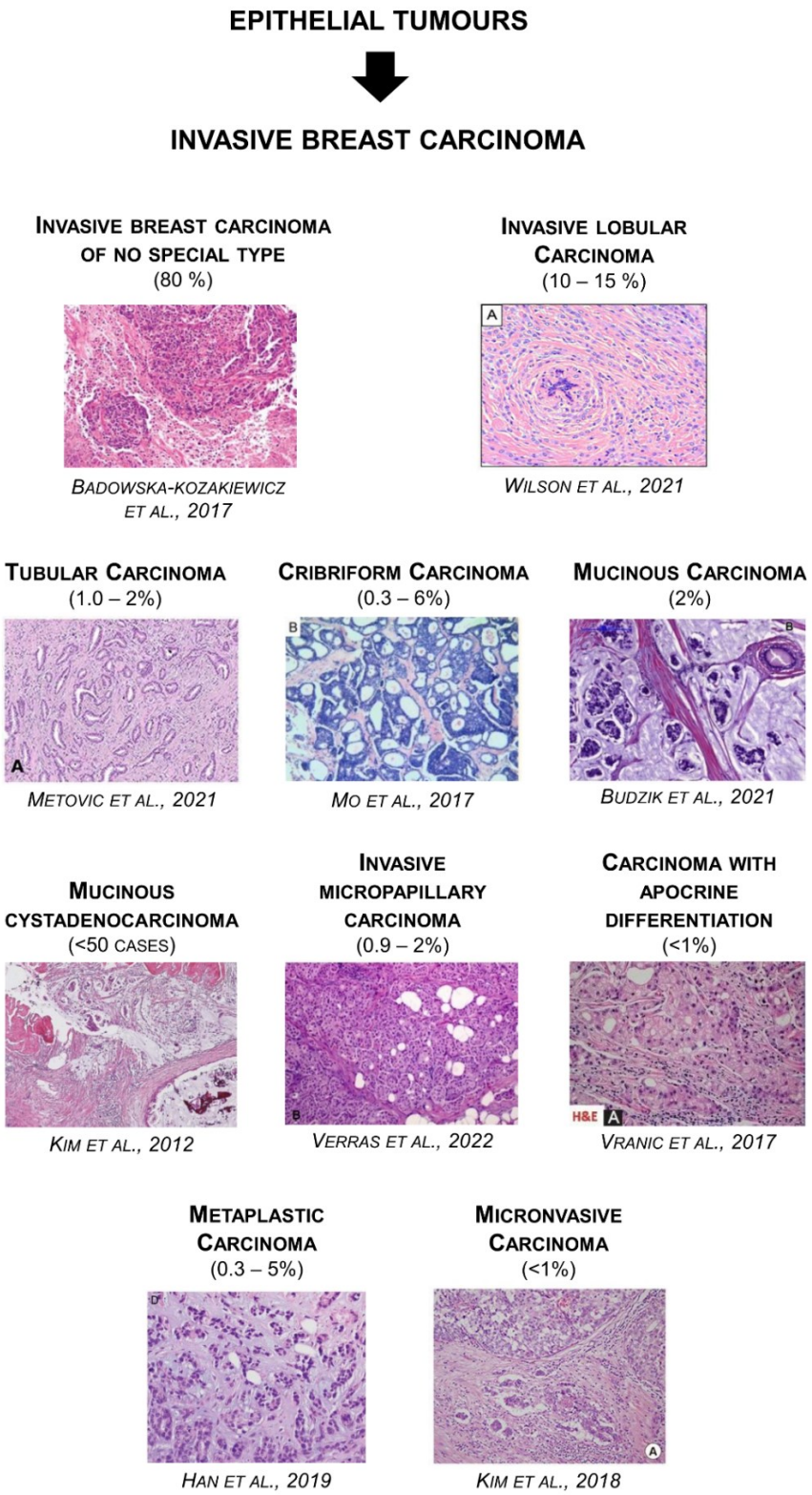

Figure 1.03 Histologic preparates exhibit excessive heterogeneity. Representative hematoxylin and eosin staining specimens of breast cancer. The prevalence of cancer is shown in parentheses. A detailed description of IBC types can be found in the cited literature.

1.1.2 Molecular characterization of breast cancer

Molecular traits of BC have been unravelled with the incorporation of modern high-throughput analytical methods over the last two decades. A seminal cDNA microarray-based survey in this field has identified four "intrinsic" molecular subtypes of BC by unsupervised hierarchical clustering of 65 surgical specimens according to the expression pattern of 496 intrinsic genes (**Perou et al., 2000**). The term "intrinsic genes" refers to the genes differing in expression between unrelated tumour samples than between paired samples taken from the same tumour. Based on estrogen receptor expression (ER), breast cancer samples branched into luminal/ER-positive (ER+) and ER-negative (ER-) clusters.

Studies with extended tumour samples and intrinsic genes were consistent with most of the gross subtyping of BC. Merely refining the ER+ cluster resulted in luminal A and luminal B subtypes. Basal-like and HER2-enriched subtypes remained in ER- cluster (**Sorlie et al., 2001 and 2003**). The normal-like subtype is now inferred to be an artefact due to outnumbering normal adjacent non-tumour cells in analyzed specimens. The study also assigned 17 BC cell lines into four biologically-relevant groups.

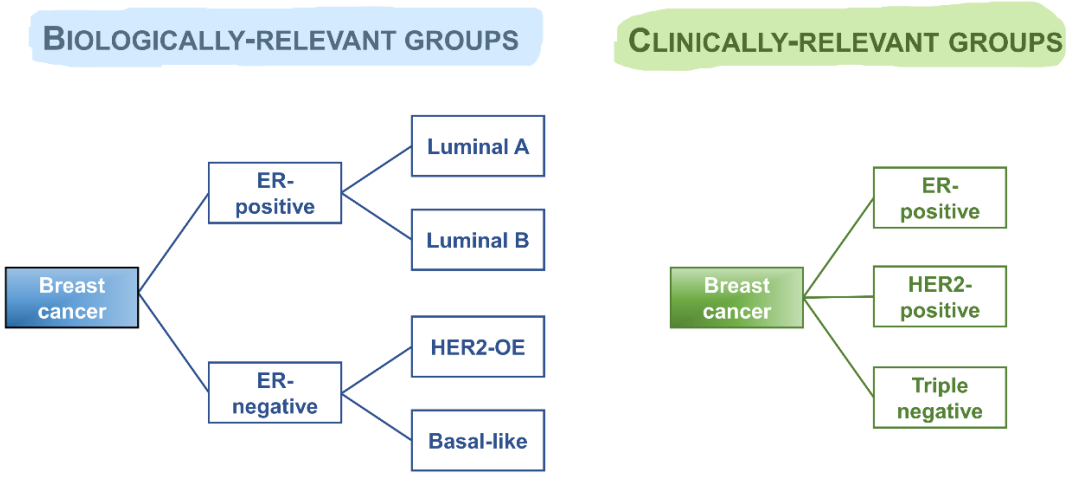

Figure 1.04 Current breast cancer categorization as used in basic research and clinic. Centroid-based prediction analysis of the microarray method (PAM50) precisely defines breast cancer subtypes. By contrast, cost-effective immunohistochemistry (IHC) and fluorescence *in situ* hybridization (FISH) methods dominate in clinics.

Luminal A tumours have high expression of luminal/ER-regulated genes such as *PGR* (progesterone receptor, 11q22.1), *GATA3* (GATA binding protein 3, 10p14*)*, *SLC39A6* (solute carrier family 39 member 6*,*18q12.2), *XBP1* (X-box binding protein 1*,* 22q12.1*)*, *FOXA1* (forkhead box A1, 14q21.1)*, TFF3* (*trefoil factor 3,* 21q22.3) and low expression of cell cycle-related *MKI67* (marker of proliferation 67, 10q26.2). Luminal A tumours tend to be slowly growing malignancies, low grade and are therefore associated with the most favourite outcome when considering overall survival and time to development of metastasis (**Perou et al., 2000; Sorlie et al., 2001 and 2003; Cardoso et al., 2019**).

Luminal B subtypes are markedly enriched for cell cycle-associated genes such as *MKI67* (**Sorlie et al., 2003**). Luminal B cancers are generally high-grade and highly proliferative, the factors reflecting intermediate to poor outcomes (**Cardoso et al., 2019**).

Basal-like subtype was named owing to high expression of basal cell-specific keratins (*KRT5* and *KRT17*), laminin and fatty acid binding protein 7 (*FABP7*). Patients with diagnosed basal-like BC have the worst prognosis (**Perou et al., 2000; Sorlie et al., 2003**).

Next, cancers of the ERBB2-overexpressing subtype (known as HER2-enriched) harbour amplification of the 17q22.24 locus. As a consequence, they overexpress a cluster of genes in close vicinity to *ERBB2* (Erb-b2 receptor tyrosine kinase 2, 17q12) and *GRB7* (growth factor receptor bound protein 7, 17q12) loci (**Sorlie et al., 2001**).

Although intrinsic subtyping by microarrays turns out to be a reliable method, high-cost demands of consumables block its usage in clinics. Hence, the reduced variant, PAM50 assay, has been developed (**Parker et al., 2009**). PAM50 assay has become very popular because it enables the determination of BC subtype even in formalin-fixed paraffin-embedded samples. The assay utilizes a centroid-based prediction method of expression of 50 genes to classify samples accurately into one of the recognized BC subtypes.

Copy number aberration (CNA) and inherited single nucleotide polymorphism (SNP) represent considerable expression of quantitative trait loci (eQTL) in BC. Therefore, joint clustering of somatic *cis*-acting CNA and gene

expression in 2,000 primary BC was the basis for the most detailed classification of BC so far (**Curtis et al., 2012**). Ten integrative highly prognostic clusters have been recognized. The authors highlighted IntClust2 (11q13/14 *cis*-acting) and IntClust5 subgroups with aggressive phenotypes and poor outcomes. Conversely, IntClust3 and IntClust4 subgroups with the most favourable outcomes lacked any somatic CNA. Subgroups with an intermediate outcome were IntClust1 (17q23/20q *cis*-acting), IntClust6 (8p12 *cis*-acting*),* IntClust8 (1q gain/16q loss), IntClust7 (16p gain/16q loss, 8q amplification) and highly-instable IntClust10 (5 loss/8q gain/10p gain/12p gain *cis*-acting) (**Curtis et al., 2012**).

1.1.3 Clinical view of breast cancer

Choice of the optimal treatment has been usually based on the parameters such as the number of axillary lymph nodes involved (at least ten nodes must be dissected for evaluation of lymph node infiltration), tumour size, age or menopausal status of patient (premenopausal, perimenopausal,postmenopausal and elderly), histopathology and hormone receptor status through the incorporation of intrinsic subtypes to current simplified schedule of intrinsic subtypes (**Glick et al., 1992; Goldhirsch et al., 1995, 2003, 2009, 2011; Burstein et al., 2021**).

For the clinical purpose, categories of early-stage BC and recommended therapy, lastly updated in 2021, are simplified as written in the below chapters (**Figure 1.04, page 17**).

1.1.3.1 ER-positive BC

Estrogen receptor positivity justifies adjuvant endocrine therapy (ET). Cancer with ≥10% of ER staining is considered truly ER-positive and might benefit from systemic ET, whereas cancer with ≤1% ER positivity will benefit from chemotherapy (CT) (**Burstein et al., 2021**). The choice of therapy in luminal type entirely depends on the marker of proliferation activity Ki-67 (*MKI67*). The luminal A subtype characterizes a high number of ER/PR positive cells and low (≤5%) Ki-67 staining, the markers favouring endocrine therapy. In contrast, luminal B cancer is ER/PR negative but has a high Ki-67 level (≤30%) and will therefore benefit from chemotherapy (**Burstein et al., 2021**).

Another clue in clinical management of ER+/HER2- node-negative patients who will beneft from chemotherapy can provide Oncotype DX® (Genomic Health, Redwood City, CA) and MammaPrint® (Agendia, Amsterdam, The Netherlands) (**Paik et al., 2006; Knauer et al., 2010**). Only patients with high-risk scores should receive chemotherapy (**Burstein et al., 2021**).

For pre-menopausal women with micro-invasive ER+ BC, *ovarian function suppression* (OFS) by gonadotrophin-releasing hormone agonist (GnRH) such as goserelin (Zoladex®) or triptorelin (Decapeptyl) combined with tamoxifen (TAM), an estrogen receptor nonsteroidal antagonist, is an appropriate option (**Figure 1.05**) (**Goldhirsch et al., 2003**). Aromatase inhibitors (AIs) such as Exemestane (Aromasin®) can substitute TAM when contraindicated (**Goldhirsh et al., 2009**). Recently, 5-year TAM monotherapy has been sufficient for most patients, except for younger (<35 years) or patients having at least two lymph nodes infiltrated with tumour cells (**Burstein et al., 2021**).

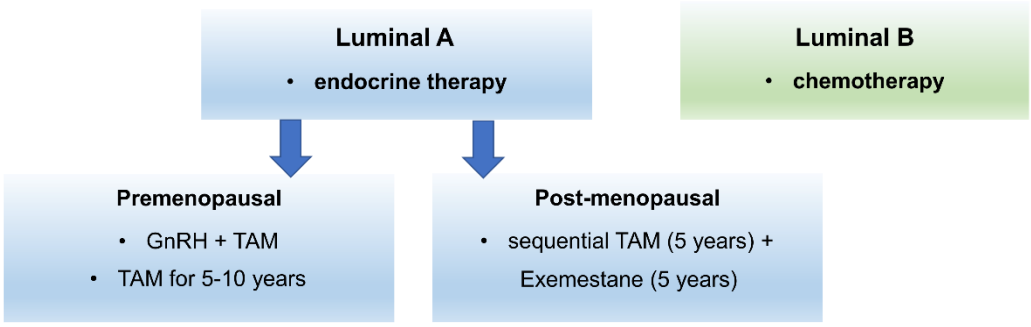

Figure 1.05 Current treatment modalities for early ER-positive BC. Therapy can be modified respectfully to cancer attributes/patient characteristics. Alternative therapies and experimental therapies are not shown. TAM – tamoxifen, a selective estrogen receptor modulator (SERM); GnRH – gonadotrophin-releasing hormone agonist; Exemestane – a type of aromatase inhibitor (AI).

The ATAC study (Arimidex, Tamoxifen, Alone or in Combination) demonstrated that post-menopausal women benefit from AI monotherapy rather than TAM monotherapy or AI/TAM combined therapy (**Duffy et al., 2003**). The sequential therapy by TAM for 2-3 years, followed by AI monotherapy for 2-3 years in post-menopausal women, turned out to be a game-changer, significantly

reducing the risk of disease relapse. Furthermore, extended therapy, i.e. five years of TAM followed by five years of AI, is superior for high-risk stage III or node-positive stage II patients. A five years monotherapy with AI or TAM remains standard for cancer of stage I (**Burstein et al., 2021**).

1.1.3.2 HER2-positive BC

Cancer is considered as HER2-positive when ≥ 30% of cancer cells are positively stained for HER2 or when HER2/CEP17 ratio ≥ 2.2 by ISH (**Cardoso et al., 2019**; **Burstein et al., 2021**). HER2-positive cancer associates with poor outcome and high risk of relapse (**Yang et al., 2021**).

The standard therapy for early HER2-positive BC is one year dosing of recombinant monoclonal *anti*-HER2 antibody, trastuzumab (Herceptin®) (**Baselga et al., 1996; Cardoso et al., 2019**). Trastuzumab binds specifically at the extracellular domain of HER2, thereby preventing HER2 homo- and HER2 heterodimerization with HER1, HER3 and HER4. Besides inhibiting HER signaling, trastuzumab can further evoke antibody-dependent cell-mediated cytotoxicity of HER2-positive cancer cells (**Ishii et al., 2019**). Combined *anti*-HER2/docetaxel therapy turned out to be more efficacious than *anti*-HER2/anthracycline therapy since the latter regime is associated with increased risk of cardiomytoxicity.

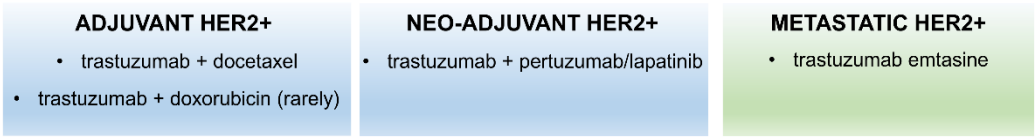

Figure 1.06 Therapy options for HER2-positive breast cancer. A monoclonal antibody specific to the human epidermal growth factor 2 receptor (HER2) is a mainstay therapy. Taxanes are preferred as part of adjuvant therapy. T – taxane; A – anthracycline.

In a neoadjuvant setting, trastuzumab in combination with pertuzumab or lapatinib (HER1 and HER2 inhibitor) showed improved long-term outcomes (**Cardoso et al., 2019**). Pertuzumab targets the same HER2 extracellular domain as trastuzumab but interacts with a different epitope, thereby specifically preventing HER2/HER3 heterodimerization (**Ishii et al., 2019**).

Metastatic HER2-positive BC is currently treated by trastuzumab emtansine (Kadczyla®), a conjugate of HER2 antibody and mertansin, an inhibitor of tubulin polymerization (**Delgado et al., 2021**).

1.1.3.3 Triple negative breast cancer

Triple-negative breast cancer (TNBC) is a highly heterogeneous group that accounts for 10-15% of all BC cases. TNBC is more commonly diagnosed as a malignancy that has just spread to axillary lymph nodes in young (≤ 35 years) African-American women (**Lehmann et al., 2011**).

Chemotherapy is inevitably recommended, as TNBC lacks ER, PR and HER2 expression. Nevertheless, a minority of patients having somatically and germinally mutated genes involved in DNA damage response, *BRCA1* (BRCA1 DNA repair associated,17q21.31), *BRCA2* (*BRCA2* DNA repair associated, 13q13.1), *PALB* (partner and localizer of BRCA2, 16p12.2) and dozen others, profit from therapy with PARPi (poly(ADP-ribose) polymerase inhibitor), for example, olaparib (Lynpanza®) and talazoparib (Talzenna®) (**Burstein et al., 2019**).

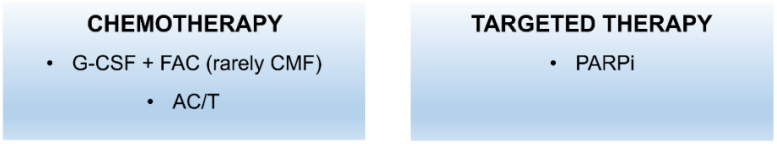

Figure 1.07 Therapy options for triple-negative breast cancer (TNBC). Most patients receive sequential AC/T therapy. When AC/T is contraindicated, prophylaxis with granulocyte colony-stimulating factor (G-CSF) prior FAC is needed. Alternatively, an older CMF regime can be administered. Patients with germinal BRCA1/BRCA2 mutations are recommended to undercome poly(ADP-ribose) polymerase inhibitors (PARPi). AC – doxorubicin plus cyclophosphamide. T – docetaxel.

Neoadjuvant chemotherapy is preferred in stages II and III for HER2-positive and TNBC. For TNBC, adjuvant chemotherapy was recommended when the primary tumour size exceeds 5 mm (**Burstein et al., 2021**). The first chemotherapy regimen, introduced in the 1970s, included a cyclophosphamide, methotrexate, and 5-fluorouracil (CMF) combination (**Martin, 2006**). Anthracyclines,

i.e. doxorubicin (Adriamycin®, A) or epirubicin (Ellence®, E), replaced methotrexate, resulting in a more efficacious FAC (or FEC) schedule. A milestone occurred in 1994 when the Food and Drug Administration (FDA) approved taxanes (paclitaxel and docetaxel) for therapy of metastatic breast cancer (**Rowinski & Donehover, 1995**). Phase II and III studies showed that TAC regimen, i.e., docetaxel (75 mg/m^2), doxorubicin (500 mg/m^2) and cyclophosphamide (500 mg/m^2), resulted in a better objective response rate, however, with severe toxicity. Thus, the TAC regime requires prior prophylaxis with granulocyte colony-stimulating factor (G-CSF). Following trials found effective treatment by four courses of dose-dense AC with the following paclitaxel or docetaxel (T) (**Sparano et al., 2008**).

Four subtypes of TNBC are recognized: basal-like 1 (BL1) subtype with high expression of genes associated with cell cycle and DNA damage), basal-like 2 (BL2) subtype with high expression of growth factor signalling genes, mesenchymal (M) subtype with high expression of epithelia-mesenchymal transition associated genes, and luminal androgen receptor (LAR) subtype with high expression of luminal genes and androgen receptor (**Lehmann et al., 2011**; **Lehmann et al., 2016**). Although the BL1 subtype superiorly responds to cisplatin, no recommendations of platinum derivatives for clinical practice have been warranted (**Burstein et al., 2021**).

1.1.4 Driver mutations and driver genes in breast cancer

Numerous sequencing studies gave an essential insight into the mutational landscape of BC (**Cancer Genome Atlas Network, 2012; Curtis et al., 2012; Pereira et al., 2016; Razavi et al., 2018; Lips et al., 2022**). Somatic changes in the cancer genome may include single nucleotide variants (SNV), insertions and deletions (referred to as indels), and large structural variants, in particular, copy number aberrations (CNA) beyond impaired epigenomic DNA patterns. Further, the most common type of SNV is a single base substitution.

Compared to other malignancies, BC belongs to a group of poorly mutated cancers, harbouring, on average, 33 non-synonymous mutations (**Vogelstein et al., 2013**). However, only a few of them genuinely contribute to cancerogenesis.

One can discern between a passenger mutation, which provides no benefit in modulating cancer growth properties and a driver mutation, which unambiguously enhances cancer cell proliferation activity. A gene harbouring a driver mutation is called *a driver gene* (**Vogelstein et al., 2013**).

The Cancer Genome Atlas Research Network (TCGA) and Molecular Taxonomy of Breast Cancer International Consortium (METABRIC) studies uniformly found *PIK3CA* (phosphatidylinositol-4,5-bisphosphate 3-kinase catalytic subunit alpha, 3q26.32) and *TP53* (tumour protein 53, 17p13.1) as the most mutated genes in BC. Mutations in *PIK3CA* are common in luminal subtypes, whereas *TP53* coding mutations dominate the HER2-enriched and basal-like subtypes. In addition, both studies highlighted prominent *GATA3* and *MAP3K1* (mitogen-activated protein kinase kinase kinase 1, also known as MEKK1, 5q11.2) mutations in luminal A subtype (**Cancer Genome Atlas Network, 2012; Pereira et al., 2016**).

Subtype	METABRIC		TCGA	
Luminal A	*PIK3CA*	57.4%	*PIK3CA*	46.4%
	GATA3	19.6%	*GATA3*	14.3%
	MAP3K1	16.2%	*MAP3K1*	13.4%
Luminal B	*PIK3CA*	34.9%	*PIK3CA*	31.5%
	TP53	24.3%	*TP53*	31.5%
	AHNAK2	14.1%	*GATA3*	15.3%

Subtype	METABRIC		TCGA	
HER2-enriched	*TP53*	70.0%	*TP53*	75.4%
	PIK3CA	41.4%	*PIK3CA*	40.4%
	AHNAK2	20.5%	*DNAH11*	10.5%
Basal-like	*TP53*	88.4%	*TP53*	82.8%
	SYNE1	20.6%	*BRCA*	15.1%
	AHNAK2	18.6%	*USH2A*	10.8%

Table 1.01. Top mutated genes in intrinsic subtypes as defined by PAM50. Two datasets (METABRIC, TCGA) were analyzed through cBioportal. *TTN* (titin) and *MUC16* (mucin 16) genes were excluded.

The TCGA study highlighted mutated genes of the PI3K signalling pathway (*PTEN*, phosphatase and tensin homolog, 10q23.31; *PIK3R1*, phosphoinositide-3-kinase regulatory subunit, 5q13.1; *AKT1*, AKT serine/threonine kinase, 14q32.33), tyrosine phosphatases *PTPRD* (protein tyrosine phosphatase receptor type D, 9p24.1-p23) and *PTPN22* (protein tyrosine phosphatase non-receptor type 22, 1p13.2), transcription factors *CBFB* (core-binding factor subunit beta, 16q22.1), *CTCF* (CCCTC-binding factor, 16q22.1), *FOXA1* (forkhead box A1, 14q21.1), *RUNX1* (RUNX family transcription factor 1. 21q22.12), *TBX3* (T-

box transcription factor 3, 12q24.21), *AFF2* (ALF transcription elongation factor 2, Xq28) and *RB1* (RB transcriptional corespressor, 13q14.2), epigenetic regulator *KMT2C* (lysine methyltransferase 2C,7q36.1), splicing factor *SF3B1* (splicing factor 3b subunit 1,2q33.1), cell cycle molecules *CCND3* (cyclin D3, 6p21.1), *CDKN1B* (cyclin-dependent kinase inhibitor 1B, p27 Kip1, 12p13.1), RAS/MAPK signalling member *NF1* (neurofibromin, 17q11.2). Most of them, particularly *TBX3*, *RUNX1*, *CBFB*, *and SF3B1*, have been identified in the follow-up METABRIC study focused on driver genes (**Cancer Genome Atlas Network, 2012; Pereira et al., 2016).**

Large deletions and insertions underpin the expression landscape of BC. METABRIC study reported copy number gains of 11q13-14 region (*CCND,* cyclin D1) and *PAK1* (p21 (RAC) activated kinase 1), 17q12 region (*ERBB2*, erb-b2 receptor tyrosine kinase 2), 8p11 region (*ZNF703*, zinc finger 703), 8q24 region (*MYC*, MYC proto-oncogene), frequent homozygous and heterozygous deletions of the regions surrounding *PPP2R2A* (protein phosphatase 2 regulatory subunit B alpha, 8p21), *MAP2K4* (mitogen-activated protein kinase kinase 4, 17p11), and *MTAP* (methylthioadenosine phosphorylase, 9p21) (**Curtis et al., 2012**).

Invasive lobular cancer (ILC) is the second histologic type of BC by prevalence (**Chapter 1.11, Figure 1.03**) (**Ciriello et al., 2015**). Most of the ILCs belong to the luminal A subtype. The high mutation rate in *CDH1* (E-cadherin, 16q22.1), *TBX3*, *RUNX1*, *FOXA1 and PIK3CA*, as well as frequent homozygous loss of *PTEN* (phosphatase and tensin homolog, 10q23.31), were observed in luminal A ILC as compared to luminal A invasive ductal carcinoma (IDC). Interestingly, significantly low incidence of *GATA3* mutations in ILC was found (**Ciriello et al., 2015**).

1.2 Taxanes and mechanism of their action

1.2.1 The discovery of paclitaxel (Taxol®)

In 1962, botanist Dr Arthur S. Barclay gathered plant samples, including bark, leaves, twigs, and fruit of the western pacific yew tree (*Taxus brevifolia Nutt.*) in Washington state in the northwest region of the United States (**Wani &**

Horwitz, 2014). He supplied the samples to the hands of Dr Jonathan L. Hartwell, a principal investigator of an antitumour drug screening program at the National Institute of Cancer (NCI). Unfortunately, despite an early experiment showing promising antitumour activity of crude extracts against 9KB cancer cells, reiterated efforts in P-388 and L-1210 leukaemia cells and mice models, supply complications and unsolved structure of the active compound led to discontinuation of taxane research for a decade.

Inspired by their previous triumph with camptothecin (a drug from *Camptotheca acuminata)*, Drs Mansukh Wani and Monroe E. Wall, both working at Research Triangle Institute (RTI), requested for *T. brevifolia* samples in 1965. In the following years, Wani and Monroe discovered the chemical structure of Taxol® (paclitaxel) by the X-ray analysis of α-hydroxy methyl ester and tetraol, two products of paclitaxel methanolysis (**Wani et al., 1971**).

The family *Taxeaceae* of conifers (*Pinophyta*) comprises of globally distributed six genera (*Amentotaxus*, *Austrotaxus Cephalotaxus*, *Pseudotaxus*, *Torreya* and *Taxus*) (**Lange & Conner, 2021**). Depending on one's idea, there are 8 to 10 recognized species in *Taxus* genera. Taxus species are slowly-growing plants confined to the northern hemisphere; some are endemic, such as Himalayan *T. wallichiana* sp. or *T. floridana* in the northwest Florida peninsula, while others are growing in a large area (**Maheshwari et al., 2008**). Besides *Taxus brevifolia*, paclitaxel has been found, however, in a less amount in *Taxus yunnanensis*, *Taxus baccata* and *Taxus wallichiana*.

Figure 1.05 Tree yews in nature. *Taxus baccata* and detailed view on a female twig with red arils and immature male yellow cones. *Taken and modified from Lange & Conner, 2021.*

Bark gathering causes irreversible damage of hundred years old trees, and poor yield of paclitaxel from *Taxus brevifolia* limited further taxane usage in clinics. For example, a 100-year-old tree provides about 300 mg of Taxol® (**Tabata, 2004**). The Discovery of a more common paclitaxel precursor, 10-deacetyl baccatin (10-DAB), in *T. baccata* leaves and research efforts in the chemistry of taxanes resulted in practical semi-synthesis of paclitaxel from 10-DAB and a pure enantiomer of C-13 isoserine side chain via Ojima-Holton coupling reaction (**Figure 1.06**) (**Ojima et al., 1992**). Additionally, automated production of paclitaxel from callus cell cultures of *T. baccata* has been developed (**Tabata et al., 2004**).

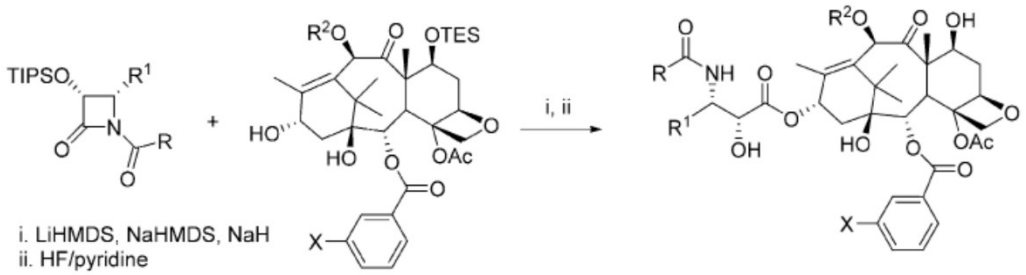

Figure 1.06 Semi-synthesis of taxanes from 10-deacetyl baccatin (10-DAB). Ojima-Holton coupling reaction of β-lactams with 10-DAB. *Taken and modified from Ojima et al., 2018.*

1.2.2 Microtubules

Microtubules appear in the microscope as large hollow tubes with a diameter of 25 nm that arise from the single-site microtubule organizing center (MTOC) near the nucleus in the interphasic cell. In contrast, microtubules grow from two spindle pole bodies in mitosis. Microtubules possess multiple roles in the eukaryotic cell, for example, the movement of whole organelles such as mitochondria, cell motility (as a component of the flagellum, cilia), forming cell shape and separation of daughter chromosomes during mitosis (**Figure 1.07**) (**Gudimchuk & McIntosh, 2021**).

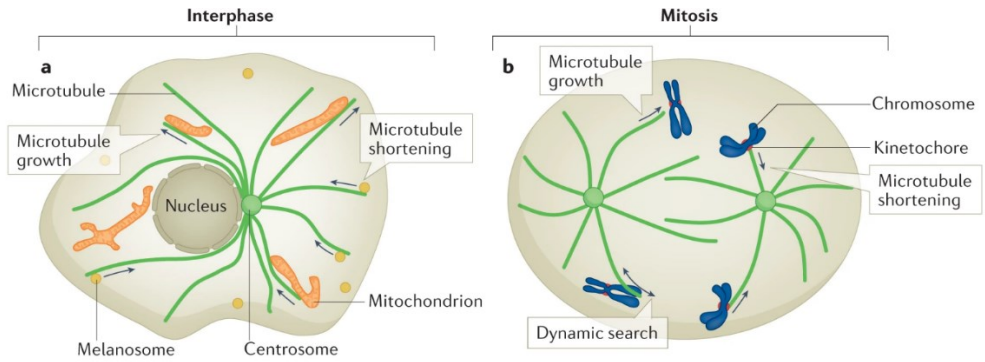

Figure 1.07 Visualization of microtubules in nondividing and dividing eukaryotic cell. *Taken from Gudimchuk & McIntosh, 2021.*

The basic unit of microtubule is a heterodimer of alpha and beta-tubulin (α- and β-tubulin), encoded by two separate genes (**Kavallaris, 2010**). There are nine genes for α-tubulin and ten for β-tubulin in a human genome with tissue-specific expression patterns (**Amargant et al., 2018**). Tubulin heterodimers assemble into protofilaments, and 13 protofilaments are parallelly organized into a microtubule.

Despite α- and β-tubulin sharing only 40% sequence homology, their overall fold is similar. The N-terminal domain of tubulin (1-206) acquires the Rossmann fold (six beta-strands and six alpha helices) essential for GTP binding. The GTP binding site in α-tubulin never hydrolyzes GTP and thus refers to "non-exchangeable" N-site. GTP hydrolysis occurs in "exchangeable" E-site in β-tubulin when the site is entirely formed by a newly incorporated tubulin heterodimer (**Orr et al., 2003; Nogales & Zhang, 2016**). The helices in the central domain (207-384) play an essential role in tubulins' longitudinal and lateral contact. Most lateral contacts occur between α-α and β-β subunits, except a seam (**Figure 1.08**). The C-terminal is less conserved between α-tubulin and β-tubulin and between tubulin isotypes. The C-terminal domain interacts with several microtubule-associated proteins (MAPs) and motor proteins like kinesins and dyneins. Tubulins are extensively modified by polyglutamylation, polyglycylation, acetylation, phosphorylation and tyrosination.

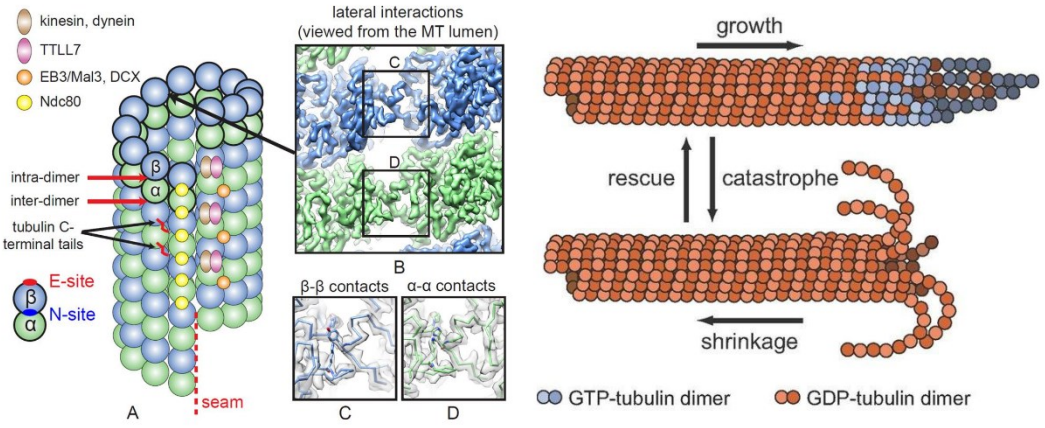

Figure 1.08 Microtubules and their dynamic behaviour. Tubulin dimers (αβ-tubulin) are basic units assembled into protofilaments. The left figure shows a detailed view of a seam in the microtubule. Microtubules can rapidly grow or shrink (right). The bending of protofilaments accompanies microtubule treadmilling. *Taken from Nogales & Zhang, 2016 (left) and Bowne-Anderson et al., 2013 (right)*.

PF is a polar structure; one end of PF ends with GTP-bound β-tubulin ("plus end") and the other end with GTP-bound α-tubulin ("minus end") (**Nogales & Zhang, 2016**). A straight GTP-α-tubulin/GTP-β-tubulin dimer can be incorporated, making a tiny GTP cap structure at the tip of the growing microtubule. Strong evidence indicates stabilizing function for GTP cap structure (**Gudimchuk & McIntosh, 2021**). Tubulin acquires straight conformation in the microtubule core, but GDP-bound tubulin dimer is curved, as seen in shrinking microtubules. GTP occupying the E-site is hydrolyzed after incorporation of heterodimer into the microtubule as α-tubulin of the other dimer completes the active catalytic site.

Microtubules are dynamic structures, stochastically oscillating between growth and shrinkage (**Mitchinson & Kirschner, 1984**). A catastrophe happens when a microtubule stops growth and initiates shrinkage, and rescue happens when a microtubule stops shrinkage and starts growth. Such a rapid oscillation is termed dynamic instability.

Two types of drugs interact with microtubules, microtubule-destabilizing and microtubule-stabilizing agents. The former represents vinca alkaloids (vinblastine, vincristine) or colchicine, and the latter represents taxanes (paclitaxel) and epothilones (epothilone B) (**McGrogan et al., 2008**).

1.2.3 Taxanes, taxoids and taxane-related compounds

More than 600 taxanes have been ascribed as yew tree metabolites. According to ring structure, taxanes are classified into 11 groups (**Lange & Conner, 2021**). Taxol® belongs to the group of taxanes with an oxetane ring and C-13 phenylisoserine side chain in the largest class of 6/8/6 ring taxanes, also referred to as normal taxanes (**Lange & Conner, 2021**).

As stated above, 10-deacetyl baccatin (10-DAB) is a presursor for synthesis of all taxanes in clinical use as well as for Stony Brook Taxanes (**Figure 1.09**).

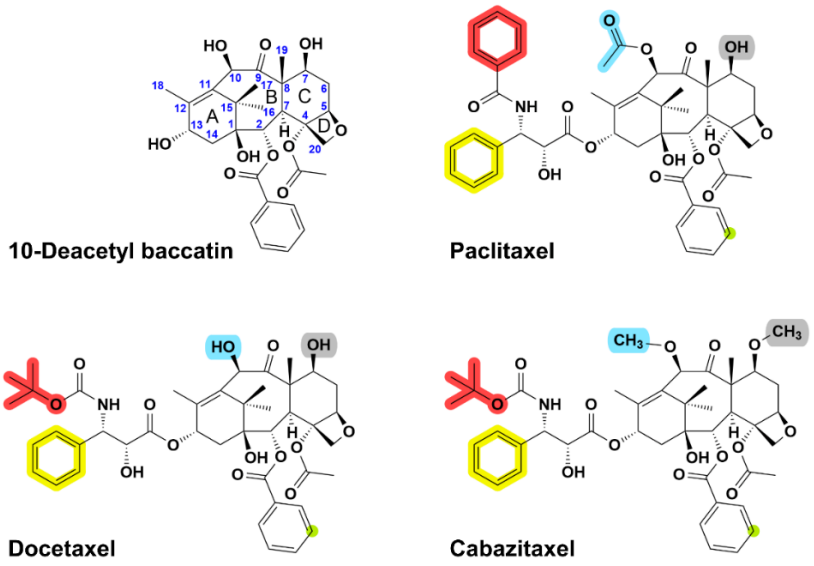

Figure 1.09 Structures of clinically-relevant taxanes. 10-Deacetyl baccatin (10-DAB) is an abundant metabolite in *Taxus* sp. (on the left). It is extracted and used for the semi-synthesis of paclitaxel (Taxol®, top right), docetaxel (Taxotere®, bottom left) and cabazitaxel (Jevtana®, bottom right). The C2, C3', C3'N and C10 positions are coloured by light green, yellow, red and light blue, respectively. *Based on Ojima et al., 2014*.

1.2.3.1 Paclitaxel (Taxol®)

Paclitaxel inhibits the process of microtubule depolymerization even upon destabilizing conditions like low-temperature or calcium (**Horwitz, 1992**). Microtubule dynamic instability is crucial for properly binding of microtubules to kinetochores and equal distribution of chromosomes into daughter cells (**Jordan et al., 1993**). Sustained metaphase/anaphase arrest induced by paclitaxel results into

activation of caspase-dependent cell death. However, gentle scenarios for cancer cells' fate, such as unequal division or premature escape from mitosis, continued in cell cycling arrest, large aneuploid cells or cell death (**Gascoigne & Taylor 2009**).

From chemical point of view, paclitaxel is a diterpene made of tricyclic 6/8/6 taxane ring (A-, B- and C-), one oxetane ring (D-ring), small flexible C2 (benzoyl group), C4 (acetyl group), C10 (acetyl group) side chains and large flexible N-benzoyl-(2R,3S)-phenylisoserine side chain attached at the C13 (**Hodge et al., 2009**) (**Figure 1.09**). Three carbon atoms in large side chain are labelled C1', C2' and C3'. The C3' position is branched into the phenyl group (C3') and benzoyl group (C3'N).

Horwitz and Schiff demonstrated that Taxol® interacts with the N-terminal domain of β-tubulin employing radio-labelled paclitaxel analogues (**Rao et al., 1992, 1994, 1995**). In consent, cryo-electron microscopy of Zn^{2+} stabilized bovine microtubules with T-shaped Taxol (T-Taxol®, butterfly Taxol(R)) proved these early results (**Löwe et al., 2001**). Rotational-echo, double-resonance nuclear magnetic resonance (REDOR-NMR) and further photoaffinity labelling revealed another biologically active Taxol conformer, REDOR-Taxol (**Sun et al., 2009**). In contrast to T-Taxol, REDOX-Taxol interacts at C2 with glycine 370 in a refined 1JFF structure (**Figure 1.10**). Of note, Taxol® binds to β-tubulin subunit in microtubules but not in soluble tubulin heterodimers in contrast to vinca alkaloids or colchicine (**Orr et al., 2003**).

Intravenous administration of Taxol solubilized in Cremophor EL (polyoxyethylated castor oil) and ethanol associated with robust side effects. The excipient Cremophor EL causes strong hypersensitive reaction (**Feng & Mumper, 2013**). To reduce Cremophor side effects, a novel formulation of Taxol, nab-paclitaxel (Abraxane®, nano-albumin bound paclitaxel), was developed, tested and approved for metastatic breast cancer by FDA (**Feng & Mumper, 2013**). Notwithstanding, common adverse effects of paclitaxel, such as alopecia, neutropenia (low number of neutrophils in blood) and neurotoxicity, persist (**Ojima et al., 2016**).

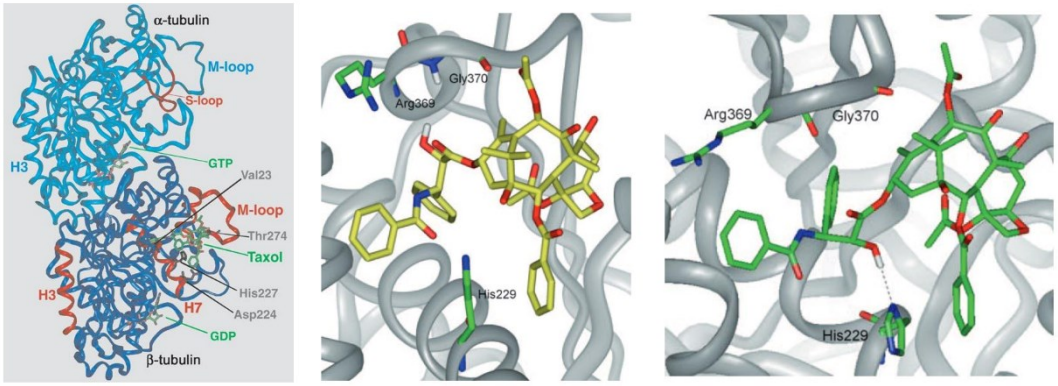

Figure 1.10 Interaction of Taxol® with β-tubulin. Taxol binding pocket is localized close to the E-site in the β-tubulin (left figure). Model of T-Taxol (yellow, middle) and REDOR-Taxol (green, right) binding to β-tubulin in refined structure 1JFF. *Taken from Orr et al., 2003 (left) and Ojima et al., 2014 (right)*.

1.2.3.2 Docetaxel (Taxotere®)

Taxotere® is a semisynthetic analogue of Taxol® bearing substituents at the C10 position (the hydroxyl group replaces an acetyl group) and at the C3' position (a *tert*-butoxycarbonyl group replaces the phenyl group) (**Figure 1.09**). The discovery of Taxotere® began when the Poitier exploited *Taxus baccata* plants that had to be chopped down to build a road on a local campus (**Guenárd et al., 1993**). Thus, the Potier group had enough material (leaves, bark, needles, wood) to find out that 10-deacetyl baccatin III (10-DAB) is a potent and more common constituent than Taxol® in needles of *T. baccata*. Poitier demonstrated that 10-DAB is unstable under acidic and basic conditions, whereas the hydroxyl group at the C-13 position is the most inert. During the semi-synthesis of Taxol® by hydroxyamination of 13-cinnamoyl derivative, the Poitier group used the *tert*-butoxycarbonyl group (t-BOC) to protect the aminogroup at the C-13 side chain due to t-BOC group can be readily removed under mild conditions.

The structure-activity relationship (SAR) studies demonstrated that Taxotere® is more potent than Taxol® in tubulin polymerization assay and dose-response assessment. In general, docetaxel seems to be weakly effective in cross-resistant cells than paclitaxel (**Ojima et al., 2008**). Docetaxel is used in combined therapy for breast cancer, gastric cancer, non-small cell lung cancer, prostate can-

cer and head and neck cancer (**Ojima et al., 2014**). Due to altered hydrophobicity, injectable docetaxel is solubilized in ethanol.

1.2.3.3 Cabazitaxel (Jevtana®)

The EU Commission approved Cabazitaxel (Sanofi-Aventis) for castration-resistant prostate cancer (CRPC) in early 2011 (**European Medicines Agency, 2023**). In addition to inducing a mitotic block, taxanes interact with androgen receptors (ARs), affecting the essential AR-signalling in prostate cells (**Darshan et al., 2011**). Better lipophilicity and reduced transport by membrane drug transporter are assumed to make cabazitaxel more effective than classical taxanes (**Vrignaud et al., 2014**). In CRPC patients, cabazitaxel is administered as a 1-hour lasting intravenous infusion (20-25 mg/m^2) every three weeks with daily 10 mg prednisone. In addition, cabazitaxel/ lapatinib has been tested in patients with metastatic HER2+ BC; however, this trial showed unclear results (**Yardley et al., 2018**).

Unlike docetaxel, cabazitaxel contains two methyl groups at the C7 and C10 positions (**Figure 1.09**). A common side effect of cabazitaxel is neutropenia, similar to other taxanes (**Villanueva et al., 2011**). Recently, 7,10-di-O-methylthiomethyl (MTM) cabazitaxel derivatives showed excellent potency against drug-resistant cells (**Ren et al., 2021**).

1.2.3.4 Stony Brook Taxanes

A vast number of studies have been devoted to the semi-synthesis of taxane derivatives (dubbed as "taxoids") and evaluating their potency against cancer and biological activity *in vitro* and *in vivo* (**Ojima et al., 2014**). As written below, some substitutions do not significantly improve potency of taxanes, whereas others do. Furthermore, substitutions can impact taxoids' capability to overcome drug resistance mechanisms *in vitro* and *in vivo*.

The nomenclature of some Stony Brook Taxanes (SB-T) reasonably follows the chemical composition of substituents (**Figure 1.11**). "SB-T" is an acronym for Stony Brook Taxane. The digits refer to specific functional groups. As Stony Brook Taxanes are, in fact, docetaxel analogues, the first digit is always

1 for the t-BOC group at the C3'N, the second and third digit label substituents at the C3' position, the digit at the fourth position labels substituent at the C10 position and the fifth and sixth positions label substituent at the C2 *para*-position.

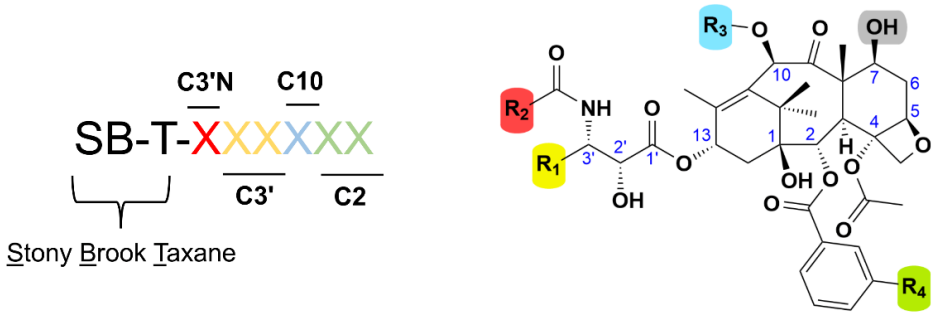

Figure 1.11 Stony Brook Taxanes (SB-Ts). A tentative nomenclature (on the left) and chemical formula of SB-T (on the right) are shown. Second-generation taxoids bear substituents at the C3'N (red), C3' (yellow) and C10 (light blue) positions, whereas third-generation taxoids are further modified at the C2 position (light green).

A less number of Stony Brook Taxanes have been derived from paclitaxel backbone reflecting better docetaxel pharmacokinetics. SB-T-0035 is a paclitaxel derivative with N,N-dimethylcarbamoyl group attached at the C10 (**Figure 1.12**) (**Jelínek et al., 2018**). Paclitaxel derivatives seldomly occur in literature, for instance, RAH-1 is a synonym for 3'-dephenyl-3'-(2-methyl-2-propenyl)paclitaxel (**Ojima et al., 1994a**). Macrocyclic paclitaxel derivatives abbreviated as SB-T-205X were used in structural studies (**Ojima and Das, 2009**).

The structure-activity relationship (SAR) studies with docetaxel derivatives concluded that the C3' phenyl group found in classical taxanes is not essential for their biological activity. A cyclohexyl group at the C3' has a comparable microtubule dissassembly activity (**Ojima et al., 1994b**). Substitution of the phenyl group by the isobutenyl group at the C3' position resulted in SB-T-1211 taxoid with slightly improved microtubule dissassembly activity, while retaining *in vitro* and *in vivo* cytotoxicity comparable to docetaxel (**Figure 1.12**) (**Ojima et al., 1994a**).

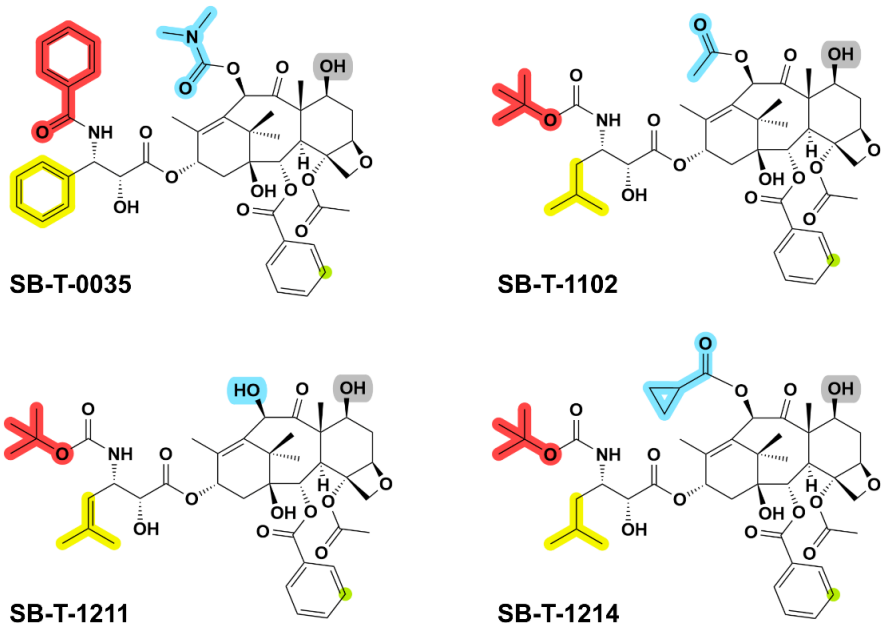

Figure 1.12 Chemical formulas of SB-T-0035 taxoid and second-generation taxoids SB-T-1102, 1211 and 1214. SB-T-0035 is a paclitaxel derivative with N,N-dimethyl-carbamoyl substituent at the C10 position. Taxoid 1102 bears the 3'-isobutyl group, whereas taxoids 1211 and 1214 bear the 3'-isobutenyl group (marked by yellow). Taxoids 1211 and 1214 differ by substituents at the C10 position (marked by light blue).

Taxoid SB-T-1212 is a highly potent chimeric derivative bearing an acetyl group at the C10 position as paclitaxel, a *tert*-butoxycarbonyl group at the C3'N as docetaxel and an isobutenyl group at the C3' position (**Figure 1.13**). Furthermore, doxorubicin-resistant MCF-7/R cells were not cross-resistant to SB-T-1212 (**Ojima et al., 1994a**).

Following SAR study evaluated whether substitutions at the C10 position in 3'-isobutyl (SB-T-110X) and 3'-isobutenyl (SB-T-121X) taxoids modify drug potency against drug-sensitive and drug-resistant cancer cells (**Figure 1.13**) (**Ojima et al., 1996**). Replacement of the hydroxyl group at the C10 position by *n*-propanoyl (SB-T-1213) or cyclopropylcarbonyl (SB-T-1214) improved anti-tumour activity (**Figure 1.12**). Significantly, taxoid SB-T-1213 showed *in vivo* better antitumour activity than docetaxel. The third most toxic taxoid SB-T-1102 bears an acetyl group at the C10 position.

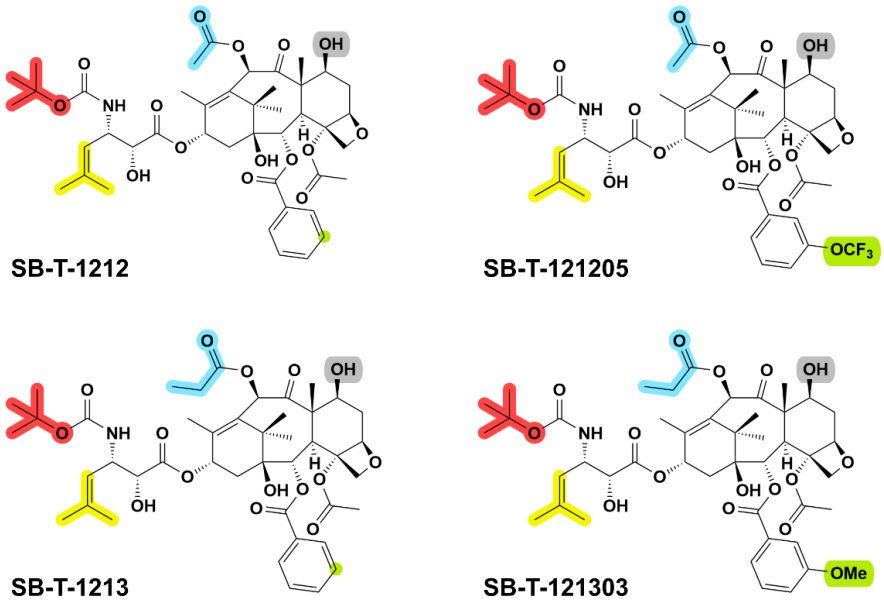

Figure 1.13 Third-generation taxoids are modified at the C2 benzoate position. Third generation taxoids SB-T-121205 and SB-T-121303 and their C3'- and C10-modified precursors SB-T-1212 and SB-T-1213 are shown for comparison. The C3', C3'N, C10 and C2 positions are highlighted by red, yellow, light blue and light green, respectively.

Aromatic groups, in particular, 4-methoxybenzoyl, 3-methoxybenzoyl and 3-(3-methoxyphenyl)propanoyl placed in acyl moiety at the C10 position in 3'-isobutenyl also resulted in highly potent taxoids with similar cytotoxicity in LCC6 and LCC6-MDR cells (the ratio IC_{50} resistant to sensitive cells, R/S = 1), (**Ojima et al., 2008**). These potent derivatives have been named *second generation taxoids*.

Early experiments with substituents (MeO, F, Cl, N_3, $CH{=}CH_2$) introduced at the meta position of C2 benzoate revealed that C2-fluoride taxoids are extremely toxic to drug-sensitive LCC6 cells and C2-methoxy taxoids exhibit better antitumour activity (R/S ≤ 1) in drug-resistant MCF-7 and LCC6-MDR cells (**Ojima et al., 1999**). Same substituents at the C2 position have been broadly investigated in a series of C3', C3'N and C10 derivatives (**Ojima et al., 2006**). The most potent derivative was SB-T-121303 (R/S = 0.9). The extremely potent compounds with modifications at the C3', C3'N, C10 and C2 positions have been dubbed third generation taxoids. Probably explanation for high potency of C2 derivatives is that

this site is recognized by cytochrome 450 oxidases as well as modifications increased affinity to β-tubulin.

Recently, C2 derivatives bearing OCF_3 and $OCFH_2$ CH_3 groups have been studied in same cell models as previous (**Wang et al., 2020**). Of note, $OCFH_2$ group can adopt various conformations with respect to polar and non-polar environment, thereby improving membrane permeability of the drug. Indeed, toxicity of taxoids decrease in the order $OCFH_2$> OCF_3> CH_3. Both $OCFH_2$ and OCF_3 groups interact by van der Waals interaction with Leu230 and Leu275 residues in β-tubulin (**Wang et al., 2020**).

1.3 Resistance to taxanes

The development of taxane resistance in cancer cells is a complex and multifactorial process involving various molecular mechanisms (**Figure 1.14**).

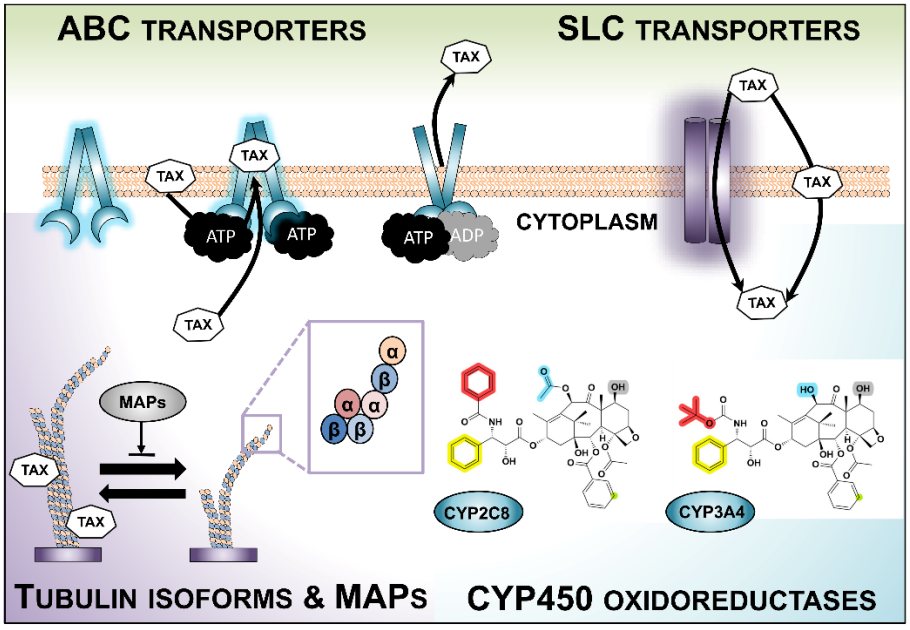

Figure 1.14. Mechanisms of taxane resistance in cancer cells. Hydrophobic taxanes easily pass through the lipid bilayer. Taxanes bind at the inner surface of assembled microtubules in the cell, promoting microtubule stabilization. In the plasma membrane, special transporters pump taxanes out of the cell (ABC transporters) or can facilitate taxane transport into the cell (SLC transporters). Microtubule-associated proteins (MAPs) and tubulin isoforms can also influence taxane resistance. Heme-containing cytochrome p450 oxidoreductases metabolize taxanes specifically.

1.3.1 Resistance associated with membrane transporters

Plasma membrane-associated transporters represent a major barrier to anti-cancer drugs. The plasma membrane is the first structure interacting with a drug. Members of the *solute carrier* (SLC) and *ATP-binding cassette* (ABC) transporters have been recognized as essential modulators of taxane sensitivity in cancer cells (**Robey et al., 2018; Girardi et al., 2020**).

1.3.1.1 SLC transporters

SLC transporters (458 genes in 65 families) participate in the movement of a broad range of substrates, i.e. macronutrients (sugars, vitamins, amino acids, nucleosides) and micronutrients (metal cations) across membranes. Moreover, recent investigations foster SLC transporters as important drug pharmacokinetics modulators. SLC transporters do not utilize ATP hydrolysis. Instead, they work as secondary active transporters and ion channels (**Colas et al., 2016**; **Pizzagalli et al., 2021**).

Silencing of *SLC31A2*, *SLC35A5*, and *SLC41A2* expression led to increased paclitaxel susceptibility in lymphoblastoid cell lines, suggesting that they can facilitate paclitaxel uptake (**Njiaju et al., 2012**). NGS revealed significant down-regulation of *SLCO1B3* expression (also known as *OATP8*) in a prostate cancer patient-derived xenograft model with acquired resistance to docetaxel. Silencing of *SLCO1B3* impaired the uptake of docetaxel and cabazitaxel (**de Morreé et al., 2016**). CRISPR-Cas9 library screen predicted a few SLC transporters being associated with paclitaxel and docetaxel resistance (**Girardi et al., 2020**). In the case of paclitaxel, but not docetaxel, *MTCH2*-specific sgRNA was found to be most enriched. It was recently found that MTCH2 (mitochondrial carrier 2) acts as an insertase of helical proteins into the outer mitochondrial membrane (**Guna et al., 2022**). However, how MTCH2 contribute to drug resistance is not clear.

1.3.1.2 ABC transporters

All living organisms harbour genes for ABC transporters in their genomes. Fourty-eight ABC transporters in seven subfamilies (ABCA-G) and 22 pseudogenes have been described in humans (**Piehler et al., 2008**). Nearly all ABC trans-

porters encompass two highly conserved *nucleotide-binding domains* (NBDs) and two less-conserved *transmembrane domains* (TMDs) in that a substrate is bound and transferred (**Robey et al., 2018; Thomas & Tampé, 2020**).

The unifying feature of ABC transporters is the dependence on ATP consumption to move the substrates in both ways (importers and exporters). The binding of ATP-Mg^{2+} into NBD ultimately evokes a switch between inward-facing (IF) and outward-facing (OF) conformation via occluded and collapsed states. Walker A and Walker B motifs, two loops (Q-loop, D-loop) and H-switch in the highly conserved *RecA ATP-binding core coordinatively contact with ATP molecule*, while Mg^{2+} is positioned by the ABCβ subdomain A-loop (**Figure 1.15**). Inserting the signature motif into the occupied ATP-binding site of other NBD promotes NBD dimerization coupled with significant structural changes in all 12 transmembrane helices and outward-facing conformation. NBD dimer disintegration, induced by ATP hydrolysis, moves back conformation to inward facing. Interestingly, due to NBD1 and TMD1 being akin to NBD2 and TMD2 in most transporters, asymmetric cleavage of ATP occurs standardly (**Thomas & Tampé, 2020**).

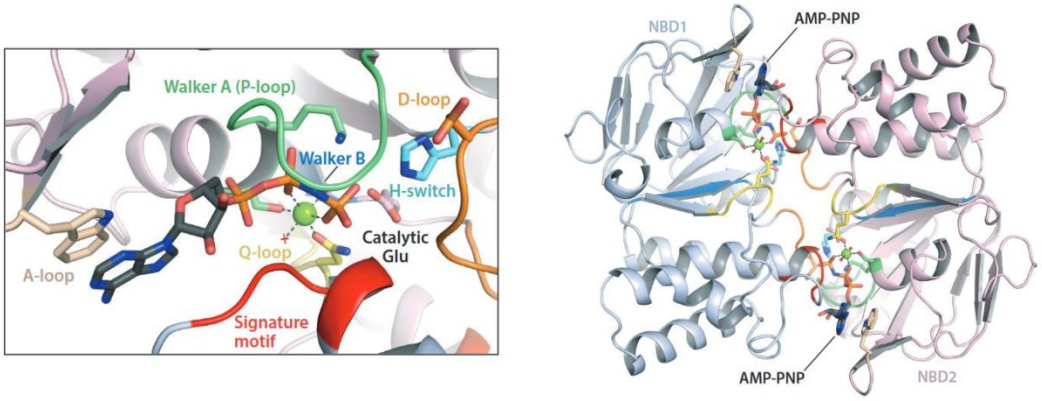

Figure 1.15 Models of ATP-Mg^{2+} positioning in the nucleotide-binding domain (NBD) and dimer formation. Binding of nonhydrolyzable AMP-PNP into NBD of MalFGK2 maltose transporter (left). NBD1 (grey) and NBD2 (light pink) form a dimer structure. A signature motif (visualized as a red line) of each NBD forms the nucleotide-binding site of other NBD. *Taken and modified from Thomas & Tampé, 2020*.

ABCB1 (also known as *MDR1*, multidrug resistance 1, 7q21.12, 1280 amino acids) encodes a 170-kDa glycosylated protein, P-glycoprotein (P-gp, permeable glycoprotein) that occupies the apical membrane of polarized cells in the bowel, kidney and liver and endothelial cells of the blood-brain barrier. As a cell guardian, ABCB1 extrudes an overwhelming number of toxins. Consequently, this protein is responsible for the poor intake of orally-administered clinically relevant drugs. This was discovered in colchicine-resistant Chinese hamster kidney cells and attributed to multidrug resistance phenotype in these cells (**Robey et al., 2018**).

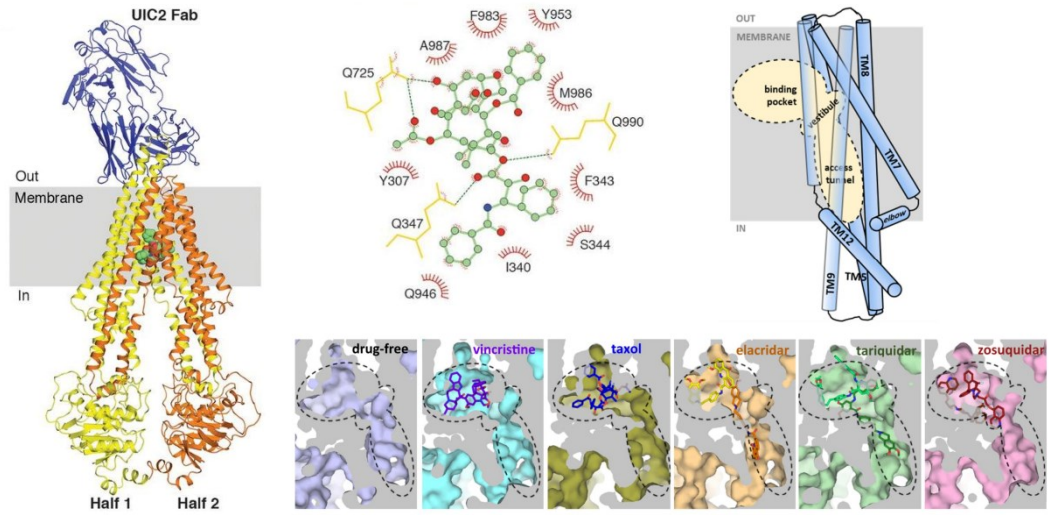

Figure 1.16 Structure of human ABCB1 multidrug transporter with paclitaxel, vincristine and inhibitors (zosuquidar, elacridarm tariquidar). Model of UIC2-FAb stabilized human ABCB1 with paclitaxel (left). Residues interacting with paclitaxel in occluded conformation (up, middle). Schematic view of the position of the binding pocket, vestibule and access tunnel found in occluded conformation (up, right). One molecule of taxol or vincristine is bound to the binding pocket, whereas two molecules of inhibitors occupy the binding pocket, vestibule and access tunnel (bottom right). Noteworthy, tariquidar and elacridar adopt and bind as conformers. *Taken and modified from Alam et al., 2019 and Nosol et al.,2020.*

Inward-facing apo and holo structures of mouse ABCB1 transporter that shares 87 % homology in amino acid sequence to human ABCB1 revealed a large 6000Å cavity in TMD with multiple binding sites (**Aller et al., 2009; Li et al.,**

2014). Recently, a series of UIC2-FAb stabilized chimeric human-mouse or human ABCB1, and MRK16-Fab stabilized human ABCB1 structures in apo or holo occluded conformations were published (**Alam et al., 2018, 2019; Nosol et al., 2020**). Notably, paclitaxel, vincristine, and third-generation inhibitors (zosuquidar, elacridar, tariquidar)-bound ABCB1 models revealed a mechanism of inhibition and residues interacting with paclitaxel in drug binding pocket (**Figure 1.16**). The access tunnel narrows in occluded conformation, effectively enclosing paclitaxel in the drug-binding cavity. A suggestion is that paclitaxel can reach the binding cavity from the inner leaflet of the membrane in an inward-facing conformation (**Nosol et al., 2020**).ABCB4 (*MDR3,* 7q21.12, 1286 amino acids) is primarily localized to the canalicular membrane of hepatocytes where transports of phosphatidylcholine from the inner to the outer leaflet of the membrane, a process that is critical for the formation of bile (**Groen et al., 2011**). Besides, ABCB4 is overexpressed with ABCB1 in drug resistant cells. ABCB4 is understood in term of paclitaxel-resistance. However, ABCB4 transporter was reported with mild reversal of resistance to paclitaxel in SK-OV-3 ovarian cells (**Duan et al., 2004**) and one study demonstrated a reduced paclitaxel uptake by F165I and S320F mutants (**Kim et al., 2013**).

ABCC2 (also known as *MRP2*, multidrug resistance protein 2, 10q24.2, 1545 amino acids) is localized on the apical membrane of kidney, liver and intestine cells (**citation**). ABCC2 transporter is involved in the eflux of endogenous substrates such as glutathione, glucurate and sulfate conjugates as well as variety of xenobiotics (**Nies & Keppler, 2007**). In particular, MDCKII cells stably transfected with human ABCC2 transporter are resistant to paclitaxel (**Huisman et al., 2005**). Experiments with *Mrp2*$^{-/-}$, *Mdr1a/1b*$^{-/-}$, and *Mdr1a/1b/Mrp2*$^{-/-}$ mice models revealed that ABCC2 transporter is crucial for billiary excretion of paclitaxel *in vivo* (**Lagas et al., 2010**).

ABCG2 transporter (also known as breast cancer resistance protein, BCRP, 4q22.1, 655 amino acids) reduces bioavailability of several chemotherapeutics including mitoxantrone and tyrosine kinase inhibitors (**Toyoda et al., 2019**). Co-selection of doxorubicin with ABCB1 inhibitor verapamil led to generation of mulidrug resistant MCF-7/AdrVp cells that were weakly cross-resistant to vinca

alkaloids and paclitaxel (**Doyle et al., 1998**). Physiological role for ABCG2 as urate transporter was independently reported by two research groups (**Matsuo et al., 2009; Woodward et al., 2009**). Structure of human ABCG2 was deciphered by Cryo-EM (**Taylor et al., 2017**).

1.3.2 Resistance associated with microtubules

Several observations promote increased microtubule dynamics as one mechanism for how a cell can acquire resistance to taxanes. Concomitantly, increased microtubule dynamics might explain why some paclitaxel-resistant cells exhibit dependency on paclitaxel, i.e., their growth is inhibited when placed into drug-free medium. Microtubule dynamics is seen as an interplay between tubulin isotypes, alterations, and microtubule-associated proteins (MAPs) (**Orr et al., 2003; Parker et al., 2017**).

Alterations in α-tubulin can induce resistance to taxanes. One study reported that overexpression of k-α1-tubulin (encoded by *TUBA1B*) in drug-selected A549 lung cells. (**Han et al., 2000**). Tyronisated alpha tubulin isoforms, like k-α1-tubulin have been shown to increase microtubule dynamics. In particular, βIII-tubulin (*TUBB3*) expression induce taxane-resistance in selected cell lines (**Kavallaris et al., 1997**).

In general, mutations in drug target can induce resistance in cancer by perturbating drug-target interaction. Truly, mutagenesis of five aminoacids (K19A, V23T, D26G, H227N and F270Y) resensitise yeast to Taxol® (**Gupta et al., 2003**). However, single mutations in beta tubulin likely affect microbutule dynamics rather than Taxol® binding. Mutations in β-tubulin that can confer resistance to taxanes occur throughout the gene as not single domain contribute to lateral and longitudinal contacts. Taxol®-resistant human cell models possess several single base substitutions, particularly D26E, A173P, E292Q, and C422Y (**Orr et al., 2003, Hari et al., 2006**). The D26E mutation has been localized to paclitaxel-binding site (**Hari et al., 2006**).

Microtubule dynamics is further regulated by several microtubule interacting proteins named MAPs. Relevant to paclitaxel resistance, protein tau (coded by *MAPT*, microtubule associated protein tau, 17q21.31) and stathmin (*STMN1*,

1p36.11) have been discussed (**McGrogan et al., 2008**). Tau protein, whose expression is specific to neuronal cells, encourages microtubule stabilization by binding to paclitaxel-binding site at the inner surface of assembled microtubule (**Smoter et al., 2011**). In contrast, destabilization of microtubule at the plus end by Stathmin is pH-dependent and is pivotal for regulation of microtubule length during mitosis (**Andersen, 2000**).

1.3.3 Resistance associated with cytochrome P450 enzymes

Cytochrome p450 (CYPs) superfamily of oxidoreductases are neccessary for hepatic clearance of drugs and toxins (**McDonnell and Hang, 2013**). Based on their aminoacid sequence similarity, 57 human genes and 58 pseudogenes for CYP450 enzymes are categorized into 18 families (assigned by number chronologically by time of their discovery) and subfamilies (assigned by letter) (**Manikandan and Nagini, 2018**). Regarding pharmacological interactions, CYP1, CYP2, CYP3 and CYP4 families are of major research concern. Some CYP450 enzymes are also expressed by cancer cells (**Nebert et al., 2013**).

Drugs can be inducers of CYP450 expression, inhibitors of CYP450 function or can be substrates for CYP450 (**McDonnell and Hang, 2013**). Taxanes concomitantly induce and are metabolized by liver microsomal CYP450 enzymes to non-toxic products (**Cresteil et al, 2002**). For instance, paclitaxel is primarily metabolized by CYP2C8 (10q23.33) to 6α-hydroxypaclitaxel and less frequently by CYP3A4 (7q22.1) to 3'-hydroxypaclitaxel (**Wang et al., 2014**). Docetaxel is metabolized by CYP3A4 at the C3'N *tert*-butoxycarbonyl group (**Cresteil et al., 2012**). In line with these results, ectopic expression of CYP3A4 confer resistance to docetaxel but not to paclitaxel (**Hofman et al., 2021**). Stony Brook Taxanes are metabolized not at the tert-butoxycarbonyl group but on the isobutyl or isobutenyl group by CYP3A4 (**Gut et al., 2006**).

Increase expression of CYP450 enzymes is hypothesised to be involved in taxane resistance *in vivo* (**Hofman et al., 2021**) Studies devoting to expression of CYP3A4 and CYP2C8 enzymes in breast cancer tissue produced mixed results (**van Eijk et al., 2019**). It is suggested that about 30-50% of breast tumor samples express CYP450 enzymes. Curiously, high expression of CYP3A4 in breast can-

cer associates with better survival rate (**Murray et al., 2010**). However, primary site of taxane detoxification in organism is outside of breast tumor tissue.

2. AIMS

The PhD thesis covers several intertwined scientific papers concerning taxane resistance in breast cancer cells. Considerable efforts were devoted to following tasks:

- What underpins acquired taxane resistance in established breast cancer cell line models (paper 1 and paper 3).
- What mechanisms contribute to enhanced ABCB1 and TRIP6 expression in taxane-resistant breast cancer cells (paper 4).
- How one would overcome acquired drug resistance to taxanes in cultured breast cancer cells (paper 2).

To accomplish these tasks, we generated a few models of drug-resistant breast cancer cell lines. We adapted MCF-7 breast cancer cell line (luminal A, ER-positive, *PIK3CA* E545K, *CASP3* -/-) to cell-death induction level of paclitaxel (300 nM) and to cell-death induction level of Stony Brook Taxane 0035 (SB-T-0035) compound (300 nM). We have also established SK-BR-3 (HER-enriched, TP53 mut) breast cancer subline resistant to cell-death induction level (100 nM).

We did most of the work with taxane-resistant MCF-7 sublines derived from the original taxane-sensitive parental MCF-7 cells. The findings enable us to compare both models to discern between common mechanism of taxane resistance and taxane-specific mechanism of resistance.

3. RESULTS AND COMMENTS

3.1 Paper 1

Characterization of acquired paclitaxel resistance of breast cancer cells and involvement of ABC transporters

In the first publication, we characterized MCF-7/PacR and SK-BR-3/PacR breast cancer cells with acquired resistance to paclitaxel. We applied a stepwise selection to an increased dose of the drug up to a concentration that is lethal to sensitive cells, i.e., 300 nM for MCF-7 cells and 100 nM for SK-BR-3 cells (**Němcová-Furstová et al., 2016**; **Jelínek et al., 2018**) (**chapter 4.1, page 59**). Since the selection procedure impacts the resistance mechanism (**Gottesman, 1998**), we expected to work with a heterogeneous population of highly resistant cells.

Acquired resistance to taxanes is notoriously linked to ABCB1 transporter (**Calcagno & Ambudkar, 2010).** Thus, we begin with assessing the expression of all human ABC transporters by real-time quantitative reverse transcription PCR with SYBR green. In both taxane-resistant cells, we identified upregulation of *ABCB1*, *ABCB4* and *ABCG2* transporters and downregulation of *the ABCC1 transporter*. Cell line-specific alterations were such as *ABCC7* (upregulated in MCF-7/PacR), *ABCC8* (downregulated in MCF-7/PacR) and *ABCC9* (upregulated in SK-BR-3) (**chapter 4.1, page 62**). In addition, the *ABCC2* transporter was altered in both resistant cells but upregulated in MCF-7/PacR and downregulated in SK-BR-3/PacR cells at the mRNA level (**chapter 4.1, page 62**).

We aimed to validate the protein expression of altered ABC transporters by modified immunoblotting protocol (**Kaur & Bachhavat, 2009**). In MCF-7/PacR cells, we showed upregulated expression of ABCB1, ABCB4, ABCC2 and ABCC3 transporters. These transporters confer resistance to paclitaxel (**Duan et al., 2004; Gao et al., 2014; Huisman et al., 2005; McCorkle et al., 2021; O'Brien et al., 2008**). In SK-BR-3/PacR cells, we found upregulated ABCB1, ABCG2, ABCC3, and ABCC4 transporters (**chapter 4.1, page 63**). Among them, ABCC4 is not considered to be able transport taxanes (**Tian et al., 2005**).

The findings point at ABCB1 and ABCC3 multidrug transporters in resistance to paclitaxel. Confocal microscopy revealed that all paclitaxel-resistant MCF-7/PacR and SK-BR-3/PacR cells uniformly express membrane-localized ABCB1 transporter (**chapter 4.1, page 65)**.

Silencing of *ABCB1* expression in paclitaxel-resistant breast cancer cells cultured with paclitaxel for 96 hours reduced the number of viable MCF-7/PacR cells to about 40% (**chapter 4.1, page 64)**. This finding suggest either an ABCB1-independent mechanism of resistance or that the cells expressed ABCB1 in such a level that is under the detection limit of the Western blot method (**Maloney et al., 2020**).

3.2 Paper 2

Substituents at the C3' and C3'N positions are critical for taxanes to overcome acquired resistance of cancer cells to paclitaxel

By employing MCF-7 and SK-BR-3 paclitaxel-resistant sublines, we tested the ability of Stony Brook Taxanes (SB-T) modified at the C3' and C3'N to overcome ABCB1-mediated drug resistance. Substituting the C3' phenyl group with alkyl and alkenyl groups in docetaxel gave more potent antitumour agents (**Ojima et al., 1994a**). Furthermore, certain C10 modifications can further increase the potency of SB-Ts (**Ojima et al., 1996**).

Ojima uses the R/S value, i.e. the ratio of resistant IC_{50} to sensitive IC_{50}, to compare the efficiency of SB-Ts in overcoming resistance (**Ojima et al., 1994a, 1994b, 1996, 2008, 2020**). Compared to classical taxanes, dose-response curves of SB-Ts differ in slope (**chapter 4.2, pages 76-78**). Hence, we use the C_{0RES}/C_{0SEN} value to compare the potency of taxanes to overcome ABCB1-mediated resistance, where C_0 is the drug concentration in that the number of cells is equivalent to the number of seeded cells after 96 hours of cultivation with SB-Ts.

Moreover, Ojima occasionally compared MCF-7 cells with NCI/ADR cells or doxorubicin-resistant MCF7/R cells (**Ojima et al., 1999**). After an intensive debate about the origin of NCI/ADR cells, they are now supposed to come

from OVCAR-8 cells but not MCF-7 cells, as it was previously mentioned (**Liscovitch & Ravid, D., 2007**).

The other source of data inconsistency might be that MCF-7 and SK-BR-3 breast cancer cells undergo caspase-dependent cell death upon taxane exposition (**Jelínek et al., 2015**). In MCF-7 cells, activated caspase-2 and other caspases participate in cell death induced by taxanes (**Jelínek et al., 2013**). We have not detected caspase-3 expression in used MCF-7 cells, likely due to a 47-base pair deletion within exon 3 (**Jänicke et al., 1998**). The expression of caspase 3 has a profound impact on cell sensitivity to drugs. For example, the restoration of caspase 3 sensitizes MCF-7 cells to drugs (**Yang et al., 2001**).

A number of papers demonstrated caspase 3 expression in MCF-7 cells, including the SB-Ts paper (**Zheng et al., 2017**). Cross-resistance of used primary antibodies is a significant source of caspase 3 detection in MCF-7 cells (**Jänicke, 2009)**. However, caspase 3 expression can also mark cross-contamination of MCF-7 cell line. Therefore, comparing results obtained in MCF-7 cells should be carefully interpreted.

We organized SB-Ts into three groups based on the substituents at the C3' and C3'N positions. Group 1 comprises 3'N-phenyl, 3'-phenyl taxanes such as paclitaxel, group 2 comprises 3'N-*tert*-butoxycarbonyl (*t*-BOC), 3'-phenyl taxanes such as docetaxel and group 3 comprises 3'N-*t*-BOC and 3'-isobutyl/isobutenyl derivatives (**chapter 4.2, page 74**).

Substituents at the C3' and C3'N positions had no substantial effect on the antitumour activity of derivatives in sensitive cells. However, as a rule, they enhanced the capability of derivatives to overcome paclitaxel resistance in the order group 1<group 2< group 3 (**chapter 4.2, page 78**). That is quite a different finding than found in the literature. For example, docetaxel (group 2) exhibited worse activity than paclitaxel (group 1) measured by R/S value (**Ojima et al., 1994b, 1996, 1999**). However, toxicity and R/S value were similar for paclitaxel and docetaxel in LCC6 versus ABCB1-transduced LCC6 cell lines (**Ojima et al., 1999**).

Furthermore, substituents at the C10 position inconsiderably affected the C_0 value (**chapter 4.2, page 78**). For example, 10-deacetyl paclitaxel was less

potent in MCF-7 cells but similarly effective as both SB-T-0035 and 10-deacetyl paclitaxel in overcoming drug resistance as paclitaxel. For group 3 of derivatives, a carbamoyl group at the C10 position made SB-T-1216 taxoid less toxic to MCF-7 and SK-BR-3 sensitive cells but two-fold more potent in overcoming resistance than SB-T-1211 (**chapter 4.2., page 78**). By contrast, SB-T-1216 was more toxic but less potent in overcoming resistance in doxorubicin-resistant MCF7/R cells (**Ojima et al., 1996**).

On the other hand, SB-T-1102 and SB-T-1214 taxoids were the most toxic in MCF-7 sensitive cells and efficiently overcame resistance to paclitaxel. In general, taxoids SB-T-1102, SB-T-1214, and SB-T-1216 were the most potent in drug-sensitive and drug-resistant cells. A similar conclusion with SB-T-1214 taxoid was reported (**Ojima et al., 1996**).

We hypothesize that taxoids lacking two phenyls, exemplified by SB-T-1216 taxoid, is a poor substrate for ABCB1. Firstly, we showed that SB-T-1216 weakly stimulated the ATPase activity of human recombinant ABCB1 transporter *in vitro* compared to paclitaxel. Secondly, we docked taxanes and SB-Ts into a human ABCB1 model derived from a mouse inward-facing ABCB1 structure. Fortunately, a human Cryo-EM structure of paclitaxel-bound ABCB1 protein in occluded conformation was published in the following years (**Alam et al., 2019; Nosol et al., 2020**). The published Cryo-EM structure differs in the orientation of paclitaxel. In the occluded conformation, paclitaxel is rotated from the vertical axis 180 degrees against our model and interacts with Q347, Q725 and Q990 residues (**chapter 1.3.1.2, page 40**). Our modelling study predicted the interaction of paclitaxel with Q945 and S337 residues in ABCB1 (**chapter 4.2, page 81**).

Notwithstanding, average docked scores calculated from the ten most probable docking poses in the ABCB1 binding cavity well elucidate the biological activity of SB-Ts (**chapter 4.2, page 81**).

The process of taxanes and taxoid transport through the access tunnel to the binding cavity can be more important than the binding affinity of paclitaxel and SB-Ts in the ABCB1 binding cavity (personal communication with Engr Jiří Černý, BIOCEV).

3.3 Paper 3

Differentially Expressed Mitochondrial Proteins in Human MCF7 Breast Cancer Cells Resistant to Paclitaxel

We asked whether another alteration in gene expression in paclitaxel-resistant breast cancer cells exists that would contribute to the resistant phenotype. In previous research, suspect proteins have been found by two-dimensional polyacrylamide gel electrophoresis (2-D PAGE) on whole-cell lysates from paclitaxel-resistant SK-BR-3/PacR cells (**Pavlikova et al., 2014**) and MCF-7/PacR cells (**Pavlíková et al., 2015**). However, low resolution, absence of low abundant proteins and mild solubilization conditions limit 2-D PAGE analyses (**Issaq & Veentra, 2008**).

Therefore, we assumed that cell fractionation could moderately circumvent these obstacles. We focused on mitochondrial proteome as the mitochondria are crucial in regulating cell death and metabolism, which can be altered in drug-resistant cells (**Fernie et al., 2004**; **Tait & Green, 2013**). To do this, we tested two commercially available kits. The QProteome Mitochondria Isolation Kit from Qiagen gave more pure fraction of undamaged mitochondria, demonstrating that the Qiagen kit was eligible for mitochondrial proteomics (**chapter 4.3, page 87; chapter 5.1, page 129**). Notwithstanding, we identified mitochondrial carbamoyl phosphate synthase I (*CPSI*, 2q34) overexpression in 2-D PAGE in both mitochondrial preparations (**chapter 4.3, page 88; chapter 5.1, page 130**).

In 2-D PAGE gels, we found significantly increased spot volumes for mitochondrial carbamoyl-phosphate synthase I (*CPS1*, 2q34) and mitochondrial ATPase family AAA domain-containing 3A and 3B (*ATAD3A*, *ATAD3B*, 1p36.33). On the other hand, we found decreased spot volumes for putative mitochondrial protein abhydrolase domain containing 11 (*ABHD11*, 7q11.23) and lysosomal cathepsin D (*CTSD*, 11p15.5). As cathepsin D is a lysosomal protease, we infer the latter finding reflected contamination of mitochondrial fraction by lysosomes (**Benes et al., 2008**).

An astonishing finding was a five-fold upregulation of the rate-limiting enzyme of the urea cycle, CPS1, in paclitaxel-resistant MCF-7/PacR cells. CPS1

expression is restricted to intestinal and hepatic cells but not non-tumour breast tissue (**Weerasinghe et al., 2014**). In cancer, elevated CPS1 expression in lung adenocarcinoma cell lines CPS1 reflects inactivating mutations in tumour suppressor liver kinase B1 (*LKB1*, known as serine-threonine kinase 11, *STK11*, 19p13.3) that strictly suppresses CPS1 via AMPK (**Kim et al., 2017**).

The physiological function of CPS1 is to convert ammonia to carbamoyl phosphate in the urea cycle in non-cancerous liver cells (**de Cima et al., 2015**). Therefore CPS1 function relative to cancer might be confusing. However, intensive research shed light on how the availability of metabolites for chromatin-modifying enzymes influences epigenetics (**Kinnaird et al., 2016**).

Cytosolic carbamoyl-phosphate, generated by carbamoyl-phosphate synthetase 2 (CAD, 2p23.3) can serve as a precursor for pyrimidine synthesis (**Li et al., 2021**). Although the pools of mitochondrial and cytosolic carbamoyl-phosphates are not linked, under specific conditions, the mitochondrial pool of carbamoyl-phosphate can replace the cytosolic pool (**Wraith, 2001**). Therefore, the role of mitochondrial CPS1 is not fully ascribed in cancer cells.

Furthermore, we looked into the cellular localization of CPS1 and found that CPS1 colocalized with diablo IAP-binding mitochondrial protein (DIABLO, 12q24.23). However, we observed heterogeneity in the expression of CPS1 in both MCF-7 and MCF-7/PacR cells (**chapter 4.3, page 91**). The population of CPS1 highly-expressing cells increased in paclitaxel-resistant MCF-7/PacR cells. Silencing of CPS1 in MCF-7/PacR cells did not affect resistance to paclitaxel, but a high number of CPS1-negative cells certainly biased this result.

Furthermore, in the MCF-7/0035R cells, the change in CPS1 expression was not observed (**chapter 5.1, page 130**). Hence, we suggest that CPS1 overexpression arose as genetic drift and is not associated with taxane resistance.

ABHD11 is a mitochondrial enzyme with downregulated expression in MCF-7/PacR cells. ABHD11 regulates the catalytic activity of 2-oxoglutarate dehydrogenase by lipoylation of the DLST subunit (**Bailey et al., 2020**). There is no evidence in the literature that ABHD11 is linked to paclitaxel resistance. In contrast, we found upregulated ABHD11 expression in Stony Brook Taxane

0035-resistant MCF-7/0035R subline (**chapter 4.3, page 90, chapter 5.2, page 131**), indicating that is likely not essential in resistance to taxanes.

3.4 Paper 4

ABCB1 Amplicon Contains Cyclic AMP Response Element-Driven TRIP6 Gene in Taxane-Resistant MCF-7 Breast Cancer Sublines

We noticed that the genes proximal to chromosome 7 centromere, such as *ABHD11 and HSPB1*, were downregulated in the MCF-7/PacR subline. Conversely, expression of genes distal to chromosome 7 centromere, such as *ABCB1*, *ABCB4*, *TRIP6 and ABCC7*, were upregulated in MCF-7/PacR subline (**Pavlíková et al., 2015, chapter 4.1, page 62**). Furthermore, ABCB1 or TRIP6 silencing reduced the number of MCF-7/PacR cells cultured with paclitaxel (**Pavlíková et al., 2015**). TRIP6 was also overexpressed concomitantly with ABCB1 in MCF-7/0035R subline (**Jelínek et al., 2018**).

Such results prompted us to thoroughly investigate the regulation of *TRIP6* expression in taxane-sensitive MCF-7 cells and taxane-resistant MCF-7 sublines. Known regulatory mechanisms of *TRIP6* expression involve *TRIP6* mRNA degradation by miRNAs and ubiquitin-dependent TRIP6 proteolysis (**Wang et al., 2017**; **Gou et al., 2019**). We found no expression of *TRIP6*-regulatory miR-138-5p in MCF-7 cells.

We assumed that chromosomal aberrations impact TRIP6 overexpression in paclitaxel-resistant MCF-7 sublines from the above findings. As expected, the *TRIP6* and *ABCB1 gene* copy number and mRNA level markedly increased in taxane-resistant MCF-7 sublines. This clue led us to investigate chromosomal aberrations in paclitaxel-resistant MCF-7 sublines by multicolour fluorescence *in situ* hybridization (mFISH). However, observation of multiple clones in early MCF-7 cell passages and increased chromosomal instability result in excessive karyotype heterogeneity (**Resnicoff et al., 1987**). Hence, we had also to analyze the karyotype of our parental taxane-sensitive MCF-7 cells, where we found highly conserved derivative chromosomes der(2)t(2;3) and der(10)t(7;10).

Regarding alterations associated with *ABCB1* and *TRIP6*, we found intact chromosome 7 in MCF-7 cells, whereas the same chromosome was aberrated in paclitaxel-resistant MCF-7 sublines. The amplified *ABCB1-TRIP6* segment formed a homogeneously stained region in chromosome 3 (MCF-7/PacR) or 19 (MCF-7/0035R). Detected chromosome 7 structural and numerical aberrations in taxane-resistant MCF-7 sublines favour a breakage-fuse-breakage mechanism of gene amplification (**McClintock, 1941**). Notably, both taxane-resistant sublines lost derivative chromosome der(18)t(18;22) with an unknown consequence on gene expression.

We found that *TRIP6* expression is regulated by cyclic AMP response element motif in *TRIP6* proximal promoter by dual-luciferase assay and targeted mutagenesis. Full CRE motif (ATGCGTCA) encompasses the CpG site. Methylation of this CpG site suppresses transcription in *cis* (**Tinti et al., 1997**). This site is not methylated in taxane-sensitive MCF-7 cells and taxane-resistant MCF-7 sublines (**chapter 4.4, page 117**). However, methylation of CRE in the TRIP6 promoter can represent different TRIP6 expressions in cell lines and tissues.

In breast cancer patients, *TRIP6* mRNA level correlated with progesterone receptor and premenopausal status (**chapter 4.4, page 120**). In the *TRIP6* promoter, no motifs associated with hormonal signalling were predicted by the JASPAR tool (**chapter 4.4, page 116**). Thus we suppose that TRIP6 expression would be only regulated indirectly by sexual hormones. Furthermore, our findings in breast cancer patients did not validate *TRIP6* as a marker of poor overall survival and relapse-free survival (**Zhao et al., 2020**).

Assessment of the function of suspect proteins others than ABCB1 were biased by ABCB1 overexpression. Double-knock-down experiments in that ABCB1 was one of the targets produced non-sense results.

4. PAPERS

- Němcová-Fürstová V, Kopperová D, Balušíková K, Ehrlichová M, Brynychová V, Václavíková R, **Daniel P**, Souček P, Kovář J. Characterization of acquired paclitaxel resistance of breast cancer cells and involvement of ABC transporters. *Toxicol. Appl. Pharmacol.* 310:215-228, **2016**. doi: 10.1016/j.taap.2016.09.020.

- Jelínek M, Balušíková K, **Daniel P**, Němcová-Fürstová V, Kirubakaran P, Jaček M, Wei L, Wang X, Vondrášek J, Ojima I, Kovář J. Substituents at the C3' and C3'N positions are critical for taxanes to overcome acquired resistance of cancer cells to paclitaxel. *Toxicol. Appl. Pharmacol.* 347:79-91, **2018**. doi: 10.1016/j.taap.2018.04.002.

- **Daniel P**, Halada P, Jelínek M, Balušíková K, Kovář J. Differentially Expressed Mitochondrial Proteins in Human MCF7 Breast Cancer Cells Resistant to Paclitaxel. *Int. J. Mol. Sci.* 20(12):2986, **2019**. doi: 10.3390/ijms20122986.

- **Daniel P**, Balušíková K, Václavíková R, Šeborová K, Ransdorfová Š, Valeriánová M, Wei L, Jelínek M, Tlapáková T, Fleischer T, Kristensen VN, Souček P, Ojima I, Kovář J. *ABCB1* Amplicon Contains Cyclic AMP Response Element-Driven *TRIP6* Gene in Taxane-Resistant MCF-7 Breast Cancer Sublines. *Genes*. 14:296, **2023**. doi: 10.3390/genes14020296.

4.1 Paper 1

CHARACTERIZATION OF ACQUIRED PACLITAXEL RESISTANCE OF BREAST CANCER CELLS AND INVOLVEMENT OF ABC TRANSPORTERS

Němcová-Fürstová, V., Kopperová, D., Balušíková, K., Ehrlichová, M., Brynychová, V., Václavíková, R., **Daniel, P.,** Souček, P., & Kovář, J. (**2016**)

Toxicology and applied pharmacology, *310*, 215–228

https://doi.org/10.1016/j.taap.2016.09.02

Toxicology and Applied Pharmacology 310 (2016) 215–228

Contents lists available at ScienceDirect

Toxicology and Applied Pharmacology

journal homepage: www.elsevier.com/locate/ytaap

Characterization of acquired paclitaxel resistance of breast cancer cells and involvement of ABC transporters

Vlasta Němcová-Fürstová [a,*], Dana Kopperová [a], Kamila Balušíková [a], Marie Ehrlichová [b], Veronika Brynychová [b], Radka Václavíková [b], Petr Daniel [a], Pavel Souček [b], Jan Kovář [a]

[a] Division of Cell and Molecular Biology, Third Faculty of Medicine, Charles University, Prague, Czech Republic
[b] Toxicogenomics Unit, National Institute of Public Health, Prague, Czech Republic

ARTICLE INFO

Article history:
Received 12 May 2016
Revised 2 September 2016
Accepted 20 September 2016
Available online 21 September 2016

Keywords:
ABCB1
ABC transporter
Breast cancer cells
Doxorubicin
Paclitaxel resistance
Taxane SB-T-1216

ABSTRACT

Development of taxane resistance has become clinically very important issue. The molecular mechanisms underlying the resistance are still unclear. To address this issue, we established paclitaxel-resistant sublines of the SK-BR-3 and MCF-7 breast cancer cell lines that are capable of long-term proliferation in 100 nM and 300 nM paclitaxel, respectively. Application of these concentrations leads to cell death in the original counterpart cells. Both sublines are cross-resistant to doxorubicin, indicating the presence of the MDR phenotype. Interestingly, resistance in both paclitaxel-resistant sublines is circumvented by the second-generation taxane SB-T-1216. Moreover, we demonstrated that it was not possible to establish sublines of SK-BR-3 and MCF-7 cells resistant to this taxane. It means that at least the tested breast cancer cells are unable to develop resistance to some taxanes. Employing mRNA expression profiling of all known human ABC transporters and subsequent Western blot analysis of the expression of selected transporters, we demonstrated that only the ABCB1/PgP and ABCC3/MRP3 proteins were up-regulated in both paclitaxel-resistant sublines. We found up-regulation of ABCG2/BCRP and ABCC4 proteins only in paclitaxel-resistant SK-BR-3 cells. In paclitaxel-resistant MCF-7 cells, ABCB4/MDR3 and ABCC2/MRP2 proteins were up-regulated. Silencing of ABCB1 expression using specific siRNA increased significantly, but did not completely restore full sensitivity to both paclitaxel and doxorubicin. Thus we showed a key, but not exclusive, role for ABCB1 in mechanisms of paclitaxel resistance. It suggests the involvement of multiple mechanisms in paclitaxel resistance in tested breast cancer cells.

1. Introduction

Breast cancer is the second most common cancer in the world and, by far, the most frequent cancer among women (www.globocan.iacr.fr). Taxanes are classical chemotherapeutics originally isolated from the bark of the Pacific yew (*Taxus brevifolia*). Taxanes have been used in breast cancer therapy since the 1990s and have been shown effective against metastatic breast cancer as well as early breast cancer (Murray et al., 2012).

Commonly used taxanes include the classical taxane paclitaxel (Taxol®) and its semi-synthetic derivative docetaxel (Taxotere®). They are microtubule-stabilizing agents that induce cell death due to beta-tubulin binding and microtubule stabilization that leads to G2/M arrest and results in induction of apoptosis (Jordan et al., 1996). Besides breast cancer, taxanes are also used in the treatment of many other malignancies, e.g. lung cancer, prostate cancer, Kaposi's sarcoma, squamous cell carcinoma of the head and neck, gastric cancer, esophageal cancer, and bladder cancer (Markman, 2008; Miller and Ojima, 2001; Tubiana-Hulin, 2005; Yared and Tkaczuk, 2012). Unfortunately, effective and successful therapy of patients is commonly limited by de novo or acquired resistance, including multidrug resistance (MDR), to taxanes.

In effort to overcome MDR, a series of second-generation taxanes with systematic modifications at C2, C10, C3′ and C3′N positions of paclitaxel was developed in laboratory of prof. Iwao Ojima, Stony Brook University, including taxane SB-T-1216 (Ojima et al., 1996). They were shown to be more effective particularly in drug-resistant cancer cells (Ehrlichova et al., 2005a; Kovar et al., 2009; Ojima et al., 2008).

Resistance to taxanes is thought to be a multifaceted phenomenon, however, despite intensive research, its mechanisms are far from being elucidated. It has been shown that resistance can result from metabolic inactivation of paclitaxel and docetaxel via the cytochrome P450 (CYP) system (CYP3A4/5 and CYP2C8, Harris et al., 1994). Other mechanisms of resistance are related to microtubules, i.e. presence of mutations in both α and β1 tubulin, aberrant expression of βIII tubulin and increased microtubule dynamics associated with altered expression of

* Corresponding author at: Division of Cell and Molecular Biology, Third Faculty of Medicine, Charles University, Ruská 87, 100 00 Prague 10, Czech Republic.
E-mail address: vlasta.furstova@lf3.cuni.cz (V. Němcová-Fürstová).

http://dx.doi.org/10.1016/j.taap.2016.09.020
0041-008X/

microtubule-associated proteins (Goncalves et al., 2001; Kavallaris, 2010; McGrogan et al., 2008; Yin et al., 2010). Altered cell cycle regulation and aberrant induction of apoptosis represent other features leading to taxane resistance (Ehrlichova et al., 2005b; Orr et al., 2003). These refer, e.g. to the altered status of p53 (Elledge et al., 1993), deregulation of expression of apoptosis regulatory proteins (e.g. Bcl-2, Bcl-X_L and IAPs) (Luo et al., 2015; Sharifi et al., 2014; Wang et al., 2009), activation of the Akt signaling pathway (Wang et al., 2011) and suppression of the checkpoint genes Mad2 and BubR1 (Sudo et al., 2004). Epigenetic changes, e.g. gene promoter DNA hypermethylation, also emerge as other important contributor to acquired drug resistance, including taxane resistance (Reed et al., 2008; Kastl et al., 2010; Brown et al., 2014). Recently, several miRNAs (e.g. miRNAs of miR200 family) have also been shown to play a role in taxane resistance (Cui et al., 2013). Finally, altered membrane transport of different compounds, including chemotherapeutics, as well as nutrients, can significantly influence drug resistance. Among the key molecules controlling uptake into and efflux from the cell and organelles are transporters of the ABC (ATP-binding cassette) family.

ABC transporters represent a large family of specific transmembrane ATP-binding proteins that translocate low-molecular weight substrates (Vtorushin et al., 2014). Presently, 48 human ABC transporters and one pseudogene have been identified. The ABC transporter family is divided into 7 subfamilies, i.e. ABCA, ABCB, ABCC, ABCD, ABCE, ABCF, and ABCG. The participation of ABC transporters in MDR is well established in various types of cancer, including breast cancer (Tamaki et al., 2011; Fletcher et al., 2016). Here, transporters ABCB1 (MDR1) (Chang et al., 2009; Fazeny-Dorner et al., 2003; Hansen et al., 2015; Hembruff et al., 2008; Li et al., 2014), ABCC1 (MRP1) (Fazeny-Dorner et al., 2003; Kars et al., 2006; Li et al., 2013; Litviakov et al., 2013), ABCC2 (MRP2) (Hembruff et al., 2008; Litviakov et al., 2013), ABCC3 (O'Brien et al., 2008) and ABCG2 (BCRP) (Fazeny-Dorner et al., 2003; Litviakov et al., 2013; Zhang et al., 2011) have been shown to be involved in taxane resistance, as seen in both in vitro experimental models as well as patient studies.

Taken together, development of taxane resistance has become a clinically very important issue due to the number of patients on taxane therapy. However, molecular mechanisms of acquired taxane resistance remain elusive. In this paper, we took advantage of paclitaxel-resistant counterparts of SK-BR-3 and MCF-7 breast cancer cell lines that were established in our laboratory. We used these new sublines to address the characterization and molecular mechanisms of acquired taxane resistance with respect to the involvement of ABC transporters. We compared their expression in paclitaxel-resistant and parental, paclitaxel-sensitive lines. We found that ABCB1, ABCB4, ABCC3 and ABCC2 were up-regulated in paclitaxel-resistant MCF-7 cells, while ABCB1, ABCC3 and ABCG2 were up-regulated in paclitaxel-resistant SK-BR-3 cells. We also demonstrated an important role for ABCB1 in the resistance to paclitaxel in both cell lines.

2. Materials and methods

2.1. Materials

Paclitaxel, doxorubicin and all other chemicals came from Sigma-Aldrich (St. Louis, MO, USA), unless otherwise indicated. SB-T-1216 (Ojima et al., 1996) was obtained from Prof. I. Ojima (Stony Brook University, NY, USA). Paclitaxel and SB-T-1216 were dissolved in DMSO (tissue culture quality) to obtain 10 mM stock solution. For real-time PCR analysis of ABC transporters, assays described in Mohelnikova-Duchonova et al. (2013) were used. For reference genes, assays Hs99999904_m1 (PPIA), Hs00430290_m1 (UBB), Hs00152844_m1 (ELF1) were used. For Western blot analysis, the following primary and secondary antibodies were used: *anti*-ABCB1 (ab3366, dilution 1:50), *anti*-ABCB4 (ab71792, dilution 1:100), *anti*-ABCC1 (Ab24102, dilution 1:20), *anti*-ABCC2 (Ab3373, dilution 1:50), *anti*-ABCC7 (Ab2784, dilution 1:200), *anti*-ABCC9 (Ab84299, dilution 1:500) from Abcam (Cambridge, UK), *anti*-ABCG2 (ALX-801-029, dilution 1:200) from Enzo Life Sciences (Farmingdale, NY, USA), *anti*-ABCB4 (PAB4698, dilution 1:100) from Abnova (Taipei City, Taiwan), *anti*-ABCC8 (ARP43622_P050, dilution 1:1000) from Aviva System Biology (San Diego, CA, USA), *anti*-MRP3/ABCC3 (#14182, dilution 1:500), *anti*-MRP4/ABCC4 (#12705, dilution 1:500), *anti*-cleaved caspase-3 (#9661, dilution 1:750), *anti*-cleaved caspase-7 (#9491, dilution 1:750) and *anti*-PARP (#9542, dilution 1:1000) from Cell Signaling Technology (Danvers, MA, USA), *anti*-actin (clone AC-40, dilution 1:1000) from Sigma-Aldrich (St. Louis, MO, USA) and HRP-linked goat *anti*-mouse (sc-2005, dilution 1:6000) and goat *anti*-rabbit (sc-2004, dilution 1:6000) antibody from Santa Cruz (Santa Cruz, CA, USA).

2.2. Cells and culture conditions

Human breast carcinoma cell lines MCF-7 and SK-BR-3 were obtained from the National Cancer Institute (Frederick, MD, USA) and the American Type Culture Collection (ATCC) (Manassas, VA, USA), respectively. The cells were maintained at 37 °C in a humidified atmosphere of 5% CO_2 in air in RMPI-1640 based culture medium containing extra L-glutamine (300 μg/ml), sodium pyruvate (110 μg/ml), HEPES (15 mM), penicillin (100 U/ml) and streptomycin (100 μg/ml), and supplemented with 10% heat-inactivated fetal bovine serum, as described previously (Musilkova and Kovar, 2001).

2.3. Establishment of paclitaxel-resistant SK-BR-3 and MCF-7 cell sublines

Paclitaxel-resistant SK-BR-3 and MCF-7 cell sublines, referred to as SK-BR-3/PacR and MCF-7/PacR cells, were established by gradual adaptation of the original cell lines to increasing paclitaxel concentrations. The starting concentration of paclitaxel was 1 nM. Paclitaxel concentrations increased as follows: 1 nM → 3 nM → 5 nM → 10 nM → 20 nM → 30 nM → 50 nM → 70 nM → 100 nM → 300 nM (the highest concentration only for MCF-7 cells). Cells were maintained at a particular paclitaxel concentration for approximately 10 passages or until they displayed, more or less, standard growth and survival after subculture. Cells were passaged twice a week if appropriate. Otherwise, the medium was changed twice a week until the cell culture reached conditions allowing passaging. The final concentration of paclitaxel achieved was 100 nM for SK-BR-3 cells and 300 nM for MCF-7. Long-term growth and survival of SK-BR-3/PacR in 100 nM paclitaxel and of MCF-7/PacR in 300 nM paclitaxel were similar to cells without paclitaxel. On the other hand, most of the original SK-BR-3 cells when exposed to 100 nM paclitaxel, and the original MCF-7 cells exposed to 300 nM paclitaxel, died within 96 h.

2.4. Establishment of SK-BR-3 and MCF-7 cell sublines resistant to second-generation taxane SB-T-1216

Similarly, we tried to establish resistant sublines to the second-generation taxane SB-T-1216. However, despite repeated attempts, we were unable to adapt both cell lines to long-term growth and survival (15 passages) in the presence of SB-T-1216 at concentrations higher than 5 nM.

2.5. Assessment of cell growth and survival

Cells were seeded at 20×10^3 cells/100 μl of culture medium into the wells of 96-well plastic plates. After a 24-h pre-incubation period allowing cells to attach, the culture medium was replaced by culture medium without taxane (control), with one of the tested taxanes (paclitaxel or SB-T-1216) or doxorubicin at the desired concentrations. Cell growth and survival were evaluated after 96 h of incubation. The number of living cells was determined using a hemocytometer counting after staining with trypan blue. IC_{50} values (the half maximal inhibitory

concentration) were calculated following curve fitting to the cell survival data.

2.6. Quantitative assessment of apoptosis

Cells (approximately 2.4×10^6 cells per sample) were seeded into standard growth media and after a 24-h preincubation period allowing cells to attach, the culture medium was replaced by medium containing paclitaxel at 100 nM for SK-BR-3 cells, or 300 nM for MCF-7 cells, or control media without taxane (Control). After the required period of treatment, cells were harvested using low-speed centrifugation. The percentage of apoptotic cells was determined by flow cytometry employing FACS Calibur cytometer (Becton Dickinson, San Jose, CA, USA) and Annexin V-FITC Apoptosis Detection Kit (Abcam, Cambridge, UK). Annexin V staining was performed according to manufacturer's instructions. Annexin V-positive cells were considered as apoptotic cells.

2.7. Cell cycle analysis

Cells (approximately 500×10^3 cells per sample) were seeded into standard growth media and after a 24 h pre-incubation period allowing cells to attach, the culture medium was replaced with medium containing paclitaxel at 100 nM concentration for SK-BR-3 cells, or at 300 nM concentration for MCF-7 cells, or control media without taxane (Control). After the desired period of treatment (6 h and 24 h for SK-BR-3 cells and 12 h and 36 h for MCF-7 cells), cell cycle analysis was performed as described previously (Ehrlichova et al., 2012). Briefly, cells were harvested using low-speed centrifugation and fixed in cold 70% ethanol overnight at 4 °C. Fixed cells were washed with PBS, stained with a propidium iodide solution (40 μg/ml propidium iodide and 100 μg/ml RNase in PBS) for 45 min and the fluorescence was measured on a FACS Calibur cytometer (Becton Dickinson, San Jose, CA, USA).

2.8. Assessment of expression of ABC transporters on the mRNA level

Total RNA was isolated using Trizol reagent according to instructions of the producer (Sigma-Aldrich, St. Louis, MO, USA). cDNA was synthesized from total RNA using random hexamer primers (RevertAid First Strand cDNA Synthesis Kit, Fermentas, Vilnius, Lithuania). Real-time PCR was performed using a ViiA7 Real-Time PCR System (Life Technologies, Carlsbad, CA, USA). The reaction mixture contained 2.5 μl of TaqMan Gene Expression Master Mix, 0.25 μl of a specific TaqMan Gene Expression Assay (see Materials and methods), 2.0 μl of cDNA and nuclease-free water to make a final volume of 5.0 μl. Cycling parameters were an initial hold at 50 °C for 2 min and denaturation at 95 °C for 10 min followed by 45 cycles consisting of denaturation at 95 °C for 15 s and annealing/extension at 60 °C for 60 s. A non-template control, containing nuclease-free water instead of cDNA, was used. Fluorescence values were acquired after each extension phase. Real-time PCR analysis of mRNA levels was performed in two separate determinations and samples were analyzed in duplicates. Samples with standard deviation of duplicates larger than 0.5 Ct were reanalyzed. If no fluorescence was detected during first 40 cycles, it was evaluated as no mRNA expression of the respective gene. Reference genes were selected on the basis of the analysis of stability of 11 potential reference genes chosen from the literature (EIF2B1, ELF1, GUSB, HPRT1, IPO8, MRPL19, POLR2A, PPIA, PSMB6, PSMC4, and UBB) in a set of all analyzed samples. Stability of reference genes was analyzed by geNorm (Vandesompele et al., 2002) and NormFinder (Andersen et al., 2004) software programs. PPIA (assay no. Hs99999904_m1), UBB (Hs00430290_m1), and ELF1 (Hs00152844_m1) were selected as the most stable reference genes. One sample of normal breast tissue was used as a calibrator for preparation of standard curves for each gene to assess their reaction efficiency. The calibration curve points were prepared by five subsequent serial five-times dilutions of the calibrator. The resulting standard curve was used for calculation of PCR efficiency (E) according to the following formula: $E = 10^{-1/\text{slope}} - 1$. Differences in the acquired raw cycle threshold (Ct) data between compared samples were analyzed by Relative Expression Software Tool (REST) 2009 program (Qiagen, Hildesheim, Germany). REST is routinely used for the determination of differences between different types of sample and control groups and considers both normalization to numerous reference genes and reaction efficiency (Pfaffl et al., 2002).

2.9. Western blot analysis

Cells (approximately 5×10^6 cells per sample) were seeded into standard growth media and after a 24-h preincubation period allowing cells to attach, the culture medium was replaced by medium containing paclitaxel at 100 nM for SK-BR-3 cells, or 300 nM for MCF-7 cells, or control media without taxane (Control). After the required period of treatment, cells were harvested using low-speed centrifugation and cell lysates were prepared using RIPA lysis buffer containing protease and phosphatase inhibitors (Roche). Protein concentrations were measured using the BCA method. Western blot analysis was performed as described previously (Nemcova-Furstova et al., 2011) with minor modifications concerning specific conditions for sample denaturation. Modifications were as follows: sample denaturation was done at 70 °C for 15 min for ABCB1 detection and at 37 °C for 5 min for ABCB4 and ABCC2 detection. ABCG2 samples were denatured at 37 °C for 5 min and after blotting, membranes were treated as described in Kaur and Bachhawat (2009). For dilution of the antibodies see "Materials and methods." The chemiluminescent signal was detected using a Carestream Gel Logic 4000 PRO Imaging System equipped with Carestream Molecular Imaging Software (Carestream Health, New Haven, CT, USA) for image acquisition and analysis. Densitometry was performed using the Carestream v5.2 program (Carestream Health).

2.10. Silencing of ABCB1 expression by siRNA and its effect on cell growth and viability

Inhibition of ABCB1 expression, employing specific siRNA, was performed similarly as already reported (Jelinek et al., 2015). Opti-MEM® Reduced Serum Medium (Life Technologies, Calsbad, CA, USA), ABCB1 specific siRNA (catalog no: 4427037, ID: s10419, Life Technologies) and INTERFERin (PolyPlus-Transfection, Illkirch, France) as a transfection reagent were used according to manufacturer instructions. Nonspecific siRNA (catalog no.: AM4635, Life Technologies) was used as a negative control.

For ABCB1 silencing, 2.1×10^5 cells in antibiotics-free medium were seeded into Petri dishes (Ø 6 cm). After 24 h for cells to attach, the culture medium of both sensitive and resistant cells was changed to paclitaxel-free medium containing the siRNA transfection mixture. In the transfection mixture, ABCB1 or nonspecific siRNAs were diluted in Opti-MEM® Reduced Serum Medium to a final concentration of 5 nM of siRNA in culture medium together with INTERFERin transfection reagent at a 1:250 dilution.

After 72 h of incubation with siRNA, cells were harvested into their cultivation media and seeded in the same media at a concentration of 2×10^5 cells/ml into culture plates. After 24 h for cells to attach, the media was replaced by media containing paclitaxel or doxorubicin (at required concentrations) or control media. After 96 h of treatment, the number of surviving cells was determined using a hemocytometer after trypan blue staining and persistence of ABCB1 silencing throughout the experiment was analyzed using Western blot (see above).

2.11. Confocal microscopy

Confocal microscopy analysis was performed with minor modifications as previously described (Nemcova-Furstova et al., 2013). Paclitaxel-resistant cells without and after ABCB1 silencing (see above) were seeded onto coverslips (approximately 1×10^5 cells per coverslip)

After 24 h of incubation, cells were fixed with methanol for 10 min or acetone for 5 min at −20 °C. After washing with PBS, cells were blocked with Image-iT™ FX signal enhancer (Molecular Probes, Invitrogen, Eugene, OR, USA) for 45 min. Next, cells were stained with *anti*-ABCB1 antibody (JSB1, dilution 1:50) at 4 °C overnight. Cells were than washed with PBS and incubated with *anti*-mouse Alexa Fluor 488-labeled secondary antibody (dilution 1:100, Life Technologies, Carlsbad, USA) for 2 h in the dark at room temperature. Finally, cells were washed again with PBS. Coverslips with stained cells were transferred onto a droplet of Vectashield® Mounting Medium with DAPI (Vector Laboratories, Burlingame, CA, USA) and sealed. Samples were analyzed using a Leica TCS SP5 confocal microscope (Bannockburn, IL, USA) with relevant excitation and emission wavelengths.

2.12. DNA methylation analysis

Bisulfite conversion and methylation-sensitive high resolution melting (MS-HRM) analysis was developed (manuscript under preparation) and performed in genomic DNA samples (500 ng) from each cell line. DNA was bisulfite modified using the EpiTect® Bisulfite Kit (Qiagen) following the manufacturer's protocol. Bisulfite-converted DNA was evaluated in 40 μl of elution buffer and 10 ng of converted DNA sample was used for particular MS-HRM analysis. CpG islands covering promoter of ABCB1 were identified using Methprimer software (Li and Dahiya, 2002). HRM analysis was then used for estimation of methylation status in all identified CpG islands divided to seven regions with optimal product length (100–150 bp) for HRM analysis. PCR amplification and subsequent HRM analysis was performed on Rotor Gene 6000 machine (Corbett Research, Sydney, Australia) by help of EpiTect HRM Kit (Qiagen) according to recommendations of producer. Real-time PCR cycling and conditions and primers for HRM analysis of all examined *ABCB1* regions are available upon request. A standard curve was constructed by diluting bisulfite converted-fully methylated human control DNA (EpiTect® Control DNA, methylated, Qiagen) with unmethylated DNA (EpiTect® Control DNA, unmethylated, Qiagen) to 0, 5, 10, 20, 30, 40, 50, 60, 70, 80, 90, and 100%. The standard curve was included in each run. Collected HRM data were analyzed using Rotor-Gene software version 6.0 (Corbett-Research) and expressed in percentage of methylated DNA derived from the calibration curve. The average values of methylation for all CpGs islands were calculated as means of methylation levels of all seven regions and for each cell line.

2.13. Statistical analysis

Statistical significance of differences was determined by the Student's *t*-test and ANOVA. $p < 0.05$ was considered statistically significant. *p*-Values for difference between methylation and expression levels in sensitive and resistant cell lines were calculated by the Spearman test.

3. Results

3.1. Establishment of paclitaxel-resistant cell sublines

Via long-term culturing of original paclitaxel-sensitive SK-BR-3 and MCF-7 cells in media with gradually increasing paclitaxel concentrations, we successfully established paclitaxel-resistant variants (sublines) SK-BR-3/PacR and MCF-7/PacR. The established paclitaxel-resistant SK-BR-3/PacR and MCF-7/PacR cells are capable of long-term survival and proliferation in media containing 100 nM paclitaxel (SK-BR-3) and 300 nM paclitaxel (MCF-7). These paclitaxel concentrations lead to cell death in most cells of the original cell lines within 96 h (Fig. 1). The growth rate of SK-BR-3/PacR and MCF-7/PacR cells, at the respective paclitaxel concentration, was similar to that of the original paclitaxel-sensitive cell lines without paclitaxel (Fig. 1). Comparison of IC_{50} values (the half maximal inhibitory concentration) in sensitive and paclitaxel-resistant cells shows that paclitaxel resistance is increased 20.5-fold in SK-BR-3/PacR cells and 96.6-fold in MCF-7/PacR cells (Table 1).

Paclitaxel treatment induced significant increase in the number of annexin V-positive cells in both sensitive cell lines, whereas there was no increase in the number of annexin V-positive cells in both paclitaxel-resistant sublines (Fig. 2C, D). No apoptosis in SK-BR-3/PacR and MCF-7/PacR cells after 100 nM and 300 nM paclitaxel treatment, respectively, was also demonstrated by no activation of caspase-3 (only in SK-BR-3 cells) and caspase-7 when compared with original cell lines (Fig. 2A, B). There is no functional caspase-3 in MCF-7 cells.

In order to assess mechanisms that were involved in the development of paclitaxel resistance in our cell lines, we also tested whether the resistance would persist in the absence of paclitaxel in the culture medium. We found that both paclitaxel-resistant cell sublines do not display any prominent changes in cell growth and survival when cultured without paclitaxel and, more importantly, they keep the paclitaxel-resistance even when allowed to grow without paclitaxel for >10 passages (Fig. 3). This indicates that paclitaxel resistance does not

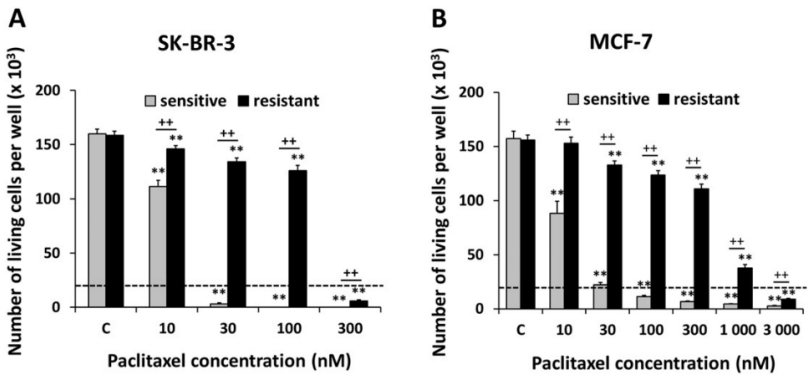

Fig. 1. Effect of paclitaxel on the growth and survival of paclitaxel-sensitive and -resistant (A) SK-BR-3 and (B) MCF-7 cells. Control cells (C) were incubated without taxane. The number of cells of the inoculum (20×10^3 cells/100 μl of medium per well) is shown as a dashed line. The number of living cells was determined after 96 h of incubation (see "Materials and methods"). Each column represents the mean of 4 separate cultures ± SEM. $^{**}p < 0.01$ when comparing paclitaxel-treated cells with their respective control cells, $^{++}p < 0.01$ when comparing the effect in sensitive and resistant cells. The data shown were obtained in one representative experiment of three independent experiments.

Table 1
IC_{50} values (nM) for paclitaxel, SB-T-1216 and doxorubicin in paclitaxel-sensitive and paclitaxel-resistant SK-BR-3 and MCF-7 cells. Data are shown as mean ± SEM of at least three independent experiments. Resistance index was calculated as fold increase in resistance when comparing resistant vs. sensitive cells (IC_{50} of resistant cells/IC_{50} of sensitive cells).

SK-BR-3	Sensitive	Resistant	Resistance index
Paclitaxel	14.8 ± 4.6	303.8 ± 99.4	20.5
SB-T-1216	5.3 ± 0.5	10.8 ± 2.1	2.1
Doxorubicin	31.8 ± 4.5	130.2 ± 6.2	4.1
MCF-7	**Sensitive**	**Resistant**	**Resistance index**
Paclitaxel	10.5 ± 0.7	1014.3 ± 295.0	96.6
SB-T-1216	3.2 ± 1.2	9.9 ± 5.7	3.1
Doxorubicin	57.9 ± 8.9	660.8 ± 310.5	11.4

represent a metabolic adaptation but rather represents a selection of genetically or epigenetically modified clones.

3.2. Establishment of SB-T-1216-resistant cell sublines

By the same approach, we also tried to establish resistance to second-generation taxane SB-T-1216 (Ojima et al., 1996). Despite our repeated attempts, the cells were not able to adapt to concentrations higher that 5 nM. Moreover, the paclitaxel-resistant SK-BR-3/PacR and MCF-7/PacR cells displayed similar sensitivity to SB-T-1216 as the original paclitaxel-sensitive cell line. Only at low SB-T-1216 concentrations (10 and 20 nM), both resistant sublines were significantly more resistant (Fig. 4 and Table 1). This suggests that the molecular mechanisms involved in resistance to paclitaxel do not work sufficiently when exposed to SB-T-1216.

3.3. Cell cycle analysis

We compared the effect of paclitaxel on the cell cycle in paclitaxel-sensitive vs. paclitaxel-resistant cells regularly maintained in paclitaxel-containing (100 nM for SK-BR-3 and 300 nM for MCF-7) medium (SK-BR-3/PacR and MCF-7/PacR) and paclitaxel-resistant cells maintained in paclitaxel-free (drug-free) medium for at least 10 passages (SK-BR-3/$PacR^{DF}$ and MCF-7/$PacR^{DF}$). According to the known mechanism of paclitaxel effect on microtubules, we demonstrated a G2/M block in both original sensitive SK-BR-3 and MCF-7 cells 6 h and 12 h after paclitaxel application (100 nM for SK-BR-3 and 300 nM for MCF-7, data not shown). This effect persisted 24 h and 36 h after the application, respectively. In contrast, a G2/M block was not induced by paclitaxel treatment

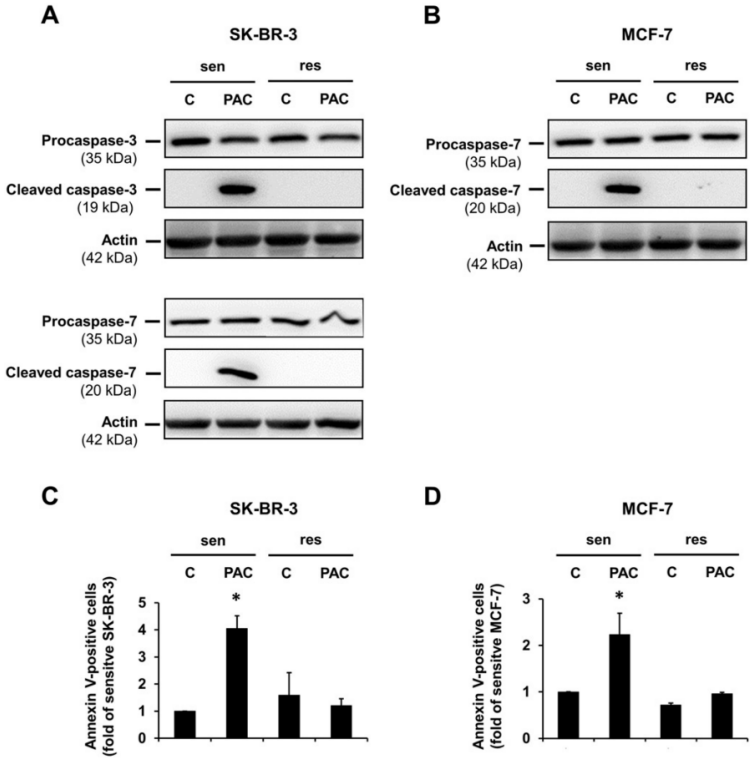

Fig. 2. Effect of paclitaxel (A) on the level of procaspase-3 and -7 and cleaved caspase-3 and 7 in paclitaxel-sensitive (sen) and paclitaxel-resistant (res) SK-BR-3 cells, (B) on the level of procaspase-7 and cleaved caspase-7 in paclitaxel-sensitive and paclitaxel-resistant MCF-7 cells and on the level of annexin V-positive cells in (C) paclitaxel-sensitive and paclitaxel-resistant SK-BR-3 cells and (D) paclitaxel-sensitive and paclitaxel-resistant MCF-7 cells. After (A, C) 24 h and (B, D) 36 h of incubation without paclitaxel (C, control cells) or with paclitaxel (PAC, 100 nM for SK-BR-3 cells and 300 nM for MCF-7 cells), levels of procaspases and cleaved caspases (A, B) were determined using Western blot analysis and relevant antibodies. The number of annexin V-positive cells (C, D) was measured employing flow cytometry and commercial Annexin V-Staining Kit (see "Materials and methods"). (A, B) Actin levels were used to confirm equal protein loading. The data shown were obtained in one representative experiment of three independent experiments. (C, D) Number of annexin-V positive cells is expressed as fold increase against control sensitive cells. Data are shown as mean ± SEM. *$p < 0.05$ when comparing the effect with control cells.

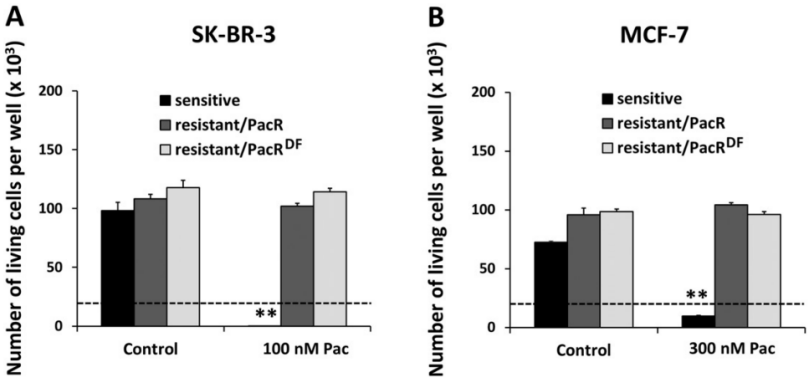

Fig. 3. Effect of paclitaxel (Pac) on the growth and survival of paclitaxel-sensitive cells (sensitive), paclitaxel-resistant cells regularly maintained in paclitaxel-containing (100 nM for SK-BR-3 and 300 nM for MCF-7) medium (resistant/PacR) and paclitaxel-resistant cells maintained in paclitaxel-free (DF, i.e. drug-free) medium at least 10 passages (resistant/PacR^{DF}) for (A) SK-BR-3 and (B) MCF-7 cells. Control cells were incubated without paclitaxel. The number of cells of the inoculum (20×10^3 cells/100 μl of medium per well) is shown as a dashed line. The number of living cells was determined after 96 h of incubation (see "Materials and methods"). Each column represents the mean of 4 separate cultures ± SEM. $^{**}p < 0.01$ when comparing paclitaxel-treated cells with their respective control cells. The data shown were obtained in one representative experiment of three independent experiments.

in paclitaxel-resistant cells SK-BR-3/PacR and MCF-7/PacR cells or in SK-BR-3/PacR^{DF} and MCF-7/PacR^{DF} cells. A G2/M block was not induced in paclitaxel-resistant cells irrespective of the long-term presence or absence of paclitaxel in the maintenance culture medium (Fig. 5).

3.4. Expression of ABC transporters on the mRNA level

In order to better characterize the resistant cells, we compared expression of all known 48 ABC transporter genes (ABCA1-10, ABCA12, ABCA13, ABCB1-11, ABCC1-12, ABCD1-4, ABCE1, ABCF1-3, ABCG1-2, ABCG4-5, ABCG8) and one pseudogene (ABCC13) on the mRNA level in paclitaxel-sensitive and paclitaxel-resistant cells. We found that only 44 of the transporters were expressed at detectable levels in cell lines and sublines tested. Transporters ABCA13, ABCB5, ABCB11, ABCG5 and ABCG8 were not detected in either cell line or subline. Transporters with a significant difference in the level of expression found between paclitaxel-sensitive and paclitaxel-resistant cells are shown in Table 2. Transporter ABCC4, which has been recently shown to be important determinant of docetaxel resistance in prostate cancer cells, is also included (Oprea-Lager et al., 2013).

In summary, only the expression of ABCB1, ABCB4 and ABCG2 mRNA was significantly increased in both paclitaxel-resistant sublines compared to their respective original sensitive cell lines. Moreover, the expression of ABCB1 and ABCB4 transporters was under the detection limit for the method we used in sensitive SK-BR-3 cells. Expression of ABCC1 was significantly decreased in both paclitaxel-resistant sublines compared to sensitive ones. Expression of other estimated ABC transporters differed in SK-BR-3 and MCF-7 cell lines. In resistant SK-BR-3/PacR cells, the expression of ABCC2 and ABCC3 was significantly decreased and the expression of ABCC9 was significantly increased compared to sensitive SK-BR-3 cells. In resistant MCF-7/PacR cells, expression of ABCC2 and ABCC7 was significantly increased compared to sensitive cells. A significant decrease of mRNA expression was found only for ABCC8.

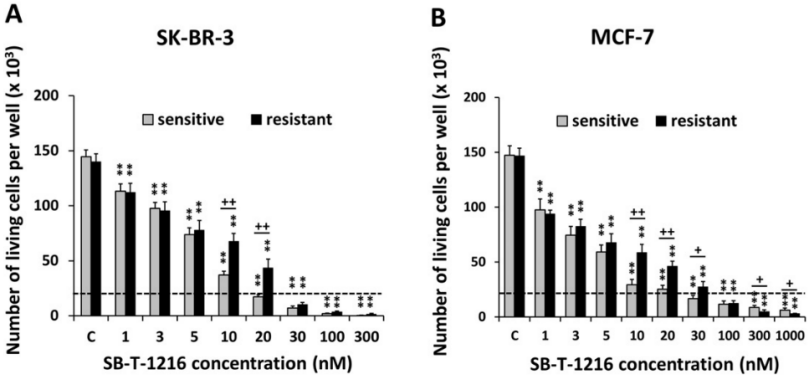

Fig. 4. Effect of SB-T-1216 on the growth and survival of paclitaxel-sensitive and -resistant (A) SK-BR-3 and (B) MCF-7 cells. Control cells (C) were incubated without taxane. The number of cells of the inoculum (20×10^3 cells/100 μl of medium per well) is shown as a dashed line. The number of living cells was determined after 96 h of incubation (see "Materials and methods"). Each column represents the mean of 4 separate cultures ± SEM. $^{**}p < 0.01$ when comparing SB-T-1216-treated cells with their respective control cells, $^{+}p < 0.05$ when comparing the effect in sensitive and resistant cells, $^{++}p < 0.01$ when comparing the effect in sensitive and resistant cells. The data shown were obtained in one representative experiment of three independent experiments.

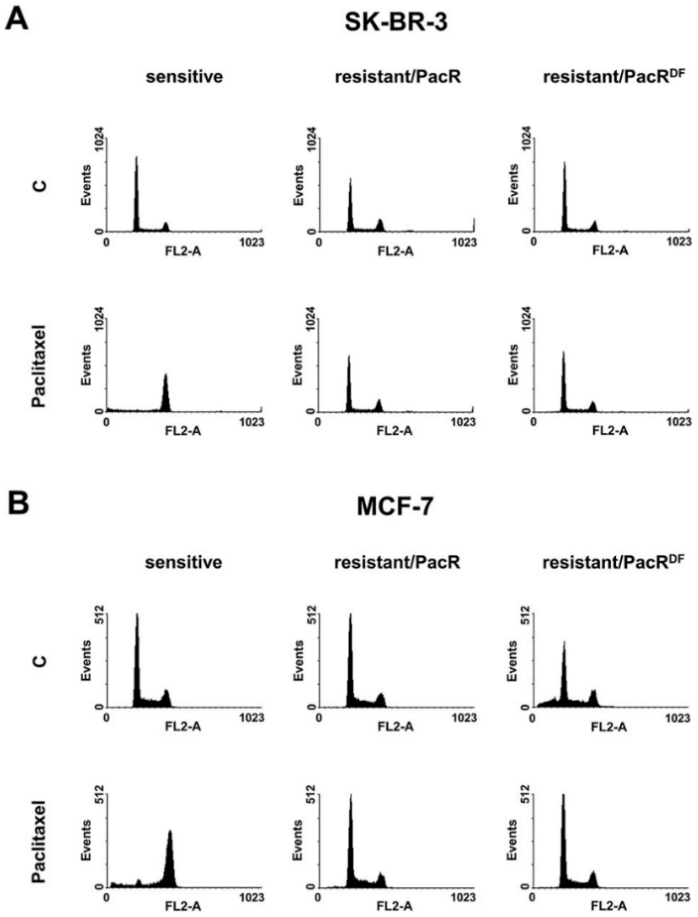

Fig. 5. Effect of paclitaxel on DNA histogram of paclitaxel-sensitive cells (sensitive), paclitaxel-resistant cells regularly maintained in paclitaxel-containing (100 nM) medium (resistant/PacR) and paclitaxel-resistant cells maintained in paclitaxel-free (DF, i.e. drug-free) medium at least 10 passages (resistant/PacR^{DF}) for (A) SK-BR-3 and (B) MCF-7 cells. Control cells (C) were incubated without taxane. After 24 h (SK-BR-3) and 36 h (MCF-7) of incubation, the cells were stained with propidium iodide (see "Materials and methods") and analyzed using flow cytometry. The data shown were obtained in one representative experiment of three independent experiments.

Table 2
Relative expression of selected ABC transporters on the mRNA level in paclitaxel-sensitive and paclitaxel-resistant SK-BR-3 and MCF-7 cells. Expression is presented as fold increases on mRNA level compared to expression in sensitive cells (calibrator, set as "1"). ND = not detectable (expression under the sensitivity threshold of the method used). *No mRNA expression of the respective gene was detected in the sensitive cells. In these cases, Ct 40.0 was used to calculate the fold differences in gene expression.

SK-BR-3	ABCB1*	ABCB4*	ABCC1	ABCC2	ABCC3	ABCC4	ABCC7	ABCC8	ABCC9	ABCG2
Resistant vs. sensitive cells	47,780	35.05	0.77	0.13	0.47	1.30	ND	0.69	1880	2.45
Up/down-regulation	↑	↑	↓	↓	↓	–	ND	–	↑	↑
p-Value	**0.002**	**0.004**	**0.020**	**0.005**	**0.023**	0.094	ND	0.489	**0.023**	**0.005**
MCF-7	ABCB1	ABCB4	ABCC1	ABCC2	ABCC3	ABCC4	ABCC7*	ABCC8	ABCC9	ABCG2
Resistant vs. sensitive cells	44,640	237.6	0.68	5.74	0.94	1.17	93.24	0.38	1.82	1.47
Up/down-regulation	↑	↑	↓	↑	–	–	↑	↓	–	↑
p-Value	**0.002**	**0.026**	**0.023**	**0.007**	0.706	0.370	<**0.001**	**0.004**	0.588	**0.030**

Differences with statistical significance ($p < 0.05$) are shown in bold.

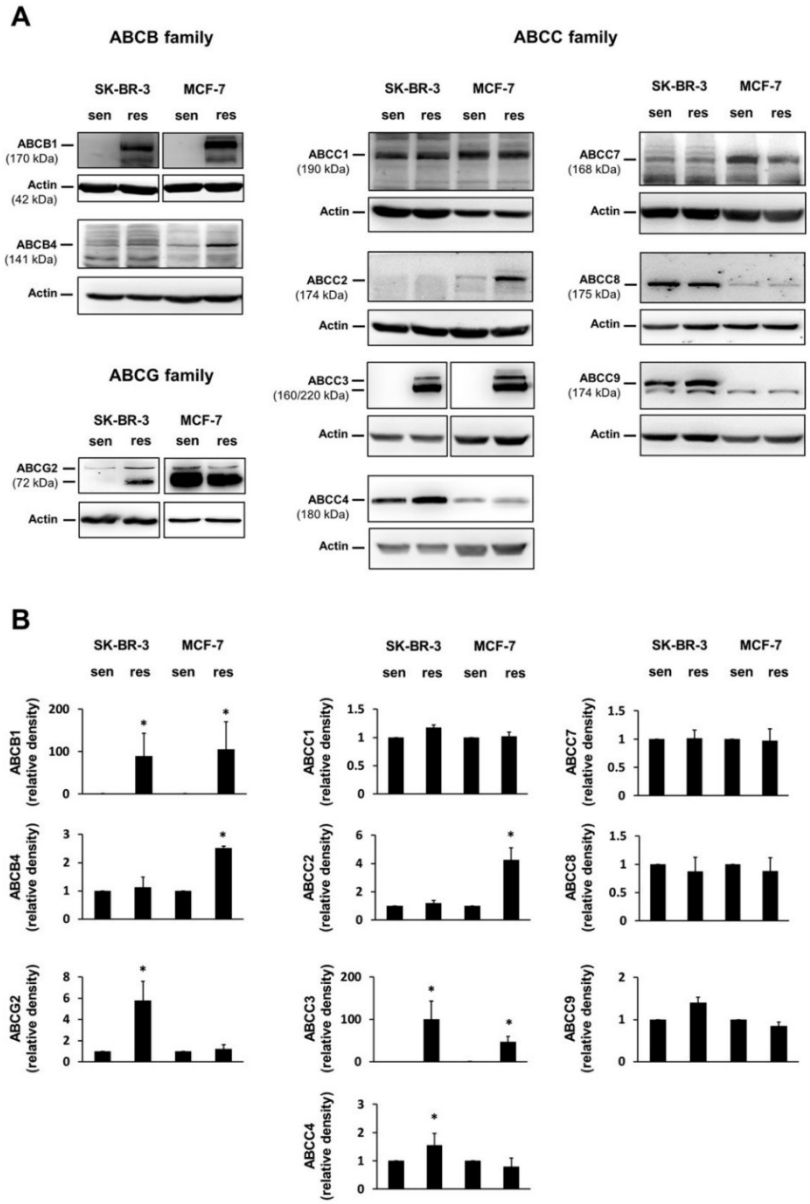

Fig. 6. The level of ABCB1, ABCB4, ABCC1, ABCC2, ABCC7, ABCC8, ABCC9 and ABCG2 transporters in paclitaxel-sensitive (sen) and paclitaxel-resistant (res) SK-BR-3 and MCF-7 cells. (A) After 24 h of incubation with paclitaxel (100 nM for SK-BR-3/PacR cells and 300 nM for MCF-7/PacR cells) the levels of ABC transporters of interest were determined using Western blot analysis and relevant antibodies (see "Materials and methods"). Actin levels were used to confirm equal protein loading. The data shown were obtained in one representative experiment of at least three independent experiments. (B) Western blot quantification was done by densitometry. Data are presented as fold increase ± SEM against the respective sensitive cells after normalization of the band intensities to actin levels. *$p < 0.05$ when comparing the effect in sensitive and resistant cells.

3.5. Expression of ABC transporters on the protein level

Next, we tried to verify mRNA expression data on the protein level. ABC transporters listed in Table 2 were subjected to Western blot analysis. We found that only ABCB1 and also ABCC3 were significantly overexpressed on protein level in resistant SK-BR-3/PacR as well as resistant MCF-7/PacR cells. Their levels were hardly detectable in both of the original paclitaxel-sensitive cell lines (Fig. 6).

Concerning overexpression of ABCB4 mRNA in both paclitaxel-resistant cell sublines, we found its up-regulation on protein level only in paclitaxel-resistant MCF-7/PacR cells. Next, we confirmed significant up-regulation of ABCC2 protein in paclitaxel-resistant MCF-7/PacR cells. Moreover, the mRNA data correlated with protein data for ABCG2 whose level was significantly increased in paclitaxel-resistant SK-BR-3/PacR cells. ABCC4 protein was also significantly up-regulated in paclitaxel-resistant SK-BR-3/PacR cells. However, except for the above listed transporters, no other changes on the protein level between paclitaxel-sensitive and paclitaxel-resistant sublines were found (Fig. 6). Nevertheless, we are aware that due to existence of many levels of protein expression regulation (regulation of mRNA stability, regulation of protein degradation, etc.) also expression of some other transporters may differ between sensitive cell lines and their paclitaxel-resistant counterpart sublines despite no detected change on mRNA expression level.

3.6. Effect of ABCB1 silencing

Employing ABCB1 silencing by specific siRNA, we tested whether ABCB1 over-expression was responsible for the observed paclitaxel resistance. We found that silencing ABCB1 expression to almost undetectable levels resulted in a significant decrease in cell survival after 96 h of paclitaxel treatment in both resistant cell sublines (67 ± 7% of the control for SK-BR-3/PacR cells and 19 ± 1% of the control for MCF-7/PacR) when compared to resistant cells not treated with siRNA (Fig. 7). The sensitivity to paclitaxel of SK-BR-3/PacR cells and MCF-7/PacR was increased approximately 2-fold and 4-fold, in comparison with nonspecific siRNA-treated cells (Table 3). Control nonspecific siRNA alone also affected ABCB1 expression to some extent. However, this silencing did not influence cell survival during paclitaxel treatment (Fig. 7).

Employing ABCB1 silencing and confocal microscopy, we demonstrated predominant localization of the ABCB1 protein in the plasma membrane of resistant cells of both tested cell lines. We also confirmed the specificity of the ABCB1 antibody used, since there was a significant decrease in the ABCB1 protein signal intensity after specific ABCB1 silencing (Fig. 8).

3.7. ABCB1 methylation status

In order to assess for potential epigenetic mechanisms involved in development of acquired paclitaxel resistance in our model cell lines, ABCB1 promoter methylation status was analyzed. Global methylation status of CpG islands of *ABCB1* promoter in SK-BR-3 and MCF-7 cells and their resistant sublines was relatively high ranging 60–100%. A significant hypermethylation of *ABCB1* in the resistant subline of SK-BR-3 cells in comparison to sensitive SK-BR-3 cells was observed (Table 4). Nevertheless, a significant correlation between *ABCB1* promoter

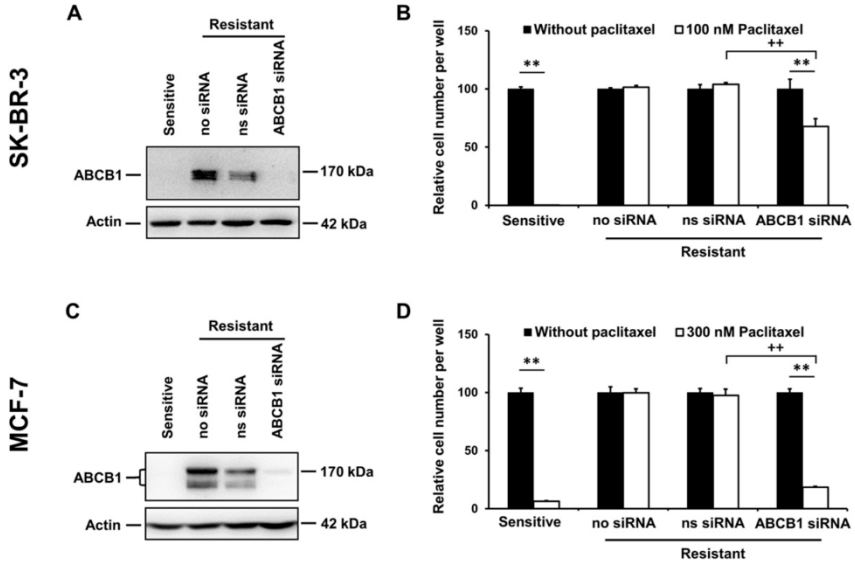

Fig. 7. The effect of ABCB1 silencing on the growth and survival of paclitaxel-resistant (A, B) SK-BR-3 and (C, D) MCF-7 cells after paclitaxel treatment. (A, C) Demonstration of ABCB1 expression after its silencing at the end of cell growth and survival experiment in (A) SK-BR-3 and (C) MCF-7 cells. The level of ABCB1 expression in sensitive cells, resistant cells, resistant cells treated with nonspecific siRNA (ns siRNA), and resistant cells treated with ABCB1 specific siRNA (ABCB1 siRNA) was assessed using Western blot analysis and relevant antibodies (see "Materials and methods"). Actin levels were used to confirm equal protein loading. The data shown were obtained in one representative experiment of three independent experiments. (B, D) Effect of silencing of ABCB1 expression on the growth and survival of (B) SK-BR-3 and (D) MCF-7 cells after paclitaxel treatment. The cells were prepared as described in "Materials and methods" and seeded at 20×10^3 cells/100 μl of medium per well. The relative number of living sensitive cells, resistant cells (no siRNA), resistant cells treated with nonspecific siRNA (ns siRNA) and resistant cells treated with ABCB1 specific siRNA (ABCB1 siRNA) was determined after 96 h of incubation with paclitaxel (100 nM for SK-BR-3 cells and 300 nM for MCF-7 cells). Each column represents the mean of 4 separate cultures ± SEM. $^{**}p < 0.01$ when comparing the effect in cells without paclitaxel and treated with paclitaxel. $^{++}p < 0.01$ when comparing the effect in ABCB1 siRNA-treated and ns siRNA-treated cells after paclitaxel application. The data shown were obtained in one representative experiment of three independent experiments.

Table 3
Effect of ABCB1 silencing employing specific ABCB1 siRNA on IC_{50} values (nM) for paclitaxel and doxorubicin in resistant SK-BR-3 (SK-BR-3/PacR) and MCF-7 (MCF-7/PacR). Control cells were treated with nonspecific siRNA (ns siRNA). Data are shown as mean ± SEM of at least two independent experiments. Resistance index was calculated as fold change in resistance when comparing the effect of specific ABCB1 siRNA vs. effect of ns siRNA (IC_{50} of ABCB1 siRNA-treated cells/IC_{50} of ns siRNA-treated cells).

SK-BR-3/PacR	Ns siRNA	ABCB1 siRNA	Resistance index
Paclitaxel	432. 8 ± 34.2	203.0 ± 54.6	0.47
Doxorubicin	125.4 ± 1.9	66.7 ± 4.1	0.53
MCF-7/PacR	Ns siRNA	ABCB1 siRNA	Resistance index
Paclitaxel	957.4 ± 70.1	262.7 ± 62.7	0.27
Doxorubicin	669.9 ± 124.8	255.3 ± 157.4	0.38

methylation and the gene expression level in sensitive and/or resistant breast cancer cells was not found (Table 4).

3.8. Multidrug resistance phenotype of paclitaxel-resistant cells

In order to assess the presence of the multidrug resistance (MDR) phenotype in our paclitaxel-resistant variants of SK-BR-3 and MCF-7 cells, we tested whether they displayed a decreased sensitivity to doxorubicin, another commonly used chemotherapeutic agent. We found that the paclitaxel-resistant SK-BR-3 and MCF-7 cells are able to survive and grow in 100 nM and 1000 nM doxorubicin, respectively. Such concentrations of doxorubicin in sensitive cells resulted in a significant decrease of the number of seeded cells. The resistance of SK-BR-3/PacR and MCF-7/PacR cells to doxorubicin was increased approximately 4-fold and 11-fold, respectively, compared to parental sensitive cell lines (Table 1). Silencing of ABCB1 by specific siRNA increased the sensitivity of SK-BR-3/PacR and MCF-7/PacR cells to doxorubicin 2-times and 3-times, respectively. However, it did not restore it to the level of sensitive cells (Table 3 and Fig. 9).

4. Discussion

We established paclitaxel-resistant variants of two commonly used breast cancer cell lines, i.e. ERα-positive and HER2-negative MCF-7 cells and ERα-negative and HER2-positive SKBR3 cells. We achieved a level of resistance that was much higher than the levels reported for most breast cancer cell lines, where resistance to paclitaxel was developed by stepwise adaptation to increasing drug concentrations (Ajabnoor et al., 2012; Chen et al., 2013; Coley et al., 2007; Guo et al., 2004; Hembruff et al., 2008; Lv et al., 2012; Kenicer et al., 2014; Tokuda et al., 2012; Wen et al., 2015). Concerning MCF-7 cells, only the group of Prof. Gündüz has reported the establishment of a variant resistant to 400 nM paclitaxel which was comparable with our model (Kars et al., 2008). As far as we know, establishment of paclitaxel-resistant variant of SK-BR-3 cells have only been reported in one other laboratory (Yang et al., 2014). Moreover, in contrast to some of the paclitaxel-resistant cell lines reported, our cells did not only display reduced paclitaxel apoptosis-inducing effects, but they were completely resistant to paclitaxel concentrations that killed nearly all cells of the original cell lines. In addition, our paclitaxel-resistant variants also displayed cross-resistance to doxorubicin, indicating the presence of the MDR phenotype. Taxane resistance was retained even in the absence of paclitaxel, similar as described by others (Kenicer et al., 2014). The long-term stability of paclitaxel resistance in absence of paclitaxel may point at the existence of some type of "genetic fixation" mechanism, e.g. gains and losses of chromosomal regions which were already described to be linked with acquired paclitaxel resistance in paclitaxel-resistant MDA-MB-231 cells (Kenicer et al., 2014) or may refer to existence of some epigenetic mechanism. However, based on

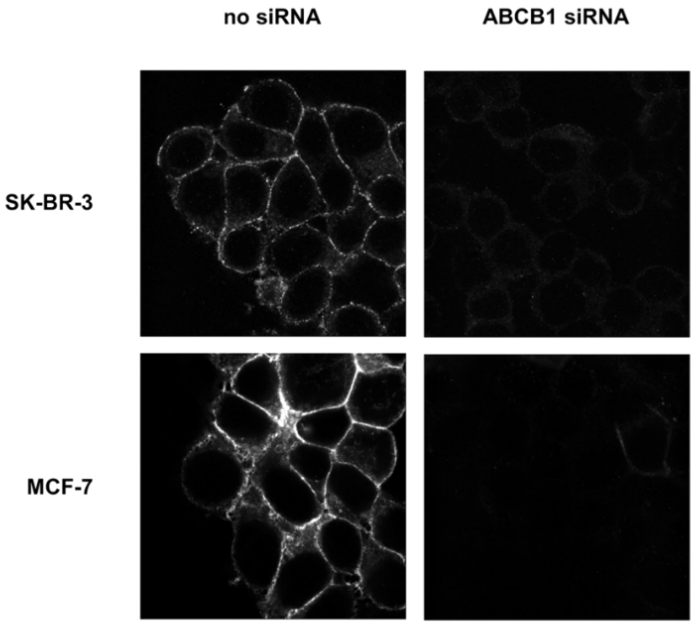

Fig. 8. Localization of ABCB1 protein in paclitaxel-resistant SK-BR-3 and MCF-7 cells. ABCB1 specific siRNA (ABCB1 siRNA) was used for silencing of ABCB1 expression. Control cells (no siRNA) were incubated in standard growth media but without the specific siRNA. Localization of ABCB1 within cells was assessed using confocal microscopy (see "Materials and methods"). Representative result from one of two independent experiments is shown.

Table 4
Relative methylation levels of CpG islands in promoter of *ABCB1* gene in paclitaxel-sensitive and paclitaxel-resistant SK-BR-3 and MCF-7 cells. Methylation is presented as percentage subtracted from the calibration curve as described in "Materials and methods". *p-Values for global methylation difference between sensitive and resistant cells were calculated by the paired *t*-test. **p-Values for difference between methylation and expression levels in sensitive and resistant cells was calculated by the Spearman test.

Cell line	Methylation of CpG islands in *ABCB1* promoter (%)	Methylation difference in sensitive vs. resistant cells (*p*-value*)	Methylation vs. gene expression (*p*-value**)
SK-BR-3 sensitive	82 ± 11		0.684
SK-BR-3 resistant	96 ± 8	**0.011**	0.225
MCF-7 sensitive	63 ± 19		0.684
MCF-7 resistant	62 ± 19	0.766	0.600

Differences with statistical significance ($p < 0.05$) are shown in bold.

our data, this putative epigenetic mechanisms does not involve changes in methylation of ABCB1 promoter. We believe that our isogenic experimental models represent very good platforms for studies concerning the processes and mechanisms linked with acquired paclitaxel resistance as well as multidrug resistance.

In this study, we took advantage of a clear-cut model system for analyzing the involvement of ABC transporters in acquired paclitaxel resistance. As far as we know, such a comprehensive analysis of expression of all known ABC transporters in paclitaxel-resistant cells has never been previously completed.

Comparing the properties of various cell lines with reported acquired paclitaxel resistance, it is evident that there is little consensus about the molecular explanation underlying this type of resistance. A consensus concerning the key player in paclitaxel resistance was achieved as to the up-regulation of ABCB1 in paclitaxel-resistant variants of various breast cancer cell lines, which has been demonstrated

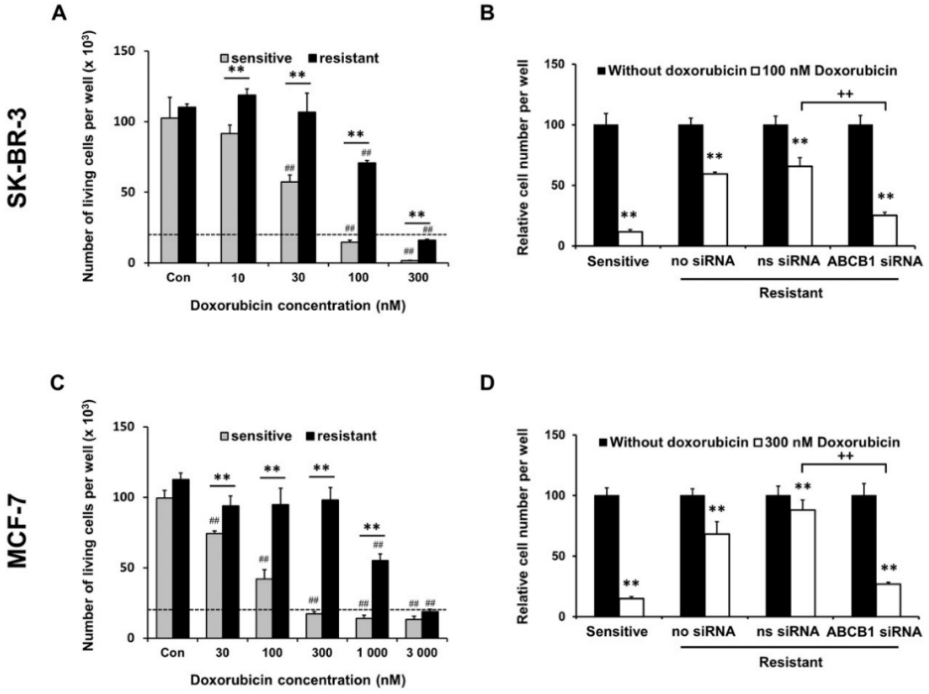

Fig. 9. (A, C) Effect of doxorubicin on the growth and survival of paclitaxel-sensitive and -resistant (A) SK-BR-3 and (C) MCF-7 cells, and (B, D) effect of ABCB1 silencing on the growth and survival of paclitaxel-sensitive and resistant (B) SK-BR-3 and (D) MCF-7 cells after doxorubicin treatment. (A, C) Control cells (Con) were incubated without doxorubicin. The number of cells of the inoculum (20×10^3 cells/100 μl of medium per well) is shown as a dashed line. The number of living cells was determined after 96 h of incubation (see "Materials and methods"). Each column represents the mean of 4 separate cultures ± SEM. $^{**}p < 0.01$ when comparing the effect in sensitive and resistant cells, $^{\#\#}p \le 0.01$ when comparing doxorubicin-treated cells with their respective control cells. The data shown were obtained in one representative experiment of three independent experiments. (B, D) The cells were prepared as described in "Materials and methods" and seeded at 20×10^3 cells/100 μl of medium per well. The relative number of living sensitive cells, resistant cells (no siRNA), resistant cells treated with nonspecific siRNA (ns siRNA) and resistant cells treated with ABCB1 specific siRNA (ABCB1 siRNA) was determined after 96 h of incubation with doxorubicin (100 nM for SK-BR-3 cells and 300 nM for MCF-7 cells). Each column represents the mean of 4 separate cultures ± SEM. $^{**}p < 0.01$ when comparing the effect in cells without doxorubicin and treated with doxorubicin. $^{++}p < 0.01$ when comparing the effect in ABCB1 siRNA-treated and ns siRNA-treated cells after doxorubicin application. The data shown were obtained in one representative experiment of two independent experiments.

on both the mRNA level (Chen et al., 2014; Duan et al., 2005; Hembruff et al., 2008; Kars et al., 2006; Kars et al., 2010; Tao et al., 2013) and the protein level (Ajabnoor et al., 2012; Chen et al., 2014; Guo et al., 2004; Hembruff et al., 2008; Kars et al., 2010; Reed et al., 2010; Tao et al., 2013; Shi et al., 2014). We also found ABCB1 over-expression on both the mRNA as well as the protein level in paclitaxel-resistant variants of both cell lines used, i.e. MCF-7 and SK-BR-3. Interestingly, ABCB1 over-expression does not appear to be essential for defense against lower paclitaxel concentrations since no ABCB1 over-expression was found during the early phases of development of paclitaxel and docetaxel resistance in MCF-7 cells (Kars et al., 2006). Furthermore, there was no ABCB1 protein expression found in paclitaxel-resistant MDA-MB-231 breast cancer cells in contrast to paclitaxel-resistant ZR75-14 breast cancer cells (Kenicer et al., 2014). This indicates that ABCB1, at least in some cases, was dispensable for the development of paclitaxel resistance. It means that also other protective mechanisms could exist. When searching for the underlying mechanism we found that the methylation status of the main CpG islands in the *ABCB1* gene promoter does not have an effect on ABCB1 transcript levels, although resistant subclones of SK-BR-3 cells presented hypermethylation in comparison to sensitive cells. Thus, the methylation pattern of *ABCB1* promoter does not explain the observed upregulation of ABCB1 in both resistant subclones and perhaps some other epigenetic mechanisms (e.g., micro RNA or posttranslational events as protein stabilization) may be responsible for the ABCB1 upregulation. This remains to be elucidated.

Concerning other transporters, the evidence of their linkage with taxane resistance is even more ambiguous. In studies concerning paclitaxel-resistant cells, ABCB4/MDR3, ABCG2/BCRP, and ABCC1/MRP1 were shown to be commonly up-regulated (Chen et al., 2014; Duan et al., 2005; Guo et al., 2004; Januchowski et al., 2014; Kars et al., 2006; Villeneuve et al., 2006). Unfortunately, some of these studies focused exclusively on mRNA results and information about expression on the protein level was missing. In our model, we identified clear over-expression of ABCB4 mRNA in paclitaxel-resistant variants of both cell lines used, however, we showed over-expression on the protein level only in paclitaxel-resistant MCF-7 cells. ABCB4 was found up-regulated, together with ABCB1, in the paclitaxel-resistant ovarian cell lines SKOV-3 and OVCAR. However, its contribution to paclitaxel resistance was only modest in comparison with ABCB1, as demonstrated by siRNA silencing (Duan et al., 2004). Thus the role of ABCB4 in paclitaxel resistance does not seem to be crucial, despite the fact that its up-regulation was commonly found. We also demonstrated over-expression of ABCG2 protein in paclitaxel-resistant SK-BR-3 cells, which confirmed the mRNA data. However, we did not observe over-expression of ABCG2 or ABCC1 in paclitaxel-resistant MCF-7 cells, which was in contrast to the report of Cai et al. (2014).

In paclitaxel-resistant MCF-7 cells, we found up-regulation of ABCC2 on both mRNA and protein level. Nevertheless, ABCC2 was also found over-expressed in the tamoxifen-resistant MCF-7 breast cancer cells (Choi et al., 2013). Interestingly, as to transporter ABCC2, the cellular distribution seems to play role in resistance, since localization of ABCC2 in the nuclear envelope was shown to predict poor clinical outcomes in breast cancer (Maciejczyk et al., 2012).

We also found significant up-regulation of ABCC3 protein in both paclitaxel-resistant sublines used despite no change (MCF-7/PacR) or significant down-regulation (SK-BR-3/PacR) was demonstrated on mRNA level. ABCC3 was already shown to mediate in vitro resistance to paclitaxel. Moreover, amplification of ABCC3 was found to be present in primary breast tumors and occur predominantly in HER2-amplified and luminal tumors (O'Brien et al., 2008). ABCC3 expression was shown to be induced by chemotherapeutics application in vitro as well as in patient samples and its role in breast cancer chemoresistance was proposed (Balaji et al., 2016). It seems to be induced by chemotherapy also in ovarian cancer (Auner et al., 2010). Taken together, transporter ABCC3 seems to be important player in MDR development and deserves further attention.

As to ABCC family of ABC transporters, ABCC4 was also upregulated on protein level in paclitaxel-resistant SK-BR-3 cells. ABCC4 was already demonstrated to confer resistance to docetaxel in docetaxel-resistant prostate cancer cells (Oprea-Lager et al., 2013). In contrast, we found no significant changes in protein levels of ABCC1, ABCC7, ABCC8, and ABCC9 for both cell lines tested. It would indicate no role for these transporters in taxane resistance in our cells. However, significant associations of intratumoral levels of ABCC1 and ABCC8 with tumor grade and expression of hormonal receptors were found in breast carcinoma patients (Hlavac et al., 2013). Taken together, concerning the transporters tested, only over-expression of ABCB1 and also ABCC3 was found on the protein level in both paclitaxel-resistant cell lines. This fact disqualifies the other transporters tested as universal enhancers of taxane resistance. The likely explanation for the observed inconsistencies between expression of some ABC transporters on the mRNA and protein level is probably the presence of multiple levels of expression regulation. The existence of a block in mRNA translation has already been shown for ABCB1 in K562 cells (Gomez-Martinez et al., 2007; Yague et al., 2003).

The level of expression of caspases, key triggers of apoptosis execution, has also been reported as a possible regulator of drug resistance, including taxanes (Janssen et al., 2007; Mielgo et al., 2009). Nevertheless, we did not observe any changes in levels of executioner caspase-3 (relevant only to SK-BR-3 cells) and caspase-7 between sensitive and paclitaxel-resistant cells in both cells lines tested. Similar data were obtained in studies of Guo et al. (2004) and Villeneuve et al. (2006) using paclitaxel-resistant MCF-7 cells. In contrast, data from Ajabnoor et al. (2012) and Sharifi et al. (2014) indicate that the loss of caspase-7 and caspase-9 expression was associated with emerging paclitaxel resistance in paclitaxel-resistant MCF-7 cells.

To sum up, when comparing properties of various cell lines with reported acquired paclitaxel resistance, it is evident that there is more than one universal molecular pattern underlying the resistance. Differences concerning the involvement of particular ABC transporters and other proteins in paclitaxel-resistant cells originating from the same parental cell line can stem from a different level of resistance achieved or, more likely, from accidental selection of specific clones displaying a specific type of gene expression pattern resulting in paclitaxel-resistance.

Very interestingly, we found that both paclitaxel resistant variants of SK-BR-3 and MCF-7 cells maintained sensitivity to the second-generation taxane SB-T-1216 (Ojima et al., 1996) that was similar to the sensitivity of the original cell lines. We have previously shown in a variety of cell lines that this second-generation taxane is comparable or even more effective than paclitaxel, especially in cells exerting higher resistance (Jelinek et al., 2013; Jelinek et al., 2015; Kovar et al., 2009; Voborilova et al., 2011). Moreover, despite repeated efforts, we were not able to establish variants of SK-BR-3 and MCF-7 cells resistant to SB-T-1216. This indicates that the second-generation taxane SB-T-1216 does not exhibit identical molecular effects as paclitaxel and instead activates cellular pathways/mechanisms that are not prone to easy development of effective defense mechanisms. This finding justifies, together with other possible advantages of usage, the development of new generations of taxanes as alternative treatment for breast cancers resistant to conventional therapy.

In both paclitaxel-resistant sublines, ABCB1 knockdown increased significantly paclitaxel and doxorubicin sensitivity, however, it did not restore the sensitivity to the level of the original cells. This indicates that multiple mechanisms besides ABCB1 over-expression are behind paclitaxel and doxorubicin resistance. One of possible players in paclitaxel sensitivity could be TRIP 6, which has been recently shown to be up-regulated in our paclitaxel-resistant MCF-7 cells and which significantly influences the sensitivity of MCF-7 cells to paclitaxel (Pavlikova et al., 2015). Additionally, there are other molecules and mechanisms reported to influence paclitaxel sensitivity, e.g. ERα-mediated ABCB1 over-expression (Shi et al., 2014), activation of MAPK/Erk1/2 signaling pathway followed by increased Egr-1 and MDR expression (Tao et al.,

2013), increased autophagy, and mitophagy (Ajabnoor et al., 2012; Wen et al., 2015). Furthermore, there are proteins that are known to be deregulated in paclitaxel-resistant MCF-7 cells, e.g. cathepsin L (Villeneuve et al., 2006), cathepsin D (Pavlikova et al., 2015), caveolin (Villeneuve et al., 2006), Bcl-2 (Villeneuve et al., 2006), SET nuclear oncogene, and transgelin 2 (Chen et al., 2014). In addition, we have demonstrated up-regulation of serpin B3, serpin B4, and heat shock protein 27 as well as down-regulation of cytokeratin 18 in paclitaxel-resistant SK-BR-3 cells (Pavlikova et al., 2014).

To conclude, we established paclitaxel-resistant variants of the SK-BR-3 and MCF-7 breast cancer cell lines that can serve as a good model for analyses of mechanisms involved in taxane resistance. Analysis of the expression of human ABC transporters has revealed that only transporters ABCB1 and ABCC3 were significantly over-expressed on the protein level in both paclitaxel-resistant sublines. Silencing of ABCB1 expression leads to a significant increase, but not complete restoration, of paclitaxel sensitivity. This indicates involvement of multiple mechanisms in paclitaxel resistance. Based on our data, transporters ABCB4, ABCC2, ABCC4 and ABCG2 may also contribute to paclitaxel resistance. Resistance to paclitaxel in both resistant sublines was circumvented by the second-generation taxane SB-T-1216. Moreover, we demonstrated that it was not possible to develop resistance to this taxane in SK-BR-3 and MCF-7 cells. It indicates that tested breast cancer cells are unable to develop an effective defense mechanism against some second-generation taxanes.

Transparency document

The Transparency document associated with this article can be found in the online version.

Acknowledgement

This work was supported by grant NT 13679-4 of the Internal Grant Agency, Ministry of Health of the Czech Republic, the Ministry of Health of the Czech Republic, project no. 15-25618A and grant KONTAKT II LH 14096 of the Ministry of Education, Youth and Sports of the Czech Republic. We would like to thank Prof. I. Ojima (Stony Brook University, NY, USA) for providing us with the taxane SB-T-1216 and Dr. Jaroslav Truksa (Institute of Molecular Genetics, Academy of Sciences, Prague, Czech Republic) for providing us with ABCC3 and ABCC4 antibodies.

References

Ajabnoor, G.M., Crook, T., Coley, H.M., 2012. Paclitaxel resistance is associated with switch from apoptotic to autophagic cell death in MCF-7 breast cancer cells. Cell Death Dis. 3, e260.

Andersen, C.L., Jensen, J.L., Orntoft, T.F., 2004. Normalization of real-time quantitative reverse transcription-PCR data: a model-based variance estimation approach to identify genes suited for normalization, applied to bladder and colon cancer data sets. Cancer Res. 64, 5245–5250.

Auner, V., Sehouli, J., Oskay-Oezcelik, G., Horvat, R., Speiser, P., Zeillinger, R., 2010. ABC transporter gene expression in benign and malignant ovarian tissue. Gynecol. Oncol. 117, 198–201.

Balaji, S.A., Udupa, N., Chamallamudi, M.R., Gupta, V., Rangarajan, A., 2016. Role of the drug transporter ABCC3 in breast cancer chemoresistance. PLoS One 11, e0155013.

Brown, R., Curry, E., Magnani, L., Wilhelm-Benartzi, C.S., Borley, J., 2014. Poised epigenetic states and acquired drug resistance in cancer. Nat. Rev. Cancer 14, 747–753.

Cai, J., Chen, S., Zhang, W., Hu, S., Lu, J., Xing, J., Dong, Y., 2014. Paeonol reverses paclitaxel resistance in human breast cancer cells by regulating the expression of transgelin 2. Phytomedicine 21, 984–991.

Chang, H., Rha, S.Y., Jeung, H.C., Im, C.K., Ahn, J.B., Kwon, W.S., Yoo, N.C., Roh, J.K., Chung, H.C., 2009. Association of the ABCB1 gene polymorphisms 2677G > T/A and 3435C > T with clinical outcomes of paclitaxel monotherapy in metastatic breast cancer patients. Ann. Oncol. 20, 272–277.

Chen, S.Y., Hu, S.S., Dong, Q., Cai, J.X., Zhang, W.P., Sun, J.Y., Wang, T.T., Xie, J., He, H.R., Xing, J.F., Lu, J., Dong, Y.L., 2013. Establishment of paclitaxel-resistant breast cancer cell line and nude mice models, and underlying multidrug resistance mechanisms in vitro and in vivo. Asian Pac. J. Cancer Prev. 14, 6135–6140.

Chen, S., Dong, Q., Hu, S., Cai, J., Zhang, W., Sun, J., Wang, T., Xie, J., He, H., Xing, J., Lu, J., Dong, Y., 2014. Proteomic analysis of the proteins that are associated with the resistance to paclitaxel in human breast cancer cells. Mol. BioSyst. 10, 294–303.

Choi, H.K., Cho, K.B., Phuong, N.T., Han, C.Y., Han, H.K., Hien, T.T., Choi, H.S., Kang, K.W., 2013. SIRT1-mediated FoxO1 deacetylation is essential for multidrug resistance-associated protein 2 expression in tamoxifen-resistant breast cancer cells. Mol. Pharm. 10, 2517–2527.

Coley, H.M., Labeed, F.H., Thomas, H., Hughes, M.P., 2007. Biophysical characterization of MDR breast cancer cell lines reveals the cytoplasm is critical in determining drug sensitivity. Biochim. Biophys. Acta 1770, 601–608.

Cui, S.Y., Wang, R., Chen, L.B., 2013. MicroRNAs: key players of taxane resistance and their therapeutic potential in human cancers. J. Cell. Mol. Med. 17, 1207–1217.

Duan, Z., Brakora, K.A., Seiden, M.V., 2004. Inhibition of ABCB1 (MDR1) and ABCB4 (MDR3) expression by small interfering RNA and reversal of paclitaxel resistance in human ovarian cancer cells. Mol. Cancer Ther. 3, 833–838.

Duan, Z., Lamendola, D.E., Duan, Y., Yusuf, R.Z., Seiden, M.V., 2005. Description of paclitaxel resistance-associated genes in ovarian and breast cancer cell lines. Cancer Chemother. Pharmacol. 55, 277–285.

Ehrlichova, M., Vaclavikova, R., Ojima, I., Pepe, A., Kuznetsova, L.V., Chen, J., Truksa, J., Kovar, J., Gut, I., 2005a. Transport and cytotoxicity of paclitaxel, docetaxel, and novel taxanes in human breast cancer cells. Naunyn Schmiedeberg's Arch. Pharmacol. 372, 95–105.

Ehrlichova, M., Koc, M., Truksa, J., Nadova, Z., Vaclavikova, R., Kovar, J., 2005b. Cell death induced by taxanes in breast cancer cells: cytochrome C is released in resistant but not in sensitive cells. Anticancer Res. 25, 4215–4224.

Ehrlichova, M., Ojima, I., Chen, J., Vaclavikova, R., Nemcova-Furstova, V., Voborilova, J., Simek, P., Horsky, S., Soucek, P., Kovar, J., Brabec, M., Gut, I., 2012. Transport, metabolism, cytotoxicity and effects of novel taxanes on the cell cycle in MDA-MB-435 and NCI/ADR-RES cells. Naunyn Schmiedeberg's Arch. Pharmacol. 385, 1035–1048.

Elledge, R.M., Fuqua, S.A., Clark, G.M., Pujol, P., Allred, D.C., McGuire, W.L., 1993. Prognostic significance of p53 gene alterations in node-negative breast cancer. Breast Cancer Res. Treat. 26, 225–235.

Fazeny-Dorner, B., Piribauer, M., Wenzel, C., Fakhrai, N., Pirker, C., Berger, W., Sedivy, R., Rudas, M., Filipits, M., Okamoto, I., Marosi, C., 2003. Cytogenetic and comparative genomic hybridization findings in four cases of breast cancer after neoadjuvant chemotherapy. Cancer Genet. Cytogenet. 146, 161–166.

Fletcher, J.I., Williams, R.T., Henderson, M.J., Norris, M.D., Haber, M., 2016. ABC transporters as mediators of drug resistance and contributors to cancer cell biology. Drug Resist. Updat. 26, 1–9.

Gomez-Martinez, A., Garcia-Morales, P., Carrato, A., Castro-Galache, M.D., Soto, J.L., Carrasco-Garcia, E., Garcia-Bautista, M., Guaraz, P., Ferragut, J.A., Saceda, M., 2007. Post-transcriptional regulation of P-glycoprotein expression in cancer cell lines. Mol. Cancer Res. 5, 641–653.

Goncalves, A., Braguer, D., Kamath, K., Martello, L., Briand, C., Horwitz, S., Wilson, L., Jordan, M.A., 2001. Resistance to taxol in lung cancer cells associated with increased microtubule dynamics. Proc. Natl. Acad. Sci. U. S. A. 98, 11737–11742.

Guo, B., Villeneuve, D.J., Hembruff, S.L., Kirwan, A.F., Blais, D.E., Bonin, M., Parissenti, A.M., 2004. Cross-resistance studies of isogenic drug-resistant breast tumor cell lines support recent clinical evidence suggesting that sensitivity to paclitaxel may be strongly compromised by prior doxorubicin exposure. Breast Cancer Res. Treat. 85, 31–51.

Hansen, S.N., Westergaard, D., Thomsen, M.B., Vistesen, M., Do, K.N., Fogh, L., Belling, K.C., Wang, J., Yang, H., Gupta, R., Ditzel, H.J., Moreira, J., Brunner, N., Stenvang, J., Schrohl, A.S., 2015. Acquisition of docetaxel resistance in breast cancer cells reveals upregulation of ABCB1 expression as a key mediator of resistance accompanied by discrete upregulation of other specific genes and pathways. Tumour Biol. 36, 4327–4338.

Harris, J.W., Rahman, A., Kim, B.R., Guengerich, F.P., Collins, J.M., 1994. Metabolism of taxol by human hepatic microsomes and liver slices: participation of cytochrome P450 3A4 and an unknown P450 enzyme. Cancer Res. 54, 4026–4035.

Hembruff, S.L., Laberge, M.L., Villeneuve, D.J., Guo, B., Veitch, Z., Cecchetto, M., Parissenti, A.M., 2008. Role of drug transporters and drug accumulation in the temporal acquisition of drug resistance. BMC Cancer 8, 318.

Hlavac, V., Brynychova, V., Vaclavikova, R., Ehrlichova, M., Vrana, D., Pecha, V., Kozevnikovova, R., Trnkova, M., Gatek, J., Kopperova, D., Gut, I., Soucek, P., 2013. The expression profile of ATP-binding cassette transporter genes in breast carcinoma. Pharmacogenomics 14, 515–529.

Janssen, K., Pohlmann, S., Janicke, R.U., Schulze-Osthoff, K., Fischer, U., 2007. Apaf-1 and caspase-9 deficiency prevents apoptosis in a bax-controlled pathway and promotes clonogenic survival during paclitaxel treatment. Blood 110, 3662–3672.

Januchowski, R., Zawierucha, P., Rucinski, M., Andrzejewska, M., Wojtowicz, K., Nowicki, M., Zabel, M., 2014. Drug transporter expression profiling in chemoresistant variants of the A2780 ovarian cancer cell line. Biomed. Pharmacother. 68, 447–453.

Jelinek, M., Balusikova, K., Kopperova, D., Nemcova-Furstova, V., Sramek, J., Fidlerova, J., Zanardi, I., Ojima, I., Kovar, J., 2013. Caspase-2 is involved in cell death induction by taxanes in breast cancer cells. Cancer Cell Int. 13, 42.

Jelinek, M., Balusikova, K., Schmiedlova, M., Nemcova-Furstova, V., Sramek, J., Stancikova, J., Zanardi, I., Ojima, I., Kovar, J., 2015. The role of individual caspases in cell death induction by taxanes in breast cancer cells. Cancer Cell Int. 15, 8.

Jordan, M.A., Wendell, K., Gardiner, S., Derry, W.B., Copp, H., Wilson, L., 1996. Mitotic block induced in HeLa cells by low concentrations of paclitaxel (taxol) results in abnormal mitotic exit and apoptotic cell death. Cancer Res. 56, 816–825.

Kars, M.D., Iseri, O.D., Gunduz, U., Ural, A.U., Arpaci, F., Molnar, J., 2006. Development of rational in vitro models for drug resistance in breast cancer and modulation of MDR by selected compounds. Anticancer Res. 26, 4559–4568.

Kars, M.D., Iseri, O.D., Gunduz, U., Molnar, J., 2008. Reversal of multidrug resistance by synthetic and natural compounds in drug-resistant MCF-7 cell lines. Chemotherapy 54, 194–200.

Kars, M.D., Iseri, O.D., Gunduz, U., 2010. Drug resistant breast cancer cells overexpress ETS1 gene. Biomed. Pharmacother. 64, 458–462.

Kastl, L., Brown, I., Schofield, A.C., 2010. Altered DNA methylation is associated with docetaxel resistance in human breast cancer cells. Int. J. Oncol. 36, 1235–1241.

Kaur, J., Bachhawat, A.K., 2009. A modified Western blot protocol for enhanced sensitivity in the detection of a membrane protein. Anal. Biochem. 384, 348–349.

Kavallaris, M., 2010. Microtubules and resistance to tubulin-binding agents. Nat. Rev. Cancer 10, 194–204.

Kenicer, J., Spears, M., Lyttle, N., Taylor, K.J., Liao, L., Cunningham, C.A., Lambros, M., MacKay, A., Yao, C., Reis-Filho, J., Bartlett, J.M., 2014. Molecular characterisation of isogenic taxane resistant cell lines identify novel drivers of drug resistance. BMC Cancer 14, 762.

Kovar, J., Ehrlichova, M., Smejkalova, B., Zanardi, I., Ojima, I., Gut, I., 2009. Comparison of cell death-inducing effect of novel taxane SB-T-1216 and paclitaxel in breast cancer cells. Anticancer Res. 29, 2951–2960.

Li, L.C., Dahiya, R., 2002. MethPrimer: designing primers for methylation PCRs. Bioinformatics 18, 1427–1431.

Li, W.J., Zhong, S.L., Wu, Y.J., Xu, W.D., Xu, J.J., Tang, J.H., Zhao, J.H., 2013. Systematic expression analysis of genes related to multidrug-resistance in isogenic docetaxel- and adriamycin-resistant breast cancer cell lines. Mol. Biol. Rep. 40, 6143–6150.

Li, W., Zhai, B., Zhi, H., Li, Y., Jia, L., Ding, C., Zhang, B., You, W., 2014. Association of ABCB1, beta tubulin I, and III with multidrug resistance of MCF7/DOC subline from breast cancer cell line MCF7. Tumour Biol. 35, 8883–8891.

Litviakov, N.V., Cherdyntseva, N.V., Tsyganov, M.M., Denisov, E.V., Garbukov, E.Y., Merzliakova, M.K., Volkomorov, V.V., Vtorushin, S.V., Zavyalova, M.V., Slonimskaya, E.M., Perelmuter, V.M., 2013. Changing the expression vector of multidrug resistance genes is related to neoadjuvant chemotherapy response. Cancer Chemother. Pharmacol. 71, 153–163.

Luo, Y., Wang, X., Wang, H., Xu, Y., Wen, Q., Fan, S., Zhao, R., Jiang, S., Yang, J., Liu, Y., Li, X., Xiong, W., Ma, J., Peng, S., Zeng, Z., Li, X., Phillips, J.B., Li, G., Tan, M., Zhou, M., 2015. High Bak expression is associated with a favorable prognosis in breast cancer and sensitizes breast cancer cells to paclitaxel. PLoS One 10, e0138955.

Lv, K., Liu, L., Wang, L., Yu, J., Liu, X., Cheng, Y., Dong, M., Teng, R., Wu, L., Fu, P., Deng, W., Hu, W., Teng, L., 2012. Lin28 mediates paclitaxel resistance by modulating p21, Rb and Let-7a miRNA in breast cancer cells. PLoS One 7, e40008.

Maciejczyk, A., Jagoda, E., Wysocka, T., Matkowski, R., Gyorffy, B., Lage, H., Surowiak, P., 2012. ABCC2 (MRP2, cMOAT) localized in the nuclear envelope of breast carcinoma cells correlates with poor clinical outcome. Pathol. Oncol. Res. 18, 331–342.

Markman, M., 2008. Pharmaceutical management of ovarian cancer: current status. Drugs 68, 771–789.

McGrogan, B.T., Gilmartin, B., Carney, D.N., McCann, A., 2008. Taxanes, microtubules and chemoresistant breast cancer. Biochim. Biophys. Acta 1785, 96–132.

Mielgo, A., Torres, V.A., Clair, K., Barbero, S., Stupack, D.G., 2009. Paclitaxel promotes a caspase 8-mediated apoptosis through death effector domain association with microtubules. Oncogene 28, 3551–3562.

Miller, M.L., Ojima, I., 2001. Chemistry and chemical biology of taxane anticancer agents. Chem. Rec. 1, 195–211.

Mohelnikova-Duchonova, B., Brynychova, V., Oliverius, M., Honsova, E., Kala, Z., Muckova, K., Soucek, P., 2013. Differences in transcript levels of ABC transporters between pancreatic adenocarcinoma and nonneoplastic tissues. Pancreas 42, 707–716.

Murray, S., Briasoulis, E., Linardou, H., Bafaloukos, D., Papadimitriou, C., 2012. Taxane resistance in breast cancer: mechanisms, predictive biomarkers and circumvention strategies. Cancer Treat. Rev. 38, 890–903.

Musilkova, J., Kovar, J., 2001. Additive stimulatory effect of extracellular calcium and potassium on non-transferrin ferric iron uptake by HeLa and K562 cells. Biochim. Biophys. Acta 1514, 117–126.

Nemcova-Furstova, V., James, R.F., Kovar, J., 2011. Inhibitory effect of unsaturated fatty acids on saturated fatty acid-induced apoptosis in human pancreatic beta-cells: activation of caspases and ER stress induction. Cell. Physiol. Biochem. 27, 525–538.

Nemcova-Furstova, V., Balusikova, K., Sramek, J., James, R.F., Kovar, J., 2013. Caspase-2 and JNK activated by saturated fatty acids are not involved in apoptosis induction but modulate ER stress in human pancreatic beta-cells. Cell. Physiol. Biochem. 31, 277–289.

O'Brien, C., Cavet, G., Pandita, A., Hu, X., Haydu, L., Mohan, S., Toy, K., Rivers, C.S., Modrusan, Z., Amler, L.C., Lackner, M.R., 2008. Functional genomics identifies ABCC3 as a mediator of taxane resistance in HER2-amplified breast cancer. Cancer Res. 68, 5380–5389.

Ojima, I., Slater, J.C., Michaud, E., Kuduk, S.D., Bounaud, P.Y., Vrignaud, P., Bissery, M.C., Veith, J.M., Pera, P., Bernacki, R.J., 1996. Syntheses and structure-activity relationships of the second-generation antitumor taxoids: exceptional activity against drug-resistant cancer cells. J. Med. Chem. 39, 3889–3896.

Ojima, I., Chen, J., Sun, L., Borella, C.P., Wang, T., Miller, M.L., Lin, S., Geng, X., Kuznetsova, L., Qu, C., Gallager, D., Zhao, X., Zanardi, I., Xia, S., Horwitz, S.B., Mallen-St, C.J., Guerriero, J.L., Bar-Sagi, D., Veith, J.M., Pera, P., Bernacki, R.J., 2008. Design, synthesis, and biological evaluation of new-generation taxoids. J. Med. Chem. 51, 3203–3221.

Oprea-Lager, D.E., Bijnsdorp, I.V., Van Moorselaar, R.J., Van Den Eertwegh, A.J., Hoekstra, O.S., Geldof, A.A., 2013. ABCC4 decreases docetaxel and not cabazitaxel efficacy in prostate cancer cells in vitro. Anticancer Res. 33, 387–391.

Orr, G.A., Verdier-Pinard, P., McDaid, H., Horwitz, S.B., 2003. Mechanisms of taxol resistance related to microtubules. Oncogene 22, 7280–7295.

Pavlikova, N., Bartonova, I., Dincakova, L., Halada, P., Kovar, J., 2014. Differentially expressed proteins in human breast cancer cells sensitive and resistant to paclitaxel. Int. J. Oncol. 45, 822–830.

Pavlikova, N., Bartonova, I., Balusikova, K., Kopperova, D., Halada, P., Kovar, J., 2015. Differentially expressed proteins in human MCF-7 breast cancer cells sensitive and resistant to paclitaxel. Exp. Cell Res. 333, 1–10.

Pfaffl, M.W., Horgan, G.W., Dempfle, L., 2002. Relative expression software tool (REST) for group-wise comparison and statistical analysis of relative expression results in real-time PCR. Nucleic Acids Res. 30, e36.

Reed, K., Hembruff, S.L., Laberge, M.L., Villeneuve, D.J., Cote, G.B., Parissenti, A.M., 2008. Hypermethylation of the ABCB1 downstream gene promoter accompanies ABCB1 gene amplification and increased expression in docetaxel-resistant MCF-7 breast tumor cells. Epigenetics 3, 270–280.

Reed, K., Hembruff, S.L., Sprowl, J.A., Parissenti, A.M., 2010. The temporal relationship between ABCB1 promoter hypomethylation, ABCB1 expression and acquisition of drug resistance. Pharmacogenomics J. 10, 489–504.

Sharifi, S., Barar, J., Hejazi, M.S., Samadi, N., 2014. Roles of the Bcl-2/Bax ratio, caspase-8 and 9 in resistance of breast cancer cells to paclitaxel. Asian Pac. J. Cancer Prev. 15, 8617–8622.

Shi, J.F., Yang, N., Ding, H.J., Zhang, J.X., Hu, M.L., Leng, Y., Han, X., Sun, Y.J., 2014. ERalpha directly activated the MDR1 transcription to increase paclitaxel-resistance of ERalpha-positive breast cancer cells in vitro and in vivo. Int. J. Biochem. Cell Biol. 53, 35–45.

Sudo, T., Nitta, M., Saya, H., Ueno, N.T., 2004. Dependence of paclitaxel sensitivity on a functional spindle assembly checkpoint. Cancer Res. 64, 2502–2508.

Tamaki, A., Ierano, C., Szakacs, G., Robey, R.W., Bates, S.E., 2011. The controversial role of ABC transporters in clinical oncology. Essays Biochem. 50, 209–232.

Tao, W., Shi, J.F., Zhang, Q., Xue, B., Sun, Y.J., Li, C.J., 2013. Egr-1 enhances drug resistance of breast cancer by modulating MDR1 expression in a GGPPS-independent manner. Biomed. Pharmacother. 67, 197–202.

Tokuda, E., Seino, Y., Arakawa, A., Saito, M., Kasumi, F., Hayashi, S., Yamaguchi, Y., 2012. Estrogen receptor-alpha directly regulates sensitivity to paclitaxel in neoadjuvant chemotherapy for breast cancer. Breast Cancer Res. Treat. 133, 427–436.

Tubiana-Hulin, M., 2005. How to maximize the efficacy of taxanes in breast cancer. Cancer Treat. Rev. 31 (Suppl 4), S3–S9.

Vandesompele, J., De Preter, K., Pattyn, F., Poppe, B., Van Roy, N., De Paepe, A., Speleman, F., 2002. Accurate normalization of real-time quantitative RT-PCR data by geometric averaging of multiple internal control genes. Genome Biol. 3 (RESEARCH0034).

Villeneuve, D.J., Hembruff, S.L., Veitch, Z., Cecchetto, M., Dew, W.A., Parissenti, A.M., 2006. cDNA microarray analysis of isogenic paclitaxelsand doxorubicin-resistant breast tumor cell lines reveals distinct drug-specific genetic signatures of resistance. Breast Cancer Res. Treat. 96, 17–39.

Voborilova, J., Nemcova-Furstova, V., Neubauerova, J., Ojima, I., Zanardi, I., Gut, I., Kovar, J., 2011. Cell death induced by novel fluorinated taxanes in drug-sensitive and drug-resistant cancer cells. Investig. New Drugs 29, 411–423.

Vtorushin, S.V., Khristenko, K.Y., Zavyalova, M.V., Perelmuter, V.M., Litviakov, N.V., Denisov, E.V., Dulesova, A.Y., Cherdyntseva, N.V., 2014. The phenomenon of multidrug resistance in the treatment of malignant tumors. Exp. Oncol. 36, 144–156.

Wang, M.Y., Chen, P.S., Prakash, E., Hsu, H.C., Huang, H.Y., Lin, M.T., Chang, K.J., Kuo, M.L., 2009. Connective tissue growth factor confers drug resistance in breast cancer through concomitant up-regulation of Bcl-xL and cIAP1. Cancer Res. 69, 3482–3491.

Wang, X., Yi, L., Zhu, Y., Zou, J., Hong, Y., Zheng, W., 2011. AKT signaling pathway in invasive ductal carcinoma of the breast: correlation with ERa, ERbeta and HER-2 expression. Tumori 97, 185–190.

Wen, J., Yeo, S., Wang, C., Chen, S., Sun, S., Haas, M.A., Tu, W., Jin, F., Guan, J.L., 2015. Autophagy inhibition re-sensitizes pulse stimulation-selected paclitaxel-resistant triple negative breast cancer cells to chemotherapy-induced apoptosis. Breast Cancer Res. Treat. 149, 619–629.

Yague, E., Armesilla, A.L., Harrison, G., Elliott, J., Sardini, A., Higgins, C.F., Raguz, S., 2003. P-glycoprotein (MDR1) expression in leukemic cells is regulated at two distinct steps, mRNA stabilization and translational initiation. J. Biol. Chem. 278, 10344–10352.

Yang, Q., Huang, J., Wu, Q., Cai, Y., Zhu, L., Lu, X., Chen, S., Chen, C., Wang, Z., 2014. Acquisition of epithelial-mesenchymal transition is associated with Skp2 expression in paclitaxel-resistant breast cancer cells. Br. J. Cancer 110, 1958–1967.

Yared, J.A., Tkaczuk, K.H., 2012. Update on taxane development: new analogs and new formulations. Drug Des Devel. Ther. 6, 371–384.

Yin, S., Bhattacharya, R., Cabral, F., 2010. Human mutations that confer paclitaxel resistance. Mol. Cancer Ther. 9, 327–335.

Zhang, W., Ding, W., Chen, Y., Feng, M., Ouyang, Y., Yu, Y., He, Z., 2011. Up-regulation of breast cancer resistance protein plays a role in HER2-mediated chemoresistance through PI3K/Akt and nuclear factor-kappa B signaling pathways in MCF7 breast cancer cells. Acta Biochim. Biophys. Sin. Shanghai 43, 647–653.

4.2 Paper 2

SUBSTITUENTS AT THE C3' AND C3'N POSITIONS ARE CRITICAL FOR TAXANES TO OVERCOME ACQUIRED RESISTANCE OF CANCER CELLS TO PACLITAXEL

Jelínek, M., Balušíková, K., **Daniel, P.,** Němcová-Fürstová, V., Kirubakaran, P., Jaček, M., Wei, L., Wang, X., Vondrášek, J., Ojima, I., & Kovář, J. (**2018**).

Toxicology and applied pharmacology, *347*, 79–91

https://doi.org/10.1016/j.taap.2018.04.002

Toxicology and Applied Pharmacology 347 (2018) 79–91

Contents lists available at ScienceDirect

Toxicology and Applied Pharmacology

journal homepage: www.elsevier.com/locate/taap

Substituents at the C3′ and C3′N positions are critical for taxanes to overcome acquired resistance of cancer cells to paclitaxel

Michael Jelínek[a], Kamila Balušíková[a], Petr Daniel[a], Vlasta Němcová-Fürstová[a], Palani Kirubakaran[b], Martin Jaček[c], Longfei Wei[d], Xin Wang[d], Jiří Vondrášek[b], Iwao Ojima[d], Jan Kovář[a,*]

[a] Department of Cell and Molecular Biology, Third Faculty of Medicine, Charles University, Ruská 87, 110 00 Prague, Czech Republic
[b] Institute of Organic Chemistry and Biochemistry, Czech Academy of Science, Flemingovo náměstí 542/2, 166 10 Prague, Czech Republic
[c] Department of Hygiene, Epidemiology and Preventive Medicine, Third Faculty of Medicine, Charles University, Ruská 87, 110 00 Prague, Czech Republic
[d] Department of Chemistry, Institute of Chemical Biology and Drug Discovery, State University of New York at Stony Brook, Stony Brook, NY 11794-3400, USA

ARTICLE INFO

Keywords:
Taxane derivates
Acquired resistance to paclitaxel
Breast cancer cells
ABCB1 transporter
Molecular docking

ABSTRACT

We tested the role of substituents at the C3′ and C3′N positions of the taxane molecule to identify taxane derivatives capable of overcoming acquired resistance to paclitaxel. Paclitaxel-resistant sublines SK-BR-3/PacR and MCF-7/PacR as well as the original paclitaxel-sensitive breast cancer cell lines SK-BR-3 and MCF-7 were used for testing. Increased expression of the ABCB1 transporter was found to be involved in the acquired resistance. We tested three groups of taxane derivatives: (1) phenyl group at both C3′ and C3′N positions, (2) one phenyl at one of the C3′ and C3′N positions and a non-aromatic group at the second position, (3) a non-aromatic group at both C3′ and C3′N positions. We found that the presence of phenyl groups at both C3′ and C3′N positions is associated with low capability of overcoming acquired paclitaxel resistance compared to taxanes containing at least one non-aromatic substituent at the C3′ and C3′N positions. The increase in the ATPase activity of ABCB1 transporter after the application of taxanes from the first group was found to be somewhat higher than after the application of taxanes from the third group. Molecular docking studies demonstrated that the docking score was the lowest, i.e. the highest binding affinity, for taxanes from the first group. It was intermediate for taxanes from the second group, and the highest for taxanes from the third group. We conclude that at least one non-aromatic group at the C3′ and C3′N positions of the taxane structure, resulting in reduced affinity to the ABCB1 transporter, brings about high capability of taxane to overcome acquired resistance of breast cancer cells to paclitaxel, due to less efficient transport of the taxane compound out of the cancer cells.

1. Introduction

Paclitaxel (Taxol®), a natural product from the bark of *Taxus brevifolia*, and the semisynthetic analog docetaxel (Taxotere®) from the needles of *Taxus baccata*, are taxanes used for the treatment of many solid cancers including breast, lung, prostate, ovarian and head and neck cancers (Chu et al., 2005; Markman, 2008; Nabholtz and Gligorov, 2005; Yared and Tkaczuk, 2012). A third taxane in clinical use, cabazitaxel (Jevtana ®), was approved by the Food and Drug Administration for treatment of metastatic castration-resistant prostate cancer in 2010 (Paller and Antonarakis, 2011).

The antitumor activity of taxanes is associated with their ability to bind to the β-tubulin subunit on the luminal side of the assembled microtubule (Parness and Horwitz, 1981; Rao et al., 1995; Rao et al., 1999; Snyder et al., 2001). Taxane treatment causes a mitotic arrest due to the binding of taxanes to the mitotic spindle. After prolonged exposure to taxane, the mitochondrial pathway of apoptosis induction is often initiated (Jordan et al., 1996; Woods et al., 1995).

The effectiveness of taxane treatment is influenced by innate and/or acquired resistance of tumor cells. Several mechanisms of taxane resistance have been proposed (Murray et al., 2012). Taxane resistance involves drug efflux mediated by transporters of the ATP-binding

Abbreviations: ABC, ATP-binding casette; ABCB1/MRP1, ATP-binding cassette B1/multidrug resistance protein 1; ABCC3/MRP3, ATP-binding cassette C3/multidrug resistance protein 3; MAPs, microtubule associated proteins; Pgp, P-glycoprotein

* Corresponding author at: Department of Cell and Molecular Biology, Third Faculty of Medicine, Charles University, Ruská 87, 100 00 Prague 10, Czech Republic.
E-mail addresses: michael.j@email.cz (M. Jelínek), kamilabalusikova@seznam.cz (K. Balušíková), petr85daniel@gmail.com (P. Daniel), vlasta.furstova@lf3.cuni.cz (V. Němcová-Fürstová), kirubakaran.palani@uochb.cas.cz (P. Kirubakaran), martin.jacek@volny.cz (M. Jaček), longfei.wei@stonybrook.edu (L. Wei), xin.wang@stonybrook.edu (X. Wang), jiri.vondrasek@uochb.cas.cz (J. Vondrášek), iwao.ojima@stonybrook.edu (I. Ojima), jan.kovar@lf3.cuni.cz (J. Kovář).

https://doi.org/10.1016/j.taap.2018.04.002
Received 8 December 2017; Received in revised form 26 March 2018; Accepted 2 April 2018
Available online 04 April 2018

casette transporter (ABC) family that can be responsible for poor bioavailability of classical taxanes (Fojo and Menefee, 2005). Mutations in the taxol-binding site of β-tubulin (Orr et al., 2003), alterations in β-tubulin isotype expression, especially β-III tubulin (Kavallaris et al., 1997), and the effect of microtubule associated proteins (MAPs), which can either affect tubulin dynamics or bind to the taxol-binding site, have all been observed in cell line models (Alli et al., 2007; Smoter et al., 2011; Sun et al., 2015).

To overcome resistance to classical taxanes, modified taxanes such as Cabazitaxel (Jevtana ®) (de Bono et al., 2010) and Ortataxel (SB-T-101131, *IDN*-5109, BAY 59-8862) have been developed with the goal of overcoming P-glycoprotein-associated resistance (Geney et al., 2005).

Classical taxanes containing a baccatin III core (paclitaxel) or 10-deacetylbaccatin (docetaxel) are esterified at the C13 position and thus they have a specific side chain at this position. The side chain contains two phenyl groups at the C3′ and C3′N positions in paclitaxel or a phenyl group at C3′ position and *tert*-butoxycarbonyl at the C3′N position in docetaxel. A series of second generation taxanes modified at the C2, C3′, C3′N, C10 and C13 positions, have been synthetized and their potency to overcome resistance to taxanes mediated by P-glycoprotein (Pgp) or mutations in β-tubulin has been assessed in some cancer cell lines or in mouse models (Matesanz et al., 2014; Ojima et al., 1994; Ojima et al., 1996; Ojima et al., 2008). These structure-activity relationship studies have revealed that novel taxanes are extremely efficient in overcoming some mechanisms of the acquired resistance described above.

We have established paclitaxel-resistant breast cancer cell sublines, SK-BR-3/PacR and MCF-7/PacR, capable of long-term proliferation in a medium containing concentrations of paclitaxel that are death-inducing for original sensitive cell lines SK-BR-3 and MCF-7 (100 nM and 300 nM, respectively). Both resistant sublines overexpress multi-drug resistance transporters ABCB1 and ABCC3 (Němcová-Fürstová et al., 2016). Moreover, both sublines also express other proteins which may be involved in resistance to paclitaxel (Pavlíková et al., 2014; Pavlíková et al., 2015). Our previous results have showed that novel taxanes with modified structures, especially at the C′3 and C3′N positions (Jelínek et al., 2013; Kovář et al., 2009; Vobořilová et al., 2011), were able to overcome paclitaxel resistance and induced cell death in tested paclitaxel-resistant breast cancer sublines (Němcová-Fürstová et al., 2016).

In the present study we tested the role of substituents at the C3′ and C3′N positions of the taxane structure to assess the capability of taxanes to overcome acquired resistance to paclitaxel in SK-BR-3 and MCF-7 cancer cells. We found that taxanes with phenyl groups at the C3′ and at C3′N positions are able to induce apoptosis in paclitaxel-resistant cells only at very high concentrations. However, taxanes with a nonaromatic group instead of a phenyl group at least at either the C3′or C3′N position are able to overcome acquired resistance to paclitaxel. These taxanes induce apoptosis at significantly lower concentrations. These acquired resistance to paclitaxel results from a dramatically increased expression of the ABCB1 (Pgp) transporter. Mechanism of the capability of taxanes to overcome this acquired resistance is based on lower affinity to ABCB1 transporter and thus lower export from resistant cells.

2. Materials and methods

2.1. Materials

The following primary and secondary antibodies were used for the detection of proteins: *anti*-ABCB1 (#12683, dilution 1:1000) from Cell Signaling Technology (Danvers, MA, USA), *anti*-actin (AC-40, A3853, dilution 1:1000) from Sigma-Aldrich, HRP-linked goat *anti*-mouse (sc-2005, dilution 1:6000) and HRP-linked goat *anti*-rabbit (sc-2004, dilution 1:6000) antibody from Santa Cruz (Santa Cruz, CA, USA).

Paclitaxel and docetaxel were purchased from Sigma-Aldrich (St. Louis, MO, USA), deacetyl paclitaxel from Santa Cruz (Santa Cruz, CA, USA). Acetyl docetaxel, SB-T-0035, SB-T-1102, SB-T-1211, SB-T-1212N1, SB-T-1214 and SB-T-1216 were synthesized at the Institute of Chemical Biology and Drug Discovery (Stony Brook, NY, USA), (Ojima et al., 1996; Ojima et al., 1997). Taxanes were dissolved in DMSO (tissue culture quality) to obtain 10 mM stock solution.

2.2. Cells and culture conditions

Human breast carcinoma cell lines MCF-7 and SK-BR-3 were obtained from the National Cancer Institute (Frederick, MD, USA) and the American Type Culture Collection (ATCC) (Manassas, VA, USA), respectively. The cells were maintained at 37 °C in a humidified atmosphere of 5% CO_2 in air in RMPI-1640 based culture medium containing extra L-glutamine (300 μg/ml), sodium pyruvate (110 μg/ml), HEPES (15 mM), penicillin (100 U/ml) and streptomycin (100 μg/ml), and supplemented with 10% heat-inactivated fetal bovine serum.

Taxane-resistant cell sublines were maintained as long-term culture in a taxane-containing medium. Concentrations were as follows: 100 nM paclitaxel for the SK-BR-3/PacR cell subline, 300 nM paclitaxel for the MCF7/PacR cell subline, 300 nM SB-T-0035 for the MCF7/SB-T-0035R cell subline.

2.3. Assessment of cell growth and survival

Cells were harvested and seeded into 96-well plate at a density of 2×10^4 cells per well in 100 μl of culture medium. After 24 h pre-incubation period allowing cells to attach, the culture medium was replaced by a culture medium without taxane (control) or with a medium containing tested taxane at desired concentrations. The number of living cells was determined after 96 h of incubation using a hemocytometer after staining with trypan blue.

2.4. Establishment of MCF7 subline resistant to SB-T-0035

The MCF7 cell subline resistant to the effect of SB-T-0035, referred to as MCF7/SB-T-0035R, was established in a similar way as the paclitaxel-resistant SK-BR-3/PacR and MCF7/PacR sublines (Němcová-Fürstová et al., 2016). The MCF7/SB-T-0035R subline was established by gradual adaptation of the original cell line to increasing concentrations of SB-T-0035. The starting concentration of SB-T-0035 was 1 nM. SB-T-0035 concentration then was increased as follows: 1 nM → 3 nM → 5 nM → 10 nM → 20 nM → 30 nM → 50 nM → 70 nM → 100 nM → 300 nM. Cells were maintained at a particular SB-T-0035 concentration for approximately 10 passages or until they displayed, more or less, standard growth and survival. The final concentration of SB-T-0035 achieved was 300 nM. Long-term growth and survival of MCF7/SB-T-0035R in 300 nM SB-T-0035 was similar to cells without SB-T-0035. On the other hand, most of the original MCF-7 cells exposed to 300 nM SB-T-0035 died within 96 h.

2.5. Preparation of cell lysates

Cells were harvested and seeded to 60 mm Petri dish at the density 1.5×10^6 cells in 5 ml of culture medium. After a 24 h pre-incubation period allowing cells to attach, the culture medium was replaced with taxane-free medium or taxane-containing medium. After each particular period of incubation, cells were harvested by trypsinization, washed three-times with ice-cold PBS and centrifuged at 500*g* for 10 min. Cell pellets were frozen at− 80 °C for 1 h and then dissolved in the RIPA lysis buffer containing protease and phosphatase inhibitors (described in detail in Jelínek et al., 2015). Protein concentrations were determined using the BCA method (Pierce BCA Protein Assay Kit, Thermofisher Scientific, MA, USA).

2.6. Western blot analysis

Protein samples (20 μg) were mixed with sample buffer (0.125 M

Tris/HCl pH 6.8, 10% glycerol, 4% SDS, 0.25 M DTT) and heated for 5 min at 100 °C. For detection of the ABCB1 transporter, samples were heated for 5 min at 37 °C. Samples were separated in 10% acrylamide gels using protein electrophoresis (Bio-Rad, Hercules, CA). Proteins separated by SDS-PAGE were blotted onto 0.2 μm nitrocellulose membrane PROTRAN BA 83 (Whatman-Schleicher and Schuell, Maidstone, UK) for 3 h at 0.25 A, using a MiniProtean II blotting apparatus (Bio-Rad). The membrane was blocked with 5% BSA in TBS for 20 min and incubated with the primary antibody at 4 °C overnight. After incubation, the membrane was washed three times (5–10 min) with TBS containing 0.1% Tween-20. Then the membrane was incubated for 1–2 h with the corresponding horseradish peroxidase-conjugated secondary antibody (Santa Cruz Biotechnology, Santa Cruz, CA, USA). Afterwards, the membrane was washed (as described above) and the chemiluminescence signal was detected using the Supersignal reagents from Pierce (Thermo Fisher Scientific, MA, USA) and a CCD camera (Carestream).

2.7. Silencing by siRNA

ABCB1 knock-down was performed similarly to a protocol already reported (Němcová-Fürstová et al., 2016). The following siRNA were used: ABCB1 specific siRNA (catalog no: 4427037, ID: s10419, Life Technologies) and nonspecific siRNA (catalog no.: AM4635, Life Technologies) as a negative control.

The siRNA transfection mixture was prepared using INTERFERin (PolyPlus-Transfection, Illkirch, France) according to manufacturer` instructions. In the transfection mixture, ABCB1 or nonspecific siRNAs were diluted with the Opti-MEM® Reduced Serum Medium to a final concentration of 5 nM of siRNA in the culture medium together with INTERFERin transfection reagent at a 1:250 dilution.

2.8. Assessment of ABC transporter ATPase activity

The effect of tested taxanes on P-glycoprotein ATPase activity was assessed using the Pgp-Glo™ Assay System with a P-glycoprotein kit (Promega, CA, USA) according to the manufacturer's protocol. Briefly, membranes (25 μg) containing human recombinant P-glycoprotein were incubated with verapamil (positive control), sodium orthovanadate (inhibitor of ATPase activity), tested compound (paclitaxel, SB-T-1216, SB-T-0035) or Pgp-Glo buffer (as a control) with non-limiting concentration of ATP in Nunc™ F96 MicroWell™ (Thermofisher Scientific, MA, USA) white plate for 120 min at 37 °C. Afterwards, ATP-detection reagent, containing recombinant Ultra-Glo™ Luciferase and luciferin substrate, was added to the samples and luciferase activity signal was determined using a TECAN Infinite M200 Pro luminometer (TECAN, Männedorf, Switzerland).

2.9. Assesment of intracellular taxane level

Cells were harvested and lysed by buffer containing 8 μg/μl digitonin (Sigma Aldrich) (see Jelínek et al., 2015).

Samples were prepared by mixing 200 μl of acetonitrile (ACN) with 100 μl of cell lysate. After centrifugation, 50 μl of the supernatant was injected onto HPLC system equipped with a column Ascentis Express C18 (150 × 4.6 mm, 5 μm, Supelco, Bellefonte, PA, USA). Our method was based on principles of previously published work (Kim et al., 2005). As a mobile phase, mixture of deionized water and ACN was used. Flow rate was 1 ml/min, maintaining first 5 min ACN concentration of 34% and increasing by linear gradient to ACN concentration of 61% by 23rd min. It was followed by purifying gradient with ACN (99%) from 24th min to 28th min and finished by the decrease of ACN concentration back to 34%.

For UV detection, the wave length λ = 228 nm was used, retention time was 17.82 min for paclitaxel, 17.87 min for SB-T-0035 and 20.85 min for SB-T-1216. The areas of peaks of individual taxanes were finally compared for tested cell lines to determine relative taxane level.

2.10. Molecular modeling studies

The human ABCB1 sequence was retrieved from the UniProt database with the accession ID: P08183. An ABCB1 homology model was constructed using the Swiss-Model automated homology model server (Biasini et al., 2014). The sequence identity of the target and template protein was 87.36%. This value indicated that the P-glycoprotein (PDB: 4Q9I) was a good model for use as a template (Szewczyk et al., 2015). The homology model of ABCB1 was further utilized for the docking studies.

The protein was prepared using the Protein Preparation Vizard in Schrodinger following a standard protocol described elsewhere (Sastry et al., 2013). Hydrogen atoms were added and minimization was done using OPLS_2005 force field. This ABCB1-homology model was further used to predict the potential small-molecule binding site using the SiteMap (SiteMap, version 3.3, Schrodinger, LCC, New York, 2014). This module in Schrodinger employs three stages of calculation-finding of appropriate sites, mapping the sites and evaluating the sites for possible binding region of ligand molecules. The receptor grid was generated around the predicted binding site with a scaling factor of 1 Å and a partial cutoff charge of 0.25 Å. Ligand docking was confined to the enclosing box of 20 Å to the selected binding site. The compounds were prepared using the LigPrep module (LigPrep, version 3.2, Schrodinger, LCC, New York, 2014) and possible ionization states were generated for neutral pH. The docking calculations were carried out using the Glide Extra Precision (Glide XP) mode with default parameters (Glide, version 6.5, Schrodinger, LCC, New York, 2014), followed by post-docking minimization to maintain the accuracy of the binding complex. The 10 most favorable docking poses for each ligand were selected for structural analysis. The mean docking scores, and hydrogen bond amino acids were provided for each protein-ligand complex.

2.11. Statistical analysis

Statistical significance of differences was determined using the Student's *t*-test. $P < 0.05$ and $P < 0.01$ were considered statistically significant at the 5% and 1% levels, respectively.

3. Results

3.1. Three groups of tested taxanes

In this study we tested three groups of taxanes. The first group, including classical paclitaxel, is represented by taxanes containing phenyl groups at both the C3′(R_1) and C3′N (R_2) positions, i.e. deacetyl paclitaxel, paclitaxel, and SB-T-0035. Taxanes from this group have different chemical groups at the C10 (R_3) position (Fig. 1).

The second group contains taxanes with a phenyl at either the C3′(R_1) or C3′N (R_2) positions and with a non-aromatic group at the second position, i.e. *tert*-butoxycarbonyl at the C3′N position or 2-methylpropenyl at the C3′ position. This group of taxanes includes classical docetaxel, acetyl docetaxel, and SB-T-1212N1. The analogs of this group have two different types of substituents at the C10 (R_3) position (Fig. 1).

The third group is represented by taxanes bearing a non-aromatic 2-methylpropenyl group at the C3′ (R_1) position and a non-aromatic *tert*-butoxycarbonyl group at the C3′N (R_2) position. This group of taxanes is represented by SB-T-1211, SB-T-1102, SB-T-1216, and SB-T-1214. Taxanes of this group have different substituents at the C10 (R_3) position (Fig. 1).

A

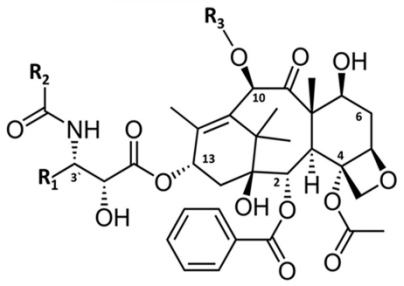

B

GROUP OF TAXANES	TAXANE	C3′ (R_1)	C3′N (R_2)	C10 (R_3)
1	DEACETYL PACLITAXEL	phenyl	phenyl	- H
	PACLITAXEL	phenyl	phenyl	- CO-CH_3
	SB-T-0035	phenyl	phenyl	- CO-N$(CH_3)_2$
2	DOCETAXEL	phenyl	- O-$C(CH_3)_3$	- H
	ACETYL DOCETAXEL	phenyl	- O-$C(CH_3)_3$	- CO-CH_3
	SB-T-1212N1	- CH=$C(CH_3)_2$	phenyl	- CO-CH_3
3	SB-T-1211	- CH=$C(CH_3)_2$	- O-$C(CH_3)_3$	- H
	SB-T-1102	- CH-CH$(CH_3)_2$	- O-$C(CH_3)_3$	- CO-CH_3
	SB-T-1216	- CH=$C(CH_3)_2$	- O-$C(CH_3)_3$	- CO-N$(CH_3)_2$
	SB-T-1214	- CH=$C(CH_3)_2$	- O-$C(CH_3)_3$	- CO-◁

- CH=$C(CH_3)_2$: 2-methylpropenyl, -CH-CH$(CH_3)_2$: 2-methylpropyl, -O-$C(CH_3)_3$: *tert*-butoxycarbonyl, -CO-CH_3: acetyl, -CO-N$(CH_3)_2$: dimethylcarbamoyl, -CO-◁ : cyclopropanecarboxyl

Fig. 1. A) Chemical structure of taxanes. R_1, R_2 and R_3 represent substituents at the C3′, C3′N and C10 positions, respectively. B) Groups of tested taxanes. Substituents at the positions C3′ (substituent R1), C3′N (substituent R_2) and C10 (substituent R_3) are described.

3.2. Characterization of paclitaxel-sensitive and paclitaxel-resistant counterpart cells

We established, from original paclitaxel-sensitive SK-BR-3 and MCF-7 cell lines, paclitaxel-resistant counterpart cell sublines SK-BR-3/PacR and MCF-7/PacR *via* adaptation to gradually increasing concentrations of paclitaxel. The established paclitaxel-resistant SK-BR-3/PacR and MCF-7/PacR cells display long-term survival and proliferation in a culture medium with 100 nM paclitaxel (SK-BR-3/PacR) or 300 nM paclitaxel (MCF-7/PacR). Application of these concentrations of paclitaxel results in cell death in most cells of the original lines within 36 h (Němcová-Fürstová et al., 2016).

Activation of executioner caspase-3 and caspase-7 was not detected in SK-BR-3/PacR cells after 100 nM paclitaxel application, while activation of these caspases in original sensitive SK-BR-3 was clearly seen. Similar data were obtained for caspase-7 in MCF-7/PacR versus original MCF-7 cells. There is no functional caspase-3 in MCF-7 cells (Němcová-Fürstová et al., 2016).

We found that the expression of ABCB1 (PgP) and ABCC3/MRP3 transporters are significantly upregulated in both resistant sublines SK-BR-3/PacR and MCF-7/PacR (Fig. 2A). Employing ABCB1 silencing by a specific siRNA, we tested whether the overexpression of ABCB1 was responsible for developed resistance to paclitaxel. Silencing of the ABCB1 expression to nearly undetectable level resulted in a significant decrease in the number of surviving cells 96 h after paclitaxel application in both resistant sublines. It was a decrease to about 70% of the number of control cells (without paclitaxel) for SK-BR-3/PacR cells and about 20% for MCF-7/PacR cells (Fig. 2B). Such differing effects of ABCB1 silencing on the number of surviving SK-BR-3/PacR cells and MCF-7/PacR cells after paclitaxel application could simply reflect differing dependence of the resistance of these sublines on ABCB1 transporter.

3.3. Effect of tested taxanes on growth and survival of paclitaxel-sensitive and paclitaxel-resistant cells

We assessed the effect of tested taxanes on growth and survival of paclitaxel-sensitive and corresponding paclitaxel-resistant cells. Taxane concentrations 10–300 nM for SK-BR-3 cells and 3–3000 nM for MCF-7 cells were used.

Data for the first group (phenyl groups at both C3′ and C3′N positions) of tested taxanes are shown in Fig. 3. Data for the second group (phenyl at either C3′or C3′N position and a non-aromatic substituent at the other position) of taxanes are shown in Fig. 4. Data for the third group (non-aromatic substituents at both C3′ and C3′N positions) are in Fig. 5.

The results are summarized in Table 1. The C_0 values (taxane concentration for which there is no increase or decrease in the number of cells of the inoculum after 96-hour incubation) concerning individual tested taxanes for sensitive and resistant SK-BR-3 as well as MCF-7 cells are presented. Furthermore, fold increase of the C_0 value for resistant cells compared with the C_0 value for sensitive cells is also presented. In the first group of taxanes, the increase in the C_0 value for resistant cells was between 8.6× and > 13.6× in the case of SK-BR-3 cells and between 26× and 132× in the case of MCF-7 cells. In the second group, the increase in the C_0 value was between 0.5× and 4.5× for SK-BR-3 cells and between 8.0× and 14.1× for MCF-7 cells. As to the third group, the increase in the C_0 value was between 1.6× and 3.5× for SK-BR-3 cells and between 2.8× and 5.9× for MCF-7 cells. We can see that the C_0 increase in the first group of taxanes was noticeably higher when compared with the C_0 increase in the second and third group of taxanes for both SK-BR-3 and MCF-7 cells.

3.4. Establishment of MCF-7 subline resistant to SB-T-0035

Like in the case of established paclitaxel-resistant counterpart cell sublines, we established SB-T-0035-resistant cell subline MCF-7/SB-T-0035R, from the original SB-T-0035-sensitive MCF-7 cell line, by adaptation to gradually increasing concentrations of SB-T-0035.

Cells of the established SB-T-0035-resistant subline MCF-7/SB-T-0035R display long-term survival and proliferation in a medium containing 300 nM SB-T-0035. Cells of the original sensitive MCF-7 line cultured with such SB-T-0035 concentration die nearly completely within 96 h (see Fig. 7).

3.5. Characterization of SB-T-0035-resistant cells

As with the paclitaxel-resistant sublines, we found that the expression of ABCB1 (PgP) transporter is significantly upregulated in the SB-T-0035-resistant subline of MCF-7 cells (Fig. 6A).

Again, we tested whether the overexpression of ABCB1 was responsible for the developed resistance using ABCB1 silencing. Silencing of ABCB1 expression by a specific siRNA to suitable level led to a significant decrease in the number of surviving cells 96 h after SB-T-0035 application in SB-T-0035-resistant cells. It was a decrease to about 30% of the number of control cells (without SB-T-0035) (Fig. 6B).

3.6. Effect of tested taxanes on growth and survival of SB-T-0035-resistant cells

We also assessed the effect of some of the tested taxanes on growth and survival of SB-T-0035-sensitive and SB-T-0035-resistant MCF-7 cells (see previous two sections) over a range of concentrations

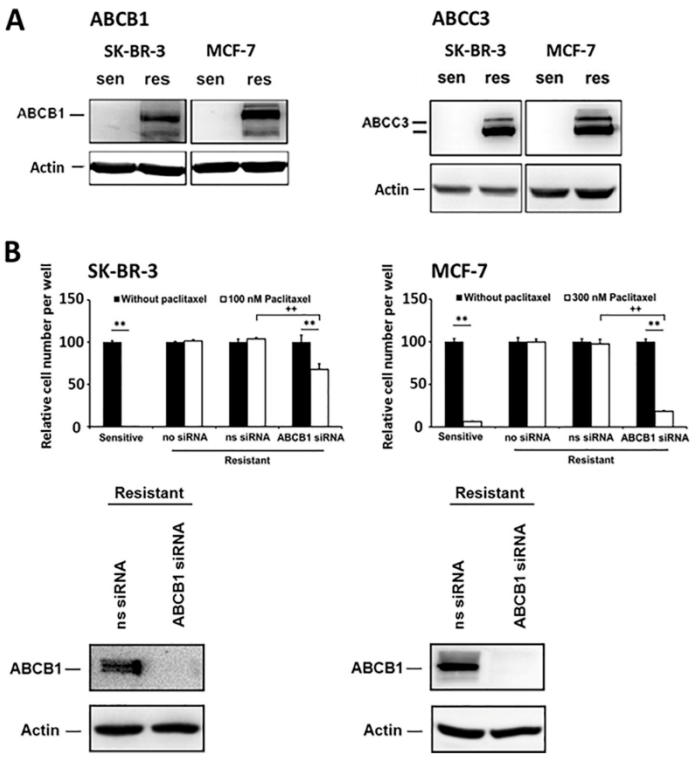

Fig. 2. (A) The level of ABCB1 and ABCC3 transporters in paclitaxel-sensitive (sen) and paclitaxel-resistant (res) SK-BR-3 and MCF-7 cells. (B) The effect of ABCB1 silencing on the growth and survival of paclitaxel-resistant SK-BR-3 and MCF-7 cells after paclitaxel treatment. (A) After 24 h of incubation with paclitaxel (100 nM for SK-BR-3 and 300 nM for MCF-7) the levels of ABC transporters were determined using western blot analysis and relevant antibodies (see "Materials and methods"). Actin levels were used to confirm equal protein loading. The data shown were obtained in one representative experiment of three independent experiments. Western blot quantification by densitometry is shown. Data are presented as the mean of relative density ± SEM. *P < 0.05 when comparing the density in sensitive and resistant cells. (B) The cells were prepared as described in "Materials and methods" and seeded at 20 × 10^3 cells/100 µl of medium per well. The relative number of living sensitive cells, resistant cells (no siRNA), resistant cells treated with non-specific siRNA (ns siRNA) and resistant cells treated with an ABCB1 specific siRNA (ABCB1 siRNA) was determined after 96 h of incubation without paclitaxel (control cells) or with paclitaxel (100 nM for SK-BR-3 and 300 nM for MCF-7). Each column represents the mean of 4 separate culture ± SEM. **P < 0.01 when comparing the effect in cells without paclitaxel and treated with paclitaxel. $^{++}$P < 0.01 when comparing the effect in ns siRNA-treated and ABCB1 siRNA-treated cells after paclitaxel application. The data shown were obtained in one representative experiment of three independent experiments. The effect of non-specific siRNA (ns siRNA) and specific siRNA (ABCB1 siRNA) on ABCB1 expression in paclitaxel-resistant SK-BR-3 and MCF-7 cells is also shown. Actin levels were used to confirm equal protein loading.

(3–3000 nM).

Data for paclitaxel and SB-T-0035 (the first group of taxanes with phenyl groups at both C3′ and C3′N positions) and SB-T-1216 (the third group of taxanes with non-aromatic substituents at both C3′ and C3′N positions) are in Fig. 7. The results are summarized in Table 2. The C_0 values concerning individual tested taxanes for sensitive and resistant MCF-7 cells are presented. Fold increase of the C_0 value for resistant cells compared with the C_0 value for sensitive cells is also shown. The increase in the C_0 value for resistant MCF-7 cells was 95× and 133× for paclitaxel and SB-T-0035 (the first group of taxane derivatives), respectively, and 2.0× for SB-T-1216 (the third group of taxanes). Again, we can see that the C_0 increase in the first group of taxanes was significantly higher compared with the C_0 increase in the third group of taxanes.

3.7. Effect of tested taxanes on ATPase activity of ABCB1 transporter

We assessed the effect of some of the tested taxanes (300 nM) on the ATPase activity of the ABCB1 (PgP) transporter employing a non-cellular system, i.e. membranes containing human recombinant ABCB1 (see "Materials and methods").

We found that all three tested taxanes (paclitaxel, SB-T-0035, and SB-T-1216) increased basal activity of the ATPase. However, the increase in the ATPase activity was 1.7–2.1 times higher for taxanes from the first group (paclitaxel, SB-T-0035) than for the taxane from the third group (SB-T-1216). The difference was not found to be statistically significant. When comparing the increase in the basal ATPase activity after the application of tested taxanes and the application of verapamil (plus control), the increase after the application of taxanes was 2.8–5.8 times lower than after verapamil application (Fig. 8).

3.8. Intracellular level of tested taxanes after their application in paclitaxel-resistant and SB-T-0035-resistant cells

Using a HPLC system (see "Materials and methods"), we assessed intracellular level of some of tested taxanes after their application (300 nM) in sensitive, paclitaxel-resistant and SB-T-0035-resistant MCF-7 cells. We supposed that intracellular level of particular taxane after the incubation of the cells with this taxane reflects the efficacy of taxane transport out of the cells.

We found that both taxanes from the first group (paclitaxel, SB-T-0035) were transported out of paclitaxel-resistant as well as SB-T-0035-resistant MCF-7 cell very efficiently. Intracellular level of both taxanes in resistant cells represented only about 5% or less of the level in control sensitive MCF-7 cells. However, intracellular level of the taxane from the third group (SB-T-1216) in resistant cells represented about 40–50% of the level in sensitive cells. It showed that transport of SB-T-1216 out of both types of resistant cells was much less efficient (Fig. 9).

3.9. Molecular docking of tested taxanes to the ABCB1 transporter

We performed molecular docking of some of tested taxanes to the human ABCB1 (PgP) transporter (Fig. 10) using Schrodinger docking suite (see "Materials and methods").

To investigate the binding affinities computationally, deacetyl paclitaxel, paclitaxel, SB-T-0035, SB-T-1212N1, acetyl docetaxel and SB-T-1216 were docked into the active site of the homology model of the ABCB1 protein. The obtained docking scores were divided into three

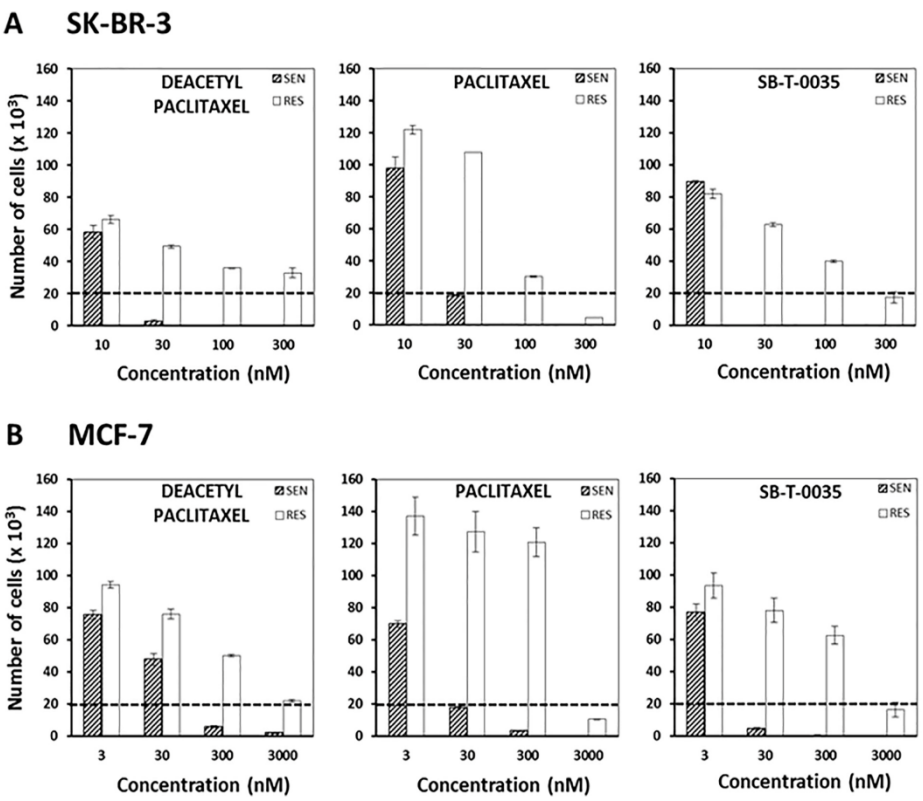

Fig. 3. Effect of deacetyl paclitaxel, paclitaxel and SB-T-0035 on the growth and survival of paclitaxel-sensitive (sen) and paclitaxel-resistant (res) (A) SK-BR-3 cells (10–300 nM taxane) and (B) MCF-7 cells (3–3000 nM taxane). The number of cells of the inoculum (20×10^3 cells/100 μl of medium per well) is shown as a dotted line. The number of living cells was determined after 96 h of incubation (see "Materials and methods"). Each column represents the mean of three separate experiments ± SEM.

groups based on the respective substitution of the side chains in the ligand molecules. The first group of taxanes included deacetyl paclitaxel (−10.77 ± 0.21), paclitaxel (−10.12 ± 0.19) and SB-T-0035 (−10.02 ± 0.15) and exhibited the lowest docking scores, i.e. highest predicted binding affinity. This probably reflects the importance of the two phenyl groups at the C3′ and C3′N positions in their structures. The second group contained SB-T-1212N1 (−9.89 ± 0.07) and acetyl docetaxel (−9.49 ± 0.18). These taxanes, lacking one phenyl group at either C′3 or C3′N position in their structures, had worse docking scores compared to taxanes of the first group. The last taxane SB-T-1216 (8.15 ± 0.25), from the third group, bearing no phenyl group at the C′3 and C3′N positions, had a docking score reflecting the lowest predicted binding affinity compared to the other taxanes. The docking predictions are summarized in Table 3.

These results demonstrated that the docking energy score reflecting the predicted free energies of individual taxanes to the ABCB1 transporter, was the lowest (the highest predicted free energy) for taxanes from the first group (deacetyl paclitaxel, paclitaxel, SB-T-0035), i.e. from −10.02 to −10.77. The taxanes from the second group (acetyl docetaxel, SB-T-1212N1) had lower predicted free energy compared to taxanes from the first group, i.e. from −9.49 to −9.89. SB-T-1216 from the third group had the lowest predicted free energy to ABCB1, i.e. −8.15 (Table 3).

Schemes showing molecular interactions of individual taxanes with the ABCB1 transporter at their binding sites are shown in Fig. 11.

4. Discussion

Previously we have established paclitaxel-resistant sublines of the original sensitive breast cancer cell lines SK-BR-3 and MCF-7 by adaptation to gradually increasing concentrations of paclitaxel (Němcová-Fürstová et al., 2016). Interestingly, we found that both paclitaxel-resistant sublines maintained their sensitivity to taxane SB-T-1216 (Ojima et al., 1996) that was similar to the sensitivity of the original sensitive lines. Furthermore, despite repeated efforts, we were unable to establish variants of the original cell lines resistant to SB-T-1216 (Němcová-Fürstová et al., 2016). These findings together with results of subsequent pilot experiment with other taxanes led us to hypothesize that substituents at the C3′and C3′N positions of the taxane structure are critical with regard to capability of overcoming resistance to paclitaxel.

We have decided to test this hypothesis. As an experimental model, we used our previously established paclitaxel-resistant sublines SK-BR-3/PacR and MCF-7/PacR versus original paclitaxel-sensitive lines SK-BR-3 and MCF-7. Resistant sublines are capable of long-term survival and near-normal proliferation in a medium with such concentrations of paclitaxel (100 nM for SK-BR-3/PacR and 300 nM for MCF-7/PacR) in which most cells of the original sensitive lines die within 96 h (Němcová-Fürstová et al., 2016). Later, within the framework of this

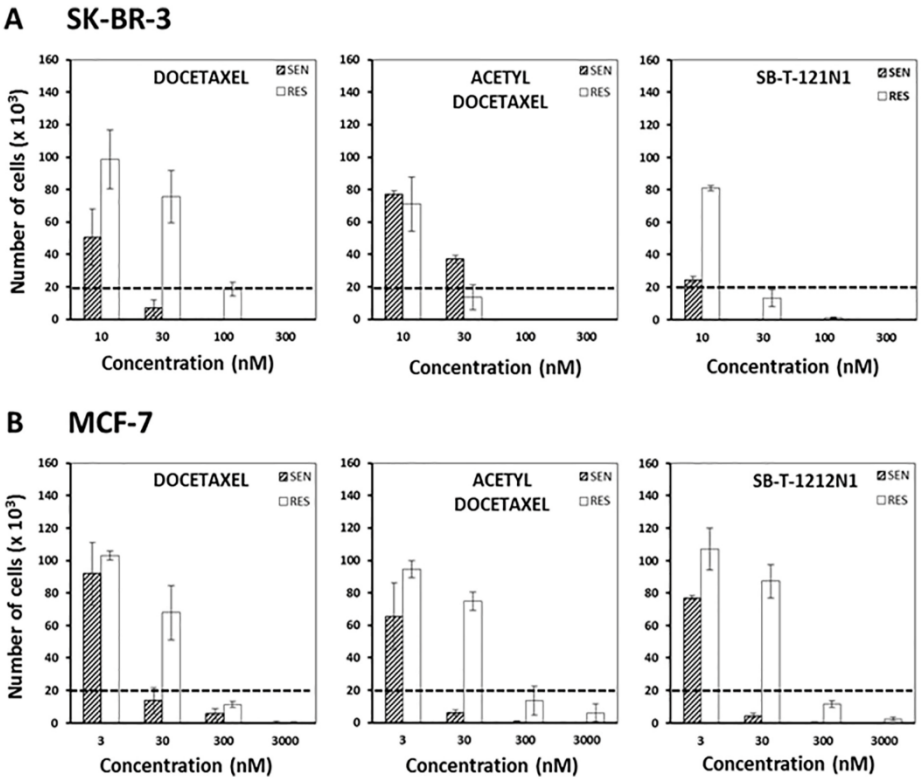

Fig. 4. Effect of docetaxel, acetyl docetaxel and SB-T-1212 N1 on the growth and survival of paclitaxel-sensitive (sen) and paclitaxel-resistant (res) (A) SK-BR-3 cells (10–300 nM taxane) and (B) MCF-7 cells (3–3000 nM taxane). The number of cells of the inoculum (20×10^3 cells/100 μl of medium per well) is shown as a dotted line. The number of living cells was determined after 96 h of incubation (see "Materials and methods"). Each column represents the mean of three separate experiments ± SEM.

study, we established SB-T-0035-resistant subline from the original sensitive MCF-7 cell line using similar approach as used for paclitaxel-resistant sublines (see "Results"). Taxane SB-T-0035 has the same substituents at the C3′and C3′N positions as paclitaxel. We used the model of established SB-T-0035-resistant MCF-7 cells versus the original sensitive MCF-7 cells in our experiments in order to confirm results regarding paclitaxel-resistant versus paclitaxel-sensitive cells.

Previously, we also found that both paclitaxel-resistant sublines significantly upregulated the expression of ABCB1 (PgP) or ABCC3 (MRP3) transporters which was detected by western blot analysis. Furthermore, effective silencing of ABCB1 expression employing a specific siRNA significantly decreased resistance to paclitaxel in the paclitaxel-resistant cells. It suggests the important role for ABCB1 in mechanisms of paclitaxel resistance (Němcová-Fürstová et al., 2016). In this study, we also found that ABCB1 expression in SB-T-0035-resistant sublines of MCF-7 cells is significantly upregulated. Together with this, we confirmed that effective silencing of ABCB1 expression by a specific siRNA results in a significant decrease in resistance to SB-T-0035 in SB-T-0035-resistant cells (see Fig. 6). Upregulation of ABCB1 and ABCC3 expression in taxane-resistant variants of breast cancer cells has been demonstrated by several authors (Ajabnoor et al., 2012; Hembruff et al., 2008; O'Brien et al., 2008; Reed et al., 2010; Shi et al., 2014; Wang et al., 2014). However, there are papers indicating that ABCB1 upregulation is not required for the development of paclitaxel resistance in breast cancer cells (Kars et al., 2006; Kenicer et al., 2014).

Data from our pilot experiments pointed to the possibility that only the presence of phenyl groups at both C3′ and C3′N positions are responsible for low capability of taxane to overcome acquired resistance to paclitaxel as well as a high probability of developing resistance to this taxane. When there is a non-aromatic group at one or both C3′ and C3′N positions, such taxane has higher capability of overcoming resistance to paclitaxel and there is low probability of developing resistance to this taxane. In further studies we tested this hypothesis. In order to do that we compared three groups of taxanes. Taxanes of the first group have phenyl groups at both C3′ and C3′N positions. Taxanes of the second group have a phenyl group at either C3′ or C3′N position and a non-aromatic group at the other position. The third group involves taxanes with non-aromatic groups at both C3′and C3′N positions (see Fig. 1). The role of substituents at the C3′and C3′N positions of the taxane structure in resistance of tumor cells has been previously studied (Ojima et al., 1994; Ojima et al., 1996; Ojima et al., 1997; Ojima et al., 2000). However, these studies were not focused on acquired resistance to paclitaxel.

The effect of individual taxanes from the three mentioned groups on tested cells was assessed by the C_0 value (see "Results"). Then the degree of resistance of paclitaxel-resistant cells to individual taxanes was assessed by the increase of the C_0 value of resistant cells when compared with the C_0 value of corresponding sensitive cells (see Table 1). In

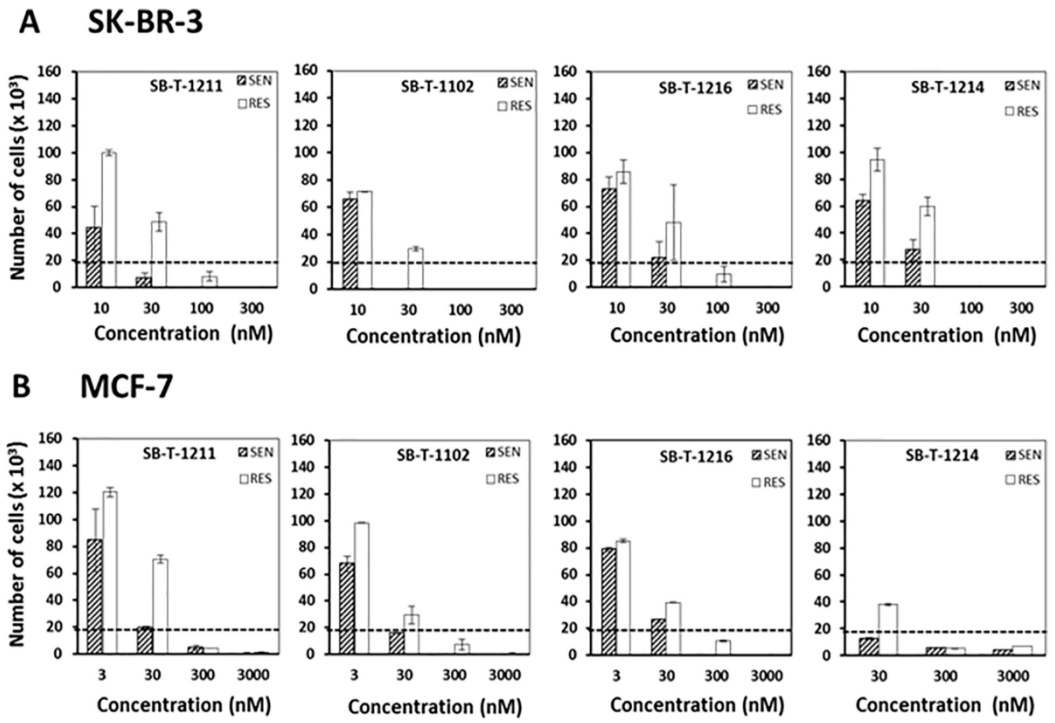

Fig. 5. Effect of SB-T-1211, SB-T-1102, SB-T-1216 and SB-T-1214 on the growth and survival of paclitaxel-sensitive (sen) and paclitaxel-resistant (res) (A) SK-BR-3 cells (10–300 nM taxane) and (B) MCF-7 cells (3–3000 nM taxane). The number of cells of the inoculum (20×10^3 cells/100 µl of medium per well) is shown as a dotted line. The number of living cells was determined after 96 h of incubation (see "Materials and methods"). Each column represents the mean of three separate experiments ± SEM.

Table 1
Comparison of the effect of tested taxanes on the growth and survival of paclitaxel-sensitive (SEN) and paclitaxel-resistant (RES) SK-BR-3 and MCF-7 cells.

TAXANE	SK-BR-3			MCF-7		
	C_0/SEN (nM)	C_0/RES (nM)	INCREASE (x)	C_0/SEN (nM)	C_0/RES (nM)	INCREASE (x)
DEACETYL PAC.	22	> 300	> 13.6	138	3600	26.1
PACLITAXEL	29	250	8.6	27	2500	92.6
SB-T-0035	23	260	11.3	19	2500	132
DOCETAXEL	22	98	4.5	25	200	8.0
ACETYL DOC.	52	26	0.5	17	240	14.1
SB-T-1212 N1	12	27	2.2	18	230	12.8
SB-T-1211	20	70	3.5	29	170	5.9
SB-T-1102	22	45	2.0	25	84	3.4
SB-T-1216	32	72	2.2	51	141	2.8
SB-T-1214	41	67	1.6	< 30	114	> 3.8

C_0 represents taxane concentration (nM) for which there is not any increase or any decrease of the number of cells of the inoculum (20×10^3 cells/100 µl of medium per well) after 96 h of incubation. Fold increase (x) of C_0 value for resistant cells in comparison with C_0 value for sensitive cells is shown.

the third group of taxanes with non-aromatic groups at both C3′and C3′N positions, the increase in the C_0 value of resistant cells was 1.6–3.5 times for SK-BR-3 cells and 2.8–5.9 times for MCF-7 cells. As to the second group of taxanes with one phenyl and one non-aromatic group at the C3′and C3′N positions respectively, the increase in the C_0 value for resistant cells was similar or somewhat higher. It was 0.5–4.5 times for SK-BR-3 cells and 8.0–14.1 times for MCF-7 cells. Presented unexpected increase (only 0.5 times) in the C_0 value for acetyl docetaxel and resistant SK-BR-3 cells (see Table 1) may represent just a stochastic fluctuation. However, in the first group of taxanes with phenyl groups at both C3′and C3′N positions, the increase in the C_0 value was noticeable. It was 8.6–13.6 times for SK-BR-3 cells and 26–132 times for MCF-7 cells. The data show that the increase in the C_0 value for resistant cells is significantly higher for taxanes of the first group compared with the increase in the C_0 value for taxanes of the second and third group. Thus, these results confirm our hypothesis that phenyl group at both C3′and C3′N positions of taxane is associated with low capability of taxane to overcome acquired paclitaxel resistance compared with taxanes containing at least one non-aromatic substituent at the C3′and C3′N positions. To the best of our knowledge, this is the first direct confirmation of such fact (see Ojima et al., 1994; Ojima et al., 1996; Ojima et al., 1998; Ojima et al., 2008). Our finding is strongly supported by the data obtained with SB-T-0035-resistant cells (see Table 2). Similarly to paclitaxel, SB-T-0035 has phenyl groups at both C3′and C3′N positions.

As with paclitaxel-resistant SK-BR-3 and MCF-7 cells (Němcová-Fürstová et al., 2016), we detected significant upregulation of the expression of ABCB1 (PgP) transporter in SB-T-0035-resistant MCF-7 cells (see Fig. 6A). It points at the possibility that upregulation of ABCB1 transporter can play an important role in acquired resistance to paclitaxel, as it was shown by several groups previously (Aldonza et al., 2016; Kathawala et al., 2015; Reed et al., 2010), and also to SB-T-0035.

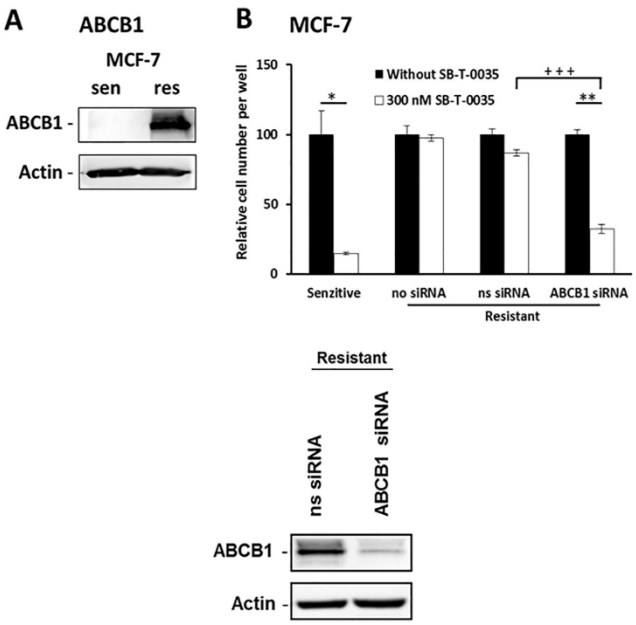

Fig. 6. (A) The level of ABCB1 transporter in SB-T-0035-sensitive (sen) and SB-T-0035-resistant (res) MCF-7 cells. (B) The effect of ABCB1 silencing on the growth and survival of SB-T-0035-resistant MCF-7 cells after SB-T-0035 treatment. (A) After 24 h of incubation with 300 nM SB-T-0035 the level of ABCB1 transporter was determined using western blot analysis and relevant antibody (see "Materials and methods"). Actin levels were used to confirm equal protein loading. The data shown were obtained in one representative experiment of two independent experiments. (B) The cells were prepared as described in "Materials and Methods" and seeded at 20×10^3 cells/100 µl of medium per well. The relative number of living sensitive cells, resistant cells (no siRNA), resistant cells treated with nonspecific siRNA (ns siRNA) and resistant cells treated with an ABCB1 specific siRNA (ABCB1 siRNA) was determined after 96 h of incubation without SB-T-0035 (control cells) or with 300 nM SB-T-0035. Each column represents the mean of 4 separate culture ± SEM. *P < 0.05, **P < 0.01 when comparing the effect in cells without SB-T-0035 and treated with SB-T-0035. $^{+++}$P < 0.001 when comparing the effect in ns siRNA-treated and ABCB1 siRNA-treated cells after SB-T-0035 application. The data shown were obtained in one representative experiment of three independent experiments. The effect of non-specific siRNA (ns siRNA) and specific siRNA (ABCB1 siRNA) on ABCB1 expression in SB-T-0035-resistant MCF-7 cells is also shown. Actin levels were used to confirm equal protein loading.

The possibility was confirmed by our experiments with paclitaxel-resistant and SB-T-0035-resistant cells by inhibiting ABCB1 expression using a specific siRNAs (Němcová-Fürstová et al., 2016, see Fig. 6B).

Increased level of ABCB1 in cells resistant to docetaxel and cabazitaxel (taxanes belonging to the second group of taxanes) (Duran et al., 2015, Li et al., 2014, Ojima et al., 1996, Ojima et al., 1998) and transport of novel taxane BMS-275,183 (taxane belonging to the third group of taxanes) by ABCB1 were described previously (Marchetti et al., 2014). The ability of taxanes SB-T-1212 and SB-T-1213 (with non-aromatic groups at C3′and C3′N positions) to overcome established P-glycoprotein-related resistance was also described (Ferlini et al., 2000; Ojima et al., 1996). Thus the hydrophobicity of molecules, which was highest for taxanes from the first group of taxanes, seems to be a key feature of molecules to be transported by ABCB1 (Liu et al., 2013;

Table 2
Comparison of the effect of tested taxanes on the growth and survival of SB-T-0035-sensitive (SEN) and SB-T-0035-resistant (RES) MCF-7 cells.

TAXANE	MCF-7		
	C_0/SEN (nM)	C_0/RES (nM)	INCREASE (x)
PACLITAXEL	20	1900	95
SB-T-0035	18	2400	133
SB-T-1216	66	135	2.0

C_0 represents taxane concentration (nM) for which there is not any increase or any decrease of the number of cells of the inoculum (20×10^3 cells/100 µl of medium per well) after 96 h of incubation. Fold increase (x) of C_0 value for resistant cells in comparison with C_0 value for sensitive cells is shown.

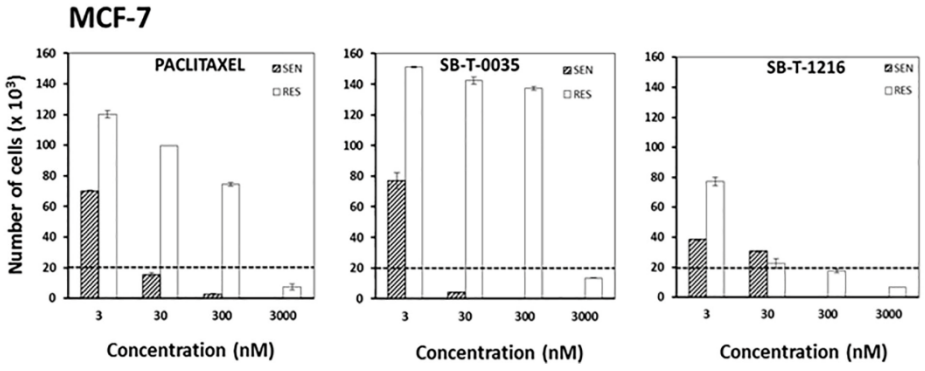

Fig. 7. Effect of paclitaxel, SB-T-0035 and SB-T-1216 (3–3000 nM) on the growth and survival of SB-T-0035-sensitive (sen) and SB-T-0035-resistant (res) MCF-7 cells. The number of cells of the inoculum (20×10^3 cells/100 µl of medium per well) is shown as a dotted line. The number of living cells was determined after 96 h of incubation (see "Materials and methods"). Each column represents the mean of three separate experiments ± SEM.

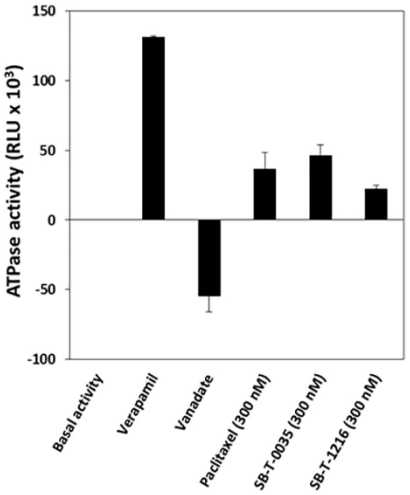

Fig. 8. Effect of paclitaxel, SB-T-0035 and SB-T-1216 (300 nM) on the ATPase activity of ABCB1 transporter. To assess the ATPase activity of ABCB1 (PgP) transporter, commercial Pgp-Glo™ Assay System with P-glycoprotein kit (Promega) using membranes with human recombinant P-glycoprotein was used (see "Materials and methods"). The ATPase activity is expressed as relative light units (RLU). The ATPase activity after verapamil application was used as a positive control and after sodium orthovanadate application as a negative control. Basal ATPase activity of ABCB1 transporter (without taxane, verapamil or vanadate application) is shown. Each column represents the mean of two independent experiments ± SEM.

Ojima et al., 1998).

The visual inspection of the docking poses of deacetyl paclitaxel, paclitaxel and SB-T-0035, from the first group of taxanes, acetyl docetaxel and SB-T-1212N1, from the second group of taxanes, and SB-T-1216 from the third group of taxanes, provided almost identical interactions with few exceptions in the binding conformation/orientation of the compounds to the active site of the ABCB1 protein (see Fig. 11). The 5 Å surrounding region of the bound compound was mostly occupied by hydrophobic amino acid residues. The two phenyl groups at the C3′and C3′N positions are buried into the hydrophobic cleft of the ABCB1 protein, indicating a tight binding of deacetyl paclitaxel, paclitaxel, SB-T-0035, acetyl docetaxel and SB-T-1212 N1. Docking energy scores of

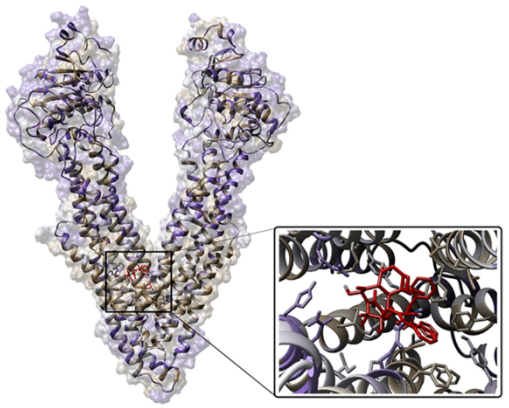

Fig. 10. Structure of the human ABCB1 transporter with bound deacetyl paclitaxel.

taxanes of all three taxane groups reflect the importance of substitutions at the C3′and C3′N positions of the C13 side chain of taxanes. The importance of hydrophobic interactions was documented previously. Phe 339 of ABCB1 molecule was found to form a gate for entry of paclitaxel into its binding site, while several other Phe residues (Phe71, Phe332, Phe728) helped paclitaxel to be stabilized in the binding site of ABCB1 (Zhang et al., 2015).

Further, hydrogen bonding interaction was predicted between the protein-ligand complexes. The hydrogen bond involving the polar carboxyl group of Ser337 is maintained by the oxygen atom (=O) near the NH of all reported taxanes and it helps to keep the same orientation and position of the phenyl group in deacetyl paclitaxel, paclitaxel, SB-T-0035 and SB-T-1212 N1. On the other hand, acetyl docetaxel and SB-T-1216 lack the phenyl group near the oxygen atom (=O), which results in the slight change in the orientation of the binding pose. Moreover, the interaction of Gln347 was observed with the carbonyl oxygen atom, which is connected to the phenyl group at the C2 position of deacetyl paclitaxel, SB-T-0035, acetyl docetaxel and SB-T-1212 N1. For so far unknown reason, this interaction is not present in complexes with paclitaxel and SB-T-1216. Additionally, the interaction of side chain of the Gln946 was predicted in the baccatin core of all tested taxanes.

Docking scores reflecting predicted free energy of taxanes to ABCB1 transporter correspond to the three groups of tested taxanes (see

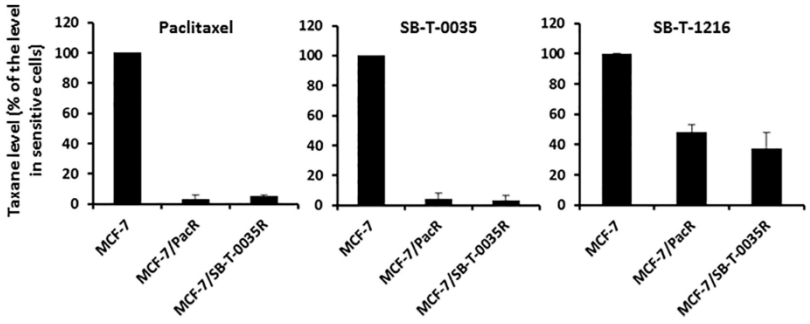

Fig. 9. Level of paclitaxel, SB-T-0035 and SB-T-1216 after their application in sensitive MCF-7 cells, paclitaxel-resistant MCF-7/PacR cells and SB-T-0035-resistant MCF-7/SB-T-0035R cells. After 24 h of incubation with 300 nM concentration of tested taxane relative taxane levels were assessed using a HPLC system (see "Materials and methods"). Levels of individual taxanes in sensitive MCF-7 cells were used as controls (100%). Each column represents mean of two independent experiments ± SEM.

Table 3
The docking score and hydrogen bond interactions of the ABCB1 transporter with tested taxanes. The values are based on the average score of top ten conformations.

Taxane	Docking conformations	Score (kcal/mol)	Hydrogen bond
DEACETYL PACLITAXEL	10	−10.77 ± 0.21	S 337, Q 347, Q 946
PACLITAXEL	10	−10.12 ± 0.19	S 337, Q 946
SB-T-0035	10	−10.02 ± 0.15	S 337, Q 347, Q 946
SB-T-1212 N1	10	−9.89 ± 0.07	S 337, Q 347, Q 946
ACETYL DOCETAXEL	10	−9.49 ± 0.18	S 337, Q 347, Q 946
SB-T-1216	10	−8.15 ± 0.25	S 337, Q 946

Table 3). Taxanes from the first group (two phenyl groups at the C3′and C3′N positions) have the highest predicted free energy, taxanes from the second group (one phenyl and one non-aromatic substituent at the C3′and C3′N positions) have intermediate predicted free energy, and taxane from the third group (two non-aromatic substituents at the C3′and C3′N positions) has the lowest predicted free energy. Lower predicted free energy means less effective transport out of cancer cell and *vice versa*. These data are in agreement with our data concerning the efficacy of taxane transport out of cells (see Fig. 9). The higher capability of taxanes, with at least one non-aromatic group at the C3′and C3′N positions, to overcome acquired resistance to paclitaxel as well as reduced probability of developing resistance is very likely based on their less effective transport out of cancer cell. The affinity of taxane to the ABCB1 transporter was reported to be strongly affected by the substituent at the position C10 previously (Ferlini et al., 2000). However, authors did not use the human ABCB1 transporter in their

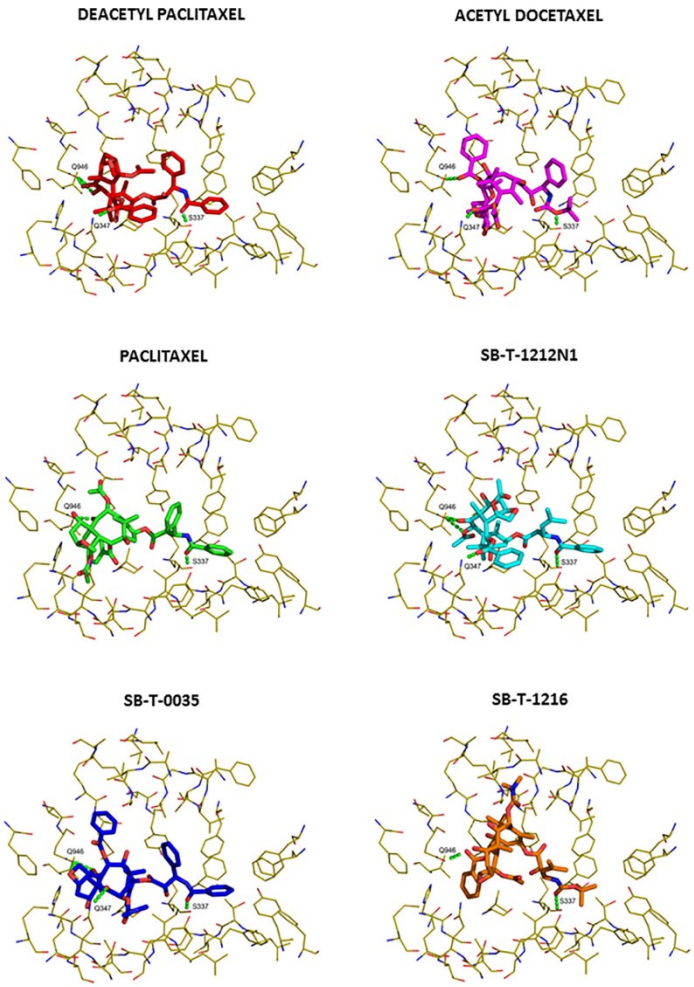

Fig. 11. Visualization of representative docking poses of tested taxanes (deacetyl paclitaxel, paclitaxel, SB-T-0035, acetyl docetaxel, SBT-1212N1, and SB-T-1216) into the ABCB1 binding site. The hydrogen bonding interactions are shown as green dotted lines. (For interpretation of the references to colour in this figure legend, the reader is referred to the web version of this article.)

molecular docking study. We did not confirm that finding in our study when comparing taxanes from the first group.

We can summarize that the high capability of a taxane to overcome acquired resistance of breast cancer cells to paclitaxel and the low probability of developing resistance to this taxane correspond to the type of substituents at the C3′ and C3′N positions of the taxane molecule. At least one non-aromatic group at these positions means high capability to overcome acquired resistance and low probability to develop resistance to the taxane. On the other hand, the presence of phenyl groups at both C3′and C3′N positions leads to low capability of overcoming acquired resistance and high probability of developing resistance. These findings are related to the function of the ABCB1 transporter which plays a crucial role in acquired resistance to taxanes.

Acknowledgement

The authors thank Mr. Thomas Secrest for English revision.

Funding

This work was supported by grant KONTAKT II LH 14096 from the Ministry of Education, Youth and Sports of the Czech Republic, project PROGRES Q28 from the Charles University, Prague as well as grant from the National Institutes of Health, USA (CA 103314 to I.O.).

Author's contributions

MJ carried out some western blot analyses, analyzed dose responses and significantly contributed to manuscript preparation, KB performed siRNAs experiments, PD carried out ATPase assay and helped with manuscript preparation, VNF carried out some western blot analyses, PK realized molecular docking studies, MJ carried out HPLC method, LW and XW were involved in the preparation of taxane derivatives, JV designed molecular docking studies, IO designed taxane derivatives and contributed to manuscript preparation and JK was main coordinator of the research and manuscript preparation. All authors read and approved the final manuscript.

Competing interest

The authors declare that they have no competing interests.

References

Ajabnoor, G.M., Crook, T., Coley, H.M., 2012. Paclitaxel resistance is associated with switch from apoptotic to autophagic cell death in MCF-7 breast cancer cells. Cell Death Dis. 26, e260.
Aldonza, M.B., Hong, J.Y., Alinsug, M.V., Song, J., Lee, S.K., 2016. Multiplicity of acquired cross-resistance in paclitaxel-resistant cancer cells is associated with feedback control of TUBB3 via FOXO3a-mediated ABCB1 regulation. Oncotarget 7, 34395–34419.
Alli, E., Yang, J.M., Ford, J.M., Hait, W.N., 2007. Reversal of stathmin-mediated resistance to paclitaxel and vinblastine in human breast carcinoma cells. Mol. Pharmacol. 71, 1233–1240.
Biasini, M., Bienert, S., Waterhouse, A., Arnold, K., Studer, G., Schmidt, T., Kiefer, F., Gallo Cassarino, T., Bertoni, M., Bordoli, L., Schwede, T., 2014. SWISS-MODEL: modelling protein tertiary and quaternary structure using evolutionary information. Nucleic Acids Res. 42, W252–8.
de Bono, J.S., Oudard, S., Ozguroglu, M., Hansen, S., Machiels, J.P., Kocak, I., Gravis, G., Bodrogi, I., Mackenzie, M.J., Shen, L., Roessner, M., Gupta, S., Sartor, A.O., TROPIC Investigators, 2010. Prednisone plus cabazitaxel or mitoxantrone for metastatic castration-resistant prostate cancer progressing after docetaxel treatment: a randomised open-label trial. Lancet 376, 1147–1154.
Chu, Q., Vincent, M., Logan, D., Mackay, J.A., Evans, W.K., 2005. Lung Cancer Disease Site Group of Cancer Care Ontario's program in evidence-based care. Taxanes as first-line therapy for advanced non-small cell lung cancer: a systematic review and practice guideline. Lung Cancer 50, 355–374.
Duran, G.E., Wang, Y.C., Francisco, E.B., Rose, J.C., Martinez, F.J., Coller, J., Brassard, D., Vrignaud, P., Sikic, B.I., 2015. Mechanisms of resistance to cabazitaxel. Mol. Cancer Ther. 14, 193–201.
Ferlini, C., Distefano, M., Pignatelli, F., Lin, S., Riva, A., Bombardelli, E., Mancuso, S., Ojima, I., Scambia, G., 2000. Antitumour activity of novel taxanes that act at the same time as cytotoxic agents and P-glycoprotein inhibitors. Br. J. Cancer 83, 1762–1768.
Fojo, A.T., Menefee, M., 2005. Microtubule targeting agents: basic mechanisms of multidrug resistance (MDR). Semin. Oncol. 32, S3–8.
Geney, R., Chen, J., Ojima, I., 2005. Recent advances in the new generation taxane anticancer agents. Med. Chem. 1, 125–139.
Hembruff, S.L., Laberge, M.L., Villeneuve, D.J., Guo, B., Veitch, Z., Cecchetto, M., Parissenti, A.M., 2008. Role of drug transporters and drug accumulation in the temporal acquisition of drug resistance. BMC Cancer 8, 318.
Jelínek, M., Balušíková, K., Kopperová, D., Němcová-Fürstová, V., Šrámek, J., Fidlerová, J., Zanardi, I., Ojima, I., Kovář, J., 2013. Caspase-2 is involved in cell death induction by taxanes in breast cancer cells. Cancer Cell Int. 13, 42.
Jelínek, M., Balušíková, K., Schmiedlová, M., Němcová-Fürstová, V., Šrámek, J., Stančíková, J., Zanardi, I., Ojima, I., Kovář, J., 2015. The role of individual caspases in cell death induction by taxanes in breast cancer cells. Cancer Cell Int. 15, 8.
Jordan, M.A., Wendell, K., Gardiner, S., Derry, W.B., Copp, H., Wilson, L., 1996. Mitotic block induced in HeLa cells by low concentrations of paclitaxel (Taxol) results in abnormal mitotic exit and apoptotic cell death. Cancer Res. 56, 816–825.
Kars, M.D., Iseri, O.D., Gündüz, U., Ural, A.U., Arpaci, F., Molnár, J., 2006. Development of rational in vitro models for drug resistance in breast cancer and modulation of MDR by selected compounds. Anticancer Res. 26, 4559–4568.
Kathawala, R.J., Wang, Y.J., Shukla, S., Zhang, Y.K., Alqahtani, S., Kaddoumi, A., Ambudkar, S.V., Ashby Jr., C.R., Chen, Z.S., 2015. ATP-binding cassette subfamily B member 1 (ABCB1) and subfamily C member 10 (ABCC10) are not primary resistance factors for cabazitaxel. Chin. J. Cancer 34, 115–120.
Kavallaris, M., Kuo, D.Y., Burkhart, C.A., Regl, D.L., Norris, M.D., Haber, M., Horwitz, S.B., 1997. Taxol-resistant epithelial ovarian tumors are associated with altered expression of specific beta-tubulin isotypes. J. Clin. Invest. 100, 1282–1293.
Kenicer, J., Spears, M., Lyttle, N., Taylor, K.J., Liao, L., Cunningham, C.A., Lambros, M., MacKay, A., Yao, C., Reis-Filho, J., Bartlett, J.M., 2014. Molecular characterization of isogenic taxane resistant cell lines identify novel drivers of drug resistance. BMC Cancer 14, 762.
Kim, S.C., Yu, J., Lee, J.W., Park, E.S., Chi, S.C., 2005. Sensitive HPLC method for quantitation of paclitaxel (Genexol) in biological samples with application to preclinical pharmacokinetics and biodistribution. J. Pharm. Biomed. Anal. 39, 170–176.
Kovář, J., Ehrlichová, M., Smejkalová, B., Zanardi, I., Ojima, I., Gut, I., 2009. Comparison of cell death-inducing effect of novel taxane SB-T-1216 and paclitaxel in breast cancer cells. Anticancer Res. 29, 2951–2960.
Li, W., Zhai, B., Zhi, H., Li, Y., Jia, L., Ding, C., Zhang, B., You, W., 2014. Association of ABCB1, β tubulin I, and III with multidrug resistance of MCF7/DOC subline from breast cancer cell line MCF7. Tumour Biol. 35, 8883–8891.
Liu, H., Ma, Z., Wu, B., 2013. Structure-activity relationships and in silico models of P-glycoprotein (ABCB1) inhibitors. Xenobiotica 43, 1018–1026.
Marchetti, S., Pluim, D., Beijnen, J.H., Mazzanti, R., van Tellingen, O., Schellens, J.H., 2014. Effect of the drug transporters ABCB1, ABCC2, and ABCG2 on the disposition and brain accumulation of the taxane analog BMS-275,183. Invest. New Drugs 32, 1083–1095.
Markman, M., 2008. Pharmaceutical management of ovarian cancer: current status. Drugs 68, 771–789.
Matesanz, R., Trigili, C., Rodríguez-Salarichs, J., Zanardi, I., Pera, B., Nogales, A., Fang, W.S., Jímenez-Barbero, J., Canales, A., Barasoain, I., Ojima, I., Díaz, J.F., 2014. Taxanes with high potency inducing tubulin assembly overcome tumoural cell resistances. Bioorg. Med. Chem. 22, 5078–5090.
Murray, S., Briasoulis, E., Linardou, H., Bafaloukos, D., Papadimitriou, C., 2012. Taxane resistance in breast cancer: mechanisms, predictive biomarkers and circumvention strategies. Cancer Treat. Rev. 38, 890–903.
Nabholtz, J.M., Gligorov, J., 2005. The role of taxanes in the treatment of breast cancer. Expert. Opin. Pharmacother. 6, 1073–1094.
Němcová-Fürstová, V., Kopperová, D., Balušíková, K., Ehrlichová, M., Brynychová, V., Václavíková, R., Daniel, P., Souček, P., Kovář, J., 2016. Characterization of acquired paclitaxel resistance of breast cancer cells and involvement of ABC transporters. Toxicol. Appl. Pharmacol. 310, 215–228.
O'Brien, C., Cavet, G., Pandita, A., Hu, X., Haydu, L., Mohan, S., Toy, K., Rivers, C.S., Modrusan, Z., Amler, L.C., Lackner, M.R., 2008. Functional genomics identifies ABCC3 as a mediator of taxane resistance in HER2-amplified breast cancer. Cancer Res. 68, 5380–5389.
Ojima, I., Duclos, O., Zucco, M., Bissery, M.C., Combeau, C., Vrignaud, P., Riou, J.F., Lavelle, F., 1994. Synthesis and structure-activity relationships of new antitumor taxoids. Effects of cyclohexyl substitution at the C-3′ and/or C-2 of taxotere (docetaxel). J. Med. Chem. 37, 2602–2608.
Ojima, I., Slater, J.C., Michaud, E., Kuduk, S.D., Bounaud, P.Y., Vrignaud, P., Bissery, M.C., Veith, J.M., Pera, P., Bernacki, R.J., 1996. Syntheses and structure-activity relationships of the second-generation antitumor taxoids: exceptional activity against drug-resistant cancer cells. J. Med. Chem. 39, 3889–3896.
Ojima, I., Slater, J.C., Kuduk, S.D., Takeuchi, C.S., Gimi, R.H., Sun, C.M., Park, Y.H., Pera, P., Veith, J.M., Bernacki, R.J., 1997. Syntheses and structure-activity relationships of taxoids derived from 14 beta-hydroxy-10-deacetylbaccatin III. J. Med. Chem. 40, 267–278.
Ojima, I., Bounaud, P.Y., Takeuchi, C., Pera, P., Bernacki, R.J., 1998. New taxanes as highly efficient reversal agents for multidrug resistance in cancer cells. Bioorg. Med. Chem. Lett. 8, 189–194.
Ojima, I., Lin, S., Slater, J.C., Wang, T., Pera, P., Bernacki, R.J., Ferlini, C., Scambia, G., 2000. Syntheses and biological activity of C-3′-difluoromethyl-taxoids. Bioorg. Med. Chem. 8, 1619–1628.
Ojima, I., Chen, J., Sun, L., Borella, C.P., Wang, T., Miller, M.L., Lin, S., Geng, X., Kuznetsova, L., Qu, C., Gallager, D., Zhao, X., Zanardi, I., Xia, S., Horwitz, S.B.,

Mallen-StClair, J., Guerriero, J.L., Bar-Sagi, D., Veith, J.M., Pera, P., Bernacki, R.J., 2008. Design, synthesis, and biological evaluation of new-generation taxoids. J. Med. Chem. 51, 3203–3221.
Orr, G.A., Verdier-Pinard, P., McDaid, H., Horwitz, S.B., 2003. Mechanisms of Taxol resistance related to microtubules. Oncogene 22, 7280–7295.
Paller, C.J., Antonarakis, E.S., 2011. Cabazitaxel: a novel second-line treatment for metastatic castration-resistant prostate cancer. Drug Des. Devel. Ther. 5, 117–124.
Parness, J., Horwitz, S.B., 1981. Taxol binds to polymerized tubulin in vitro. J. Cell. Biol. 91, 479–487.
Pavlikova, N., Bartonova, I., Dincakova, L., Halada, P., Kovar, J., 2014. Differentially expressed proteins in human breast cancer cells sensitive and resistant to paclitaxel. Int. J. Oncol. 45, 822–830.
Pavlíková, N., Bartoňová, I., Balušíková, K., Kopperova, D., Halada, P., Kovář, J., 2015. Differentially expressed proteins in human MCF-7 breast cancer cells sensitive and resistant to paclitaxel. Exp. Cell. Res. 333, 1–10.
Rao, S., Orr, G.A., Chaudhary, A.G., Kingston, D.G., Horwitz, S.B., 1995. Characterization of the taxol binding site on the microtubule. 2-(m-Azidobenzoyl)taxol photolabels a peptide (amino acids 217–231) of beta-tubulin. J. Biol. Chem. 270, 20235–20238.
Rao, S., He, L., Chakravarty, S., Ojima, I., Orr, G.A., Horwitz, S.B., 1999. Characterization of the Taxol binding site on the microtubule. Identification of Arg(282) in beta-tubulin as the site of photoincorporation of a 7-benzophenone analogue of Taxol. J. Biol. Chem. 274, 37990–37994.
Reed, K., Hembruff, S.L., Sprowl, J.A., Parissenti, A.M., 2010. The temporal relationship between ABCB1 promoter hypomethylation, ABCB1 expression and acquisition of drug resistance. Pharmacogenomics J. 10, 489–504.
Sastry, G.M., Adzhigirey, M., Day, T., Annabhimoju, R., Sherman, W., 2013. Protein and ligand preparation: parameters, protocols, and influence on virtual screening enrichments. J. Comput. Aided. Mol. Des. 27, 221–234.
Shi, J.F., Yang, N., Ding, H.J., Zhang, J.X., Hu, M.L., Leng, Y., Han, X., Sun, Y.J., 2014. ERα directly activated the MDR1 transcription to increase paclitaxel-resistance of ERα-positive breast cancer cells in vitro and in vivo. Int. J. Biochem Cell Biol. 53, 35–45.
Smoter, M., Bodnar, L., Duchnowska, R., Stec, R., Grala, B., Szczylik, C., 2011. The role of Tau protein in resistance to paclitaxel. Cancer Chemother. Pharmacol. 68, 553–557.
Snyder, J.P., Nettles, J.H., Cornett, B., Downing, K.H., Nogales, E., 2001. The binding conformation of Taxol in beta-tubulin: a model based on electron crystallographic density. Proc. Natl. Acad. Sci. U S A 98, 5312–5316.
Sun, R., Liu, Z., Wang, L., Lv, W., Liu, J., Ding, C., Yuan, Y., Lei, G., Xu, C., 2015. Overexpression of stathmin is resistant to paclitaxel treatment in patients with non-small cell lung cancer. Tumour Biol. 36, 7195–7204.
Szewczyk, P., Tao, H., McGrath, A.P., Villaluz, M., Rees, S.D., Lee, S.C., Doshi, R., Urbatsch, I.L., Zhang, Q., Chang, G., 2015. Snapshots of ligand entry, malleable binding and induced helical movement in P-glycoprotein. Acta Crystallogr. D. Biol. Crystallogr. 71, 732–741.
Vobořilová, J., Němcová-Fürstová, V., Neubauerová, J., Ojima, I., Zanardi, I., Gut, I., Kovář, J., 2011. Cell death induced by novel fluorinated taxanes in drug-sensitive and drug-resistant cancer cells. Invest. New Drugs 29, 411–423.
Wang, H., Vo, T., Hajar, A., Li, S., Chen, X., Parissenti, A.M., Brindley, D.N., Wang, Z., 2014. Multiple mechanisms underlying acquired resistance to taxanes in selected docetaxel-resistant MCF-7 breast cancer cells. BMC Cancer 14, 37.
Woods, C.M., Zhu, J., McQueney, P.A., Bollag, D., Lazarides, E., 1995. Taxol-induced mitotic block triggers rapid onset of a p53-independent apoptotic pathway. Mol. Med. 1, 506–526.
Yared, J.A., Tkaczuk, K.H., 2012. Update on taxane development: new analogs and new formulations. Drug Des. Devel. Ther. 6, 371–384.
Zhang, J., Li, D., Sun, T., Liang, L., Wang, Q., 2015. Interaction of P-glycoprotein with anti-tumor drugs: the site, gate and pathway. Soft Matter 11, 6633–6641.

4.3 Paper 3

DIFFERENTIALLY EXPRESSED MITOCHONDRIAL PROTEINS IN HUMAN MCF7 BREAST CANCER CELLS RESISTANT TO PACLITAXEL

Daniel, P., Halada, P., Jelínek, M., Balušíková, K., & Kovář, J. (**2019**)

International journal of molecular sciences, *20*(12), 2986.

https://doi.org/10.3390/ijms20122986

International Journal of
Molecular Sciences

MDPI

Article

Differentially Expressed Mitochondrial Proteins in Human MCF7 Breast Cancer Cells Resistant to Paclitaxel

Petr Daniel [1,*], Petr Halada [2], Michael Jelínek [1], Kamila Balušíková [1] and Jan Kovář [1,*]

[1] Department of Biochemistry, Cell and Molecular Biology, Third Faculty of Medicine, Charles University, Ruská 87, 100 00 Prague, Czech Republic; michael.j@email.cz (M.J.); kamila.balusikova@lf3.cuni.cz (K.B.)
[2] Laboratory of Molecular Structure Characterization, Institute of Microbiology, v.v.i., Vídeňská 1083, 142 20 Prague, Czech Republic; halada@biomed.cas.cz
* Correspondence: petr.daniel@lf3.cuni.cz (P.D.); jan.kovar@lf3.cuni.cz (J.K.); Tel.: +420-267-102-658 (P.D. & J.K.)

Received: 6 May 2019; Accepted: 17 June 2019; Published: 19 June 2019

Abstract: Identification of novel proteins with changed expression in resistant cancer cells could be helpful in elucidation mechanisms involved in the development of acquired resistance to paclitaxel. In this study, we carried out a 2D-PAGE using the mitochondrial-enriched fraction from paclitaxel-resistant MCF7/PacR cells compared to original paclitaxel-sensitive MCF7 breast cancer cells. Differentially expressed proteins were identified employing mass spectrometry. We found that lysosomal cathepsin D and mitochondrial abhydrolase-domain containing protein 11 (ABHD11) had decreased expression in MCF7/PacR cells. On the other hand, mitochondrial carbamoyl-phosphate synthetase 1 (CPS1) and ATPase family AAA-domain containing protein 3A and 3B (ATAD3A, ATAD3B) were overexpressed in MCF7/PacR cells. Further, we showed that there was no difference in localization of CPS1 in MCF7 and MCF7/PacR cells. We demonstrated a significant increase in the number of CPS1 positive MCF7/PacR cells, using FACS analysis, compared to the number of CPS1 positive MCF7 cells. Silencing of CPS1 expression by specific siRNA had no significant effect on the resistance of MCF7/PacR cells to paclitaxel. To summarize, we identified several novel proteins of a mitochondrial fraction whose role in acquired resistance to paclitaxel in breast cancer cells should be further assessed.

Keywords: breast cancer cells; paclitaxel resistance; mitochondria; two-dimensional electrophoresis; carbamoyl-phosphate synthetase 1 (CPS1); abhydrolase-domain containing protein 11 (ABHD11); cathepsin D; ATPase family AAA-domain containing protein 3A and 3B (ATAD3A, 3B)

1. Introduction

Breast cancer is the most commonly diagnosed cancer in women with 1.67×10^6 newly diagnosed cases and nearly 5×10^5 deaths per year [1]. Because of the heterogeneous nature of breast cancer, chemotherapy is based on various anticancer agents [2]. Specific chemotherapy by aromatase inhibitors (i.e., Tamoxifen ®) for estrogen-positive breast cancer or monoclonal antibody (i.e., Trastuzumab ®) for HER2 positive breast cancer can be useful when used in combination with anthracyclines (Doxorubicin, Epirubicin) and taxanes (Paclitaxel, Taxol®, and Docetaxel, Taxotere®) [3,4]. Taxanes and anthracyclines are the preferred choices for the treatment of triple-negative breast cancer [4,5].

The anticancer effect of paclitaxel (Taxol ®) was discovered while testing yew (*Taxus brevifolia*) bark extract on cancer cell proliferation [6]. It was shown that taxanes, i.e., taxol-related compounds, exert their effects through binding to the beta subunit of tubulin [7,8], and thus stabilizing microtubules [9]. Cells exposed to clinical doses of taxanes trigger the spindle assembly checkpoint and subsequently

initiate apoptosis [10]. However, the cells arrested in mitosis may exit mitosis and die via various mechanisms, survive as senescent cells, or may be able to duplicate as aneuploid cells [11].

Acquired resistance has been extensively studied in cultured paclitaxel-resistant cells of breast [12–15], ovarian [16,17], lung [18], prostate [19,20] and hepatocellular [21] origins. The most common finding is that paclitaxel-resistant cells induce the expression of one or more members of the ATP-binding cassette (ABC) transporter family, particularly the ABCB1 transporter (P-glycoprotein) [14,22]. Other broadly discussed mechanisms that can contribute to taxane resistance are mutations or alterations in the expression of both tubulin subunits [21,23], expression of detoxifying enzymes [24], and expression of microtubule-associated proteins [25]. Other mechanisms of taxane resistance have also been discussed [26].

In order to elucidate the molecular mechanisms of acquired resistance to taxanes, we established an MCF7/PacR subline resistant to death-inducing concentrations of paclitaxel (300 nM) through multistep adaptation from the original paclitaxel-sensitive MCF7 cell line [14]. We analyzed the expression of 49 known human ABC transporters at the mRNA and protein level in paclitaxel-sensitive MCF7 cells versus paclitaxel-resistant MCF7/PacR cells [14]. ABCB1, ABCB4, ABCC2, and ABCC3 transporters were found to be overexpressed in MCF7/PacR cells. Concerning transporter ABCB1, it was shown to transport paclitaxel out of cancer cells [27]. Molecular docking using a humanized model of mouse ABCB1 transporter showed the binding of paclitaxel into its large binding cavity and transport of taxanes out of MCF7/PacR cells [28]. Recently, interaction and model of paclitaxel transport by ABCB1 transporter was elegantly presented [29]. Beside enhanced transporter activity, we reported that thyroid-hormone interacting protein 6 (TRIP6) is markedly upregulated (650%) whereas lysosomal protease cathepsin D and heat shock protein 27 (HSP27) are both downregulated (28% and 47%, respectively) in MCF/PacR cells [30].

Downregulation of ABCB1 expression leads to only a partial decrease in resistance to paclitaxel. It indicates that more mechanisms might be involved in paclitaxel resistance in MCF7/PacR cells [28,30]. Mitochondria, where up to 1,900 constituent proteins are present [31], play an essential role in apoptosis regulation [32] and thus it is reasonable to test the possible involvement of mitochondrial proteins in resistance to paclitaxel. Mitochondria are also essential for cell metabolism and respiration [33], cell signaling [34], and other cell functions [35,36]. Therefore, in the present study, we tested differences in protein expression in the mitochondrial fraction of paclitaxel-resistant MCF7/PacR compared to paclitaxel-sensitive MCF7 breast cancer cells, using two-dimensional polyacrylamide gel electrophoresis (2D-PAGE). We found that mitochondrial carbamoyl-phosphate synthetase I (CPS1) was significantly overexpressed (494%) in MCF7/PacR cells. It seems that its expression was not caused by increased expression in each MCF7/PacR cell but rather due to an increase in the number of CPS1 positive MCF7/PacR cells. Downregulation of CPS1 expression in MCF7/PacR cells had no effect on resistance to paclitaxel. Other proteins with changed expression were mitochondrial lipase abhydrolase domain-containing protein 11 (ABHD11) (downregulation to 68%) and ATPase family AAA-domain containing protein 3A and 3B (ATAD3A/3B) (downregulation to 154% was statistically nonsignificant). Probably as a product of contamination of mitochondrial fraction with lysosomes, we also detected lysosomal protease cathepsin D (CTSD) downregulated in MCF7/PacR cells (19%).

2. Results

2.1. Isolation of Mitochondrial Fraction

To isolate mitochondria from MCF7 breast cancer cells, we used a Mitochondria QProteome®Mitochondria Isolation Kit (Qiagen) (see Section 4). Obtained mitochondrial fractions were termed "high-purity mitochondrial fraction".

At first, we tested the integrity of the mitochondrial fraction from MCF7 cells using western blot analysis with antibodies against markers of mitochondrial compartments. We observed a CPS1 (carbamoyl-phosphate synthetase 1) (mitochondrial matrix marker) and Smac/Diablo (second

Int. J. Mol. Sci. **2019**, *20*, 2986

mitochondria-derived activator of caspase/direct inhibitor of apoptosis-binding protein with low pI) (mitochondrial intermembrane marker) signal in the mitochondrial fraction but not in the cytosolic fraction. SDHA (succinate dehydrogenase flavoprotein complex, subunit alpha) (inner mitochondrial membrane marker) was also detected in the mitochondrial fraction as well as weakly detected in the cytosolic fraction (Figure 1). These data indicate that the mitochondrial fraction contains mostly undamaged mitochondria.

To examine potential contamination of the mitochondrial fraction, we performed western blot analysis using antibodies against the endoplasmic reticulum, cytoskeleton, and cytosolic proteins. The mitochondrial fraction contained calnexin (an endoplasmic reticulum protein), β-actin (cytoskeletal protein), and GAPDH (glyceraldehyde-3-phosphate dehydrogenase) (Figure 1). Other cytoplasmic proteins, such as Hop (Hsp70-Hsp90 organizing protein) and Akt/PKB (protein kinase B) were virtually absent in the mitochondrial fraction. Taken together, the mitochondrial fraction was free of most cytosolic proteins. However, contamination with endoplasmic reticulum as well as cytoskeleton proteins was detected.

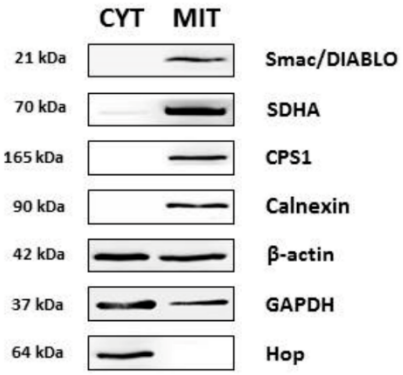

Figure 1. Comparison of the expression of selected proteins in cytosolic (CYT) and high-purity mitochondrial (MIT) fractions isolated from MCF7 cells using a QProteome Mitochondria Isolation Kit (see Section 4). The level of tested proteins was assessed using western blot analysis employing relevant antibodies (see Section 4). Smac/Diablo (Second mitochondria-derived activator of caspases/Direct IAP binding protein with low pI, mitochondrial intermembrane space), SDHA (succinate dehydrogenase complex flavoprotein subunit α, inner mitochondrial membrane), CPS1 (carbamoyl-phosphate synthetase 1, mitochondrial matrix), calnexin (endoplasmic reticulum), β-actin (representative cytoskoletal protein), GAPDH (glyceraldehyde 3-phosphate dehydrogenase, cytosol), Hop (Hsp70-Hsp90 organizing protein, cytosol).

2.2. *Two-Dimensional Electrophoresis of Mitochondrial Fraction*

We used the "high-purity mitochondrial fraction" of paclitaxel-sensitive MCF7 and paclitaxel-resistant MCF7/PacR cells for conventional 2D-PAGE analysis (see Section 4). Coomassie brilliant blue-stained pairs of gels (3-11NL, 11 cm, 125 μg of proteins) from MCF7 (served as controls) and MCF7/PacR cells, were used for spot analyses. Three independent pairs of gels were used. In these gels, we were able to detect and match approximately 600 spots per gel (Figure 2) using ImageMaster 2D Platinum 6.0 software (see Section 4). It should be noted that the observed number of spots did not correspond to the number of detected proteins. This was mainly due to post-translational modifications that affected the isoelectric point as well as the molecular weights of the proteins. Thus, some proteins occurred as multiple spots in 2D-PAGE gel, which were typically seen as a string of spots.

Int. J. Mol. Sci. **2019**, *20*, 2986

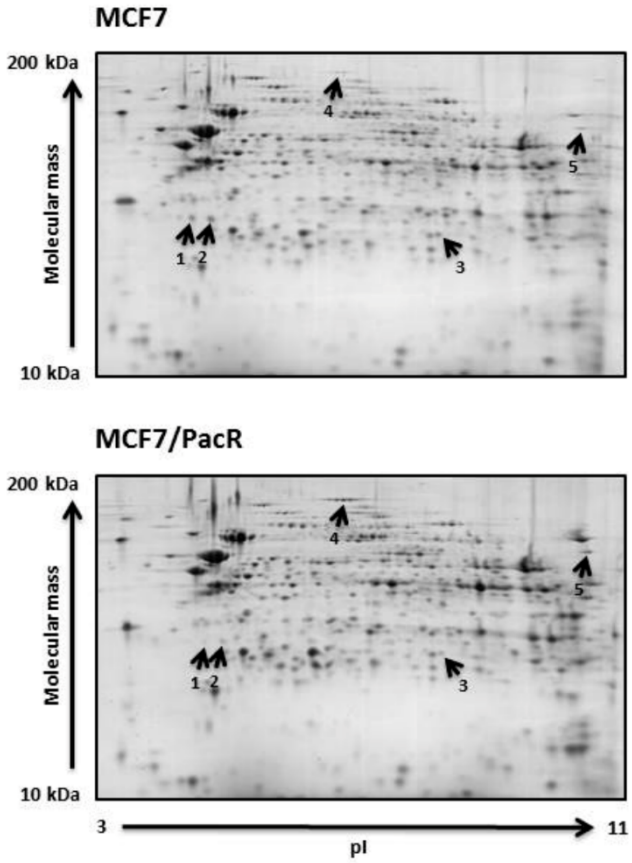

Figure 2. Differences between paclitaxel-sensitive MCF7 cells and paclitaxel-resistant MCF7/PacR cells concerning protein expression in high-purity mitochondrial fractions. Representative 2D gels of three independent pairs of gels (see Section 4) show five spots with differing expression (at least two-fold change). These five spots were identified as cathepsin D (spot 1 and spot 2), ABHD11 (abhydrolase domain-containing protein 11) (spot 3), CPS1 (carbamoyl-phosphate synthetase 1) (spot 4), and ATAD3A, ATAD3B (ATPase family AAA domain-containing protein 3A and 3B) (spot 5).

2.3. Spot Analysis and Protein Identification

Spot volumes of 600 matched spots were statistically analyzed (Student´s *t*-test). We found five spots with altered (at least a two-fold change) spot volumes in MCF7/PacR cells compared to control MCF7 cells (Figure 2). These spots were excised and digested with trypsin protease. The resulting peptides were analyzed using MALDI-TOF mass spectrometry (for details see Section 4).

Spots with downregulated expression in MCF7/PacR cells were lysosomal cathepsin D (spot 1 and 2 with volumes decreased to 16% and 23% of control cells, respectively), mitochondrial abhydrolase domain-containing protein 11 (ABHD11) (spot 3 with a volume decreased to 30% of control cells). Spots with upregulated expression were mitochondrial carbamoyl-phosphate synthetase 1 (CPS1) (spot 4 with a volume increased to 518% of control cells), mitochondrial ATPase family AAA domain-containing protein 3A and 3B (ATAD3A, ATAD3B) (spot 5 with a volume increased to 257% of control cells) (Figures 2 and 3, Table 1).

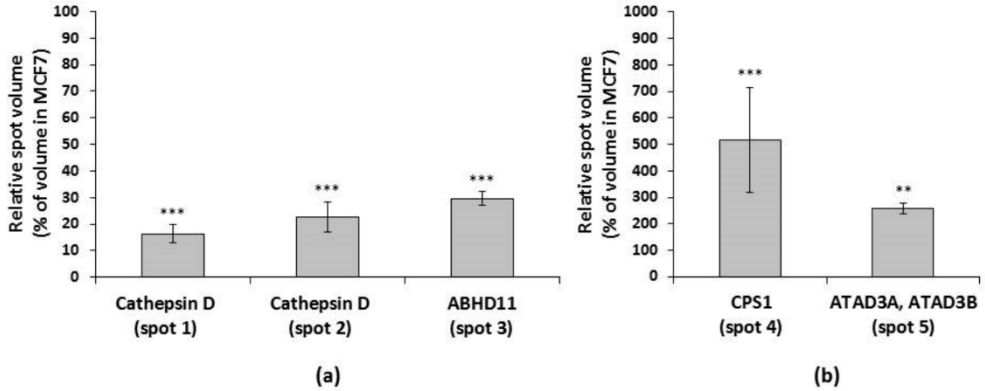

Figure 3. Expression levels of the identified proteins, (**a**) downregulated and (**b**) upregulated, in paclitaxel-resistant MCF7/PacR cells is presented as a percentage of the level in paclitaxel-sensitive MCF7 cells. Each column represents the mean value of the expression level ± SEM of the corresponding spots from three independent sets of gels. ** $p < 0.01$, *** $p < 0.001$ when compared with the level in MCF7 cells.

Table 1. Protein identification of five spots with differing expression using MALDI-TOF MS. Table includes spot number, protein name, UniProtKB database number (DTB No.), number of peptides matched to the identified protein, sequence coverage (SC), peptide sequences confirmed by MS/MS, theoretical (Th.)/experimental (Exp.) values of protein molecular weight (MW) and pI.

Spot No.	Protein Name	DTB No.	No. of Peptides	SC [%]	MS/MS Confirmation	MW [kDa] Th./Exp.	pI Th./Exp.
1	Cathepsin D	P07339	12	33	FDGILGMAYPR YYTVFDRDNNR LVDQNIFSFYLSR	45/28	6.1/4.7
2	Cathepsin D	P07339	15	38	FDGILGMAYPR YYTVFDRDNNR LVDQNIFSFYLSR ISVNNVLPVFDNLMQQK	45/28	6.1/5.0
3	Abhydrolase domain-containing protein 11, ABHD11	Q8NFV4	21	68	AINIADELPR GGAEPRPLPLSYR TAMLLALQRPELVER VNLDALTQHLDKILAFPQR	35/27	9.5/7.2
4	Carbamoyl-phosphate synthase 1 [ammonia], mitochondrial, CPS1	P31327	14	10	FVHDNYVIR GILIGIQQSFRPR SAYALGGLGSGICPNR	164/164	6.3/6.0–6.2
5	ATPase family AAA domain-containing protein 3A, ATAD3A	Q9NVI7	29	38	TAGTLFGEGFR LDSVIEFSIPDSLLIR LQAYHTQTTPLIEYYR QRYEDQLKQQQLLNEENLR	71/71	9.1/10.4–10.7
	ATPase family AAA domain-containing protein 3B, ATAD3B	Q5T9A4	17	29	LKEYEAAVEQLKSEQIR	73/73	9.3/10.4–10.7

MALDI-TOF MS data indicated that the cathepsin D spots (spots 1 and 2, approximately 28 kDa) represent the heavy-chain of catalytically active full-form cathepsin D (45 kDa) based on their ascertained sequences and molecular weight [30] (Table 1, Figure 2). These spots differ in their isoelectric point (likely due to post-translational modification). For both spots, the experimental isoelectric point (approximately 4.7 and 5.0) is lower than theoretical (6.1).

The spot determined as ABHD11 (spot 3) also differed from its predicted (35 kDa) molecular weight (Table 1). We estimated its molecular weight to be approximately 27 kDa based on its position relative to the cathepsin D heavy chains spots (28 kDa) in 2D-PAGE gels. The experimental isoelectric point (approximately 7.2) of ABHD11 significantly differs from theoretical (9.5).

Spot 4 (a string of five spots of same molecular weight) (Table 1, Figure 2) were determined to be CPS1, which likely belongs to the post-translationally modified full-length protein (we estimated the molecular weight to be more than 150 kDa). The experimental isoelectric point is in agreement with theoretical value (6.3).

Mitochondrial proteins ATAD3A and ATAD3B (spot 5) are products of two genes (ATAD3A and ATAD3B) and their molecular weight (71 and 73 kDa, respectively) corresponded to their position in the 2D-PAGE gels. The experimental isoelectric point (approximately 10.4–10.7) differs from theoretical values (9.1 and 9.3).

2.4. Western Blot of Identified Proteins

We validated the changed expression of identified proteins using western blot and subsequent densitometry. We used whole-cell lysates of MCF7 cells and MCF7/PacR cells. Expression of cathepsin D (28 kDa band) decreased to 19% in MCF7/PacR cells (compared to control sensitive cells). This band should represent both spot 1 and spot 2 due to similar molecular weights. Expression of ABHD11 (27 kDa) decreased to 68% in MCF7/PacR cells, and expression of CPS1 (164 kDa) increased to 494% in MCF7/PacR cell. Expression of ATAD3A/B (71–73 kDa) increased to 154% in MCF7/PacR cells, however, the densitometric measurement was statistically insignificant in this case (Figure 4).

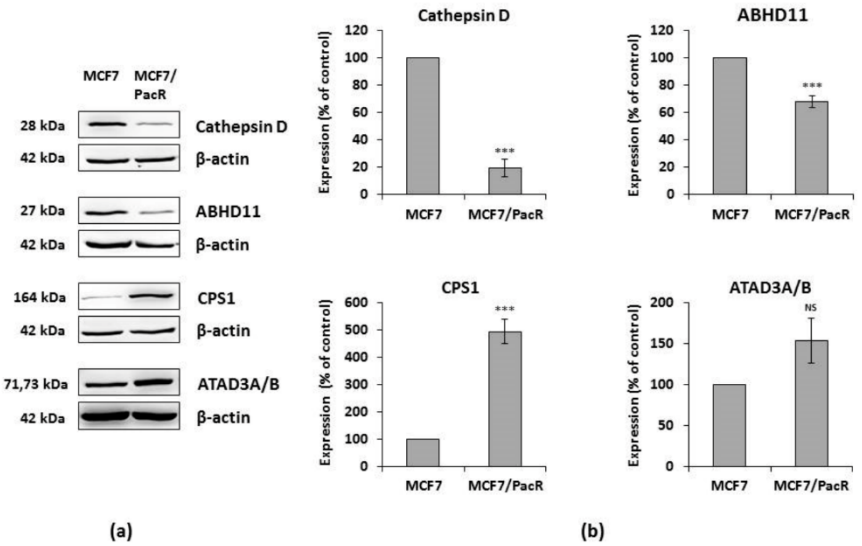

Figure 4. Confirmation of changes in protein expression detected by 2D analysis employing western blot analysis. (**a**) Western blot was performed with whole-cell lysates of paclitaxel-sensitive MCF7 cells and paclitaxel-resistant MCF7/PacR cells. Levels of tested proteins were assessed using western blot analysis employing relevant antibodies (see Section 4). β-actin served as a loading control. Representative results are from three independent experiments. (**b**) Densitometric analysis of western blots normalized to β-actin level. The expression of proteins in MCF7/PacR was compared to the expression in MCF cells (100%), and relative values were normalized to β-actin levels. Columns represent mean values of band volume ± SEM from three experimental values. *** $p < 0.001$ compared to the volume in MCF7 cells. NS = statistically non-significant difference.

2.5. Distribution of CPS1 within Cells

In order to assess the distribution of CPS1, which was the most upregulated protein in MCF7/PacR cells, we used confocal microscopy. Colocalization with the mitochondrial marker cytochrome c oxidase subunit IV (Cox IV) showed localization of CPS1 in the mitochondria of MCF7 cells as well as

Int. J. Mol. Sci. **2019**, *20*, 2986

MCF7/PacR cells. It has been proposed [37] that CPS1 is also localized in the cell nucleus. However, we did not detect CPS1 in the nuclei of either MCF7 and MCF7/PacR cells (Figure 5).

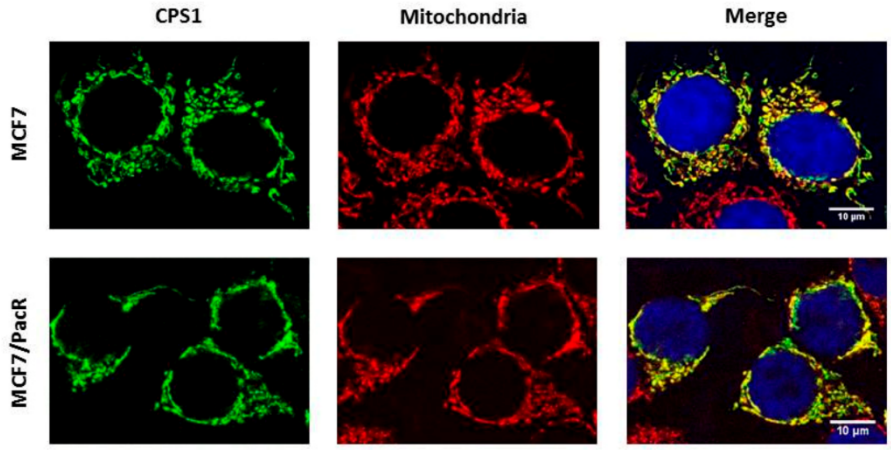

Figure 5. Cellular distribution of CPS1 (carbamoyl-phosphate synthetase 1) in paclitaxel-sensitive MCF7 cells and paclitaxel-resistant MCF7/PacR cells. The localization of CPS1 was detected using confocal microscopy (see Section 4). The localization of CPS1 (green), mitochondria (red), nuclei (blue) and the merge are shown. The data shown were obtained in one representative experiment of two independent experiments.

By using flow cytometry, we detected increased levels of CPS1 in MCF7/PacR cells (Figure 6a). However, the observed differences were due to the different number of CPS1 positive cells in MCF7 and MCF7/PacR cell populations. In MCF7 cells, only 9% were CPS1 positive cells whereas the number of CPS1 positive cells increased significantly to 30% in MCF7/PacR cells (Figure 6b). Thus, most MCF7, as well as MCF7/PacR cells, did not express CPS1. Upregulated expression of CPS1 is rather caused by the increasing number of CPS1 positive MCF7/PacR cells and not due to the increase of CPS1 expression in each MCF7/PacR cell.

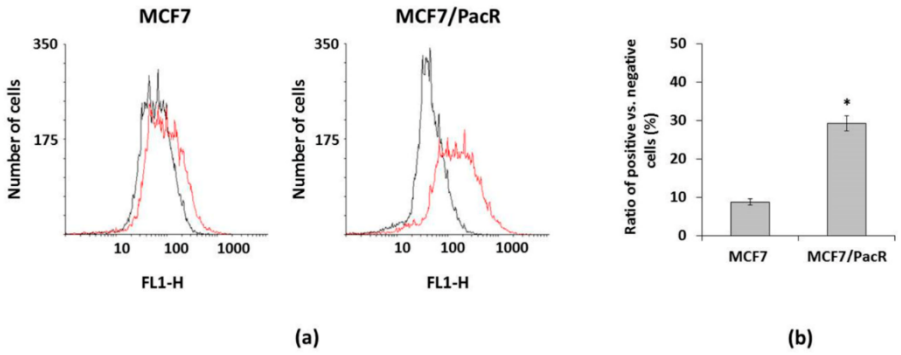

Figure 6. Expression of CPS1 (carbamoyl-phosphate synthetase 1) in paclitaxel-sensitive MCF7 cells and paclitaxel-resistant MCF7/PacR cells. The expression was assessed employing FACS (see Section 4). The data shown were obtained in one representative experiment from three independent experiments. (**a**) Histograms of MCF7 and MCF7/PacR cells, which were stained with a secondary antibody (black) or stained with a specific CPS1 antibody and then with the secondary antibody (red). (**b**) The number of CPS1 positive cells vs. negative cells (ratio) in MCF7 and MCF7/PacR cell population. Columns represent the mean value of the ratio ± SEM from two experimental values. * $p < 0.05$ compared to the ratio in paclitaxel-sensitive MCF7 cells.

Int. J. Mol. Sci. **2019**, *20*, 2986

2.6. Effect of CPS1 Silencing on Resistance to Paclitaxel

We further tested the effect of CPS1 silencing on the resistance of MCF7/PacR cells to paclitaxel. The effect was compared with the documented effect of ABCB1 silencing [27]. CPS1 and ABCB1 were knocked down in MCF7/PacR cells using Silencer®Select siRNAs (see "Materials and Methods"). Both used specific CPS1 siRNAs (A and B) efficiently (≥90%) silenced the expression of CPS1 in MCF7/PacR cells. ABCB1 knockdown was efficient to a similar extent. As a siRNA transfection control, we used MCF7/PacR cells treated with nonspecific siRNA (Figure 7b).

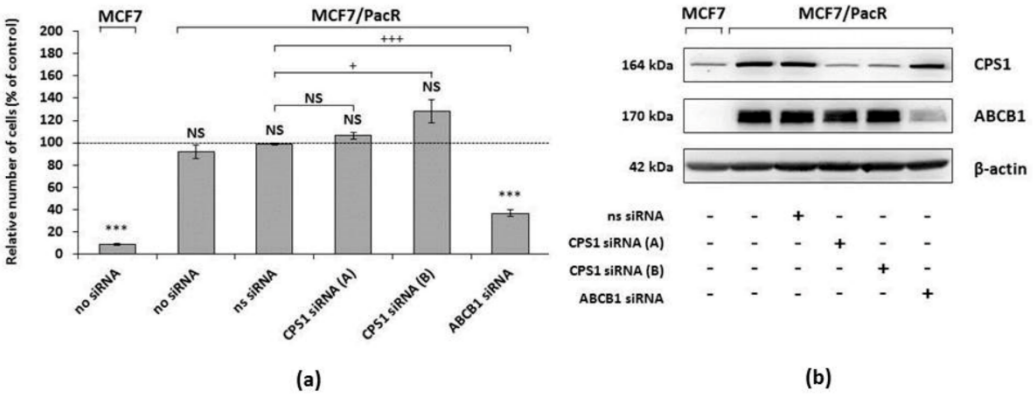

Figure 7. The effect of CPS1 (carbamoyl-phosphate synthetase 1) silencing and ABCB1 (ATP-binding cassette transporter B1) silencing on the growth and survival of paclitaxel-resistant MCF7/PacR cells in the paclitaxel-containing medium compared with the growth and survival of sensitive MCF7 cells in the paclitaxel-containing medium. (**a**) The cells were prepared and seeded as described in "Materials and Methods". The relative number of living sensitive MCF7 cells (no siRNA), resistant MCF7/PacR cells (no siRNA), resistant cells treated with non-specific siRNA (ns siRNA), and resistant cells treated with two different (A and B) CPS1 specific siRNAs (CPS1 siRNA), as well as with an ABCB1 specific siRNA (ABCB1 siRNA), was determined after 96 h of incubation (the number of sensitive MCF7 or resistant MCF7/PacR cells grown in paclitaxel-free medium represents 100%, i.e., the control). Each column represents the mean ± SEM of three independent experiments. *** $p < 0.001$ compared to the control. NS = a statistically non-significant difference. $^{+}$ $p < 0.05$, $^{+++}$ $p < 0.001$ compared to the effect of ns siRNA. (**b**) The effect of ns siRNA, specific CPS1 siRNA (A) and CPS1 siRNA (B), as well as specific ABCB1 siRNA, on the expression of CPS1 and ABCB1 in sensitive MCF7 cells and resistant MCF7/PacR cells cultured in paclitaxel-containing medium, is also shown. Levels of tested proteins were assessed using western blot analysis and the relevant antibodies (see Section 4). β-actin served as a loading control. Representative results come from three independent experiments.

MCF7/PacR cells with silenced CPS1 (CPS1 siRNA A and B) or with silenced ABCB1 were cultivated in a paclitaxel-containing medium (i.e., a 300 nM, death-inducing, concentration of paclitaxel) or paclitaxel-free medium (control representing 100% of grown cells) for 96 hours. After 96 hours, the number of living cells was determined (see "Materials and Methods"). The number of non-treated MCF7 cells, incubated with 300 nM paclitaxel for 96 hours, decreased to 9%. The number of non-treated MCF7/PacR cells, incubated with 300 nM paclitaxel for 96 hours, slightly and non-significantly decreased to 92%. The number of MCF7/PacR cells treated with nonspecific siRNA in the paclitaxel-containing medium did not change. The numbers of MCF7/PacR cells treated with both (A and B) specific CPS1 siRNAs nonsignificantly increased (106% and 128%, respectively). The number of MCF7/PacR cells treated with specific ABCB1 siRNA significantly decreased to 37% (Figure 7a).

We compared the number of MCF7/PacR cells treated with nonspecific siRNA (siRNA transfection control) with the number of MCF7/PacR cells treated with specific CPS1 or ABCB1 siRNAs in order to test the effect of CPS1 knockdown on resistance to paclitaxel compared to the effect of ABCB1

knockdown. There was no statistically significant decrease in the number of MCF7/PacR cells treated with both specific CPS1 siRNAs (A and B). Furthermore, for CPS1 siRNA B there was a slight, but statistically significant increase. In comparison, MCF7/PacR cells with knocked down ABCB1, the number of grown cells significantly decreased (Figure 7a).

These data indicate that knockdown of CPS1 does not affect the resistance of MCF7/PacR cells to paclitaxel. In contrast to CPS1, the effect of ABCB1 siRNA silencing on the resistance of MCF7/PacR cells to paclitaxel was significant.

3. Discussion

In this paper, we studied potential differences in the expression of mitochondrial proteins between paclitaxel-sensitive MCF7 and paclitaxel-resistant MCF7/PacR breast cancer cells. For 2D-PAGE analysis, we used a mitochondrial fraction isolated using a commercial kit. The mitochondrial fraction was contaminated with endoplasmic reticulum and other cytosolic proteins, such as GAPDH, although the isolated mitochondria were nearly undamaged (Figure 1). Contamination with the endoplasmic reticulum is typical for mitochondria-enriched fractions due to the close, functional contact with mitochondria [38]. It has also been shown that GAPDH can be localized in various cellular compartments depending on its function [39]. Thus, the mitochondrial fractions also likely contained vesicles of non-mitochondrial origin and endoplasmic reticulum.

Therefore, it is not surprising that in addition to the mitochondrial proteins, we found lysosomal protein cathepsin D during the 2D-PAGE analysis (Figure 2, Table 1) likely as a result of lysosomal contamination of the mitochondrial fraction. Cathepsin D is a lysosomal aspartyl endoproteinase whose mature form consists of non-covalent interactions between light (14 kDa) and heavy (34 kDa) chains [40]. The heavy chain of cathepsin D (approximately 28 kDa in our study) was shown to be downregulated in paclitaxel-resistant MCF7/PacR cells (to 25% of the level in paclitaxel-sensitive MCF7 cells) [30]. In the present study, cathepsin D most likely represents a contamination product in the mitochondrial fraction. Unlike our previous study [30], we observed two similarly downregulated spots for the heavy chain of cathepsin D (Figures 2 and 3, Table 1). The described spots differ only in their isoelectric point, likely reflecting their different post-translational modifications. Cathepsin D is known to be overexpressed in breast cancer cells, where it promotes growth and metastatic activity [41,42]. Signaling, via occupied intracellular estrogen receptors, stimulates cathepsin D transcription [43]. Tamoxifen was found to decrease cathepsin D expression [44]. Apart from its enzymatic role inside the lysosomes and in the tumor cell microenvironment (the secreted form of cathepsin D), it is also well known to be involved in the regulation of cell death [45–47]. Upon diverse death signals, cathepsin D translocates from lysosomes into the cytosol, where it executes its pro-apoptotic activities by cleaving specific substrates. The cleavage of these substrates contributes to the activation of the pro-apoptotic Bax protein [48]. Moreover, cathepsin D can directly cleave anti-apoptotic Bcl2 protein [49].

ABHD11 (abhydrolase domain-containing protein 11) also known as Williams–Beuren syndrome chromosomal region 21 protein (WBSCR21), is a member of the α/β-hydrolase domain family. Members of this large family are encoded by 19 human genes [50]. ABHD11 is localized in the locus that is deleted in Williams–Beuren syndrome, which is a multisystemic genetic disease [51]. It is unclear, whether ABHD11 deletion contributes to any of the symptoms associated with this syndrome. ABHD11 is a mitochondrial matrix hydrolase that processes an unknown lipid substrate [52]. Its predicted molecular mass (35 kDa) is in contrast with the observed position of the spot in our study (approximately 27 kDa) (Figure 2). This difference could be the result of the processing of ABHD11 N-terminal targeting sequence, at leucine 59, by mitochondrial processing peptidase during its transport into the mitochondria (based on MitoFates software, [53]). ABHD11 processing explains the discrepancy between its theoretical and experimental isoelectric point (Figure 2, Table 1). Processed N-terminal sequence is rich in basic amino acids (theoretical pI is 12.5). Increased enzymatic activity of ABHD11 was found in non-small lung cancer [54]. The ABHD11 locus also encodes for long non-coding RNA, termed as ABHD11-AS1 (antisense 1), whose expression is increased in gastric [55], colorectal [56],

pancreatic [57] and endometrial [58] cancer. In MCF7/PacR cells, ABHD11 is downregulated (to 68% of the level in control MCF7 cells) (Figure 4). Heat-shock protein 27, which is encoded by a neighboring gene, was also downregulated (50% of the level in control MCF7 cells) [30].

CPS1 (carbamoyl-phosphate synthetase 1) was the most upregulated mitochondrial protein found in MCF7/PacR cells (490% of the level in MCF7 cells) (Figures 4 and 5). As a mitochondrial matrix enzyme (EC 6.3.4.16), CPS1 catalyzes the first rate-limiting step of the urea cycle [59]. In this reaction, CPS1 generates carbamoyl phosphate from ammonia and bicarbonate. Recently, the CPS1 structure was elucidated in the presence of its activator, N-acetyl-L-glutamate (NAG) [59]. Unlike its prominent role in the urea cycle, there are currently no data about the participation of CPS1 in the acquired resistance to any chemotherapeutics. Remarkably, it was shown that transcription of CPS1 is negatively regulated by liver kinase B1 (also known as serine/threonine kinase 11) in lung adenocarcinoma cell lines [60,61]. In MCF7 cells, this kinase is regulated by estrogen [62]. The excess of mitochondrial carbamoyl phosphate can supply, by an unknown mechanism, the cytosolic pool that is utilized in pyrimidine synthesis [61], as well as promote cell proliferation. CPS1 could play a different role depending on the type of cancer cells. One study showed that overexpression of CPS1 associates with poor chemoradiotherapy response in rectal cancer [63]. However, in cancers of non-small intestinal origin, CPS1 expression is totally lost [64].

CPS1 gene is localized on chromosome 2 (Table 2) in the vicinity of the gene coding for a microtubule-associated protein (MAP2) which is a regulator of microtubule flexibility [65] and is known to be associated with resistance to paclitaxel [66]. Notably, we found that changes in CPS1 expression in MCF7/PacR cells (found by 2D-PAGE and western blot) (Figures 2–4, Table 1) are likely caused by an increased number of cells expressing CPS1 (Figure 6). However, for most MCF7, as well as MCF7/PacR cells, the expression of CPS1 was at a low level. Silencing of CPS1 expression in resistant MCF7/PacR cells resulted in a non-significant change in the number of MCF7/PacR cells cultivated in paclitaxel-containing medium (Figure 7). However, the high expression of ABCB1 transporter in MCF7/PacR cells could have masked the effect of specific CPS1 siRNA. Therefore, we also performed a simultaneous knock-down of ABCB1 and CPS1 in MCF7/PacR cells. However, the data were confusing, likely due to the strong off-target effects of the siRNA combination. Thus, it remains a question of whether CPS1 plays any role in acquired resistance to paclitaxel.

ATAD3A and ATAD3B (ATPase family AAA-domain containing protein 3A and 3B) are proteins associated with the inner mitochondrial membrane, which are coded by nuclear genes [67]. In primates, the ancestral gene ATAD3A (coding for 71 kDa protein), was tandemly duplicated and mutated. It resulted in the novel ATAD3B (coding for 73 kDa protein) and ATAD3C gene (coding for 46 kDa protein) [68]. In MCF7/PacR cells, we detected both the ATAD3A and ATAD3B proteins in a single spot (with upregulation to 250% of the level in control MCF7 cells) (see Figures 2 and 3, Table 1). However, we were not able to confirm the overexpression using western blot of whole cell lysates (results were statistically insignificant) (see Figure 4). ATAD3A forms hexameric ring structures, exposing its C-terminal ATPase domain into the mitochondrial matrix [69]. ATAD3 is crucial for maintaining mitochondrial dynamics [70], the mitochondrial nucleoid [71,72], the mitochondria-endoplasmic reticulum connection [73], cholesterol metabolism [74], cristae structure [74], and chemoresistance to doxorubicin [75]. ATAD3A expression correlates with the response to chemoradiotherapy in primary glioblastoma multiforme [76]. Higher expression of ATAD3A is associated with cisplatin resistance and PSA level in prostate cancer [77]. In breast and colon cancer, ATAD3A forms and stabilizes WASF3 in a complex with endoplasmic protein GRP78 [73]. WASF3 dysregulates expression of KISS3, a regulator of NFκB signaling pathway and thus promotes cell proliferation and metastatic activity [73]. It was shown that ATAD3B is expressed in pluripotent embryonic stem cells and in cancer cells where it negatively regulates ATAD3A function [78].

Table 2. All identified protein expression change in paclitaxel-resistant MCF7/PacR cells compared to paclitaxel-sensitive MCF7 cells. The table includes protein name, protein localization within the cell, known or predicted function in the cell, localization of the gene within the human genome, expression level in MCF7/PacR cells (compared to the level in MCF7 cells) determined by western blot, and corresponding references.

Protein Name/Abbreviation	Protein Localization	Function	Gene Localizaton	Expression in MCF7/PacR Cells
ATP binding cassette subfamily B member 1, **ABCB1**	Plasma membrane	Drug efflux [14]	7q21.12	Overexpressed, concrete level not determined [14]
ATP binding cassette subfamily B member 4, ABCB4	Plasma membrane	Drug efflux [14]	7q21.12	Overexpressed, concrete level not determined [14]
ATP binding cassette subfamily C member 2, **ABCC2**	Plasma membrane	Drug efflux [14]	10q24.2	Overexpressed, concrete level not determined [14]
ATP binding cassette subfamily C member 3, **ABCC3**	Plasma membrane	Drug efflux [14]	17q21.33	Overexpressed, concrete level not determined [14]
Abhydrolase domain-containing protein 11, **ABHD11**	Mitochondria	Putative lipid hydrolase [52]	7q11.23	68% [this paper]
ATPase family AAA domain-containing protein 3A and 3B, **ATAD3A**, **ATAD3B**	Mitochondria	Multiple (mitochondrial network, cristae structure, nucleoid binding) [69,71–75]	1p36.33	154% [this paper]
Carbamoyl-phosphate synthetase 1, **CPS1**	Mitochondria	Enzyme (urea cycle) [59,61]	2q34	494% [this paper]
Cathepsin D, **CTSD**	Lysosomes	Protein degradation, cell death [40,48,49]	11p15.5	28% [30], 19% [this paper]
Heat shock protein family B (small) member 1, **HSP27**	Cytosol	Signaling [30]	7q11.23	47% [30]
Thyroid hormone receptor interactor 6, **TRIP6**	Cytosol	Antiapoptotic signaling [30]	7q22.1	650% [30]

Multiple mechanisms for the regulation of ABCB1 expression in cancer cell lines have been discussed [79]. Interestingly, we showed that several genes (HSP27, ABHD11, ABCB4, and TRIP6) (Table 2), located on the long arm of chromosome 7 close to the ABCB1 and ABCB4 genes, have altered expression in MCF7/PacR cells. Curiously, the genes localized between centromere and ABCB1 (e.g., HSP27 and ABHD11) are both underexpressed and the gene for TRIP6, localized between the telomere and ABCB1, is overexpressed in MCF7/PacR. Changes in the expression of the mentioned genes could reflect genetic changes (like chromosome rearrangement) occurring in the long arm of chromosome 7.

4. Materials and Methods

4.1. Materials

All reagents were purchased from Sigma-Aldrich (St. Louis, MO, USA) unless otherwise specified. The following primary and secondary antibodies were used to detect protein expression: anti-CPS1 (B1) (sc376190, 1:500) from Santa-Cruz Biotechnology (Santa Cruz, CA, USA), anti-actin (clone AC-40, dilution 1:1000), anti-CPS1 [EPR7493-3] (ab129076, 1:1000), anti-GAPDH (ab9485, 1:1000) from Abcam (Cambridge, UK), anti-SDHA (D6J9M) XP®(#11998, 1:1000), anti-Smac/Diablo (79-1-83) (#2954, 1:1000), anti-COX IV (#11967S, 1:200), anti-Hop (D10E2) (#5670, 1:1000), anti-Calnexin (C5C9) (#2679, 1:1000) from Cell Signaling Technology (Danvers, MA, USA). Secondary antibodies HRP-linked goat anti-rabbit (sc-2004, 1:5000) or goat anti-mouse (sc-2005, 1:5000) were from Santa-Cruz Biotechnology (Santa Cruz, CA, USA). Secondary goat anti-rabbit IgG H&L Alexa Fluor®488 (ab150077) was from Abcam (Cambridge, UK), and goat anti-mouse IgG H&L $F(ab)_2$ Alexa Fluor®594 (#8890S) was from Cell Signaling Technology (Danvers, MA, USA).

4.2. Cell Culture

Human breast cancer cell line MCF7 was purchased from ATCC (Manassas, VA, USA). The establishment of the paclitaxel-resistant subline MCF7/PacR was described previously [14]. The MCF7 breast cancer cell line was cultivated in RPMI medium supplemented with 10% fetal bovine serum, whereas the MCF7/PacR subline was cultivated in RPMI medium containing 10% FBS and 300 nM paclitaxel. The cells were cultivated at 37 °C in a humidified atmosphere with 5% CO_2.

4.3. Preparation of Mitochondria-Enriched Fraction

For isolation of the mitochondria-enriched fraction, cells were seeded at a density of 2.0×10^6 cells into six Petri dishes (Ø 10 cm, i.e., 1.2×10^7 cells/experiment). After 24 h, media were replaced for the fresh ones. After 72 h, the cells were harvested with the trypsin-EDTA solution into 10 mL of ice-cold PBS and centrifuged (500 *g*, 10 min, 4 °C). Mitochondria were enriched using a QProteome®mitochondria isolation kit (Qiagen, Hilden, Germany) according to the manufacturer´s protocol with the following modifications. Briefly, cell pellets (approximately 6.0×10^7 cells) were washed with 3 ml of 0.9% NaCl and resuspended in 3 ml of lysis buffer (with protease inhibitors). The resuspended cells were then incubated on an end-on-end shaker for 10 min at 4 °C and centrifuged (1000 *g* for 10 min, 4 °C). The supernatant (cytosolic fraction) was carefully removed for further analysis. Cell pellets were resuspended in 3 ml of disruption buffer (with protease inhibitors), and organelles were released by passing the suspension ten times through a 26 G needle. Samples were centrifuged (1000 *g*, 10 min, 4 °C) and the supernatant was transferred into new tubes. Cell pellets were resuspended in 1 mL of disruption buffer (with protease inhibitors), and the lysis was repeated by passing the suspension ten times through a 26 G needle. Samples were centrifuged (1000 *g*, 10 min, 4 °C), cell pellets (unbroken cells and nuclei) were kept for further analysis. Supernatants were mixed and centrifuged (6000 *g*, 10 min, 4 °C). The resulting supernatant (microsomal fraction) was kept for further analysis. Cell pellets (crude mitochondria fractions) were dissolved in 750 µL of mitochondria purification buffer and purified using a density gradient according to the manufacturer´s protocol. Finally, the pellets were resuspended in RIPA buffer (for western blot analysis) or protein extraction buffer V (for 2D-PAGE).

4.4. Two-Dimensional Electrophoresis

Pellets containing mitochondria-enriched fractions were resuspended in protein extraction buffer V (PEB V) with protease and phosphatase inhibitors and nuclease mix (GE Healthcare, Uppsala, Sweden). Protein concentrations were determined using a 2-D quant kit (GE Healthcare, Uppsala, Sweden). Due to the low amounts of isolated proteins in each sample, lysates were not cleaned using the precipitation method (i.e., 2-D Clean-Up Kit). Each sample (120 µg of proteins) was mixed with 4 µL bromophenol blue solution 0.1%, 2 µL IPG buffer 3-11NL (ampholytes), and 4 µL Destreak reagent (GE Healthcare, Uppsala, Sweden). Samples were passively rehydrated onto 11 cm 3-11NL IPG strips (GE Healthcare, Uppsala, Sweden) at 20 °C for at least 24 h. Isoelectric focusing was performed using an Ettan IPGPhor II unit with the following protocol: gradient 150 V for 1 h → 150 V for 1 h → gradient 300 V for 0.5 h → 300 V for 2 h → gradient 1500 V for 2.5 h → 1500 V for 1 h → gradient 5000 V for 5 h → 5000 V for 9 h. The total voltage-hour was 65 KV·h.

After IEF, the strips were equilibrated in equilibration (EQ) buffer (6 M urea, 30% glycerol, 2% SDS, 50mM Tris-HCl pH 8.8) containing 2% DTT (EQ-DTT) for 20 min at room temperature and then equilibrated in EQ buffer containing 2.5% iodoacetamide (EQ-IAA) using the same conditions. Polyacrylamide gels (12% pH 8.8 resolving, and 4% pH 8.8 stacking gels) were hand cast in criterion empty cassettes (13.3 × 8.7cm) (Biorad, Hercules, CA, USA). The equilibrated strips were placed on top of the stacking gels and covered with agarose sealing solution (0.5% agarose, Laemmli running buffer, bromophenol blue). The electrophoresis was run at a constant voltage of 60 V.

Gels were rinsed three times with distilled water for 5 min and stained overnight in 100 mL colloidal Coomassie Brilliant Blue G-250 (distilled water, 10% ethanol, 2% orthophosphoric acid, 0.02% Coomassie Brilliant Blue G-250). Gels were rinsed three times with distilled water and destained in destaining solution (10% ethanol, 2% orthophosphoric acid, distilled water) for 20 min. Gels were stored in 1% acetic acid at 4°C.

4.5. Analysis of Two-Dimensional Electrophoresis Gels

Gels were scanned using a UMAX PowerLook 1120 scanner and Labscan software (GE Healthcare, Uppsala, Sweden) at 600 dpi. Images were analyzed using Image Master™ 2D Platinum 6.0 software (GE Healthcare, Uppsala, Sweden). Spots were manually detected and analyzed using three independent sets of gels (sensitive MCF7 versus paclitaxel-resistant MCF7/PacR). The statistical significance of the change in expression of matched spots was determined using the Student´s *t*-test. Spots with at least a two-fold change in the signal were selected for MALDI-TOF mass spectrometry (MS) analysis.

4.6. Mass Spectrometry

Mass spectrometry was performed as previously described [30]. Cut spots were destained with 50 mM 4-ethylmorpholine acetate (pH 8.1) in 50% acetonitrile (MeCN). After complete destaining, gels were washed with water, reduced in size via dehydration in MeCN and reconstituted again in water. The supernatant was removed, and gels were partly dried in a SpeedVac concentrator. Gel pieces were then incubated overnight at 37 °C in a cleavage buffer containing 25 mM 4-ethylmorpholine acetate, 5% MeCN, and trypsin (100 ng, Promega, Madison, WI, USA). The resulting peptides were extracted with 40% MeCN/0.1% trifluoroacetic acid (TFA).

An aqueous 50% MeCN/0.1% TFA solution of α-cyano-4-hydroxycinnamic acid (5 mg/mL, Sigma-Aldrich, St. Louis, MO, USA) was used as a MALDI matrix. The peptide mixture (1 µL) was deposited on a MALDI plate, allowed to air-dry at room temperature and overlaid with 0.4 µL of the matrix. Mass spectra were measured using an Ultraflex III MALDI-TOF (Bruker Daltonics, Bremen, Germany), mass range of 700–4000 Da, calibrated internally using monoisotopic $[M+H]^+$ ions of trypsin auto-proteolytic fragments (842.5 and 2211.1 Da). The peak lists, created using the flexAnalysis 3.3 program, were searched using an in-house MASCOT search engine against the

SwissProt 2013_12 database subset of human proteins with the following search settings: peptide tolerance of 30 ppm, missed cleavage site value set to one, variable carbamidomethylation of cysteine, oxidation of methionine and protein N-term acetylation. Proteins with MOWSE scores over the threshold of 56 (calculated for the settings used) were considered as identified. The identities of protein candidates were determined using MS/MS analysis.

4.7. Whole-Cell Lysate Preparation

Whole-cell lysates were prepared from cells growing on Petri dishes (Ø 6 cm). The cells (approximately 3.0×10^6) were harvested with trypsin-EDTA solution into 10 mL of ice-cold phosphate-buffered saline (PBS) and centrifuged (500 *g*, 10 min, 4 °C). Cell pellets were washed twice with ice-cold PBS and centrifuged (500 *g*, 10 min, 4 °C). The resulting pellets were resuspended in RIPA™ buffer (Merck Millipore, Burlington, MA, USA) using the cOmpleteTM Mini protease inhibitor cocktail mix (Roche, Rotkreuz, Switzerland). After incubation for 20 min on ice, the lysate was centrifuged (16,000 *g*, 20 min, 4 °C) and the supernatant (whole-cell lysate) was transferred into a new tube. Protein concentrations were determined using a Pierce BCA Protein Assay Kit (Thermo Fisher Scientific, Waltham, MA, USA).

4.8. Western Blot Analysis

Immunoblotting was performed as previously described [28,80,81]. Whole-cell lysates samples (20 µg) or cell fractions (12 µg) were mixed with sample buffer (0.125M Tris/HCl pH6.8, 10% glycerol, 4% SDS, 0.25M DTT) and heated for 5 min at 95 °C. Samples were separated in 12% hand casted polyacrylamide gels using protein electrophoresis (Bio-Rad, Hercules, CA, USA). Separated proteins were blotted onto 0.2 µm nitrocellulose membranes PROTRAN BA 83 (Whatman-Schleicher and Schuell, Maidstone, UK) at 0.25 A for 3 h using a MiniProtean II blotting apparatus (Bio-Rad, Hercules, CA, USA). The membrane was blocked with 5% BSA in TBS for 30min and incubated with the primary antibody at 4 °C overnight. Membranes were washed three times with TBS containing 0.1% Tween-20 (TBS-T). Then the membranes were incubated for 2 h with the corresponding horseradish peroxidase-conjugated secondary antibody. The membrane was again washed three times with TBS-T. The chemiluminescence signal was detected using SuperSignal™ West Pico PLUS Chemiluminescent Substrate (Thermo Fisher Scientific, Waltham, MA, USA) and a CCD camera GEL Logic 4000 Pro (Carestream Health, New Haven, CT, USA).

4.9. Confocal Microscopy

Cells were seeded at a density of 5–6 × 10^4 cells onto coverslips. After an attachment period, the cells were fixed with 4% paraformaldehyde for 20 min, washed three times with PBS (10 min), and permeabilized with 0.3% Triton X-100 for 15–20 min. After three washing steps, the cells were blocked for 60 min with 1% BSA and stained with the primary antibodies diluted 1:200 in 1% BSA anti-CPS1 [EPR7493-3] (Abcam, Cambridge, UK) and anti-COX IV (#11967S) (Cell Signaling Technology, Danvers, MA, USA) at 4 °C overnight. The cells were then washed three times with PBS and incubated with secondary antibodies goat anti-rabbit IgG H&L Alexa Fluor®488 (ab150077) and goat anti-mouse IgG H&L F(ab)$_2$ Alexa Fluor®594 (#8890S) (Abcam, Cambridge, UK) for 2 h in the dark, at room temperature. Finally, cells were washed again with PBS. Next, cells were transferred onto a droplet of Vectashield®Mounting Medium with DAPI (Vector Laboratories, Burlingame, CA, USA) and sealed. Samples were analyzed using a Leica TCS SP5 confocal microscope (Bannockburn, IL, USA).

4.10. FACS Analysis

The cells (approximately 2.5×10^6 cells per sample) were seeded into Petri dishes. After an attachment period, cells were harvested into PBS and sedimented by low-speed centrifugation (500 *g*, 10 min, 4 °C). Next, cells were fixed by 3–4% formaldehyde at 37 °C for 10 min, centrifuged, washed with PBS, and permeabilized using 90% methanol on ice for 30 min. Subsequently, cells were washed

with PBS. Nonspecific reactions were prevented by incubation in 3% BSA for 60 min. Cells were incubated with primary antibody anti-CPS1 [EPR7493-3] (Abcam, Cambridge, UK) diluted 1:80 in 3% BSA for 60 min. Then cells were washed with PBS and incubated 60 min with Goat anti-rabbit IgG H&L Alexa Fluor®488 (ab150077) (Abcam, Cambridge, UK) diluted 1:200 in 3% BSA. Finally, cells were washed with PBS, and the intensity of cell fluorescence was measured using a FACS Calibur cytometer (Becton Dickinson, San Jose, CA, USA).

4.11. siRNA Silencing and Its Effect on Resistance to Paclitaxel

CPS1 expression was knockdown using Silencer®Select siRNA ID s3462 ("siRNA CPS1 A", transcription variant 1, 3) and ID s528702 ("siRNA CPS1 B" transcription variant 1, 2, 3). ABCB1 was knock-downed using Silencer®Select siRNA ID s10419. Nonspecific Silencer®Select siRNA 4390844 was used as a negative control. All siRNAs were purchased from Life Technologies (Carlsbad, CA, USA). Cells were transiently transfected with INTERFERin reagent (PolyPlus-Transfection, Illkirch, France) in Opti-MEM®Reduced Serum Medium (Life Technologies, Carlsbad, CA, USA) according to manufacturer instructions.

The cells were seeded at a density of 2.1×10^5 cells per Petri dish (Ø 6 cm) in antibiotic-free medium. After 24 h both paclitaxel-sensitive (MCF7) and paclitaxel-resistant (MCF7/PacR) cells were transfected in paclitaxel-free medium. In the transfection mixture, CPS1, ABCB1, or non-specific siRNAs were diluted in Opti-MEM®Reduced Serum Medium to a final concentration of 5 nM of siRNA (for double siRNA transfection the final concentration was 10 nM siRNA in total, i.e., 5 nM each) in the culture medium together with the INTERFERin transfection reagent at a 1:250 dilution. After 72 h of incubation with siRNA, cells were harvested and seeded in the fresh media at a concentration of 2.0×10^5 cells/ml into culture plates. After 24 h, allowing cells to attach, the media was replaced by media containing paclitaxel. After 96 h of treatment, the number of surviving cells was determined using a hemocytometer after trypan blue staining, and the persistence of CPS1 and ABCB1 silencing throughout the experiment was analyzed using western blot (see above).

4.12. Statistical Analysis

The statistical significance of differences was determined using the Student's *t*-test. $p < 0.05$, $p < 0.01$, and $p < 0.001$ were considered statistically significant at the 5%, 1%, and 0.1% levels, respectively. NS means statistically insignificant.

5. Conclusions

In this study, we detected three mitochondrial proteins (CPS1, ATAD3A/ATAD3B, and ABHD11) and one lysosomal protein (cathepsin D) with different expressions in paclitaxel-resistant MCF7/PacR breast cancer cells compared to paclitaxel-sensitive MCF7 breast cancer cells. None of these mitochondrial proteins have previously been associated with acquired resistance of breast cancer cells to paclitaxel.

In the case of mitochondrial ATAD3A and ATAD3B proteins, we detected increased expression in the spot containing peptides of both proteins in MCF7/PacR cells. However, this result was not confirmed with western blot and whole-cell lysates. Mitochondrial lipase ABHD11 was downregulated in MCF7/PacR cells. Owing to its position in human genome (i.e. on the long arm of chromosome 7, close to ABCB1, ABCB4, and HSP27), the change in ABHD11 expression likely reflect genetic changes (e.g., chromosome rearrangement) during selection of paclitaxel-resistant cells having a high expression of the ABCB1 transporter rather than its direct involvement in acquired resistance to paclitaxel. Downregulation of cathepsin D expression in MCF7/PacR cells is in accordance with its described role as an effector molecule in lysosomal cell death.

For CPS1, which was the most upregulated protein in MCF7/PacR cells, we observed the same mitochondrial localization, using confocal microscopy, of CPS1 in both sensitive and resistant cells.

The role of CPS1 in acquired resistance to paclitaxel was not demonstrated during the CPS1 knockdown experiment, which used specific siRNA.

Author Contributions: P.D. carried out the isolation of mitochondrial fractions, two-dimensional electrophoresis, western blot, and prepared the manuscript; P.H. carried out the mass spectrometry; K.B. carried out siRNA techniques; M.J. carried out the confocal microscopy and flow cytometry; J.K. coordinated the experiments and helped to complete the manuscript.

Funding: This research was funded by Charles University, project GA UK 664216 and by the Grant Agency of the Czech Republic, project 19-03063S.

Acknowledgments: Authors thank to Thomas Secrest for language revision.

Conflicts of Interest: The authors declare no conflict of interest.

Abbreviations

2D-PAGE	Two-dimensional polyacrylamide gel electrophoresis
ABCB1	ATP-binding cassette transporter member B1
ABCB4	ATP-binding cassette transporter member B4
ABCC2	ATP-binding cassette transporter member C2
ABCC3	ATP-binding cassette transporter member C3
ABHD11	Alpha/beta hydrolase domain-containing protein 11
ATAD3A	ATPase family AAA domain-containing protein 3A
ATAD3B	ATPase family AAA domain-containing protein 3B
CPS1	Carbamoyl phosphate synthetase 1
COX IV	Cytochrome c oxidase subunit IV
Diablo	Direct inhibitor of apoptosis-binding protein with low pI
GAPDH	Glyceraldehyde-3-phosphate dehydrogenase
HER2	Human epidermal growth factor receptor 2
Hop	Hsp70-Hsp90 organizing protein
HSP27	Heat-shock protein 27
MALDI-TOF	Matrix-assisted laser desorption/ionization-time-of-flight
MAP2	Microtubule-associated protein 2
MCF7	Michigan Cancer Foundation 7
SDHA	Succinate dehydrogenase complex flavoprotein, subunit alpha
STK11	Serine/threonine kinase 11
Smac	Second mitochondria-derived activator of caspase
WBSCR21	Williams–Beuren syndrome chromosomal region 21 protein

References

1. Ferlay, J.; Soerjomataram, I.; Dikshit, R.; Eser, S.; Mathers, C.; Rebelo, M.; Parkin, D.M.; Forman, D.; Bray, F. Cancer incidence and mortality worldwide: Sources, methods and major patterns in GLOBOCAN 2012. *Int. J. Cancer* **2015**, *136*, 359–386. [CrossRef] [PubMed]
2. Anampa, J.; Makower, D.; Sparano, J.A. Progress in adjuvant chemotherapy for breast cancer: An overview. *BMC Med.* **2015**, *13*, 195. [CrossRef] [PubMed]
3. Theriault, R.L.; Carlson, R.W.; Allred, C.; Anderson, B.O.; Burstein, H.J.; Edge, S.B.; Farrar, W.B.; Forero, A.; Giordano, S.H.; Goldstein, L.J.; et al. National comprehensive cancer network. Breast cancer, version 3.2013: Featured updates to the NCCN guidelines. *J. Natl. Compr. Cancer Netw.* **2013**, *11*, 753–760. [CrossRef]
4. Coates, A.S.; Winer, E.P.; Goldhirsch, A.; Gelber, R.D.; Gnant, M.; Piccart-Gebhart, M.; Thürlimann, B.; Senn, H.J. Panel members. Tailoring therapies—Improving the management of early breast cancer: St Gallen international expert consensus on the primary therapy of early breast cancer 2015. *Ann. Oncol.* **2015**, *26*, 1533–1546. [CrossRef] [PubMed]
5. Mustacchi, G.; De Laurentiis, M. The role of taxanes in triple-negative breast cancer: Literature review. *Drug Des. Dev. Ther.* **2015**, *9*, 4303–4318. [CrossRef]
6. Weaver, B.A. How Taxol/paclitaxel kills cancer cells. *Mol. Biol. Cell* **2014**, *25*, 2677–2681. [CrossRef]

7. Manfredi, J.J.; Parness, J.; Horwitz, S.B. Taxol binds to cellular microtubules. *J. Cell Biol.* **1982**, *94*, 688–696. [CrossRef]
8. Snyder, J.P.; Nettles, J.H.; Cornett, B.; Downing, K.H.; Nogales, E. The binding conformation of Taxol in beta-tubulin: A model based on electron crystallographic density. *Proc. Natl. Acad. Sci. USA* **2001**, *98*, 5312–5316. [CrossRef]
9. Xiao, H.; Verdier-Pinard, P.; Fernandez-Fuentes, N.; Burd, B.; Angeletti, R.; Fiser, A.; Horwitz, S.B.; Orr, G.A. Insights into mechanism of microtubule stabilization by Taxol. *Proc. Natl. Acad. Sci. USA* **2006**, *103*, 10166–10173. [CrossRef]
10. Woods, C.M.; Zhu, J.; McQueney, P.A.; Bollag, D.; Lazarides, E. Taxol-induced mitotic block triggers rapid onset of a p53-independent apoptotic pathway. *Mol. Med.* **1995**, *1*, 506–526. [CrossRef]
11. Gascoigne, K.E.; Taylor, S.S. How do anti-mitotic drugs kill cancer cells? *J. Cell Sci.* **2009**, *122*, 2579–2585. [CrossRef] [PubMed]
12. Ajabnoor, G.M.; Crook, T.; Coley, H.M. Paclitaxel resistance is associated with switch from apoptotic to autophagic cell death in MCF-7 breast cancer cells. *Cell Death Dis.* **2012**, *3*, e260. [CrossRef] [PubMed]
13. Chen, S.Y.; Hu, S.S.; Dong, Q.; Cai, J.X.; Zhang, W.P.; Sun, J.Y.; Wang, T.T.; Xie, J.J.; He, H.R.; Xing, J.F.; et al. Establishment of paclitaxel-resistant breast cancer cell line and nude mice models, and underlying multidrug resistance mechanisms in vitro and in vivo. *Asian Pac. J. Cancer Prev.* **2013**, *14*, 6135–6140. [CrossRef] [PubMed]
14. Němcová-Fürstová, V.; Kopperová, D.; Balušíková, K.; Ehrlichová, M.; Brynychová, V.; Václavíková, R.; Daniel, P.; Souček, P.; Kovář, J. Characterization of acquired paclitaxel resistance of breast cancer cells and involvement of ABC transporters. *Toxicol. Appl. Pharmacol.* **2016**, *310*, 215–228. [CrossRef] [PubMed]
15. Boichuk, S.; Galembikova, A.; Sitenkov, A.; Khusnutdinov, R.; Dunaev, P.; Valeeva, E.; Usolova, N. Establishment and characterization of a triple negative basal-like breast cancer cell line with multi-drug resistance. *Oncol. Lett.* **2017**, *14*, 5039–5045. [CrossRef] [PubMed]
16. Zhang, J.; Zhao, J.; Zhang, W.; Liu, G.; Yin, D.; Li, J.; Zhang, S.; Li, H. Establishment of paclitaxel-resistant cell line and the underlying mechanism on drug resistance. *Int. J. Gynecol. Cancer* **2012**, *22*, 1450–1456. [CrossRef] [PubMed]
17. Duran, G.E.; Wang, Y.C.; Moisan, F.; Francisco, E.B.; Sikic, B.I. Decreased levels of baseline and drug-induced tubulin polymerisation are hallmarks of resistance to taxanes in ovarian cancer cells and are associated with epithelial-to-mesenchymal transition. *Br. J. Cancer* **2017**, *116*, 1318–1328. [CrossRef]
18. Gonçalves, A.; Braguer, D.; Kamath, K.; Martello, L.; Briand, C.; Horwitz, S.; Wilson, L.; Jordan, M.A. Resistance to Taxol in lung cancer cells associated with increased microtubule dynamics. *Proc. Natl. Acad. Sci. USA* **2001**, *98*, 11737–11742. [CrossRef]
19. Sobue, S.; Mizutani, N.; Aoyama, Y.; Kawamoto, Y.; Suzuki, M.; Nozawa, Y.; Ichihara, M.; Murate, T. Mechanism of paclitaxel resistance in a human prostate cancer cell line, PC3-PR, and its sensitization by cabazitaxel. *Biochem. Biophys. Res. Commun.* **2016**, *479*, 808–813. [CrossRef]
20. Takeda, M.; Mizokami, A.; Mamiya, K.; Li, Y.Q.; Zhang, J.; Keller, E.T.; Namiki, M. The establishment of two paclitaxel-resistant prostate cancer cell lines and the mechanisms of paclitaxel resistance with two cell lines. *Prostate* **2007**, *67*, 955–967. [CrossRef]
21. Zhou, J.; Cheng, S.C.; Luo, D.; Xie, Y. Study of multi-drug resistant mechanisms in taxol-resistant hepatocellular carcinoma QGY-TR 50 cell line. *Biochem. Biophys. Res. Commun.* **2001**, *280*, 1237–1242. [CrossRef] [PubMed]
22. Vaidyanathan, A.; Sawers, L.; Gannon, A.L.; Chakravarty, P.; Scott, A.L.; Bray, S.E.; Ferguson, M.J.; Smith, G. ABCB1 (MDR1) induction defines a common resistance mechanism in paclitaxel- and olaparib-resistant ovarian cancer cells. *Br. J. Cancer* **2016**, *115*, 431–441. [CrossRef] [PubMed]
23. Orr, G.A.; Verdier-Pinard, P.; McDaid, H.; Horwitz, S.B. Mechanisms of Taxol resistance related to microtubules. *Oncogene* **2003**, *22*, 7280–7295. [CrossRef] [PubMed]
24. Martínéz, C.; García-Martín, E.; Pizarro, R.M.; García-Gamito, F.J.; Agúndez, J.A.G. Expression of paclitaxel-inactivating CYP3A activity in human colorectal cancer: Implications for drug therapy. *Br. J. Cancer* **2002**, *87*, 681–686. [CrossRef] [PubMed]
25. Smoter, M.; Bodnar, L.; Duchnowska, R.; Stec, R.; Grala, B.; Szczylik, C. The role of Tau protein in resistance to paclitaxel. *Cancer Chemother. Pharmacol.* **2011**, *68*, 553–557. [CrossRef] [PubMed]

26. Murray, S.; Briasoulis, E.; Linardou, H.; Bafaloukos, D.; Papadimitriou, C. Taxane resistance in breast cancer: Mechanisms, predictive biomarkers and circumvention strategies. *Cancer Treat. Rev.* **2012**, *38*, 890–903. [CrossRef]
27. Gao, B.; Russell, A.; Beesley, J.; Chen, X.Q.; Healey, S.; Henderson, M.; Wong, M.; Emmanuel, C.; Galletta, L.; Johnatty, S.E.; et al. Paclitaxel sensitivity in relation to ABCB1 expression, efflux and single nucleotide polymorphism in ovarian cancer. *Sci. Rep.* **2014**, *4*, 4669. [CrossRef] [PubMed]
28. Jelínek, M.; Balušíková, K.; Daniel, P.; Němcová-Fürstová, V.; Kirubakaran, P.; Jaček, M.; Wei, L.; Wang, X.; Vondrášek, J.; Ojima, I.; et al. Substituents at the C3′ and C3′N positions are critical for taxanes to overcome acquired resistance of cancer cells to paclitaxel. *Toxicol. Appl. Pharmacol.* **2018**, *347*, 79–91. [CrossRef]
29. Alam, A.; Kowal, J.; Broude, E.; Roninson, I.; Locher, K.P. Structural insight into substrate and inhibitor discrimination by human P-glycoprotein. *Science* **2019**, *363*, 753–756. [CrossRef]
30. Pavlíková, N.; Bartoňová, I.; Balušíková, K.; Kopperová, D.; Halada, P.; Kovář, J. Differentially expressed proteins in MCF-7 breast cancer cells sensitive and resistant to paclitaxel. *Exp. Cell Res.* **2015**, *333*, 1–10. [CrossRef]
31. Palmfeldt, J.; Bross, P. Proteomics of human mitochondria. *Mitochondrion* **2017**, *33*, 2–14. [CrossRef] [PubMed]
32. Tait, S.W.; Green, D.R. Mitochondrial regulation of cell death. *Cold Spring Harb. Perspect. Biol.* **2013**, *5*, a008706. [CrossRef] [PubMed]
33. Fernie, A.R.; Carrari, F.; Sweetlove, L.J. Respiratory metabolism: Glycolysis, the TCA cycle and mitochondrial electron transport. *Curr. Opin. Plant. Biol.* **2004**, *7*, 254–261. [CrossRef] [PubMed]
34. Tait, S.W.; Green, D.R. Mitochondria and cell signalling. *J. Cell Sci.* **2012**, *125*, 807–815. [CrossRef] [PubMed]
35. McBride, H.M.; Neuspiel, M.; Wasiak, S. Mitochondria: More than just a powerhouse. *Curr. Biol.* **2006**, *16*, R551–R560. [CrossRef] [PubMed]
36. Weinberg, S.E.; Sena, L.A.; Chandel, N.S. Mitochondria in the regulation of innate and adaptive immunity. *Immunity* **2015**, *42*, 406–417. [CrossRef]
37. Joshi, A.D.; Mustafa, M.G.; Lichti, C.F.; Elferink, C.J. Homocitrullination is a novel histone H1 epigenetic mark dependent on aryl hydrocarbon receptor recruitment of carbamoyl-phosphate synthase 1. *J. Biol. Chem.* **2015**, *290*, 27767–27778. [CrossRef]
38. Rowland, A.A.; Voeltz, G.K. Endoplasmic reticulum-mitochondria contacts: Function of the junction. *Nat. Rev. Mol. Cell Biol.* **2012**, *13*, 607–625. [CrossRef]
39. Tristan, C.; Shahani, N.; Sedlak, T.W.; Sawa, A. The diverse functions of GAPDH: Views from different subcellular compartments. *Cell. Signal.* **2011**, *23*, 317–323. [CrossRef]
40. Benes, P.; Vetvicka, V.; Fusek, M. Cathepsin ᴅ-many functions of one aspartic protease. *Crit. Rev. Oncol. Hematol.* **2008**, *68*, 12–28. [CrossRef]
41. Achour, O.; Ashraf, Y.; Bridiau, N.; Kacem, M.; Poupard, N.; Bordenave-Juchereau, S.; Sannier, F.; Lamerant-Fayel, N.; Kieda, C.; Liaudet-Coopman, E.; et al. Alteration of cathepsin D trafficking induced by hypoxia and extracellular acidification in MCF-7 breast cancer cells. *Biochimie* **2016**, *121*, 123–130. [CrossRef] [PubMed]
42. Zhan, Y.; Wang, K.; Li, Q.; Zou, Y.; Chen, B.; Gong, Q.; Ho, H.I.; Yin, T.; Zhang, F.; Lu, Y.; et al. The novel autophagy inhibitor alpha-hederin promoted paclitaxel cytotoxicity by increasing reactive oxygen species accumulation in non-small cell lung cancer cells. *Int. J. Mol. Sci.* **2018**, *19*, 3221. [CrossRef] [PubMed]
43. Xing, W.; Archer, T.K. Upstream stimulatory factors mediate estrogen receptor activation of the cathepsin D promoter. *Mol. Endocrinol.* **1998**, *12*, 1310–1321. [CrossRef] [PubMed]
44. Dabrosin, C.; Johansson, A.C.; Ollinger, K. Decreased secretion of cathepsin D in breast cancer in vivo by tamoxifen: Mediated by the mannose-6-phosphate/IGF-II receptor? *Breast Cancer Res. Treat.* **2004**, *85*, 229–238. [CrossRef] [PubMed]
45. Johansson, A.C.; Steen, H.; Ollinger, K.; Roberg, K. Cathepsin D mediates cytochrome c release and caspase activation in human fibroblast apoptosis induced by staurosporine. *Cell Death Differ.* **2003**, *10*, 1253–1259. [CrossRef] [PubMed]
46. Emert-Sedlak, L.; Shangary, S.; Rabinovitz, A.; Miranda, M.B.; Delach, S.M.; Johnson, D.E. Involvement of cathepsin D in chemotherapy-induced cytochrome c release, caspase activation, and cell death. *Mol. Cancer Ther.* **2005**, *4*, 733–742. [CrossRef] [PubMed]
47. Zuzarte-Luis, V.; Montero, J.A.; Kawakami, Y.; Izpisua-Belmonte, J.C.; Hurle, J.M. Lysosomal cathepsins in embryonic programmed cell death. *Dev. Biol.* **2007**, *301*, 205–217. [CrossRef]

48. Castino, R.; Peracchio, C.; Salini, A.; Nicotra, G.; Trincheri, N.F.; Démoz, M.; Valente, G.; Isidoro, C. Chemotherapy drug response in ovarian cancer cells strictly depends on a cathepsin D-Bax activation loop. *J. Cell. Mol. Med.* **2009**, *13*, 1096–1109. [CrossRef]
49. Jancekova, B.; Ondrouskova, E.; Knopfova, L.; Smarda, J.; Benes, P. Enzymatically active cathepsin D sensitizes breast carcinoma cells to TRAIL. *Tumour Biol.* **2016**, *37*, 10685–10696. [CrossRef]
50. Lord, C.C.; Thomas, G.; Brown, J.M. Mammalian alpha beta hydrolase domain (ABHD) proteins: Lipid metabolizing enzymes at the interface of cell signaling and energy metabolism. *Biochim. Biophys. Acta* **2013**, *1831*, 792–802. [CrossRef]
51. Pober, S. Williams-Beuren syndrome. *N. Engl. J. Med.* **2010**, *362*, 239–252. [CrossRef] [PubMed]
52. Arya, M.; Srinivasan, M.; Rajasekharan, R. Human alpha beta hydrolase domain containing protein 11 and its yeast homolog are lipid hydrolases. *Biochem. Biophys. Res. Commun.* **2017**, *487*, 875–880. [CrossRef] [PubMed]
53. Fukasawa, Y.; Tsuji, J.; Fu, S.C.; Tomii, K.; Horton, P.; Imai, K. MitoFates: Improved prediction of mitochondrial targeting sequences and their cleavage sites. *Mol. Cell. Proteomics* **2015**, *14*, 1113–1126. [CrossRef] [PubMed]
54. Wiedl, T.; Arni, S.; Roschitzki, B.; Grossmann, J.; Collaud, S.; Soltermann, A.; Hillinger, S.; Aebersold, R.; Weder, W. Activity-based proteomics: Identification of ABHD11 and ESD activities as potential biomarkers for human lung adenocarcinoma. *J. Proteom.* **2011**, *74*, 1884–1894. [CrossRef] [PubMed]
55. Yang, Y.; Shao, Y.; Zhu, M.; Li, Q.; Yang, F.; Lu, X.; Xu, C.; Xiao, B.; Sun, Y.; Guo, J. Using gastric juice lncRNA-ABHD11-AS1 as a novel type of biomarker in the screening of gastric cancer. *Tumor Biol.* **2016**, *37*, 1183–1188. [CrossRef] [PubMed]
56. Lei, X.; Li, L.; Duan, X. Long non-coding RNA ABHD11-AS1 promotes colorectal cancer development through regulation of miR-133a/SOX4 axis. *Biosci. Rep.* **2018**, BSR20181386. [CrossRef] [PubMed]
57. Qiao, X.; Lv, S.X.; Qiao, Y.; Li, Q.P.; Ye, B.; Wang, C.C.; Miao, L. Long noncoding RNA ABHD11-AS1 predicts the prognosis of pancreatic cancer patients and serves as a promoter by activation the PI3K-AKT pathway. *Eur. Rev. Med. Pharmacol. Sci.* **2018**, *22*, 8630–8639. [CrossRef] [PubMed]
58. Liu, Y.; Wang, L.L.; Chen, S.; Zong, Z.H.; Guan, X.; Zhao, Y. LncRNA ABHD11-AS1 promotes the development of endometrial carcinoma by targeting cyclin D1. *J. Cell. Mol. Med.* **2018**, *22*, 3955–3964. [CrossRef] [PubMed]
59. De Cima, S.; Polo, L.M.; Díez-Fernández, C.; Martínez, A.I.; Cervera, J.; Fita, I.; Rubio, V. Structure of human carbamoyl phosphate synthetase: Deciphering the on/off switch of human ureagenesis. *Sci. Rep.* **2015**, *5*, 16950. [CrossRef]
60. Çeliktas, M.; Tanaka, I.; Tripathi, S.C.; Fahrmann, J.F.; Aguilar-Bonavides, C.; Villalobos, P.; Delgado, O.; Dhillon, D.; Dennison, J.B.; Ostrin, E.J.; et al. Role of CPS1 in cell growth, metabolism and prognosis in LKB1-Inactivated lung adenocarcinoma. *J. Natl. Cancer Inst.* **2017**, *109*, 1–9. [CrossRef]
61. Kim, J.; Hu, Z.; Cai, L.; Li, K.; Choi, E.; Faubert, B.; Bezwada, D.; Rodriguez-Canales, J.; Villalobos, P.; Lin, Y.F.; et al. CPS1 maintains pyrimidine pools and DNA synthesis in KRAS/LKB1-mutant lung cancer cells. *Nature* **2017**, *546*, 168–172. [CrossRef] [PubMed]
62. Brown, K.A.; McInnes, K.J.; Takagi, K.; Ono, K.; Hunger, N.I.; Wang, L.; Sasano, H.; Simpson, E.R. LKB1 expression is inhibited by estradiol-17β in MCF-7 cells. *J. Steroid Biochem. Mol. Biol.* **2011**, *127*, 439–443. [CrossRef] [PubMed]
63. Lee, Y.Y.; Li, C.F.; Lin, C.Y.; Lee, S.W.; Sheu, M.J.; Lin, L.C.; Chen, T.J.; Wu, T.F.; Hsing, C.H. Overexpression of CPS1 is an independent negative prognosticator in rectal cancers receiving concurrent chemoradiotherapy. *Tumour Biol.* **2014**, *35*, 11097–11105. [CrossRef] [PubMed]
64. Cardona, D.M.; Zhang, X.; Liu, C. Loss of carbamoyl phosphate synthetase I in small-intestinal adenocarcinoma. *Am. J. Clin. Pathol.* **2009**, *132*, 877–882. [CrossRef] [PubMed]
65. Dye, R.B.; Fink, S.P.; Williams, R.C., Jr. Taxol-induced flexibility of microtubules and its reversal by MAP-2 and Tau. *J. Biol. Chem.* **1993**, *268*, 6847–6850. [PubMed]
66. Bauer, J.A.; Chakravarthy, A.B.; Rosenbluth, J.M.; Mi, D.; Seeley, E.H.; De Matos Granja-Ingram, N.; Olivares, M.G.; Kelley, M.C.; Mayer, I.A.; Meszoely, I.M.; et al. Identification of markers of taxane sensitivity using proteomic and genomic analyses of breast tumors from patients receiving neoadjuvant paclitaxel and radiation. *Clin. Cancer Res.* **2010**, *16*, 681–690. [CrossRef] [PubMed]
67. Da Cruz, S.; Xenarios, I.; Langridge, J.; Vilbois, F.; Parone, P.A.; Martinou, J.C. Proteomic analysis of the mouse liver mitochondrial inner membrane. *J. Biol. Chem.* **2003**, *278*, 41566–41571. [CrossRef] [PubMed]

68. Li, S.; Rousseau, D. ATAD3, a vital membrane bound mitochondrial ATPase involved in tumor progression. *J. Bioenerg. Biomembr.* **2012**, *44*, 189–197. [CrossRef] [PubMed]
69. Gilquin, B.; Taillebourg, E.; Cherradi, N.; Hubstenberger, A.; Gay, O.; Merle, N.; Assard, N.; Fauvarque, M.O.; Tomohiro, S.; Kuge, O.; et al. The AAA+ ATPase ATAD3A controls mitochondrial dynamics at the interface of the inner and outer membranes. *Mol. Cell. Biol.* **2010**, *30*, 1984–1996. [CrossRef] [PubMed]
70. Frickey, T.; Lupas, A.N. Phylogenetic analysis of AAA proteins. *J. Struct. Biol.* **2004**, *146*, 2–10. [CrossRef]
71. Wang, Y.; Bogenhagen, D.F. Human mitochondrial DNA nucleoids are linked to protein folding machinery and metabolic enzymes at the mitochondrial inner membrane. *J. Biol. Chem.* **2006**, *281*, 25791–25802. [CrossRef] [PubMed]
72. He, J.; Mao, C.C.; Reyes, A.; Sembongi, H.; Di Re, M.; Granycome, C.; Clippingdale, A.B.; Fearnley, I.M.; Harbour, M.; Robinson, A.J.; et al. The AAA+ protein ATAD3 has displacement loop binding properties and is involved in mitochondrial nucleoid organization. *J. Cell. Biol.* **2007**, *176*, 141–146. [CrossRef] [PubMed]
73. Teng, Y.; Ren, X.; Li, H.; Shull, A.; Kim, J.; Cowell, J.K. Mitochondrial ATAD3A combines with GRP78 to regulate WASF3 metastasis-promoting protein. *Oncogene* **2016**, *35*, 333–343. [CrossRef] [PubMed]
74. Peralta, S.; Goffart, S.; Williams, S.L.; Diaz, F.; Garcia, S.; Nissanka, N.; Area-Gomez, E.; Pohjoismäki, J.; Moraes, C.T. ATAD3 controls mitochondrial cristae structure, influencing mtDNA replication and cholesterol levels in muscle. *J. Cell. Sci.* **2018**, *131*, jcs217075. [CrossRef] [PubMed]
75. Hubstenberger, A.; Labourdette, G.; Baudier, J.; Rousseau, D. ATAD 3A and ATAD 3B are distal 1p-located genes differentially expressed in human glioma cell lines and present in vitro anti-oncogenic and chemoresistant properties. *Exp. Cell Res.* **2008**, *314*, 2870–2883. [CrossRef] [PubMed]
76. You, W.C.; Chiou, S.H.; Huang, C.Y.; Chiang, S.F.; Yang, C.L.; Sudhakar, J.N.; Lin, T.Y.; Chiang, I.P.; Shen, C.C.; Cheng, W.Y.; et al. Mitochondrial protein ATPase family AAA domain containing 3A correlates with radioresistance in glioblastoma. *Neuro. Oncol.* **2013**, *15*, 1342–1352. [CrossRef]
77. Huang, K.H.; Chow, K.C.; Chang, H.W.; Lin, T.Y.; Lee, M.C. ATPase family AAA domain containing 3A is an anti-apoptotic factor and secretion regulator of PSA in prostate cancer. *Int. J. Mol. Med.* **2011**, *28*, 9–15. [CrossRef]
78. Merle, N.; Féraud, O.; Gilquin, B.; Hubstenberger, A.; Kieffer-Jacquinot, S.; Assard, N.; Bennaceur-Griscelli, A.; Honnorat, J.; Baudier, J. ATAD3B is a human embryonic stem cell specific mitochondrial protein, re-expressed in cancer cells, that functions as dominant negative for the ubiquitous ATAD3A. *Mitochondrion* **2012**, *12*, 441–448. [CrossRef]
79. Calcagno, A.M.; Ambudkar, S.V. Molecular mechanisms of drug resistance in single-step and multi-step drug-selected cancer cells. *Methods Mol. Biol.* **2010**, *596*, 77–93. [CrossRef]
80. Jelínek, M.; Balušíková, K.; Kopperová, D.; Němcová-Fürstová, V.; Šrámek, J.; Fidlerová, J.; Zanardi, I.; Ojima, I.; Kovář, J. Caspase-2 is involved in cell death induction by taxanes in breast cancer cells. *Cancer Cell Int.* **2013**, *13*, 42. [CrossRef]
81. Jelínek, M.; Balušíková, K.; Schmiedlová, M.; Němcová-Fürstová, V.; Šrámek, J.; Stančíková, J.; Zanardi, I.; Ojima, I.; Kovář, J. The role of individual caspases in cell death induction by taxanes in breast cancer cells. *Cancer Cell Int.* **2015**, *15*, 8. [CrossRef] [PubMed]

4.4 Paper 4

ABCB1 AMPLICON CONTAINS CYCLIC AMP RESPONSE ELEMENT-DRIVEN *TRIP6* GENE IN TAXANE-RESISTANT MCF-7 BREAST CANCER SUBLINES

Daniel, P., Balušíková, K., Václavíková, R., Šeborová, K., Ransdorfová, Š., Valeriánová, M., Wei, L., Jelínek, M., Tlapáková, T., Fleischer, T., Kristensen, V. N., Souček, P., Ojima, I., & Kovář, J. (**2023**)

Genes, *14*(2), 296

https://doi.org/10.3390/genes14020296

genes

MDPI

Article

ABCB1 Amplicon Contains Cyclic AMP Response Element-Driven *TRIP6* Gene in Taxane-Resistant MCF-7 Breast Cancer Sublines

Petr Daniel [1], Kamila Balušíková [1], Radka Václavíková [2,3], Karolína Šeborová [2,3], Šárka Ransdorfová [4], Marie Valeriánová [4], Longfei Wei [5], Michael Jelínek [1], Tereza Tlapáková [6], Thomas Fleischer [7], Vessela N. Kristensen [8], Pavel Souček [2,3], Iwao Ojima [5] and Jan Kovář [1,*]

1 Department of Biochemistry, Cell and Molecular Biology, Third Faculty of Medicine, Charles University, 100 00 Prague, Czech Republic
2 Toxicogenomics Unit, National Institute of Public Health, 100 00 Prague, Czech Republic
3 Laboratory of Pharmacogenomics, Biomedical Center, Faculty of Medicine, Charles University, 323 00 Pilsen, Czech Republic
4 Department of Cytogenetics, Institute of Hematology and Blood Transfusion, 128 00 Prague, Czech Republic
5 Department of Chemistry, Institute of Chemical Biology & Drug Discovery, Stony Brook University—State University of New York, Stony Brook, NY 11794, USA
6 Department of Cell Biology, Faculty of Science, Charles University, 128 00 Prague, Czech Republic
7 Department of Cancer Genetics, Institute for Cancer Research, Oslo University Hospital, 0310 Oslo, Norway
8 Department of Medical Genetics, Institute of Clinical Medicine, Faculty of Medicine, University of Oslo, 0424 Oslo, Norway
* Correspondence: jan.kovar@lf3.cuni.cz; Tel.: +420-267-102-658

Abstract: A limited number of studies are devoted to regulating *TRIP6* expression in cancer. Hence, we aimed to unveil the regulation of *TRIP6* expression in MCF-7 breast cancer cells (with high *TRIP6* expression) and taxane-resistant MCF-7 sublines (manifesting even higher *TRIP6* expression). We found that *TRIP6* transcription is regulated primarily by the cyclic AMP response element (CRE) in hypomethylated proximal promoters in both taxane-sensitive and taxane-resistant MCF-7 cells. Furthermore, in taxane-resistant MCF-7 sublines, *TRIP6* co-amplification with the neighboring *ABCB1* gene, as witnessed by fluorescence in situ hybridization (FISH), led to *TRIP6* overexpression. Ultimately, we found high *TRIP6* mRNA levels in progesterone receptor-positive breast cancer and samples resected from premenopausal women.

Keywords: *TRIP6*; cAMP response element; gene amplification; *ABCB1*; breast cancer; CpG methylation; MCF-7

Citation: Daniel, P.; Balušíková, K.; Václavíková, R.; Šeborová, K.; Ransdorfová, Š.; Valeriánová, M.; Wei, L.; Jelínek, M.; Tlapáková, T.; Fleischer, T.; et al. *ABCB1* Amplicon Contains Cyclic AMP Response Element-Driven *TRIP6* Gene in Taxane-Resistant MCF-7 Breast Cancer Sublines. *Genes* **2023**, *14*, 296. https://doi.org/10.3390/genes14020296

Academic Editor: Robert Winqvist

Received: 12 December 2022
Revised: 18 January 2023
Accepted: 19 January 2023
Published: 23 January 2023

1. Introduction

Thyroid hormone receptor interactor 6 (*TRIP6*, 7q22.1) gene encodes for highly conserved 50 kDa protein (476 amino acid residues). TRIP6 is structurally organized into an N-terminal proline-rich domain, Crm-1-dependent nuclear export signal (NES), and three tandemly arrayed LIM domains (lin-11, Isl-1, and mec-3) followed by PDZ-binding motif TTDC (PSD95, Dlg1, ZO-1) at its C terminus [1,2]. TRIP6 belongs to small zyxin family (zyxin, ajuba, lipoma-preferred partner 1, LIM domain-containing protein 1, Wilms tumor 1-interacting protein, filamin-binding LIM protein 1) due to the presence of LIM domains [3].

Due to various modules, TRIP6 interacts with a plethora of partners extensively summarized elsewhere [4]. TRIP6 resides in the cell cytoplasm, where it accumulates at focal adhesions [5] and adherent junctions [6–8], the sites associated with the actin cytoskeleton. Additionally, TRIP6 has been described to shuttle between the cell nucleus and cytoplasm [2]. The N-terminally truncated isoform of TRIP6 (nTRIP6) entirely localizes in

the cell nucleus, where it promotes transcription of myogenesis regulatory genes [9–11]. Recently, Shukla et al. demonstrated that half of the *TRIP6* knock-out mice developed hydrocephalus as a result of impaired ciliogenesis in ependymal brain cells [12]. In conclusion, TRIP6 participates in multiple cellular processes, cell motility [6,13–15], signaling [15,16], regulation of transcription [5,9], and telomere protection [17]. Thus, TRIP6 represents an attractive molecule in cancer research.

Several lines of evidence underpin high *TRIP6* expression in MCF-7 cells. The Human Protein Atlas displays *TRIP6* mRNA as the most expressed in MCF-7 cells "https://www.proteinatlas.org/ENSG00000087077-TRIP6/cell+line (accessed on 19 January 2023)" [18]. Analysis of publicly available single cell transcriptomic data "https://bcatlas.tigem.it/tigem/dibernardo/AIRC_atlas_32_ccls/?ds=Atlas_32_ccls&gene=TRIP6 (accessed on 19 January 2023)" showed ubiquitous *TRIP6* expression in 32 evaluated breast cancer cell lines [19]. Nevertheless, BT549, MCF-7 and HCC70 cells expressed more *TRIP6* mRNA than any other breast cancer cells in the study. In line with this finding, Zhao et al. reported high *TRIP6* expression in several breast cancer cell lines [20]. Furthermore, we revealed *TRIP6* overexpression in paclitaxel-resistant MCF-7/PacR subline [21], yet the molecular mechanism(s) that drive *TRIP6* expression in MCF-7 cells as well in paclitaxel-resistant cells have not been described in detail.

To date, a few studies have investigated the regulation of *TRIP6* expression by microRNA (miRNA), in particular, miR-138-5p [22], miR-485-3p [23] in neural stem cells, and miR-7 in colorectal cancer [24]. Recently, Gou et al. demonstrated that tocopherol α transfer protein-like TTPAL protects TRIP6 from ubiquitin-mediated degradation in colorectal cancer [25].

Breast cancer is the most diagnosed cancer worldwide [25]. It exhibits a heterogeneous nature concerning histological, genetic, and clinical behavior, thus emphasizing the need for patient-tailored therapy [26]. Cost-effective but less accurate immunohistochemical and in situ hybridization methods allow systematic categorization of breast cancer into estrogen receptor-positive (ER+) luminal, HER2-positive, and triple-negative subtypes, reflecting the type of adjuvant therapy in the clinics [27]. Although molecular assays (Mammaprint®, Oncotype DX®) predict the outcome of patients with ER+ disease, they are not widespread in hospitals due to the high costs, especially in less developed countries [27], and also add limited information to existing clinical tests [28].

Notably, modern omics studies have allowed a more detailed look at breast cancer categorization and highlighted a few novel targets for its therapy [29,30]. Despite these advances, we lack data concerning the regulation of individual gene expression in the context of known drivers such as *PIK3CA* and *TP53* and more data are needed considering other less recognized or unknown drivers.

Here, we exploited parental taxane-sensitive MCF-7 cells and two taxane-resistant sublines, MCF-7/PacR (named as "PacR" subline) and MCF-7/SB-T-0035R (named as "0035R" sublines), to elucidate mechanisms regulating *TRIP6* expression in breast cancer. We discovered *cis*-acting regulatory motifs in *TRIP6* proximal promoter and clarified its function by dual-luciferase reporter assay. Consequently, we revealed stable hypomethylation in *TRIP6* proximal promoter in tested MCF-7 cells. We found a few *TRIP6* loci localized in der(7)t(7;7)ins(7;15) and one *TRIP6* locus in normal chromosome 7 in MCF-7 cell line. Co-amplified *TRIP6*/*ABCB1* region formed homogeneously stained region inserted in chromosome 3 (PacR subline) and chromosome 19 (0035R subline). Analysis of *TRIP6* expression in 95 breast cancer samples revealed associations of the *TRIP6* mRNA expression level with progesterone receptor positivity and premenopausal status.

2. Materials and Methods

2.1. Materials

Unless otherwise specified, all chemicals and oligonucleotides were purchased from Merck KGaA (Darmstadt, Germany). Stony Brook Taxane SB-T-0035 was synthesized and kindly provided by Professor Iwao Ojima [31].

2.2. Cell Culture

Human breast cancer cell line MCF-7 (RRID: CVCL_0031) was purchased from ATCC. Paclitaxel-resistant MCF-7/PacR (RRID: CVCL_B7P7) (shortened "PacR" in this study) and Stony Brook taxane 0035-resistant MCF-7/SB-T-0035R (RRID: CVCL_C0CU) (shortened "0035R" in this study) sublines were established by multi-step selection on mass populations of MCF-7 cells [32–34]. MCF-7 cells were maintained in RPMI-1640 medium supplemented with 10% fetal bovine serum and streptomycin-penicillin mix. Taxane-resistant MCF-7 sublines were cultured in the same medium supplemented with 300 nM paclitaxel (PacR subline) or 300 nM SB-T-0035 (0035R subline). The cell stocks used in this study were independently authenticated (Figures S1–S3).

2.3. Collection and Processing of Breast Cancer Tissue Samples

Breast cancer tissue samples (N = 95) were collected and snap-frozen during primary surgery in The Faculty Hospital Motol and Institute for the Care for Mother and Child (Prague, Czech Republic) between 2003 and 2009. Sample processing was described in detail previously [35,36]. Samples from 82 patients were collected during the primary surgery before any chemotherapy or hormonal therapy (adjuvant group; ACT group). Samples from the second group of patients (N = 13) were collected during the primary surgery after neoadjuvant cytotoxic therapy with regimens containing taxanes or taxanes in combination with 5-fluorouracil and/or anthracycline, and cyclophosphamide (NACT group), a standard regimen in the period of sample collection. Noteworthy, the current guidelines do not support the addition of 5-fluorouracil to the anthracycline (Doxorubicin/Epirubicin)-cyclophosphamide regimen.

A response to NACT was evaluated pre- and post-therapy by ultrasonography. Histological classification of carcinomas was performed according to standard diagnostic procedures [37]. The expression of estrogen and progesterone receptors was assessed immunohistochemically (IHC) with the 1% cut-off value for classification of tumors as hormone receptor positive. *ERBB2* status was defined as positive in samples with IHC score 2+ or 3+ confirmed by fluorescence in situ hybridization or silver in situ hybridization. The cut-off between high and low expression of proliferative marker Ki-67 was 13.25% [38]. Samples were subtyped according to hormone receptor and *ERBB2* expression as triple-negative (TNBC) subtype, *ERBB2* subtype and luminal subtype [39]. Disease-free survival (DFS) was defined as the time elapsed between surgery and disease recurrence.

2.4. Isolation of Nucleic Acids and Proteins

Cultured cells were harvested by trypsin-EDTA solution and washed. Breast cancer tissue samples were grounded to powder by mortar and pestle under liquid nitrogen. Nucleic acids and protein were isolated using Allprep DNA/RNA/protein Kit (Qiagen, Hilden, Germany) following the manufacturer's instructions. Nucleic acids were quantified using Quanti-iT^{TM} PicoGreen^{TM} dsDNA Assay Kit (Invitrogen^{TM}, Carlsbad, CA, USA) and Quant-iT RiboGreen RNA Assay Kit (Invitrogen) in Infinite M200 microplate reader (Tecan Group Ltd., Männendorf, Switzerland). RNA integrity was checked by Agilent 2100 Bioanalyzer and Agilent RNA 6000 Nano Assay Kit (Agilent Technologies, Inc., Santa Clara, CA, USA).

2.5. Quantitative Reverse Transcription PCR (qRT-PCR)

The real-time PCR study design adhered to the Minimum Information for Publication of Quantitative Real-Time PCR Experiments guidelines [40]. The synthesis of complementary DNA (cDNA) is described in Table S1. The used TaqMan® Gene Expression probes and PCR conditions are specified in Tables S2 and S3. *IPO8* and *MRPL19* were used as reference genes in patient cohorts based on their stability, as previously published [35]. To achieve the best reaction efficiency (>90%), we optimized the cycling conditions of each assay using a calibration curve as described previously [41,42]. For cell lines, the threshold cycle (Ct) of the gene of interest (GOI) was normalized to the reference gene (REF) by the following

formula $\Delta Ct = Ct_{REF} - Ct_{GOI}$. To compare gene expression between MCF-7 cells and taxane-resistant MCF-7 sublines, we calculated the ΔΔCt value by the following formula $\Delta\Delta Ct = \Delta Ct_{RES} - \Delta Ct_{MCF-7}$. Otherwise, to compare gene expression, fold change was calculated using the $2^{-\Delta\Delta Ct}$ method [43].

2.6. Assessment of Gene Copy Number

Genomic DNA (10 ng per reaction) was subjected to amplification as triplicate in ABI-PRISM 7500 Fast Real-time PCR System (Thermo Fisher Scientific, Waltham, MA, USA) with Predesigned TaqMan® Copy Number Assays (*TRIP6* FAM-MGB, Cat. No. *Hs02120646_cn; ABCB1* FAM-MGB, Cat. No. *Hs04962504_cn*) and Reference Assays (*TERT* VIC-TAMRA, Cat. No. 4403316; *RPPH1* VIC-TAMRA, Cat. No. *4403326*). The threshold cycle (Ct) value of a gene of interest (GOI) in a sample was normalized to the reference gene (REF) by the following formula $\Delta Ct = Ct_{REF} - Ct_{GOI}$. For *ABCB1* in the 0035R subline, data were not corrected by the *TERT* reference gene DNA level as the *TERT* copy number likely altered in these cells (Figure A1). To estimate gene copy number gain or loss in taxane-resistant sublines, we subtracted the normalized (ΔCt) values as follows this formula $\Delta\Delta Ct = \Delta Ct_{RES} - \Delta Ct_{MCF-7}$, where RES means taxane-resistant MCF-7 subline.

2.7. Western Blot Analysis

Western blot was performed as described elsewhere [44]. The primary antibodies that were used were *anti*-P-glycoprotein (ab3366, RRID: AB_303744), *anti*-actin (ab11003, RRID: AB_297660) from Abcam (Cambridge, UK), and *anti*-TRIP6 (HPA052813, RRID: AB_2681961) from Atlas Antibodies (Bromma, Sweden). SuperSignal™ West Pico PLUS Chemiluminescent Substrate or West Femto Maximum Sensitivity Substrate (Pierce, Rockford, IL, USA) were applied on a membrane to detect the chemiluminescence signal of secondary HRP-conjugated goat *anti*-mouse (SA00001-1, RRID: AB_272565) and HRP-conjugated goat *anti*-rabbit (SA00001-2, RRID: AB_272564) from Proteintech (Rosemont, IL, USA). Images were obtained using ChemiDoc MP imaging system (Biorad, Hercules, CA, USA).

2.8. Fluorescence In Situ Hybridization (FISH) Analysis

MCF-7 cells (60% confluency) were incubated with colchicine (0.2 µg/mL) and taxane-resistant MCF-7 sublines were incubated with colchicine and zosuquidar hydrochloride (100 nM) for 1 h. Harvested cells were resuspended in hypotonic buffer (100 mM KCl, 5 mM HEPES, 1 mM EGTA, pH 7.3) and fixed in methanol–glacial acetic acid (3:1). BAC probe mix *ABCB1*(spectrum green)/*TRIP6*(spectrum aqua) was purchased from Empire Genomics (Williamsville, NY, USA) (Figure S4). 24XCyte and XCyte 7 mBAND probes were purchased from MetaSystems (Altlussheim, Germany). All available metaphases were scanned using Metafer AxioImager Z2 – automatic mitoses finder and AxioImager Z1 fluorescence microscope (Carl Zeiss, Oberkochen, Germany) and further analyzed using Isis computer analysis system (MetaSystems). The findings are described according to ISCN2020 [45].

2.9. Cloning

pGL3-Promoter, pGL4.10[*luc2*], pGL4.24[*luc2P*/minP], and pNL1.1TK[*Nluc*/TK] vectors were purchased from Promega (Madison, WI, USA). 5′ flanking sequence of the *TRIP6* was taken from Ensembl genome browser (Homo sapiens GRCh38.p12) for *TRIP6*-201 transcript (ENST00000200457.9). Sequence −936/+111 (where +1 means *TRIP6* transcription start) was amplified from MCF-7/PacR genomic DNA by PCR and cloned into pGL3-Promoter vector via *Kpn*I and *Nco*I sites. The inserted sequence was subcloned by PCR into pGL4.10[*luc2*] and pGL4.24 vectors (Figure S5). Mutagenesis of the CRE motif was achieved by cleavage with *Aat*II-HF enzyme followed by 3′ overhangs removal (Large Klenow Fragment, NEB). The construction of plasmids, primers and PCR conditions are summarized in Figure S5 and Tables S4–S8. The constructs have been verified by restriction

endonuclease cleavage and insert sequencing (LightRun, SupremeRun, Eurofins Genomics, Ebersberg, Germany).

2.10. Dual-Luciferase Reporter Assay

Cells (2.0×10^5) were seeded into wells of Nunc™ F96 MicroWell™ plate (Cat. No. 236105, Thermo Fisher Scientific) in paclitaxel-free medium. After 24 h, enabling cells to attach to a surface, the cells were co-transfected with 100 ng of DNA per well at a 100:1 ratio (reporter to co-reporter) using jetPRIME® transfection reagent (Polyplus-Transfection, Illkirch, France) following the manufacturer's instructions. After 4 h, the transfection mix was replaced by a fresh paclitaxel-free cell culture medium. After 48 h post-transfection, samples were assayed by Nano-Glo® Dual-Luciferase Assay System I (Promega). Plates were read after 10 min of incubation in M200 Pro Plate Reader (Tecan Group Ltd.).

2.11. DNA Methylation Profiling

Bisulfite conversion of 500 ng DNA was performed with a EZ DNA Methylation™ Kit (Zymo Research, Irvine, CA, USA), according to the manufacturer's protocol. The genome-wide DNA methylation was assessed by the Infinium Human MethylationEPIC BeadChip platform (Illumina, San Diego, CA, USA) following the manufacturer's instructions. The microarray was scanned by the Illumina iScan system. The obtained data were further processed using the R language [46]. Quality control and data normalization were carried out in the *minfi* package as described previously [47,48]. Raw data were converted into β values for further analysis [49,50]. Probes mapped to single nucleotide polymorphism were removed from the analysis [51]. Differentially methylated probes were defined with $|\Delta\beta| > 0.2$ (20% difference). The β value is defined as the ratio between methylated versus unmethylated alleles.

2.12. Bisulfite Sequencing

Extracted DNA (1 µg) was bisulfite converted using the Epitect Bisulfite Kit (Qiagen) following the manufacturer's instructions. Then, 100 ng of converted DNA was subjected to 42 cycles of amplification (95 °C for 5 min, 95 °C for 30 s, 57 °C for 30 s, 68 °C for 60 s) with Epimark® Hot Start Taq DNA polymerase (NEB), pair of primers (forward: 5′-AGAAATGGTAGTTTAGGGTTTAGGGGGTTA-3′; reverse: 5′-AACCTCTAACCTTCAC CCCCTCTTC-3′) in a 50 µL reaction. PCR product was cloned into pGEM® T-Easy vector (Promega). Transformed DH5α Max Efficiency Competent Cells (Thermo Fisher Scientific) were selected on X-Gal/ampicillin plates. Sequencing data were analyzed in Quma online tool [52]. The clones with more than 93% cytosines converted outside CpG were analyzed.

2.13. Statistical Analysis

Graphs and statistical analysis were generated in Graph Pad Prism 9.2.0 (GraphPad Software, San Diego, CA, USA) regarding the recommendations described by others [53]. The SPSS v16.0 program (SPSS Inc, Chicago, IL, USA) was used for whole gene CpG methylation data and associations with breast cancer clinic pathological data. The normality of data was tested by the Shapiro–Wilk test prior to statistical analysis. Associations of transcripts with clinical data were assessed by the non-parametric Mann–Whitney, Kruskal–Wallis, and Spearman rank test. All *p*-values were obtained by two-sided tests. A *p*-value of <0.05 was considered statistically significant.

Variances were compared by F-test prior to unpaired *t*-test analysis. The distribution of residuals was checked by residual plot, homoscedasticity plot, and QQ plot. Individual statistical analysis is specified in each figure or table legend.

3. Results

3.1. TRIP6 as Well as ABCB1 Are Overexpressed in Taxane-Resistant MCF-7 Sublines

Recently, we established Stony Brook 0035-resistant MCF-7 subline (0035R subline) from the same parental MCF-7 cells as paclitaxel-resistant MCF-7 subline (PacR) [34]. SB-T-0035 is a paclitaxel derivative in that a dimethyl carbamoyl group replaces the methyl group at the C10 position of the baccatin core (Figure 1).

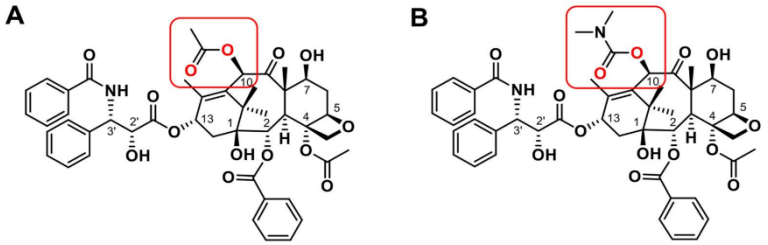

Figure 1. Structural formulas of taxanes used in the study. (**A**) Paclitaxel; (**B**) Stony Brook Taxane 0035 (SB-T-0035). Substituents bound at the C10 position of the baccatin III core are highlighted by the red frame.

We were interested in whether the *TRIP6* gene (7q22.1, 100.8Mb) is overexpressed in 0035R subline similarly to the already described PacR subline [21], and we wanted to identify what mechanisms underpin *TRIP6* overexpression in taxane-resistant MCF-7 sublines. Regarding de novo expression of the adjacent *ABCB1* gene (7q21.12, 87.5Mb), we hypothesized that co-amplification could drive enhanced levels of *TRIP6* and *ABCB1* in PacR cells [33,34].

We compared *TRIP6* and *ABCB1* copy number (Figure 2A), mRNA level (Figure 2B), and protein level (Figure 2C) between MCF-7 cells and taxane-resistant MCF-7 sublines. Due to both the target (*TRIP6*, *ABCB1*) and reference (*RPPH1*, *TERT*) gene copy numbers being unknown in all assayed cell samples, we roughly estimated copy number gain or loss from ΔΔCt values obtained by duplex real-time TaqMan® PCR (Figures 2A and A1). The *ABCB1* and *TRIP6* gene copy number increased in 0035R cells ($\Delta\Delta Ct_{ABCB1}$ = 2.32, $\Delta\Delta Ct_{TRIP6}$ = 2.38) although less than in PacR cells ($\Delta\Delta Ct_{ABCB1}$ = 3.42, $\Delta\Delta Ct_{TRIP6}$ = 3.50). The level of *TRIP6* mRNA increased in 0035R cells ($\Delta\Delta Ct_{TRIP6}$ = 1.35) although less than in PacR cells ($\Delta\Delta Ct_{TRIP6}$ = 2.16) compared to MCF-7 cells. The level of TRIP6 protein increased approximately by 3.5-fold in both taxane-resistant MCF-7 sublines compared to MCF-7 cells (Figure 2B).

Furthermore, we also found markedly elevated levels of *ABCB1* mRNA and protein in 0035R cells, although it was two-fold lower compared to PacR cells (Figure 2B,C).

Collectively, *TRIP6* copy number, mRNA level, and protein level increased in line with *ABCB1* copy number, mRNA, and protein level, suggesting that co-amplification is accountable for their increased expression.

3.2. A Few TRIP6 Loci Pre-Exists in MCF-7 Cell Line

Variation in *TRIP6* copy number might underlie high *TRIP6* mRNA and protein expression even in parental MCF-7 cells. In addition, the massive distribution and subcultivation of MCF-7 cells during the last 50 years resulted in enormous MCF-7 cell line heterogeneity [54]. Thus, we first determined the karyotype of MCF-7 cells used in this study.

The composite karyotype of MCF-7 cells assembled from 20 mitoses (of 52 analyzed) counted 67 to 69 chromosomes (Table 1). Chromosomes X, 6, 7, 9, 14, and 21 were disomic. All chromosomes possessed numerical and structural aberrations. Derivative chromosomes were formed predominantly by unbalanced translocations (Figure 3A, Table 1), while reciprocal translocations between t(3;6) and t(4;5) occurred. Chromosome 7 *p*- and q-arm

segments translocated to chromosomes X, 2, 7, 10, and 22 (Figure 3B, Figure A2). Subsequent multicolor banding (mBAND) analysis revealed rearrangements in der(7)t(7;7)ins(7;15) (Figure 3B). We detected a few *ABCB1* (7q21.12) and *TRIP6* (7q22.1) loci on both arms of der(7)t(7;7)ins(7;15). Interestingly, the other copy of chromosome 7 was intact and carried *ABCB1* and *TRIP6* loci in situ (Figure 3C).

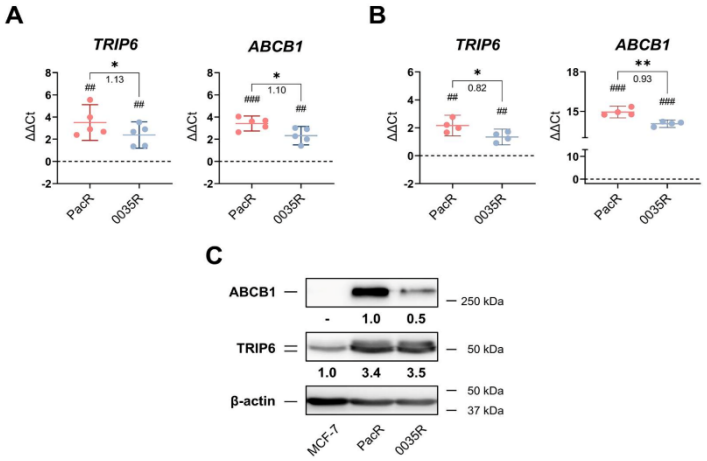

Figure 2. *TRIP6* and *ABCB1* are overexpressed in paclitaxel-resistant MCF-7 subline (PacR) and SB-T-0035-resistant MCF-7 (0035R) subline. (**A**) The DNA level of *TRIP6* and *ABCB1* plotted as ΔΔCt values (N = 5, 3 technical replicates). The dashed line represents the DNA level in parental MCF-7 cells. For *ABCB1* in the 0035R subline, data were not corrected by the *TERT* reference gene DNA level. The numbers below the zig–zag lines represent DNA level difference between PacR and 0035R sublines. Statistical analysis was performed using the one-sample *t*-test (#) and paired *t*-test (*). (**B**) *TRIP6* and *ABCB1* mRNA expression level was plotted as delta-delta threshold cycle (ΔΔCt) values (N = 4, 3 technical replicates). Dashed lines represent *TRIP6* or *ABCB1* expression in MCF-7 cells. The mean and 95% confidence interval (CI) are shown. The numbers below the zig–zag lines represent the mRNA expression level difference between PacR and 0035R sublines. Statistical significance was tested using the one-sample *t*-test (#) and paired *t*-test (*). (**C**) Western blot analysis of ABCB1 transporter and TRIP6 in MCF-7 cells and taxane-resistant MCF-7 sublines. The numbers displayed below each representative Western blot mean the fold change of band volume normalized to β-actin level (N = 4); (**D**) * $p < 0.05$, ** $p < 0.01$. ## $p < 0.01$, ### $p < 0.001$.

Table 1. Composite karyotype of parental MCF-7 cell line. Differences to taxane-resistant MCF-7 sublines are highlighted in bold.

Cell Line	Composite Karyotype
MCF-7 67~69 <3n>	X,-X,der(X)t(X;7)(p11.2;p15.3)del(X)(q21.3q28),der(1)t(9;20)(?;?)t(1;20)(p12;?)t(1;9)(q21;?),+2,der(2)t(2;3)(q?34;?),der(2)t(2;7)(p?;q32)t(2;14)(q36;q?),der(2)t(2;14)(q36;q?),der(3)del(3)(p?13p?26)t(3;6)(q27;q25),t(4;5)(q?31;p13),-6,der(6)t(3;6)(q27;q25),**-7**,der(7)t(7;7)(p15;?)ins(7;15)(p;?),der(8)t(8;15)(p11.2;q?)x2, **der(8)t(8;16)(q?24;?)**,-9,der(9)t(8;9)(q?;p22),**der(10)t(3;6)(?;?)t(6;10)(?;p14)**,der(10)t(7;10)(p21,p14), der(11)t(11;16)(p11.2;?)t(8;11)(q11.2;q13),+12,der(12)t(1;17)(?;?)t(1;9)(?;?)t(9;12)(?;p11.2),der(12)t(8;12)(?;p11.2)t(5;12)(?;q?21),+13,del(13)(q?22q?34)x2,der(13)t(6;13)(?;p11.2),-14,+15,der(15)t(15;16)(p11.2;q?)del(15)(q?22.3q?26), der(15)t(15;21)(p11.2;q?21),der(16)del(16)(p?13)del(16)(q?21),**der(17)t(17;20)(q?24;?)t(1;20)(?;?)t(1;21)(?;?),+18**, der(18)del(18)(p?11.2)del(18)(q?11.2),dup(18)(q?q?),**der(18)t(18;22)(p11.2;q11.2)**,der(19)t(12;19)(q13;p13.3), der(19)t(11;14)(?;q?)t(11;19)(?;p12),+20,der(20)t(1;21)(?;q?)t(1;20)(?;p11.2)x2,-21,der(22)t(6;22)(?;q11.2),der(22)t(7;22)(q22;q11.2)x2[cp20]

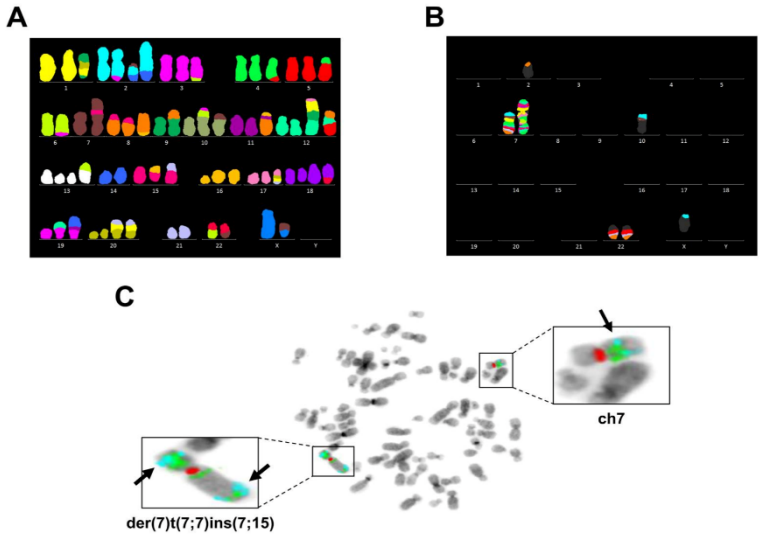

Figure 3. *TRIP6* and *ABCB1* possess increased copy numbers in parental MCF-7 cell line. (**A**) Multicolor fluorescence in situ hybridization (FISH) analysis of representative metaphase chromosomes of MCF-7 cells. (**B**) Multicolor banding (mBAND) of chromosome 7 analysis of representative metaphase chromosomes of MCF-7 cells. (**C**) Dual FISH analysis of representative metaphase chromosomes of MCF-7 cells. Labeled chromosomes are shown in detail. Arrows point to *TRIP6* loci. Detected signals come from a probe specific to *ABCB1* (green), *TRIP6* (aqua), and the centromere of chromosome 7 (red).

3.3. Chromosome 7 Is Rearranged in Taxane-Resistant MCF-7 Sublines

To validate amplification of the region encompassing *TRIP6* and *ABCB1*, we carried out similar FISH analyses in taxane-resistant MCF-7 sublines.

We karyotyped 8 mitoses (of 34 analyzed) of PacR cells, and 12 mitoses (of 36 analyzed) of 0035R cells (Figure 4, Table 2). The modal chromosome number of taxane-resistant MCF-7 sublines slightly varies from parental MCF-7 cells. Nevertheless, most derivative chromosomes have been preserved (Figure 4, Figure A2). Notably, a breakage at 7q11.2 in the intact chromosome 7 resulted in novel der(7)t(6;7) and der(7)del(7)(p12)del(7)(q11.1) in taxane-resistant MCF-7 sublines (Figure 4, Figure A3). We detected *TRIP6* co-amplification with *ABCB1* (Figure 4C,F) as a homogeneously stained region (HSR) translocated to chromosome 3 (PacR subline) or chromosome 19 (0035R subline). In a few mitoses of 0035R cells, we unambiguously detected HSR in chromosome 15 (Figure 4D), indicating that 0035R subline might consist of two subclones.

3.4. TRIP6 Expression Is Regulated by Cyclic AMP Response Element (CRE)

TRIP6 promoter has not been functionally characterized yet. Hence, we generated 5′ and 3′ truncated *TRIP6* promoter reporter constructs by cloning a human *TRIP6* promoter sequence upstream of the minimal synthetic promoter (minP) in pGL4.24[*luc2P*/minP] vector (Figure S5). In fact, the cloned full-length *TRIP6* promoter sequence encompassed *SLC12A9* exon 14 (sequence −936 to −376, relative to *TRIP6* transcription start, TSS) and *SLC12A9-TRIP6* intergenic region (sequence −375 to −1) (Figure 5).

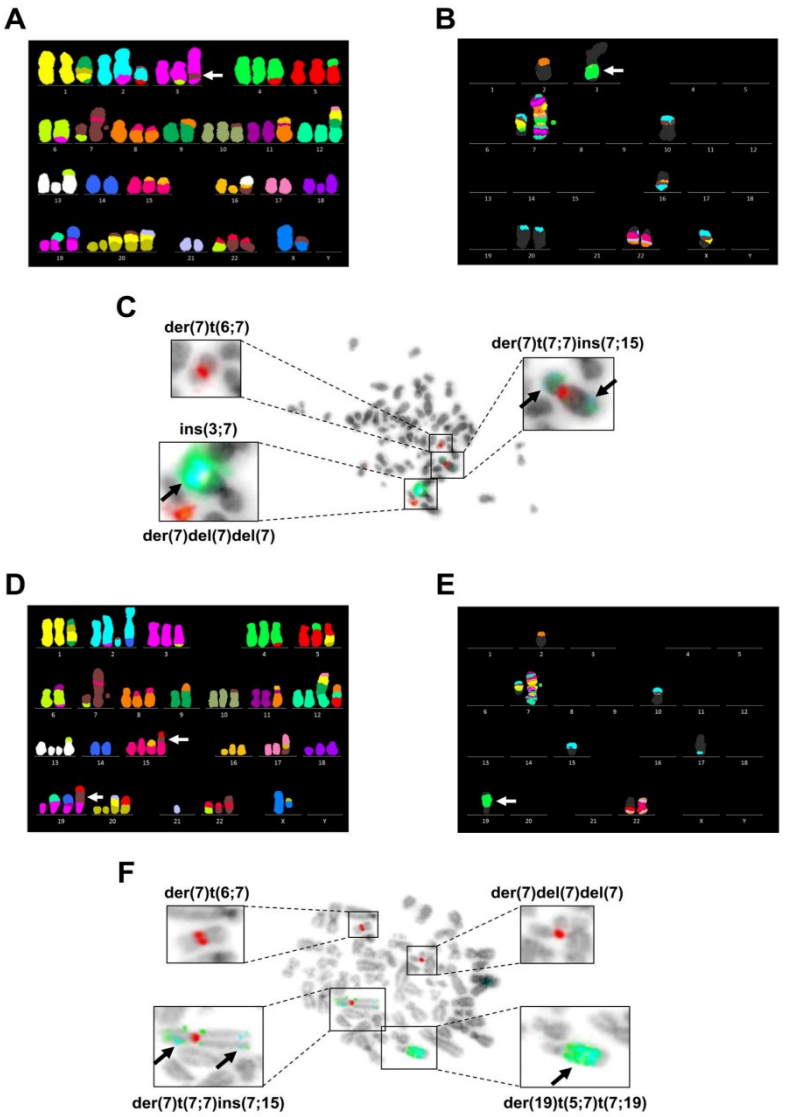

Figure 4. Co-amplification of *TRIP6* and *ABCB1* genes in taxane-resistant MCF-7 sublines (PacR, 0035R). Representative metaphase chromosomes of PacR subline analyzed by (**A**) multicolor fluorescence in situ hybridization (mFISH), (**B**) multicolor band (mBAND) of chromosome 7, and (**C**) dual FISH. Representative metaphase chromosome of 0035R subline analyzed by (**D**) mFISH, (**E**) mBAND of chromosome 7, and (**F**) dual FISH.The white arrows point at homogeneously staining regions (HSRs) harboring the *ABCB1* and *TRIP6* genes. Labeled chromosomes are shown in detail. Detected signals come from a probe specific to *ABCB1* (green), *TRIP6* (aqua), and the centromere of chromosome 7 (red).

Table 2. Composite karyotype of taxane-resistant MCF-7 sublines. Differences to parental MCF-7 cell line are highlighted in bold.

Cell Subline	Composite Karyotype
PacR 67-68 <3n>	X,-X,der(X)t(X;7)(p11.2;p15.3)del(X)(q21.3q28),der(1)t(9;20)(?;?)t(1;20)(p12;?)t(1;9)(q21;?),+2,der(2)t(2;3)(q?34;?), **der(2)t(2;7)(p?;q32)t(2;5)(q?;?)**,der(2)t(2;14)(q36;q?),der(3)del(3)(p?13p?26)t(3;6)(q27;q25),**ins(3;7)(q?23;q11.2q22)**, t(4;5)(q?31;p13),-6,der(6)t(3;6)(q27;q25),**der(7)t(6;7)(?;q11.2)**,der(7)t(7;7)(p15;?)ins(7;15)(p;?), **der(7)del(7)(p12)del(7)(q11.1)**,der(8)t(8;15)(p11.2;q?)x2,-9,der(9)t(8;9)(q?;p22),der(10)t(7;10)(p21;p14), der(11)t(11;16)(p11.2;?)t(8;11)(q11.2;q13),+12,der(12)t(1;17)(?;?)t(1;9)(?;?)t(9;12)(?;p11.2),der(12)t(8;12)(?;p11.2) t(5;12)(?;q?21),del(13)(q?22q?34),der(13)t(6;13)(?;p11.2),-14,**der(15)t(15;16)(p11.2;q?)**,der(15)t(15;16)(p11.2;q?) del(15)(q?22.3q?26),**+16**,der(16)del(16)(p?13)del(16)(q?21)x2,**der(16)t(13;16)(q?12;p11.2)t(7;16)(p15.3;q?13),-17**, der(18)del(18)(p?11.2)del(18)(q?11.2),dup(18)(q?q?),der(19)t(12;19)(q13;p13.3),der(19)t(11;14)(?;q?)t(11;19)(?;p12), **+20x2,der(20)t(1;7)(?;p21)t(1;20)(?;p11.2)x2**,der(20)t(1;21)(?;q?)t(1;20)(?;p11.2),- 21,der(22)t(6;22)(?;q11.2),der(22)t(7;22)(q22;q11.2)x2[cp8]
0035R 67~70 <3n>	X,-X,**der(X)t(X;20)(p11.2;?)del(X)(q21.3q28)**,der(1)t(9;20)(?;?)t(1;20)(p12;?)t(1;9)(q21;?),+2,der(2)t(2;3)(q?34;?), **der(2)t(2;7)(p?12;q32)del(2)(q36)**,der(2)t(2;14)(q36;q?),der(3)del(3)(p?13p?26)t(3;6)(q27;q25),t(4;5)(q?31;p13), **der(5)t(1;5)(q?13)t(1;20)(?;q?)**,-6,**der(6)t(6;11)(p?21;q?)t(3;6)(q27;q25),der(7)t(6;7)(?;q11.2)**, der(7)t(7;7)(p15;?)ins(7;15)(p;?),**der(7)del(7)(p12)del(7)(q11.1)**,der(8)t(8;15)(p11.2;q?)x2,-9,der(9)t(8;9)(q?;p22), der(10)t(7;10)(p21;p14),der(11)t(11;16)(p11.2;?)t(8;11)(q11.2;q13),+12,der(12)t(1;17)(?;?)t(1;9)(?;?)t(9;12)(?;p11.2), der(12)t(8;12)(?;p11.2)t(5;12)(?;q?21),+13,del(13)(q?22q?34)x2,der(13)t(6;13)(?;p11.2),-14,+15, der(15)t(15;16)(p11.2;q?)del(15)(q?22.3q?26),**der(15)t(5;7)(?;p22)t(7;15)(p22;p11.2)**,der(16)del(16)(p?13)del(16)(q?21) **der(17)t(17;20)(q?24;?)t(7;20)(p22;?)**,der(18)del(18)(p?11.2)del(18)(q?11.2),dup(18)(q?q?),**+19**,der(19)t(12;19) (q13;p13.3),der(19)t(11;14)(?;q?)t(11;19)(?;p12),**der(19)t(5;7)(?;q21)t(7;19)(q21;p13.3)**,+20,der(20)t(1;21)(?;q?)t(1;20) (?;p11.2),**der(20)t(5;20)(?;p?12)**,-21,der(22)t(6;22)(?;q11.2),der(22)t(7;22)(q22;q11.2), **der(22)t(7;22)(q22;p11.2)t(7;22)(q22;q11.2)**[cp12]

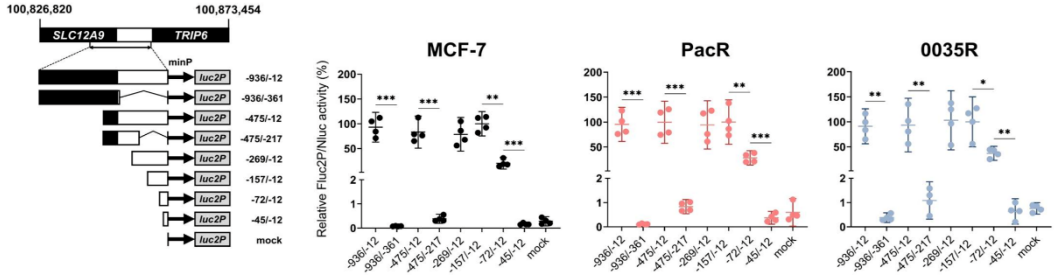

Figure 5. The *TRIP6* proximal promoter governs *TRIP6* transcription in parental MCF-7 cell line as well as in taxane-resistant MCF-7 sublines (PacR, 0035R). Schematic diagrams of the 5′ and 3′ truncated constructs (on the left) and scatter dot plots showing normalized luciferase activities (Fluc2P/Nluc) relative to the construct −157/−12 (on the right). The cloned sequence −936/−12 encompasses an intergenic region (white box, sequence −12 to −375) and a part of the *SLC12A9* upstream gene (black box, sequence −376 to −936). minP refers to synthetic minimal TATA box promoter. The mean and 95% confidence interval (CI) are displayed for each construct ($N = 4$, 3 technical replicates). Empty vector pGL4.24[*luc2P*/minP] served as a mock. Statistical significance was tested using the one-way blocked ANOVA with Geisser–Greenhouse correction followed by Tukey's post hoc test on log-transformed data. * $p < 0.05$, ** $p < 0.01$, *** $p < 0.001$.

We assessed firefly (Fluc2P) and deep-sea shrimp Nanoluc (Nluc) luciferase activities in MCF-7 cells and taxane-resistant MCF-7 sublines co-transfected with a series of 5′ and 3′ truncated constructs and the normalization pNL1.1.TK[Nluc/TK] vector. Firstly, the experiments showed that the *TRIP6* proximal promoter (sequence −157 to −12 relative to the *TRIP6* transcription start) but not the *TRIP6* distal promoter (sequence −936 to −157) is sufficient to drive *TRIP6* expression in both MCF-7 cells and taxane-resistant MCF-7 sublines (Figure 5). Secondly, the construct −72/−12 achieved significant Fluc2P/Nluc

activity (20%, 28%, and 37% of relative Fluc2P/Nluc activity of the −157/−12 construct in MCF-7, PacR, and 0035R cells, respectively).

To identify *cis*-acting regulatory elements in the active human *TRIP6* proximal promoter, we scanned the −200 to −1 sequence with Jaspar 2022 transcription factor binding profiles (≥93% relative profile score threshold) (Table S9) [55]. We manually identified core elements within most of the predicted binding sites (Figure 6A). Remarkably, we discovered a full cyclic AMP response element (CRE) motif at position −60 to −53, corresponding to the −72/−12 construct with marked activity. Mutagenesis of CRE demonstrated a 6- to 21-fold reduction in Fluc2P/Nluc activity in 5′ truncated constructs (−157/−12ΔCRE, −117/−12ΔCRE, and −72/−12ΔCRE) (Figure 6B), indicating that CRE is crucial to *TRIP6* transcription in MCF-7 cells.

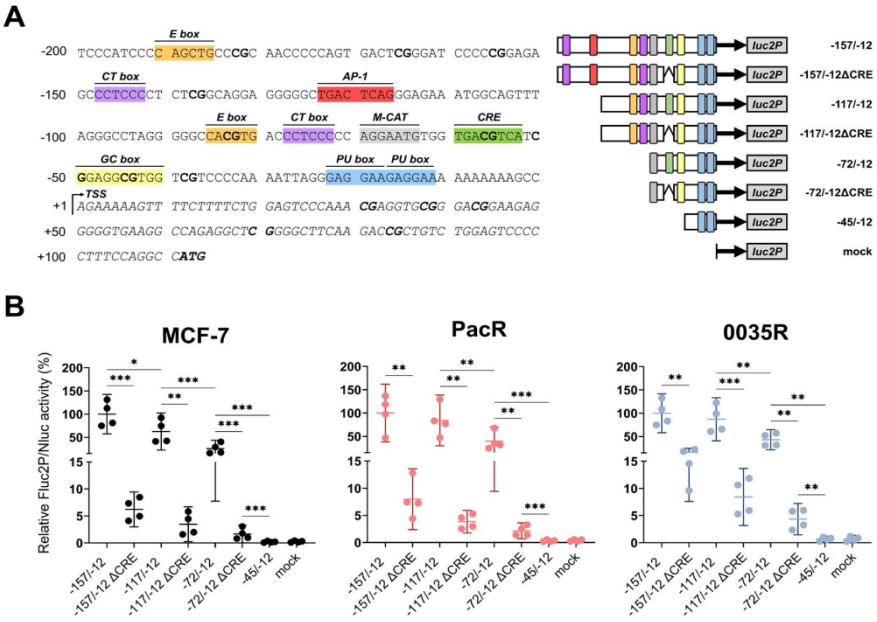

Figure 6. Cyclic AMP response element (CRE) regulates *TRIP6* proximal promoter activity in parental MCF-7 cell line as well as in taxane-resistant MCF-7 sublines (PacR, 0035R). (**A**) Predicted *cis*-regulatory elements in the human *TRIP6* proximal promoter sequence (GRCh38.p12) (on the left). The sequence also includes a 5′ untranslated region and *TRIP6* start codon. CpG dinucleotides and start codon are highlighted in bold. TSS means *TRIP6* transcription start. E box refers to enhancer box, CT box refers to CT-rich sequence, AP-1 site refers to Activator protein 1, M-CAT refers to muscle-CAT element (in reverse orientation), CRE refers to cyclic AMP response element, GC-box refers to GC-rich sequence. Schematic diagrams of the *TRIP6* proximal promoter with wild-type CRE or mutated CRE motif (on the right). Colored rectangles correspond to predicted *cis*-acting gene regulatory elements positioned at the 5′ flanking sequence of *TRIP6*. (**B**) Scatter dot plots showing Fluc2P/Nluc activities relative to the −157/−12 construct (on the right). minP refers to synthetic minimal TATA box promoter. The mean and 95% confidence interval (CI) are displayed for each construct (N = 4, 3 technical replicates). Empty vector pGL4.24[*luc2P*/minP] served as a mock. Statistical significance was tested using the one-way blocked ANOVA with Geisser–Greenhouse correction followed by Tukey's post hoc test on log-transformed data. * $p < 0.05$, ** $p < 0.01$, *** $p < 0.001$.

Furthermore, the −117/−72 construct exhibited a two-fold increase in Fluc2P/Nluc activity compared to the −72 /−12 construct in all tested cells (Figure 6B). The region −117 to −72 encompasses an enhancer box (E box) and CT box [56]. Furthermore, activating protein 1 (AP-1) motif located within the region −157 to −117 weakly stimulated (1.6-fold, $p = 0.036$) Fluc2P/Nluc activity in MCF-7 cells but not in PacR and 0035R cells (1.2-fold, $p = 0.60$, 1.1-fold, $p = 0.33$, respectively). Yet, the other element(s), probably the GC box [57] or M-CAT [58], increased basal expression as seen in the −72/−12ΔCRE construct. We recurrently detected no stimulatory activity in the region −45 to −12 in all tested cells.

Collectively, CRE unambiguously promotes *TRIP6* transcription in MCF-7 cells and taxane-resistant MCF-7 sublines. The predicted E box, GC box, CT box, and M-CAT might contribute to the *TRIP6* promoter activity; however, there would still be other unidentified motifs. In addition, the AP1 site likely enhances *TRIP6* transcription only in MCF-7 cells, as it does not appear to modulate the response in PacR and 0035R cells.

3.5. TRIP6 Proximal Promoter Is Hypomethylated in Taxane-Resistant MCF-7 Sublines

Methylation of CpG site in CRE motif hampers transcription in *cis* [59]. Considering *TRIP6* dependence on the CRE motif (Figure 6), we assessed the methylation of 8 CpG sites within the *TRIP6* proximal promoter by bisulfite PCR. As it is shown in Figure 7A, the analyzed region exhibits hypomethylation in MCF-7 cells (3.8%), PacR subline (6.0 %), and 0035R subline. Importantly, we detected an unmethylated CpG in the CRE motif in all tested cells (Figure 7A).

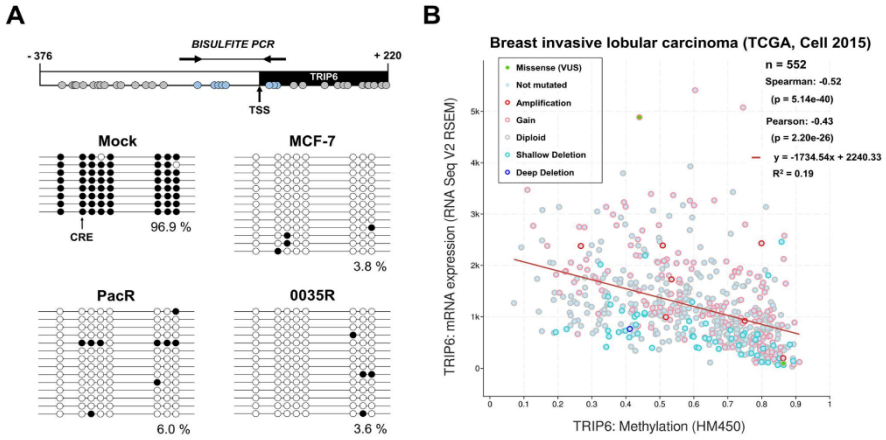

Figure 7. The *TRIP6* proximal promoter is stable hypomethylated in parental MCF-7 cell line as well as in taxane-resistant MCF-7 sublines (PacR, 0035R); (**A**) Schematic diagram (top) displaying the position of individual CpG dinucleotides (grey circles) in *TRIP6-SLC12A9* intergenic region (white rectangle, −376 to −1) and *TRIP6* exon 1 (black rectangle, +1 to +220). Methylation status of CpG sites estimated by bisulfite sequencing (bottom). In vitro methylated human diploid DNA served as an internal control (mock). The black arrow points CpG dinucleotide within the CRE motif. The white circles depict non-methylated CpG dinucleotides. Black circles depict methylated CpG dinucleotides. Analyzed CpG dinucleotides are shown as blue circles. Arrows indicate the position of the used primer pair. TSS means *TRIP6* transcription start. (**B**) Correlation of *TRIP6* mRNA level (normalized to RNA-Seq by Expectation–Maximization method, RSEM) with *TRIP6* methylation (HM450 Illumina Platform) in The Cancer Genome Atlas (TCGA) breast cancer study ($N = 552$). VUS refers to a variant of unknown significance. Shallow deletion refers to possible heterozygous deletion. Deep deletion refers to possible homozygous deletion. The graph was generated in the cBioPortal platform.

Furthermore, we assessed *TRIP6* methylation in clinical breast cancer samples (TCGA study) (Figure 7B). *TRIP6* mRNA expression negatively correlated (Spearman's coefficient = −0.52, $p < 0.001$) with CpG methylation level, indicating that DNA methylation might regulate *TRIP6* expression also in breast tumors.

To explore *TRIP6* differential methylation between MCF-7 cells and taxane-resistant MCF-7 sublines (PacR, 0035R), we employed 16 probes that targeted to defined gene regions TSS200 (−200 bases to TSS, i.e., proximal promoter), TSS1500 (−1500 to −200, i.e., distal promoter), 1st Exon, gene body (region between ATG and stop codon), and 5′ and 3′ untranslated regions (UTRs). It is worth noting that the distal promoter region substantially overlaps with the last exon of the *SLC12A9* gene. Although the whole *TRIP6* gene sequence analysis showed higher methylation in PacR cells ($p = 0.004$, FDR = 0.025), in fact, methylation of the distal *TRIP6* promoter region (TSS1500) significantly changed. We found no differential methylation between MCF-7 cells and taxane-resistant MCF-7 sublines in the *TRIP6* proximal promoter (TSS200), gene body, and 1st exon, in line with bisulfite sequencing data (Table 3).

Table 3. Altered *TRIP6* methylation level between parental MCF-7 cells and taxane-resistant MCF-7 sublines (PacR, 0035R). The absolute β value (|Δβ|) is defined as difference between β value of MCF-7 cells and PacR cells, or MCF-7 cells and 0035R cells. Statistical analysis results include *p*-value and false discovery rate (FDR). Ns means statistically insignificant result.

Region *	MCF-7 vs. PacR			MCF-7 vs. 0035R		
	|Δβ|	*p*-Value	FDR	|Δβ|	*p*-Value	FDR
Whole gene	0.41	0.004	0.025	0.36	0.2	ns
1st exon	0.23	0.121	ns	0.01	0.439	ns
Body	0.12	0.248	ns	0.11	0.248	ns
TSS1500	0.49	0.02	0.025	0.36	0.002	0.008
TSS200	0.40	0.05	ns	0.05	0.05	ns

* Gene regions as defined in Results section.

These findings suggest that the *TRIP6* proximal promoter is stably hypomethylated, thereby contributing to high *TRIP6* expression in MCF-7 cells and taxane-resistant MCF-7 sublines.

3.6. Associations of TRIP6 mRNA Level with Clinicopathological Features of Breast Cancer

In a recent study, Zhao et al. postulated *TRIP6* as a putative prognostic biomarker in breast cancer [20]. Therefore, we aimed to validate this finding by evaluating *TRIP6* expression in 95 breast tumor tissue samples and 6 non-tumor tissues collected in the Czech Republic.

Table 4 summarizes clinical data, response to the therapy, and survival of patients who provided breast cancer tissues. The median age (± SD) of patients with a breast cancer diagnosis was 56.0 ± 10.7 years. Most individuals were diagnosed with invasive ductal carcinoma (84.2%), grade 1 or 2 (75.8%), and stage II (62.1%). Nearly all breast cancer tissues expressed estrogen receptor (ER, 90.5% of samples) and progesterone receptor (PR, 70% of samples), meaning that luminal molecular subtype (91.6%) prevailed in evaluated samples. The median of disease-free survival (DFS) (± SD) of patients was 61.1 ± 28.4 months, and overall survival was 70.9 ± 28 months. Unfortunately, disease progression occurred in 9 of the 95 patients, and 8 patients died.

We assessed *TRIP6* mRNA expression in all collected breast tissue samples ($N = 95$) and protein expression only in a small number of samples ($N = 20$) due to limitations in sample size. Whereas all breast tumor tissues expressed *TRIP6* mRNA, we detected TRIP6 protein expression by immunoblotting in 17 of the 20 examined samples (Figure 8A). *TRIP6* mRNA and protein level correlated intermediately (Spearman's coefficient 0.594, $p = 0.032$) in breast cancer tissues. (Figure 8B).

Table 4. Clinicopathological characteristics of 95 breast carcinoma patients.

Characteristics	Breast Carcinoma Set
Mean age at diagnosis, years	56.0 ± 10.7
Menopausal status	**N (%)**
Premenopausal	27 (28.4)
Postmenopausal	66 (69.5)
Not available	2 (2.1)
Histological type	**N (%)**
Invasive ductal carcinoma	80 (84.2)
Others	15 (15.8)
Histological grade	**N (%)**
G1	13 (13.7)
G2	59 (62.1)
G3	22 (23.1)
Not available	1 (1.1)
Stage	**N (%)**
I	31 (32.6)
II	59 (62.1)
III	4 (4.2)
IV	1 (1.1)
Estrogen receptor status	**N (%)**
Positive	86 (90.5)
Negative	9 (9.5)
Progesterone receptor status	**N (%)**
Positive	70 (73.7)
Negative	25 (26.3)
ERBB2 status	**N (%)**
Positive	27 (28.4)
Negative	68 (71.6)
Ki67 status [1]	**N (%)**
Positive	70 (73.7)
Negative	13 (13.7)
Unknown	12 (12.6)
Molecular subtype	**N (%)**
Luminal A	60 (63.2)
Luminal B	26 (27.3)
ERBB2	7 (7.4)
Triple negative	2 (2.1)
Therapeutic regimens	**N (%)**
Neoadjuvant (NACT) [2]	13 (13.7)
Adjuvant (ACT)	82 (86.3)
Relapse	**N (%)**
Yes	9 (9.5)
No	86 (90.5)
Overall survival (OS)	
Mean (months) ± SD	70.9 ± 28.0
Disease-free survival (DFS)	
Mean (months) ± SD	61.1 ± 28.4

[1] The cut-off score was 13.25% [38]. [2] Including the individual in stage IV and undergoing a palliative care.

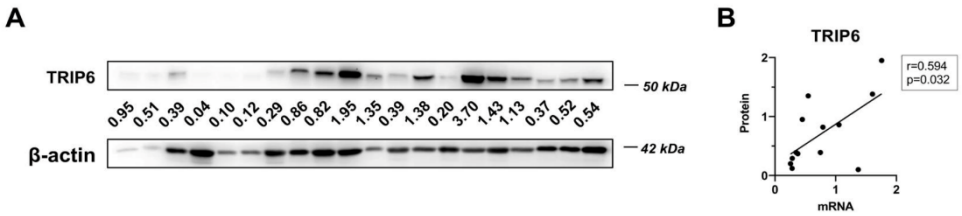

Figure 8. *TRIP6* expression in breast cancer samples. (**A**) TRIP6 protein expression in 20 breast tumor samples. The numbers displayed below the TRIP6 Western blot represent the TRIP6 level normalized to the β-actin level. (**B**) Correlation of *TRIP6* mRNA level versus TRIP6 protein in 13 breast cancer samples. Spearman's correlation coefficient and statistical significance (*p*-value) are shown.

We found no difference in *TRIP6* mRNA expression levels between adjuvant (N = 82) and neoadjuvant (N = 13) cohorts (p = 0.86). Furthermore, we found no statistically significant correlation between *TRIP6* mRNA level and DFS or OS, independent of the type of therapy. High *TRIP6* mRNA expression was observed in premenopausal (p = 0.033) and progesterone receptor positive (p = 0.020) breast cancer in the adjuvant cohort of breast cancer patients but not in the neoadjuvant cohort (p = 0.50 and p = 0.77, respectively) (Table 5).

Table 5. Significant associations of intratumoral *TRIP6* mRNA level with clinical data of breast carcinoma patients in the adjuvant chemotherapy group (N = 82).

Characteristics	*TRIP6* Expression Relative to *IPO8* and *MRPL19*	Significance (Mann–Whitney)
Premenopausal	1.05 ± 0.59	0.033
Postmenopausal	0.77 ± 0.49	
Progesterone receptor positive	0.93 ± 0.56	0.020
Progesterone receptor negative	0.61 ± 0.34	

4. Discussion

An early study demonstrated a ubiquitous 1.8-Kb *TRIP6* mRNA expression in human organs except for skeletal muscle, brain, and leukocytes [60]. Recently, Shukla et al. detected TRIP6 in ependymal and choroid plexus cells of embryonic and early post-natal (to P10) mice brains [12]. Additionally, observations of enhanced *TRIP6* expression in various neoplasms might indicate disrupted gene regulatory mechanisms during cancerogenesis [20,61]. Furthermore, we found *TRIP6* overexpression in paclitaxel-resistant MCF-7/PacR subline [62], yet the molecular mechanism(s) that drive *TRIP6* expression in MCF-7 cells as well in paclitaxel-resistant cells have not been described in detail.

Herein, we revealed that *TRIP6* copy number gain and the activity of the cyclic-AMP response element in the hypomethylated *TRIP6* proximal promoter contribute to the high TRIP6 protein level in parental MCF-7 cells. Although the AP-1 motif seems more important in parental MCF-7 cells, copy number gain but not altered regulation of the *TRIP6* promoter instead contribute to *TRIP6* overexpression in both taxane-resistant MCF-7 sublines (Figure 9).

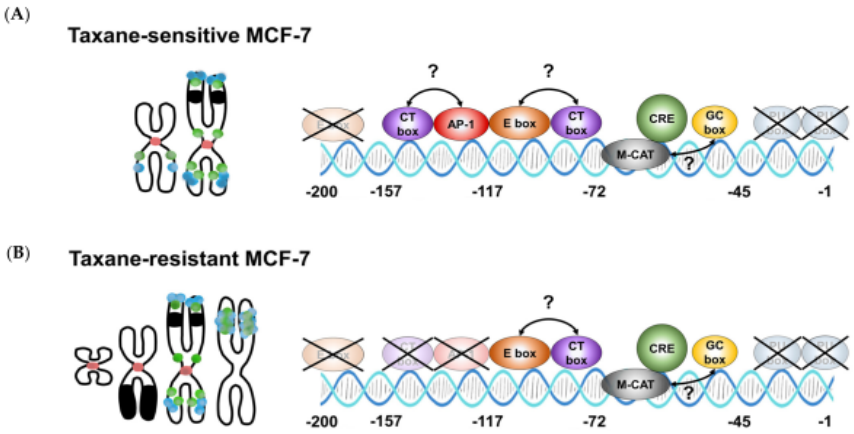

Figure 9. Chromosomal aberrations and *cis*-regulatory elements in the TRIP6 promoter contribute to enhanced TRIP6 expression in parental MCF-7 cells and taxane-resistant MCF-7 sublines. (**A**) In MCF-7 cells, copy number gain (on the left) and the activity of the cyclic AMP response element (on the right) in the hypomethylated TRIP6 proximal promoter contribute to high TRIP6 expression. The role of other putative transcription factor binding sites remains elusive. (**B**) In MCF-7 sublines, TRIP6/ABCB1 co-amplification led to the formation of a homogeneously stained region in chromosome 3 (PacR) or 19 (0035R) (on the left). In contrast, the activity of elements in the hypomethylated TRIP6 promoter remained unchanged except for the region containing the putative AP-1 site (on the right). Dots represent TRIP6 loci (blue) and ABCB1 loci (green). The red area refers to chromosome 7 centromere. The black area refers to chromosome 15 (in MCF-7 and taxane-resistant MCF-7 cells) or chromosome 6 segments (in taxane-resistant MCF-7 cells only).

While *TRIP6* mRNA levels differed between PacR cells and 0035R cells, TRIP6 protein abundance was identical and markedly higher compared to parental MCF-7 cells (Figure 2). This discrepancy might indicate the differential *TRIP6* post-transcription regulation, for instance, by putative differential *TRIP6* mRNA base modifications, miRNA, or recently observed TRIP6 ubiquitin-mediated degradation [24]. Concerning miRNA, it was reported that miR-7, miR-138-5p, miR-485-3p, and miR-589-5p regulate *TRIP6* gene expression; unfortunately, their function related to *TRIP6* in breast cancer has not been investigated [21–23,63]. However, our preliminary data suggest that miR-138-5p is not expressed in MCF-7 cells and taxane-resistant MCF-7 sublines (personal communication Dr. R. Václavíková).

Strikingly, the *TRIP6* (100.8 Mb, 7q22.1) gene copy number and mRNA level increased in parallel with the *ABCB1* (87.5 Mb, 7q21.12) gene copy number and mRNA level. In agreement, FISH analyses unambiguously validate *TRIP6*/*ABCB1* co-amplification in taxane-resistant MCF-7 sublines (Figure 4). Despite *TRIP6* amplification, our findings indicate that TRIP6 is not involved in resistance to taxanes, as silencing of the *TRIP6* does not seem to affect the response of the 0035R cells to SB-T-0035 compound (Figure S6). To date, upregulation of the *TRIP6* gene occurred in daunorubicin- (EPG85-257RDB) and mitoxantrone-resistant (EPG85-257RNOV) human gastric carcinoma cells, the former cells having also upregulated *ABCB1* [64].

The *ABCB1* amplified region, referred to as *ABCB1* amplicon, is often documented in drug-resistant sublines [64–67]. By retrospective analysis, Genovese et al. defined the *ABCB1* amplicon core as a 1 Mb region commonly detected in ABCB1 overexpressing cells [65]. By contrast, the largest reported *ABCB1* amplicon was bordered by semaphorin 3D (*SEMA3D*, 84.3 Mb) and cyclin-dependent kinase 6 (*CDK6*, 92.1 Mb) [66]. The occurrence

of *TRIP6* (7q22.1, 100.8Mb) might indicate the extraordinary size of the *ABCB1* amplicon in MCF-7 sublines.

The most famous breakage–fusion–break (BFB) mechanism of amplicon formation leverages specific sequences referred to as fragile sites [68]. What mechanism specifies fragile site selection is not well known. The breaks likely occurred at the FRA7F aphidicolin site (98.7–107.4 Mb) and the 7q11.2 region. The order of events is challenging due to the utilization of multiple selection steps and no direct observation of fusion bridges. Nevertheless, numerical aberration of chromosome 7 in taxane-resistant MCF-7 sublines might be a remnant of dicentric chromosome 7.

Beyond *ABCB1*/*TRIP6* co-amplification, we noticed the loss of der(18)t(18;22) in both taxane-resistant MCF-7 sublines. The impact of this aberration in the context of taxane resistance is unknown.

Since the enhanced *TRIP6* expression could theoretically be caused by different transcriptional regulations at the *TRIP6* promoter level, we analyzed the responsiveness of the *TRIP6* promoter by dual-luciferase assay. The *TRIP6* proximal promoter region (−157 to −45) controlled luciferase expression in MCF-7 cells (Figure 5). The most active segment spanning −72 to −45 nucleotides harbors the M-CAT motif, cyclic AMP response element (CRE), and GC box (Figure 6). Disrupting the CRE motif by mutagenesis reduced luciferase activity, highlighting its pivotal role in *TRIP6* transcription regulation (Figure 6). A genome-wide analysis has previously identified identical CRE motif within the *TRIP6* proximal promoter [69], but its role has remained elusive. The *cis*-regulating activity of the CRE motif relies on its position (< 250 bases) relative to gene transcription start [70] and methylation of the inner CpG site [59]. As tested by bisulfite sequencing (Figure 7A), the CpG site within the CRE motif was not methylated in MCF-7 cells and in both taxane-resistant cells; however, whether this particular methylation affects the expression of *TRIP6* remains to be determined in further studies.

Finally, we evaluated the clinical data of breast cancer patients with *TRIP6* mRNA expression. Recently, we revealed no clinicopathological association of the *TRIP6* mRNA expression level in ovarian cancer [71]. To highlight our findings concerning the regulation of *TRIP6* expression in sensitive and taxane-resistant MCF-7 breast cancer cell lines, we evaluated *TRIP6* mRNA expression against clinical data of breast cancer patients who had undergone taxane-containing regimens. So far, Zhao et al. have analyzed TRIP6 protein expression in breast cancer from the Chinese cohort [20]. Unfortunately, our data did not validate most of the published results, likely due to the small number of patients in our study and the heterogenous nature of breast cancer.

5. Conclusions

This study presents compelling evidence that the cyclic AMP response element (CRE) located within the stable hypomethylated proximal promoter controls *TRIP6* expression in MCF-7 cells. Furthermore, increased *TRIP6* copy number contributes to high TRIP6 expression in MCF-7 cells in vitro. Co-amplification of *TRIP6* with *ABCB1* underlies *TRIP6* upregulation in two taxane-resistant MCF-7 sublines. Cytogenetic analyses showed that amplicon arose from intact chromosome 7. In addition, we observed a loss of derivative chromosome der(18)t(18;22) in both sublines, with an unknown relation to taxane resistance. Moreover, the present study has not found direct prognostic or predictive relevance of *TRIP6* for better tailoring breast cancer management at the clinics. Instead, the analysis of breast tumor of a neoadjuvant cohort revealed *TRIP6* mRNA expression level associations with positive progesterone receptor expression status and premenopausal status.

Collectively, we propose that *TRIP6* proximal promoter might act as another important regulatory site in regulation of *TRIP6* expression. The relevance of our functionally valid observation for clinical course of breast and other cancer(s), including eventual utility of TRIP6 as a target for new therapy design, shall be evaluated by follow-up studies.

Supplementary Materials: The following supporting information can be downloaded at: https://www.mdpi.com/article/10.3390/genes14020296/s1, Figure S1: Authentication report MCF-7; Figure S2: Authentication report MCF-7/PacR subline; Figure S3: Authentication report MCF-7/0035R subline; Figure S4: Empire Genomics Certificate; Figure S5: Cloning scheme; Figure S6: Effect of *TRIP6* silencing; Table S1: Synthesis of complementary DNA; Table S2: TaqMan® Gene Expression probes list; Table S3: Reaction conditions for quantitative PCR; Table S4: Oligonucleotides used for *TRIP6* promoter cloning; Table S5: *TRIP6* promoter constructs generated by PCR fragment cloning; Table S6: PCR components and cycling conditions used for amplification of TRIP6 sequence; Table S7: Constructs generated by restriction endonuclease cleavage and blunting; Table S8: Constructs generated by restriction endonuclease cleavage; Table S9: Predicted transcription factor binding sites.

Author Contributions: Conceptualization, P.D. and J.K.; methodology, T.T. and T.F.; formal analysis, R.V., K.Š. and T.F.; investigation, P.D., K.B., R.V., K.Š., M.J., Š.R. and M.V.; resources, L.W., T.F., T.T. and I.O.; data curation, R.V.; writing—original draft preparation, P.D., R.V., K.Š. and Š.R.; writing—review and editing, J.K. and R.V.; visualization, P.D., Š.R. and M.V.; supervision, J.K., P.S., V.N.K. and I.O.; project administration, J.K. and P.S. All authors have read and agreed to the published version of the manuscript.

Funding: This work was supported by the Czech Science Foundation grant 19-03063S, by the Czech Ministry Of Education, Youth And Sports, Inter-Excellence LTA-USA, grant number 19032, by the Charles University In Prague, Cooperation Program MED ONCO 39, by the National Institutes of Health/National Cancer Institute grant, CA103314, and by the European Union–Next Generation EU, National Institute for Research of Metabolic and Cardiovascular Diseases (Programme EXCELES, ID Project No. LX22NPO5104). The APC was funded by the Charles University In Prague, Cooperation Program MED ONCO 39.

Institutional Review Board Statement: Procedures performed in the present study followed the 1964 Helsinki Declaration of the National Institute of Public Health in Prague, approved the study protocol (approval code no. 9799-4 (issued on 30 January 2008), 15-25618A (6 August 2014), and 17-28470A (22 June 2016)).

Informed Consent Statement: Informed consent was obtained from all subjects involved in the study.

Data Availability Statement: Not applicable.

Acknowledgments: The methylation array was performed at the Genomics Core Facility, Oslo University Hospital (http://oslo.genomics.no/).

Conflicts of Interest: The authors declare no conflict of interest.

Appendix A

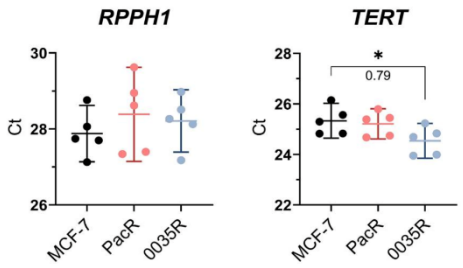

Figure A1. The DNA level of ribonuclease P RNA component H1 (*RPPH1*) and telomerase reverse transcriptase (*TERT*) plotted as Ct values (N = 5, 3 technical replicates). The mean and 95% CI are shown. The number below the zig–zag line represent DNA level difference between MCF-7 cells and 0035R cells. Statistical analysis was performed using the one-way ANOVA with Dunnett's post hoc correction test (*).

Genes **2023**, *14*, 296

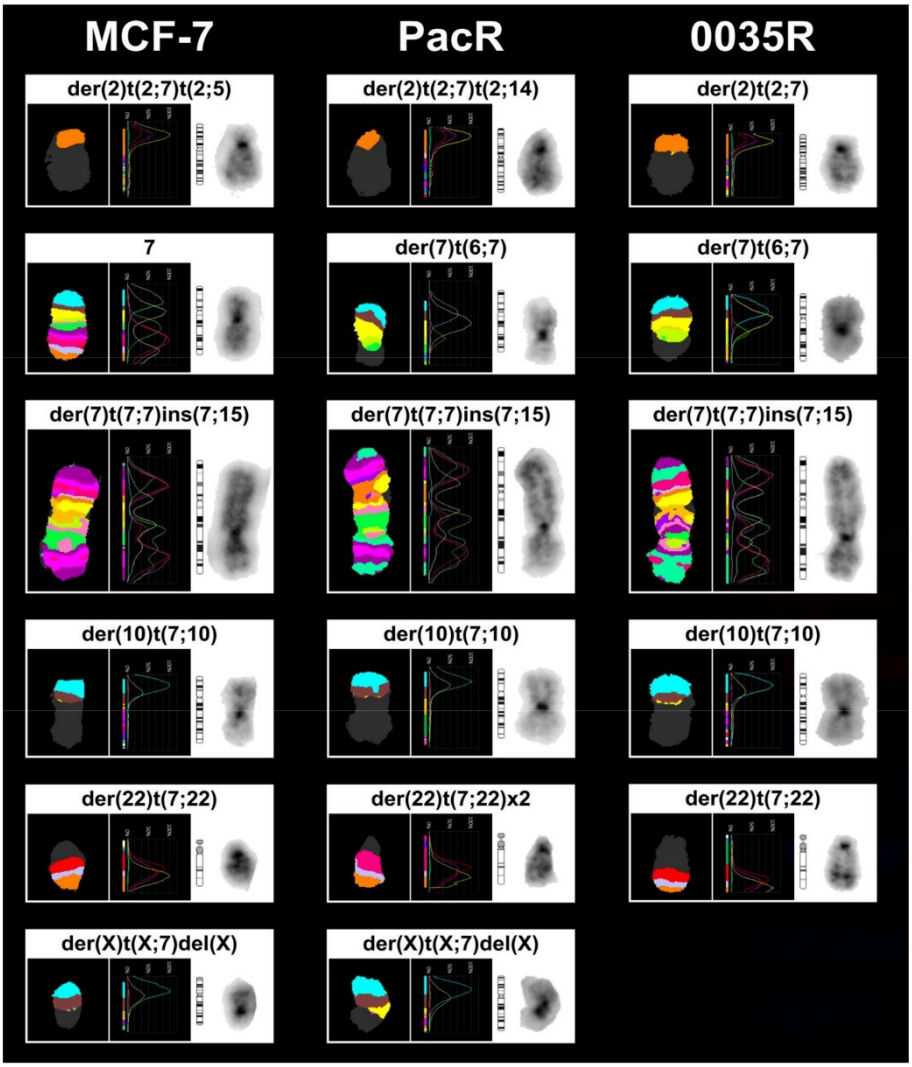

Figure A2. Multicolor fluorescence in situ hybridization (mFISH) of human chromosome 7. Displayed derivative chromosomes harboring chromosome 7 region that are present in parental taxane-sensitive MCF-7 cell line (MCF-7), paclitaxel-resistant MCF-7/PacR cell subline (PacR) and Stony Brook Taxane MCF-7/SB-T-0035R subline (0035R).

Genes **2023**, *14*, 296

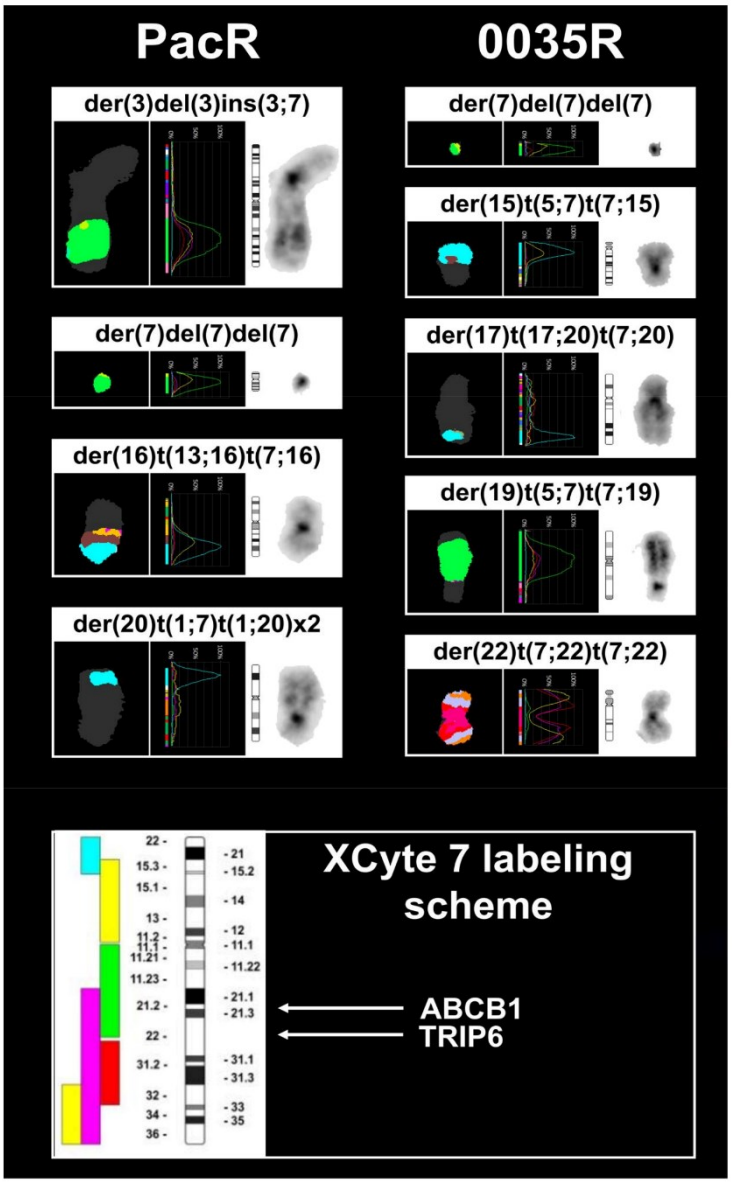

Figure A3. Multicolor fluorescence in situ hybridization (mFISH) of human chromosome 7. Displayed (**top**) novel derivative chromosomes harboring chromosome 7 region in paclitaxel-resistant MCF-7/PacR cell subline (PacR) and Stony Brook Taxane MCF-7/SB-T-0035R subline (0035R). Labeling scheme and position of the *ABCB1* and *TRIP6* genes in human chromosome 7 (**bottom**).

References

1. Yi, J.; Beckerle, M.C. The human TRIP6 gene encodes a LIM domain protein and maps to chromosome 7q22, a region associated with tumorigenesis. *Genomics* **1998**, *49*, 314–316. [CrossRef]
2. Wang, Y.; Gilmore, T.D. LIM domain protein Trip6 has a conserved nuclear export signal, nuclear targeting sequences, and multiple transactivation domains. *Biochim. Biophys. Acta* **2001**, *1538*, 260–272. [CrossRef] [PubMed]
3. Siddiqui, M.Q.; Badmalia, M.D.; Patel, T.R. Bioinformatic Analysis of Structure and Function of LIM Domains of Human Zyxin Family Proteins. *Int. J. Mol. Sci.* **2021**, *22*, 2647. [CrossRef] [PubMed]
4. Lin, V.T.; Lin, F.T. TRIP6: An adaptor protein that regulates cell motility, antiapoptotic signaling and transcriptional activity. *Cell Signal.* **2011**, *23*, 1691–1697. [CrossRef] [PubMed]
5. Xu, J.; Lai, Y.J.; Lin, W.C.; Lin, F.T. TRIP6 enhances lysophosphatidic acid-induced cell migration by interacting with the lysophosphatidic acid 2 receptor. *J. Biol. Chem.* **2004**, *279*, 10459–10468. [CrossRef] [PubMed]
6. Chastre, E.; Abdessamad, M.; Kruglov, A.; Bruyneel, E.; Bracke, M.; Di Gioia, Y.; Beckerle, M.C.; van Roy, F.; Kotelevets, L. TRIP6, a novel molecular partner of the MAGI-1 scaffolding molecule, promotes invasiveness. *FASEB J.* **2009**, *23*, 916–928. [CrossRef] [PubMed]
7. Dutta, S.; Mana-Capelli, S.; Paramasivam, M.; Dasgupta, I.; Cirka, H.; Billiar, K.; McCollum, D. TRIP6 inhibits Hippo signaling in response to tension at adherens junctions. *EMBO Rep.* **2018**, *19*, 337–350. [CrossRef] [PubMed]
8. Venkatramanan, S.; Ibar, C.; Irvine, K.D. TRIP6 is required for tension at adherens junctions. *J. Cell Sci.* **2021**, *134*, jcs247866. [CrossRef]
9. Kassel, O.; Schneider, S.; Heilbock, C.; Litfin, M.; Göttlicher, M.; Herrlich, P. A nuclear isoform of the focal adhesion LIM-domain protein Trip6 integrates activating and repressing signals at AP-1- and NF-kappaB-regulated promoters. *Genes Dev.* **2004**, *18*, 2518–2528. [CrossRef]
10. Kemler, D.; Dahley, O.; Roßwag, S.; Litfin, M.; Kassel, O. The LIM domain protein nTRIP6 acts as a co-repressor for the transcription factor MEF2C in myoblasts. *Sci. Rep.* **2016**, *6*, 27746. [CrossRef]
11. Abbariki, T.N.; Gonda, Z.; Kemler, D.; Urbanek, P.; Wagner, T.; Litfin, M.; Wang, Z.Q.; Herrlich, P.; Kassel, O. The LIM domain protein nTRIP6 modulates the dynamics of myogenic differentiation. *Sci. Rep.* **2021**, *11*, 12904. [CrossRef] [PubMed]
12. Shukla, S.; Haenold, R.; Urbánek, P.; Frappart, L.; Monajembashi, S.; Grigaravicius, P.; Nagel, S.; Min, W.K.; Tapias, A.; Kassel, O.; et al. TRIP6 functions in brain ciliogenesis. *Nat. Commun.* **2021**, *12*, 5887. [CrossRef] [PubMed]
13. Yi, J.; Kloeker, S.; Jensen, C.C.; Bockholt, S.; Honda, H.; Hirai, H.; Beckerle, M.C. Members of the Zyxin family of LIM proteins interact with members of the p130Cas family of signal transducers. *J. Biol. Chem.* **2002**, *277*, 9580–9589. [CrossRef]
14. Takizawa, N.; Smith, T.C.; Nebl, T.; Crowley, J.L.; Palmieri, S.J.; Lifshitz, L.M.; Ehrhardt, A.G.; Hoffman, L.M.; Beckerle, M.C.; Luna, E.J. Supervillin modulation of focal adhesions involving TRIP6/ZRP-1. *J. Cell Biol.* **2006**, *174*, 447–458. [CrossRef]
15. Lai, Y.J.; Lin, V.T.; Zheng, Y.; Benveniste, E.N.; Lin, F.T. The adaptor protein TRIP6 antagonizes Fas-induced apoptosis but promotes its effect on cell migration. *Mol. Cell. Biol.* **2010**, *30*, 5582–5596. [CrossRef] [PubMed]
16. Yang, Y.; Li, X.M.; Wang, J.R.; Li, Y.; Ye, W.L.; Wang, Y.; Liu, Y.X.; Deng, Z.Y.; Gan, W.J.; Wu, H. TRIP6 promotes inflammatory damage via the activation of TRAF6 signaling in a murine model of DSS-induced colitis. *J. Inflamm.* **2022**, *19*, 1. [CrossRef] [PubMed]
17. Sheppard, S.A.; Loayza, D. LIM-domain proteins TRIP6 and LPP associate with shelterin to mediate telomere protection. *Aging* **2010**, *2*, 432–444. [CrossRef] [PubMed]
18. Thul, P.J.; Åkesson, L.; Wiking, M.; Mahdessian, D.; Geladaki, A.; Blal, H.A.; Alm, T.; Asplund, A.; Björk, L.; Breckels, L.M.; et al. A subcellular map of the human proteome. *Science* **2017**, *356*, eaal3321. [CrossRef] [PubMed]
19. Gambardella, G.; Viscido, G.; Tumaini, B.; Isacchi, A.; Bosotti, R.; di Bernardo, D. A single-cell analysis of breast cancer cell lines to study tumour heterogeneity and drug response. *Nat. Commun.* **2022**, *13*, 1714. [CrossRef]
20. Zhao, X.; Jiang, C.; Xu, R.; Liu, Q.; Liu, G.; Zhang, Y. TRIP6 enhances stemness property of breast cancer cells through activation of Wnt/β-catenin. *Cancer Cell Int.* **2020**, *20*, 51. [CrossRef]
21. Wang, J.; Li, J.; Yang, J.; Zhang, L.; Gao, S.; Jiao, F.; Yi, M.; Xu, J. MicroRNA-138-5p regulates neural stem cell proliferation and differentiation in vitro by targeting TRIP6 expression. *Mol. Med. Rep.* **2017**, *16*, 7261–7266. [CrossRef] [PubMed]
22. Gu, J.; Shao, R.; Li, M.; Yan, Q.; Hu, H. MiR-485-3p modulates neural stem cell differentiation and proliferation via regulating TRIP6 expression. *J. Cell. Mol. Med.* **2020**, *24*, 398–404. [CrossRef] [PubMed]
23. Ling, Y.; Cao, C.; Li, S.; Qiu, M.; Shen, G.; Chen, Z.; Yao, F.; Chen, W. TRIP6, as a target of miR-7, regulates the proliferation and metastasis of colorectal cancer cells. *Biochem. Biophys. Res. Commun.* **2019**, *514*, 231–238. [CrossRef]
24. Gou, H.; Liang, J.Q.; Zhang, L.; Chen, H.; Zhang, Y.; Li, R.; Wang, X.; Ji, J.; Tong, J.H.; To, K.F.; et al. TTPAL Promotes Colorectal Tumorigenesis by Stabilizing TRIP6 to Activate Wnt/β-Catenin Signaling. *Cancer Res.* **2019**, *13*, 3332–3346. [CrossRef] [PubMed]
25. Sung, H.; Ferlay, J.; Siegel, R.L.; Laversanne, M.; Soerjomataram, I.; Jemal, A.; Bray, F. Global Cancer Statistics 2020: GLOBOCAN Estimates of Incidence and Mortality Worldwide for 36 Cancers in 185 Countries. *CA Cancer J. Clin.* **2021**, *71*, 209–249. [CrossRef] [PubMed]
26. Turner, K.M.; Yeo, S.K.; Holm, T.M.; Shaughnessy, E.; Guan, J.L. Heterogeneity within molecular subtypes of breast cancer. *Am. J. Physiol. Cell Physiol.* **2021**, *321*, C343–C354. [CrossRef]

27. Burstein, H.J.; Curigliano, G.; Thürlimann, B.; Weber, W.P.; Poortmans, P.; Regan, M.M.; Senn, H.J.; Winer, E.P.; Gnant, M.; Panelists of the St Gallen Consensus Conference. Customizing local and systemic therapies for women with early breast cancer: The St. Gallen International Consensus Guidelines for treatment of early breast cancer 2021. *Ann. Oncol.* **2021**, *32*, 1216–1235. [CrossRef]
28. Lashen, A.; Toss, M.S.; Fadhil, W.; Oni, G.; Madhusudan, S.; Rakha, E. Evaluation Oncotype DX® 21-Gene Recurrence Score and Clinicopathological Parameters: A single institutional experience. *Histopathology* 2023, *accepted*. [CrossRef]
29. Cancer Genome Atlas Network. Comprehensive molecular portraits of human breast tumours. *Nature* **2012**, *490*, 61–70. [CrossRef]
30. Pereira, B.; Chin, S.F.; Rueda, O.M.; Vollan, H.K.; Provenzano, E.; Bardwell, H.A.; Pugh, M.; Jones, L.; Russell, R.; Sammut, S.J.; et al. The somatic mutation profiles of 2,433 breast cancers refines their genomic and transcriptomic landscapes. *Nat. Commun.* **2016**, *7*, 11479. [CrossRef]
31. Ojima, I.; Fumero-Oderda, C.L.; Kuduk, S.D.; Ma, Z.; Kirikae, F.; Kirikae, T. Structure-activity relationship study of taxoids for their ability to activate murine macrophages as well as inhibit the growth of macrophage-like cells. *Bioorg. Med. Chem.* **2003**, *11*, 2867–2888. [CrossRef]
32. Calcagno, A.M.; Ambudkar, S.V. Molecular mechanisms of drug resistance in single-step and multi-step drug-selected cancer cells. *Methods Mol. Biol.* **2010**, *596*, 77–93. [CrossRef] [PubMed]
33. Němcová-Fürstová, V.; Kopperová, D.; Balušíková, K.; Ehrlichová, M.; Brynychová, V.; Václavíková, R.; Daniel, P.; Souček, P.; Kovář, J. Characterization of acquired paclitaxel resistance of breast cancer cells and involvement of ABC transporters. *Toxicol. Appl. Pharmacol.* **2016**, *310*, 215–228. [CrossRef] [PubMed]
34. Jelínek, M.; Balušíková, K.; Daniel, P.; Němcová-Fürstová, V.; Kirubakaran, P.; Jaček, M.; Wei, L.; Wang, X.; Vondrášek, J.; Ojima, I.; et al. Substituents at the C3′ and C3′N positions are critical for taxanes to overcome acquired resistance of cancer cells to paclitaxel. *Toxicol. Appl. Pharmacol.* **2018**, *347*, 79–91. [CrossRef] [PubMed]
35. Brynychová, V.; Hlaváč, V.; Ehrlichová, M.; Václavíková, R.; Pecha, V.; Trnková, M.; Wald, M.; Mrhalová, M.; Kubáčková, K.; Pikus, T.; et al. Importance of transcript levels of caspase-2 isoforms S and L for breast carcinoma progression. *Future Oncol.* **2013**, *9*, 427–438. [CrossRef]
36. Hubackova, M.; Vaclavikova, R.; Ehrlichova, M.; Mrhalova, M.; Kodet, R.; Kubackova, K.; Vrána, D.; Gut, I.; Soucek, P. Association of superoxide dismutases and NAD(P)H quinone oxidoreductases with prognosis of patients with breast carcinomas. *Int. J. Cancer* **2012**, *130*, 338–348. [CrossRef]
37. Tavassoli, F.A.; Devilee, P. International Agency for Research on Cancer; World Health Organization. In *Pathology and Genetics of Tumours of the Breast and Female Genital Organs*; IARC Press: Lyon, France, 2003; 432p.
38. Cheang, M.C.; Chia, S.K.; Voduc, D.; Gao, D.; Leung, S.; Snider, J.; Watson, M.; Davies, S.; Bernard, P.S.; Parker, J.S.; et al. Ki67 index, HER2 status, and prognosis of patients with luminal B breast cancer. *J. Natl. Cancer Inst.* **2009**, *101*, 736–750. [CrossRef]
39. Goldhirsch, A.; Winer, E.P.; Coates, A.S.; Gelber, R.D.; Piccart-Gebhart, M.; Thürlimann, B.; Senn, H.J.; Panel members. Personalizing the treatment of women with early breast cancer: Highlights of the St Gallen International Expert Consensus on the Primary Therapy of Early Breast Cancer 2013. *Ann. Oncol.* **2013**, *24*, 2206–2223. [CrossRef]
40. Bustin, S.A.; Benes, V.; Garson, J.A.; Hellemans, J.; Huggett, J.; Kubista, M.; Mueller, R.; Nolan, T.; Pfaffl, M.W.; Shipley, G.L.; et al. The MIQE guidelines: Minimum information for publication of quantitative real-time PCR experiments. *Clin. Chem.* **2009**, *55*, 611–622. [CrossRef]
41. Hlaváč, V.; Brynychová, V.; Václavíková, R.; Ehrlichová, M.; Vrána, D.; Pecha, V.; Koževnikovová, R.; Trnková, M.; Gatěk, J.; Kopperová, D.; et al. The expression profile of ATP-binding cassette transporter genes in breast carcinoma. *Pharmacogenomics* **2013**, *14*, 515–529. [CrossRef]
42. Elsnerova, K.; Mohelnikova-Duchonova, B.; Cerovska, E.; Ehrlichova, M.; Gut, I.; Rob, L.; Skapa, P.; Hruda, M.; Bartakova, A.; Bouda, J.; et al. Gene expression of membrane transporters: Importance for prognosis and progression of ovarian carcinoma. *Oncol. Rep.* **2016**, *35*, 2159–2170. [CrossRef]
43. Livak, K.J.; Schmittgen, T.D. Analysis of relative gene expression data using real-time quantitative PCR and the 2(-Delta Delta C(T)). *Methods* **2001**, *25*, 402–408. [CrossRef] [PubMed]
44. Daniel, P.; Halada, P.; Jelínek, M.; Balušíková, K.; Kovář, J. Differentially Expressed Mitochondrial Proteins in Human MCF7 Breast Cancer Cells Resistant to Paclitaxel. *Int. J. Mol. Sci.* **2019**, *20*, 2986. [CrossRef] [PubMed]
45. McGowan-Jordan, J.; Hastings, R.J.; Moore, S.; International Standing Committee on Human Cytogenomic nomenclature. *ISCN 2020: An International System for Human Cytogenomic Nomenclature*; Karger: Basel, Switzerland, 2020; 170p.
46. R Core Team. *R: A Language and Environment for Statistical Computing*; R Foundation for Statistical Computing: Vienna, Austria, 2020.
47. Touleimat, N.; Tost, J. Complete pipeline for Infinium® Human Methylation 450K BeadChip data processing using subset quantile normalization for accurate DNA methylation estimation. *Epigenomics* **2012**, *4*, 325–341. [CrossRef] [PubMed]
48. Fleischer, T.; Frigessi, A.; Johnson, K.C.; Edvardsen, H.; Touleimat, N.; Klajic, J.; Riis, M.L.; Haakensen, V.D.; Wärnberg, F.; Naume, B.; et al. Genome-wide DNA methylation profiles in progression to in situ and invasive carcinoma of the breast with impact on gene transcription and prognosis. *Genome Biol.* **2014**, *15*, 435. [CrossRef]
49. Fortin, J.P.; Triche, T.J., Jr.; Hansen, K.D. Preprocessing, normalization and integration of the Illumina HumanMethylationEPIC array with minfi. *Bioinformatics* **2017**, *33*, 558–560. [CrossRef]

50. Maksimovic, J.; Gordon, L.; Oshlack, A. SWAN: Subset-quantile within array normalization for illumina infinium HumanMethylation450 BeadChips. *Genome Biol.* **2012**, *13*, R44. [CrossRef]
51. Pidsley, R.; Zotenko, E.; Peters, T.J.; Lawrence, M.G.; Risbridger, G.P.; Molloy, P.; Van Djik, S.; Muhlhausler, B.; Stirzaker, C.; Clark, S.J. Critical evaluation of the Illumina MethylationEPIC BeadChip microarray for whole-genome DNA methylation profiling. *Genome Biol.* **2016**, *17*, 208. [CrossRef]
52. Kumaki, Y.; Oda, M.; Okano, M. QUMA: Quantification tool for methylation analysis. *Nucleic Acids Res.* **2008**, *36*, W170–W175. [CrossRef]
53. Weissgerber, T.L.; Milic, N.M.; Winham, S.J.; Garovic, V.D. Beyond bar and line graphs: Time for a new data presentation paradigm. *PLoS Biol.* **2015**, *13*, e1002128. [CrossRef]
54. Comşa, Ş.; Cîmpean, A.M.; Raica, M. The Story of MCF-7 Breast Cancer Cell Line: 40 years of Experience in Research. *Anticancer Res.* **2015**, *35*, 3147–3154.
55. Fornes, O.; Castro-Mondragon, J.A.; Khan, A.; van der Lee, R.; Zhang, X.; Richmond, P.A.; Modi, B.P.; Correard, S.; Gheorghe, M.; Baranašić, D.; et al. JASPAR 2020: Update of the open-access database of transcription factor binding profiles. *Nucleic Acids Res.* **2020**, *48*, D87–D92. [CrossRef]
56. Lutz, W.; Schwab, M. In vivo regulation of single copy and amplified N-myc in human neuroblastoma cells. *Oncogene* **1997**, *15*, 303–315. [CrossRef] [PubMed]
57. Ji, C.; Casinghino, S.; McCarthy, T.L.; Centrella, M. Multiple and essential Sp1 binding sites in the promoter for transforming growth factor-β type I receptor. *J. Biol. Chem.* **1997**, *272*, 21260–21267. [CrossRef] [PubMed]
58. Mar, J.H.; Ordahl, C.P. M-CAT binding factor, a novel trans-acting factor governing muscle-specific transcription. *Mol. Cell. Biol.* **1990**, *10*, 4271–4283. [CrossRef] [PubMed]
59. Iguchi-Ariga, S.M.; Schaffner, W. CpG methylation of the cAMP-responsive enhancer/promoter sequence TGACGTCA abolishes specific factor binding as well as transcriptional activation. *Genes Dev.* **1989**, *3*, 612–619. [CrossRef] [PubMed]
60. Zhao, M.K.; Wang, Y.; Murphy, K.; Yi, J.; Beckerle, M.C.; Gilmore, T.D. LIM domain-containing protein trip6 can act as a coactivator for the v-Rel transcription factor. *Gene Expr.* **1999**, *8*, 207–217. [PubMed]
61. Zhu, L.; Xu, X.; Tang, Y.; Zhu, X. TRIP6 functions as a potential oncogene and facilitated proliferation and metastasis of gastric cancer. *Biologics* **2019**, *13*, 101–110. [CrossRef] [PubMed]
62. Pavlíková, N.; Bartoňová, I.; Balušíková, K.; Kopperová, D.; Halada, P.; Kovář, J. Differentially expressed proteins in human MCF-7 breast cancer cells sensitive and resistant to paclitaxel. *Exp. Cell Res.* **2015**, *333*, 1–10. [CrossRef]
63. Wang, Y.; Dong, L.; Liu, Y. Targeting Thyroid Receptor Interacting Protein 6 by MicroRNA-589-5p Inhibits Cell Proliferation, Migration, and Invasion in Endometrial Carcinoma. *Cancer Biother. Radiopharm.* **2019**, *34*, 529–536. [CrossRef]
64. Heim, S.; Lage, H. Transcriptome analysis of different multidrug-resistant gastric carcinoma cells. *In Vivo* **2005**, *19*, 583–590.
65. Genovese, I.; Ilari, A.; Assaraf, Y.G.; Fazi, F.; Colotti, G. Not only P-glycoprotein: Amplification of the ABCB1-containing chromosome region 7q21 confers multidrug resistance upon cancer cells by coordinated overexpression of an assortment of resistance-related proteins. *Drug Resist. Updat.* **2017**, *32*, 23–46. [CrossRef] [PubMed]
66. Wang, Y.C.; Juric, D.; Francisco, B.; Yu, R.X.; Duran, G.E.; Chen, K.G.; Chen, X.; Sikic, B.I. Regional activation of chromosomal arm 7q with and without gene amplification in taxane-selected human ovarian cancer cell lines. *Genes Chromosom. Cancer* **2006**, *45*, 365–374. [CrossRef] [PubMed]
67. Lombard, A.P.; Lou, W.; Armstrong, C.M.; D'Abronzo, L.S.; Ning, S.; Evans, C.P.; Gao, A.C. Activation of the *ABCB1* Amplicon in Docetaxel- and Cabazitaxel-Resistant Prostate Cancer Cells. *Mol. Cancer. Ther.* **2021**, *20*, 2061–2070. [CrossRef] [PubMed]
68. Kumar, R.; Nagpal, G.; Kumar, V.; Usmani, S.S.; Agrawal, P.; Raghava, G.P.S. HumCFS: A database of fragile sites in human chromosomes. *BMC Genom.* **2019**, *19*, 985. [CrossRef] [PubMed]
69. Zhang, X.; Odom, D.T.; Koo, S.H.; Conkright, M.D.; Canettieri, G.; Best, J.; Chen, H.; Jenner, R.; Herbolsheimer, E.; Jacobsen, E.; et al. Genome-wide analysis of cAMP-response element binding protein occupancy, phosphorylation, and target gene activation in human tissues. *Proc. Natl. Acad. Sci. USA* **2005**, *102*, 4459–4464. [CrossRef]
70. Tinti, C.; Yang, C.; Seo, H.; Conti, B.; Kim, C.; Joh, T.M.; Kim, K.S. Structure/function relationship of the cAMP response element in tyrosine hydroxylase gene transcription. *J. Biol. Chem.* **1997**, *272*, 19158–19164. [CrossRef]
71. Seborova, K.; Kloudova-Spalenkova, A.; Koucka, K.; Holy, P.; Ehrlichova, M.; Wang, C.; Ojima, I.; Voleska, I.; Daniel, P.; Balusikova, K.; et al. The Role of TRIP6, ABCC3 and CPS1 Expression in Resistance of Ovarian Cancer to Taxanes. *Int. J. Mol. Sci.* **2021**, *23*, 73. [CrossRef]

5. UNPUBLISHED DATA

5.1 Proteomic analyses

In paper 3, we aimed to find differentially expressed mitochondrial protein in mitochondrial preparations from taxane-sensitive MCF-7 and paclitaxel-resistant MCF-7/PacR cells by 2-D PAGE. We concluded that QProteome Mitochondria Isolation Kit is eligible for this workflow when compared with KIT#1 based on evidence of mitochondrial fraction cross-contamination by specific antibodies to cytosolic, nuclear, mitochondrial and endoplasmic reticulum proteins (**chapter 3.5, page 87**).

To gain better insight into the quality of isolated fractions, we compared electrophoretic gels between mitochondrial fractions isolated by two commercially available kits. The scans looked quite different (**Figure 4.01**). For example, KIT#2 produced a mitochondrial fraction where most of the keratin 8/18 was depleted. Furthermore, enrichment for neutral to basic proteins in KIT#2 is evident.

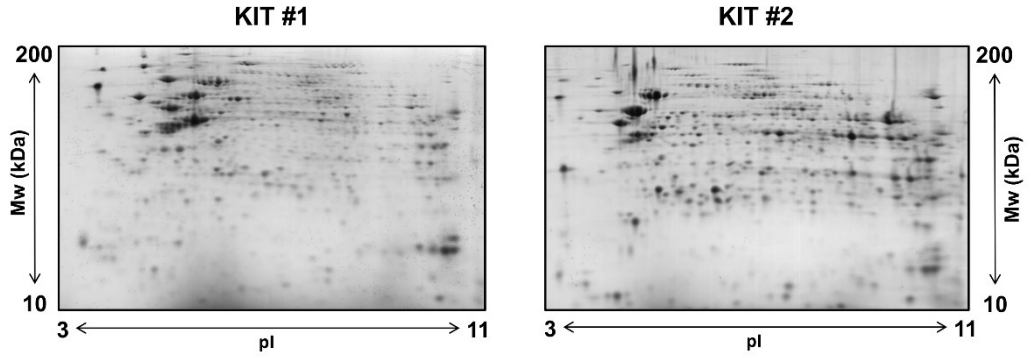

Figure 4.01 Representative 2-D PAGE of mitochondrial-enriched fraction from MCF-7 cells stained with coomassie brilliant blue. Two kits were compared (KIT#1, KIT#2). The most abundant spots obviously correspond to mitochondrial heat-shock proteins Hsp70 and Hsp90 as indicated by its molecular weight. KIT#2 – QProteome Mitochondria Isolation Kit.

Nevertheless, we found the array of spots corresponding to CPS1 (spot1) by comparing mitochondrial fractions we obtained by KIT#1. We were unable to clarify septin 2, septin 11 and peroxiredoxin 2 alterations by Western blot.

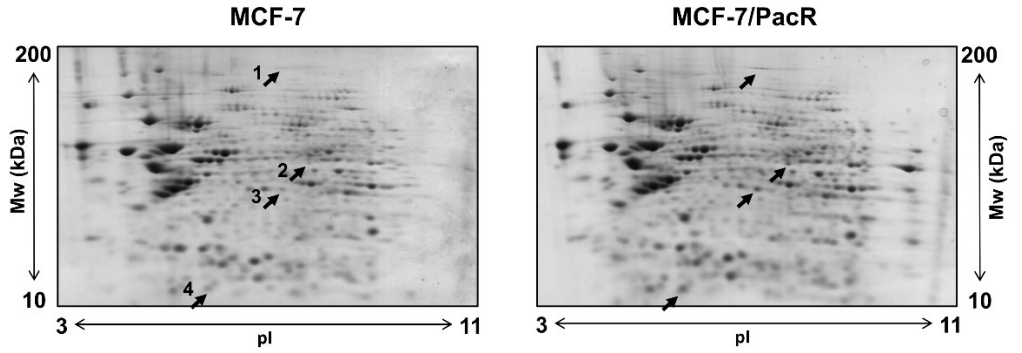

Figure 4.02 Representative 2-D PAGE of mitochondrial-enriched fraction (KIT#1) from MCF-7 cells and paclitaxel-resistant MCF-7/PacR cells. Altered spots are as follows: spot 1 – carbamoyl phosphate synthase 1 (*CPS1*), spot 2 – septin 11 (*SEPTIN11*), spot 3 – septin 2 (*SEPTIN2*), spot 4 – peroxiredoxin 2 (*PRDX2*).

We analyzed mitochondrial fractions isolated by QProteome Mitochondria Isolation Kit between MCF-7 cells and Stony Brook Taxane 0035-resistant MCF-7/0035R cells (**Figure 4.03**). The preliminary data showed a few suspect spots with two-fold difference in spot volume, including a putative ABHD11 spot no. 4. There was no change in CPS1 expression.

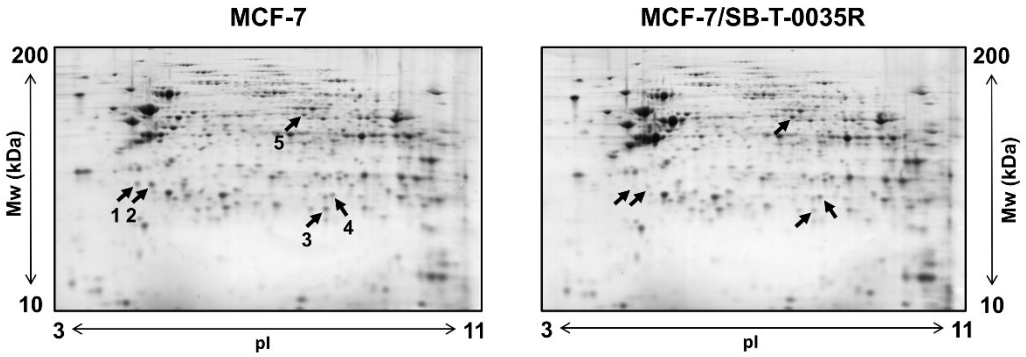

Figure 4.03 Representative 2-D PAGE of mitochondrial-enriched fraction (KIT#2) from MCF-7 cells and Stony Brook Taxane 0035-resistant MCF-7/SB-T-0035R cells. The spots with changed spot volume are depicted by arrows. Spot 1 and spot 2 is cathepsin D, spot 4 is abhydrolase domain containing 11. Spots 3 and spot 5 have not been analyzed by mass spektrometry.

5.2 ABHD11 expression in gynecological cancer

Assessment of ABHD11 expression by qPCR and Western blot confirmed 2-D PAGE data with mitochondrial-enriched fractions. In MCF-7/PacR cells, we found ABHD11 upregulation, whereas ABHD11 was downregulated in MCF-7/0035R cells. Such likely reflects alterations in ABHD11 copy number. This data also suggest that ABHD11 fluctations are tolerated in MCF-7 cells.

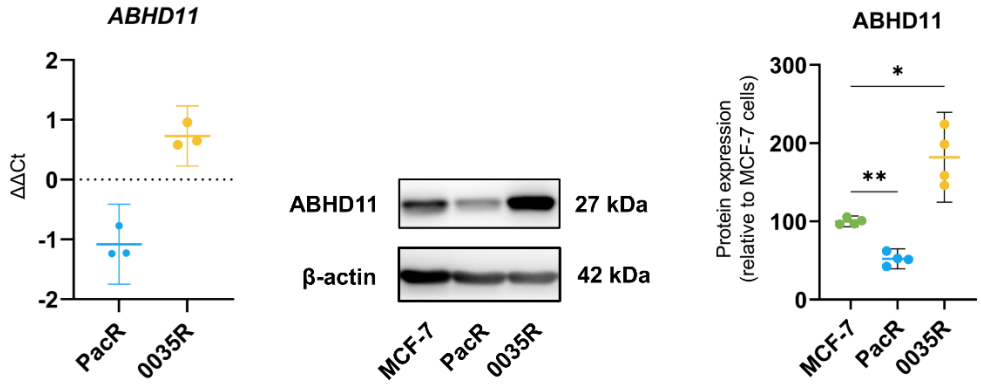

Figure 4.03 *ABHD11* is expressed concisely at mRNA and protein level in MCF-7/PacR cells and MCF-7/0035R subline. From left to right: scatter dot plot showing mRNA levels of ABHD11 in MCF-7/PacR and MCF-7/0035R cells (mean value and 95% CI is shown). The result is statistically significant since the.CI is not crossing the zero value representing ABHD11 mRNA level in MCF-7 cells. Representative western blot of ABHD11 expression. B-actin serves as a loading control and for data normalizati-on. Scatter dot plot on the right shows densitometric analysis results.

ABHD11 controls 2-oxoglutarate (2-OG) level in mitochondria by (**Bailey et al, 2020**). We compared ABHD11 expression between non-tumour and tumour ovarian tissues. As markedly seen in **Figure 4.04**, nearly all ovarian tumour specimens were positive for ABHD11, whereas non-tumour tissue were absent of ABHD11. The underlying mechanisms responsible for ABHD11 expression restricted to ovarian tumour tissue has not been investigated yet.

Analyses of *ABHD11* mRNA and protein expression in larger sample sets of ovarian non-tumour and tumour samples with defined mutation landscapes is needed.

Specific inhibitor, MLL-266, that covalently binds to ABHD11, should be screened *in vitro* and *in vivo* against patient-derived ovartian xenografts. is also available (**Bailey et al., 2020**).

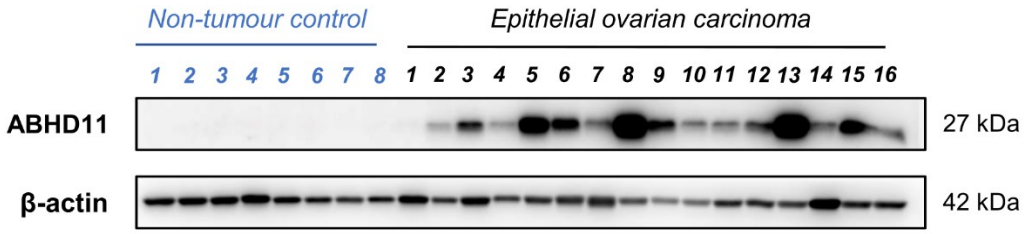

Figure 4.04 Expression of ABHD11 in ovarian carcinoma and non-tumour ovarian tissues. For comparison, β-actin expression is show

6. CONCLUSIONS

- Acquired resistance to paclitaxel and Stony Brook Taxane 0035 are mediated by ABCB1 transporter *in vitro* in MCF-7 cells and SK-BR-3 cells as documented by gene expresion analysis and function studies. Other ABC transporters such as ABCB4, ABCC2 and ABCC3 can potentially modulate resistance phenotype in these cells. Mitochondrial carbamoyl-phosphate synthase 1 (CPS1), overexpressed in MCF-7/PacR cells as a result of increased number of CPS1-positive cells, probably does not contribute to paclitaxel resistance.

- Amplification of the large segment adjacent to the *ABCB1* gene underpins ABCB1 and TRIP6 overexpression in taxane-resistant MCF-7 sublines. The amplicon was derived from the locus at intact chromosome 7. Furthermore, high TRIP6 expression in MCF-7 and taxane-resistant MCF-7 sublines is caused by combination of activity of single cyclic AMP response element in the hypomethylated TRIP6 proximal promoter.

- Taxane derivatives modified at the C3' and C3'N positions can overcome acquired resistance to paclitaxel and Stony Brook Taxane 0035 *in vitro*. Taxanes with two phenyl groups (paclitaxel, SB-T-0035, 10-deacetyl paclitaxel) are less potent in overcoming acquired resistance to paclitaxel in comparison to taxoids with one phenyl group (docetaxel, acetyl docetaxel). Taxoids SB-T-1216 and SB-T-1102 without phenyl groups at the C3 and C3'N positions are the most potent agents.

7. REFERENCES

Alam, A., Küng, R., Kowal, J., McLeod, R. A., Tremp, N., Broude, E. V., Roninson, I. B., Stahlberg, H., & Locher, K. P. (**2018**). Structure of a zosuquidar and UIC2-bound human-mouse chimeric ABCB1. *Proceedings of the National Academy of Sciences of the United States of America*, *115*(9), E1973–E1982. https://doi.org/10.1073/pnas.1717044115

Alam, A., Kowal, J., Broude, E., Roninson, I., & Locher, K. P. (**2019**). Structural insight into substrate and inhibitor discrimination by human P-glycoprotein. *Science (New York, N.Y.)*, *363*(6428), 753–756. https://doi.org/10.1126/science.aav7102

Aller, S. G., Yu, J., Ward, A., Weng, Y., Chittaboina, S., Zhuo, R., Harrell, P. M., Trinh, Y. T., Zhang, Q., Urbatsch, I. L., & Chang, G. (**2009**). Structure of P-glycoprotein reveals a molecular basis for poly-specific drug binding. *Science (New York, N.Y.)*, *323*(5922), 1718–1722. https://doi.org/10.1126/science.1168750

Amargant, F., Barragan, M., Vassena, R., & Vernos, I. (**2019**). Insights of the tubulin code in gametes and embryos: from basic research to potential clinical applications in humans†. *Biology of reproduction*, *100*(3), 575–589. https://doi.org/10.1093/biolre/ioy203

Andersen S. S. (**2000**). Spindle assembly and the art of regulating microtubule dynamics by MAPs and Stathmin/Op18. *Trends in cell biology*, *10*(7), 261–267. https://doi.org/10.1016/s0962-8924(00)01786-4

Badowska-Kozakiewicz, A. M., Sobol, M., & Patera, J. (**2017**). Expression of multidrug resistance protein P-glycoprotein in correlation with markers of hypoxia (HIF-1α, EPO, EPO-R) in invasive breast cancer with metastasis to lymph nodes. *Archives of medical science : AMS*, *13*(6), 1303–1314. https://doi.org/10.5114/aoms.2016.62723

Bailey, P. S. J., Ortmann, B. M., Martinelli, A. W., Houghton, J. W., Costa, A. S. H., Burr, S. P., Antrobus, R., Frezza, C., & Nathan, J. A. (**2020**). ABHD11 maintains 2-oxoglutarate metabolism by preserving functional lipoylation of the 2-oxoglutarate dehydrogenase complex. *Nature communications*, *11*(1), 4046. https://doi.org/10.1038/s41467-020-17862-6

Baselga, J., Tripathy, D., Mendelsohn, J., Baughman, S., Benz, C. C., Dantis, L., Sklarin, N. T., Seidman, A. D., Hudis, C. A., Moore, J., Rosen, P. P., Twaddell, T., Henderson, I. C., & Norton, L. (**1996**). Phase II study of weekly intravenous recombinant humanized anti-p185HER2 monoclonal antibody in patients with HER2/neu-overexpressing metastatic breast cancer. *Journal of clinical oncology : official journal of the American Society of Clinical Oncology*, *14*(3), 737–744. https://doi.org/10.1200/JCO.1996.14.3.737

Benes, P., Vetvicka, V., & Fusek, M. (**2008**). Cathepsin D--many functions of one aspartic protease. *Critical reviews in oncology/hematology*, *68*(1), 12–28. https://doi.org/10.1016/j.critrevonc.2008.02.008

Bowne-Anderson, H., Zanic, M., Kauer, M., & Howard, J. (**2013**). Microtubule dynamic instability: a new model with coupled GTP hydrolysis and multistep catastrophe. *BioEssays : news and reviews in molecular, cellular and developmental biology*, *35*(5), 452–461. https://doi.org/10.1002/bies.201200131

Budzik, M. P., Fudalej, M. M., & Badowska-Kozakiewicz, A. M. (**2021**). Histopathological analysis of mucinous breast cancer subtypes and comparison with invasive carcinoma of no special type. *Scientific reports*, *11*(1), 5770. https://doi.org/10.1038/s41598-021-85309-z

Burstein, H. J., Polyak, K., Wong, J. S., Lester, S. C., & Kaelin, C. M. (**2004**). Ductal carcinoma in situ of the breast. *The New England journal of medicine*, *350*(14), 1430–1441. https://doi.org/10.1056/NEJMra031301

Burstein, H. J., Curigliano, G., Loibl, S., Dubsky, P., Gnant, M., Poortmans, P., Colleoni, M., Denkert, C., Piccart-Gebhart, M., Regan, M., Senn, H. J., Winer, E. P., Thurlimann, B., & Members of the St. Gallen International Consensus Panel on the Primary Therapy of Early Breast Cancer 2019 (**2019**). Estimating the benefits of therapy for early-stage breast cancer: the St. Gallen International Consensus Guidelines for the primary therapy of early breast cancer 2019. *Annals of oncology : official journal of the European Society for Medical Oncology*, *30*(10), 1541–1557. https://doi.org/10.1093/annonc/mdz235

Burstein, H. J., Curigliano, G., Thürlimann, B., Weber, W. P., Poortmans, P., Regan, M. M., Senn, H. J., Winer, E. P., Gnant, M., & Panelists of the St Gallen Consensus Conference (**2021**). Customizing local and systemic therapies for women with early breast cancer: the St. Gallen International Consensus Guidelines for treatment of early breast cancer 2021. *Annals of oncology : official journal of the European Society for Medical Oncology*, *32*(10), 1216–1235. https://doi.org/10.1016/j.annonc.2021.06.023

Cancer Genome Atlas Network (**2012**). Comprehensive molecular portraits of human breast tumours. *Nature*, *490*(7418), 61–70. https://doi.org/10.1038/nature11412

Calcagno, A. M., & Ambudkar, S. V. (**2010**). Molecular mechanisms of drug resistance in single-step and multi-step drug-selected cancer cells. *Methods in molecular biology (Clifton, N.J.)*, *596*, 77–93. https://doi.org/10.1007/978-1-60761-416-6_5

Cardoso, F., Kyriakides, S., Ohno, S., Penault-Llorca, F., Poortmans, P., Rubio, I. T., Zackrisson, S., Senkus, E., & ESMO Guidelines Committee. Electronic address: clinicalguidelines@esmo.org (**2019**). Early breast cancer: ESMO Clinical Practice Guidelines for diagnosis, treatment and follow-up†. *Annals of oncology :*

official journal of the European Society for Medical Oncology, *30*(8), 1194–1220. https://doi.org/10.1093/annonc/mdz173

Ciriello, G., Gatza, M. L., Beck, A. H., Wilkerson, M. D., Rhie, S. K., Pastore, A., Zhang, H., McLellan, M., Yau, C., Kandoth, C., Bowlby, R., Shen, H., Hayat, S., Fieldhouse, R., Lester, S. C., Tse, G. M., Factor, R. E., Collins, L. C., Allison, K. H., Chen, Y. Y., … Perou, C. M. (**2015**). Comprehensive Molecular Portraits of Invasive Lobular Breast Cancer. *Cell*, *163*(2), 506–519. https://doi.org/10.1016/j.cell.2015.09.033

Colas, C., Ung, P. M., & Schlessinger, A. (**2016**). SLC Transporters: Structure, Function, and Drug Discovery. *MedChemComm*, *7*(6), 1069–1081. https://doi.org/10.1039/C6MD00005C

Curigliano, G., Burstein, H. J., Winer, E. P., Gnant, M., Dubsky, P., Loibl, S., Colleoni, M., Regan, M. M., Piccart-Gebhart, M., Senn, H. J., Thürlimann, B., St. Gallen International Expert Consensus on the Primary Therapy of Early Breast Cancer 2017, André, F., Baselga, J., Bergh, J., Bonnefoi, H., Brucker, S. Y., Cardoso, F., Carey, L., Ciruelos, E., … Xu, B. (**2017**). De-escalating and escalating treatments for early-stage breast cancer: the St. Gallen International Expert Consensus Conference on the Primary Therapy of Early Breast Cancer 2017. *Annals of oncology : official journal of the European Society for Medical Oncology*, *28*(8), 1700–1712. https://doi.org/10.1093/annonc/mdx308

Curtis, C., Shah, S. P., Chin, S. F., Turashvili, G., Rueda, O. M., Dunning, M. J., Speed, D., Lynch, A. G., Samarajiwa, S., Yuan, Y., Gräf, S., Ha, G., Haffari, G., Bashashati, A., Russell, R., McKinney, S., METABRIC Group, Langerød, A., Green, A., Provenzano, E., … Aparicio, S. (**2012**). The genomic and transcriptomic architecture of 2,000 breast tumours reveals novel subgroups. *Nature*, *486*(7403), 346–352. https://doi.org/10.1038/nature10983

Daniel, P., Halada, P., Jelínek, M., Balušíková, K., & Kovář, J. (**2019**). Differentially Expressed Mitochondrial Proteins in Human MCF7 Breast Cancer Cells Resistant to Paclitaxel. *International journal of molecular sciences*, *20*(12), 2986. https://doi.org/10.3390/ijms20122986

Daniel, P., Balušíková, K., Václavíková, R., Šeborová, K., Ransdorfová, Š., Valeriánová, M., Wei, L., Jelínek, M., Tlapáková, T., Fleischer, T., Kristensen, V. N., Souček, P., Ojima, I., & Kovář, J. (**2023**). *ABCB1* Amplicon Contains Cyclic AMP Response Element-Driven *TRIP6* Gene in Taxane-Resistant MCF-7 Breast Cancer Sublines. *Genes*, *14*(2), 296. https://doi.org/10.3390/genes14020296

Darshan, M. S., Loftus, M. S., Thadani-Mulero, M., Levy, B. P., Escuin, D., Zhou, X. K., Gjyrezi, A., Chanel-Vos, C., Shen, R., Tagawa, S. T., Bander, N. H., Nanus, D. M., & Giannakakou, P. (**2011**). Taxane-induced blockade to nuclear accumulation of the androgen receptor predicts clinical responses in metastatic prostate cancer. *Cancer research*, *71*(18), 6019–6029. https://doi.org/10.1158/0008-5472.CAN-11-1417

Delgado, J., Vleminckx, C., Sarac, S., Sosa, A., Bergh, J., Giuliani, R., Enzmann, H., & Pignatti, F. (**2021**). The EMA review of trastuzumab emtansine (T-DM1) for the adjuvant treatment of adult patients with HER2-positive early breast cancer. *ESMO open*, *6*(2), 100074. https://doi.org/10.1016/j.esmoop.2021.100074

de Cima, S., Polo, L. M., Díez-Fernández, C., Martínez, A. I., Cervera, J., Fita, I., & Rubio, V. (**2015**). Structure of human carbamoyl phosphate synthetase: deciphering the on/off switch of human ureagenesis. *Scientific reports*, *5*, 16950. https://doi.org/10.1038/srep16950

de Morrée, E. S., Böttcher, R., van Soest, R. J., Aghai, A., de Ridder, C. M., Gibson, A. A., Mathijssen, R. H., Burger, H., Wiemer, E. A., Sparreboom, A., de Wit, R., & van Weerden, W. M. (**2016**). Loss of SLCO1B3 drives taxane resistance in prostate cancer. *British journal of cancer*, *115*(6), 674–681. https://doi.org/10.1038/bjc.2016.251

Doyle, L. A., Yang, W., Abruzzo, L. V., Krogmann, T., Gao, Y., Rishi, A. K., & Ross, D. D. (**1998**). A multidrug resistance transporter from human MCF-7 breast cancer cells. *Proceedings of the National Academy of Sciences of the United States of America*, *95*(26), 15665–15670. https://doi.org/10.1073/pnas.95.26.15665

Duan, Z., Brakora, K. A., & Seiden, M. V. (**2004**). Inhibition of ABCB1 (MDR1) and ABCB4 (MDR3) expression by small interfering RNA and reversal of paclitaxel resistance in human ovarian cancer cells. *Molecular cancer therapeutics*, *3*(7), 833–838.

Duffy, S., Jackson, T. L., Lansdown, M., Philips, K., Wells, M., Pollard, S., Clack, G., Cuzick, J., Coibion, M., & Bianco, A. R. (**2003**). The ATAC adjuvant breast cancer trial in postmenopausal women: baseline endometrial subprotocol data. *BJOG : an international journal of obstetrics and gynaecology*, *110*(12), 1099–1106.

European Medicines Agency (**2023**, April 3). *Jevtana - European Medicines Agency*. European Medicines Agency. https://www.ema.europa.eu/en/medicines/human/EPAR/jevtana

Feng, L., & Mumper, R. J. (**2013**). A critical review of lipid-based nanoparticles for taxane delivery. *Cancer letters*, *334*(2), 157–175. https://doi.org/10.1016/j.canlet.2012.07.006

Fernie, A. R., Carrari, F., & Sweetlove, L. J. (**2004**). Respiratory metabolism: glycolysis, the TCA cycle and mitochondrial electron transport. *Current opinion in plant biology*, *7*(3), 254–261. https://doi.org/10.1016/j.pbi.2004.03.007

Gascoigne, K. E., & Taylor, S. S. (**2009**). How do anti-mitotic drugs kill cancer cells?. *Journal of cell science*, *122*(Pt 15), 2579–2585. https://doi.org/10.1242/jcs.039719

Gao, B., Russell, A., Beesley, J., Chen, X. Q., Healey, S., Henderson, M., Wong, M., Emmanuel, C., Galletta, L., Johnatty, S. E., Bowtell, D., Australian Ovarian Cancer Study Group, Haber, M., Norris, M., Harnett, P., Chenevix-Trench, G., Balleine, R. L., & deFazio, A. (**2014**). Paclitaxel sensitivity in relation to ABCB1 expression, efflux and single nucleotide polymorphisms in ovarian cancer. *Scientific reports*, *4*, 4669. https://doi.org/10.1038/srep04669

Girardi, E., César-Razquin, A., Lindinger, S., Papakostas, K., Konecka, J., Hemmerich, J., Kickinger, S., Kartnig, F., Gürtl, B., Klavins, K., Sedlyarov, V., Ingles-Prieto, A., Fiume, G., Koren, A., Lardeau, C. H., Kumaran Kandasamy, R., Kubicek, S., Ecker, G. F., & Superti-Furga, G. (**2020**). A widespread role for SLC transmembrane transporters in resistance to cytotoxic drugs. *Nature chemical biology*, *16*(4), 469–478. https://doi.org/10.1038/s41589-020-0483-3

Glick, J. H., Gelber, R. D., Goldhirsch, A., & Senn, H. J. (**1992**). Adjuvant therapy of primary breast cancer. 4th International Conference on Adjuvant Therapy of Primary Breast Cancer St. Gallen, Switzerland. *Annals of oncology : official journal of the European Society for Medical Oncology*, *3*(10), 801–807. https://doi.org/10.1093/oxfordjournals.annonc.a058099

Goldhirsch, A., Wood, W. C., Senn, H. J., Glick, J. H., & Gelber, R. D. (**1995**). Fifth International Conference on Adjuvant Therapy of Breast Cancer, St Gallen, March 1995. International Consensus Panel on the Treatment of Primary Breast Cancer. *European journal of cancer (Oxford, England : 1990)*, *31A*(11), 1754–1759. https://doi.org/10.1016/0959-8049(95)00479-3

Goldhirsch, A., Wood, W. C., Gelber, R. D., Coates, A. S., Thürlimann, B., & Senn, H. J. (**2003**). Meeting highlights: updated international expert consensus on the primary therapy of early breast cancer. *Journal of clinical oncology : official journal of the American Society of Clinical Oncology*, *21*(17), 3357–3365. https://doi.org/10.1200/JCO.2003.04.576

Goldhirsch, A., Ingle, J. N., Gelber, R. D., Coates, A. S., Thürlimann, B., Senn, H. J., & Panel members (**2009**). Thresholds for therapies: highlights of the St Gallen International Expert Consensus on the primary therapy of early breast cancer 2009. *Annals of oncology : official journal of the European Society for Medical Oncology*, *20*(8), 1319–1329. https://doi.org/10.1093/annonc/mdp322

Goldhirsch, A., Wood, W. C., Coates, A. S., Gelber, R. D., Thürlimann, B., Senn, H. J., & Panel members (**2011**). Strategies for subtypes--dealing with the diversity of breast cancer: highlights of the St. Gallen International Expert Consensus on the Primary Therapy of Early Breast Cancer 2011. *Annals of oncology : official journal of the European Society for Medical Oncology*, *22*(8), 1736–1747. https://doi.org/10.1093/annonc/mdr304

Gottesman, M. M., Cardarelli, C., Goldenberg, S., Licht, T., & Pastan, I. (**1998**). Selection and maintenance of multidrug-resistant cells. *Methods in enzymology*, *292*, 248–258. https://doi.org/10.1016/s0076-6879(98)92019-5

Gou, H., Liang, J. Q., Zhang, L., Chen, H., Zhang, Y., Li, R., Wang, X., Ji, J., Tong, J. H., To, K. F., Sung, J. J. Y., Chan, F. K. L., Fang, J. Y., & Yu, J. (**2019**). TTPAL Promotes Colorectal Tumorigenesis by Stabilizing TRIP6 to Activate Wnt/β-Catenin Signaling. *Cancer research*, *79*(13), 3332–3346. https://doi.org/10.1158/0008-5472.CAN-18-2986

Groen, A., Romero, M. R., Kunne, C., Hoosdally, S. J., Dixon, P. H., Wooding, C., Williamson, C., Seppen, J., Van den Oever, K., Mok, K. S., Paulusma, C. C., Linton, K. J., & Oude Elferink, R. P. (**2011**). Complementary functions of the flippase ATP8B1 and the floppase ABCB4 in maintaining canalicular membrane integrity. *Gastroenterology*, *141*(5), 1927–37.e374. https://doi.org/10.1053/j.gastro.2011.07.042

Guénard, D., Guéritte-Voegelein, F., Dubois, J., & Potier, P. (**1993**). Structure-activity relationships of Taxol and Taxotere analogues. *Journal of the National Cancer Institute. Monographs*, (15), 79–82.

Gudimchuk, N. B., & McIntosh, J. R. (**2021**). Regulation of microtubule dynamics, mechanics and function through the growing tip. *Nature reviews. Molecular cell biology*, *22*(12), 777–795. https://doi.org/10.1038/s41580-021-00399-x

Guna, A., Stevens, T. A., Inglis, A. J., Replogle, J. M., Esantsi, T. K., Muthukumar, G., Shaffer, K. C. L., Wang, M. L., Pogson, A. N., Jones, J. J., Lomenick, B., Chou, T. F., Weissman, J. S., & Voorhees, R. M. (**2022**). MTCH2 is a mitochondrial outer membrane protein insertase. *Science (New York, N.Y.)*, *378*(6617), 317–322. https://doi.org/10.1126/science.add1856

Gupta, M. L., Jr, Bode, C. J., Georg, G. I., & Himes, R. H. (**2003**). Understanding tubulin-Taxol interactions: mutations that impart Taxol binding to yeast tubulin. *Proceedings of the National Academy of Sciences of the United States of America*, *100*(11), 6394–6397. https://doi.org/10.1073/pnas.1131967100

Han, E. K., Gehrke, L., Tahir, S. K., Credo, R. B., Cherian, S. P., Sham, H., Rosenberg, S. H., & Ng, S. (**2000**). Modulation of drug resistance by alpha-tubulin in paclitaxel-resistant human lung cancer cell lines. *European journal of cancer (Oxford, England : 1990)*, *36*(12), 1565–1571. https://doi.org/10.1016/s0959-8049(00)00145-3

Han, M., Salamat, A., Zhu, L., Zhang, H., Clark, B. Z., Dabbs, D. J., Carter, G. J., Brufsky, A. M., Jankowitz, R. C., Puhalla, S. L., Johnson, R. R., Soran, A., Steiman, J. G., McAuliffe, P. F., Diego, E. J., & Bhargava, R. (**2019**). Metaplastic breast carcinoma: a clinical-pathologic study of 97 cases with subset analysis of response to neoadjuvant chemotherapy. *Modern pathology : an official journal of the United States and Canadian Academy of Pathology, Inc*, *32*(6), 807–816. https://doi.org/10.1038/s41379-019-0208-x

Harbeck, N., Penault-Llorca, F., Cortes, J., Gnant, M., Houssami, N., Poortmans, P., Ruddy, K., Tsang, J., & Cardoso, F. (**2019**). Breast cancer. *Nature reviews. Disease primers*, *5*(1), 66. https://doi.org/10.1038/s41572-019-0111-2

Hari, M., Loganzo, F., Annable, T., Tan, X., Musto, S., Morilla, D. B., Nettles, J. H., Snyder, J. P., & Greenberger, L. M. (**2006**). Paclitaxel-resistant cells have a mutation in the paclitaxel-binding region of beta-tubulin (Asp26Glu) and less stable microtubules. *Molecular cancer therapeutics*, *5*(2), 270–278. https://doi.org/10.1158/1535-7163.MCT-05-0190

Hassiotou, F., & Geddes, D. (**2013**). Anatomy of the human mammary gland: Current status of knowledge. *Clinical anatomy (New York, N.Y.)*, *26*(1), 29–48. https://doi.org/10.1002/ca.22165

Hodge, M., Chen, Q. H., Bane, S., Sharma, S., Loew, M., Banerjee, A., Alcaraz, A. A., Snyder, J. P., & Kingston, D. G. (**2009**). Synthesis and bioactivity of a side chain bridged paclitaxel: A test of the T-Taxol conformation. *Bioorganic & medicinal chemistry letters*, *19*(10), 2884–2887. https://doi.org/10.1016/j.bmcl.2009.03.063

Horwitz S. B. (**1992**). Mechanism of action of taxol. *Trends in pharmacological sciences*, *13*(4), 134–136. https://doi.org/10.1016/0165-6147(92)90048-b

Huisman, M. T., Chhatta, A. A., van Tellingen, O., Beijnen, J. H., & Schinkel, A. H. (**2005**). MRP2 (ABCC2) transports taxanes and confers paclitaxel resistance and both processes are stimulated by probenecid. *International journal of cancer*, *116*(5), 824–829. https://doi.org/10.1002/ijc.21013

Ishii, K., Morii, N., & Yamashiro, H. (**2019**). Pertuzumab in the treatment of HER2-positive breast cancer: an evidence-based review of its safety, efficacy, and place in therapy. *Core evidence*, *14*, 51–70. https://doi.org/10.2147/CE.S217848

Issaq, H., & Veenstra, T. (**2008**). Two-dimensional polyacrylamide gel electrophoresis (2D-PAGE): advances and perspectives. *BioTechniques*, *44*(5), 697–700. https://doi.org/10.2144/000112823

Jänicke, R. U., Sprengart, M. L., Wati, M. R., & Porter, A. G. (**1998**). Caspase-3 is required for DNA fragmentation and morphological changes associated with apoptosis. *The Journal of biological chemistry*, *273*(16), 9357–9360. https://doi.org/10.1074/jbc.273.16.9357

Jänicke R. U. (**2009**). MCF-7 breast carcinoma cells do not express caspase-3. *Breast cancer research and treatment*, *117*(1), 219–221. https://doi.org/10.1007/s10549-008-0217-9

Jelínek, M., Balušíková, K., Kopperová, D., Němcová-Fürstová, V., Šrámek, J., Fidlerová, J., Zanardi, I., Ojima, I., & Kovář, J. (**2013**). Caspase-2 is involved in cell death induction by taxanes in breast cancer cells. *Cancer cell international*, *13*(1), 42. https://doi.org/10.1186/1475-2867-13-42

Jelínek, M., Balušíková, K., Schmiedlová, M., Němcová-Fürstová, V., Šrámek, J., Stančíková, J., Zanardi, I., Ojima, I., & Kovář, J. (**2015**). The role of individual

caspases in cell death induction by taxanes in breast cancer cells. *Cancer cell international*, *15*(1), 8. https://doi.org/10.1186/s12935-015-0155-7

Jelínek, M., Balušíková, K., Daniel, P., Němcová-Fürstová, V., Kirubakaran, P., Jaček, M., Wei, L., Wang, X., Vondrášek, J., Ojima, I., & Kovář, J. (**2018**). Substituents at the C3' and C3'N positions are critical for taxanes to overcome acquired resistance of cancer cells to paclitaxel. *Toxicology and applied pharmacology*, *347*, 79–91. https://doi.org/10.1016/j.taap.2018.04.002

Jordan, M. A., Toso, R. J., Thrower, D., & Wilson, L. (**1993**). Mechanism of mitotic block and inhibition of cell proliferation by taxol at low concentrations. *Proceedings of the National Academy of Sciences of the United States of America*, *90*(20), 9552–9556. https://doi.org/10.1073/pnas.90.20.9552

Kaur, J., & Bachhawat, A. K. (**2009**). A modified Western blot protocol for enhanced sensitivity in the detection of a membrane protein. *Analytical biochemistry*, *384*(2), 348–349. https://doi.org/10.1016/j.ab.2008.10.005

Kavallaris, M., Kuo, D. Y., Burkhart, C. A., Regl, D. L., Norris, M. D., Haber, M., & Horwitz, S. B. (**1997**). Taxol-resistant epithelial ovarian tumors are associated with altered expression of specific beta-tubulin isotypes. *The Journal of clinical investigation*, *100*(5), 1282–1293. https://doi.org/10.1172/JCI119642

Kavallaris M. (**2010**). Microtubules and resistance to tubulin-binding agents. *Nature reviews. Cancer*, *10*(3), 194–204. https://doi.org/10.1038/nrc2803

Kim, S. E., Park, J. H., Hong, S., Koo, J. S., Jeong, J., & Jung, W. H. (**2012**). Primary Mucinous Cystadenocarcinoma of the Breast: Cytologic Finding and Expression of MUC5 Are Different from Mucinous Carcinoma. *Korean journal of pathology*, *46*(6), 611–616. https://doi.org/10.4132/KoreanJPathol.2012.46.6.611

Kim, T. H., Park, H. J., & Choi, J. H. (**2013**). Functional Characterization of ABCB4 Mutations Found in Low Phospholipid-Associated Cholelithiasis (LPAC). *The Korean journal of physiology & pharmacology : official journal of the Korean Physiological Society and the Korean Society of Pharmacology*, *17*(6), 525–530. https://doi.org/10.4196/kjpp.2013.17.6.525

Kim, J., Hu, Z., Cai, L., Li, K., Choi, E., Faubert, B., Bezwada, D., Rodriguez-Canales, J., Villalobos, P., Lin, Y. F., Ni, M., Huffman, K. E., Girard, L., Byers, L. A., Unsal-Kacmaz, K., Peña, C. G., Heymach, J. V., Wauters, E., Vansteenkiste, J., Castrillon, D. H., … DeBerardinis, R. J. (**2017**). CPS1 maintains pyrimidine pools and DNA synthesis in KRAS/LKB1-mutant lung cancer cells. *Nature*, *546*(7656), 168–172. https://doi.org/10.1038/nature22359

Kim, M., Kim, H. J., Chung, Y. R., Kang, E., Kim, E. K., Kim, S. H., Kim, Y. J., Kim, J. H., Kim, I. A., & Park, S. Y. (**2018**). Microinvasive Carcinoma versus Ductal Carcinoma *In Situ*: A Comparison of Clinicopathological Features and Clinical Outcomes. *Journal of breast cancer*, *21*(2), 197–205. https://doi.org/10.4048/jbc.2018.21.2.197

Knauer, M., Mook, S., Rutgers, E. J., Bender, R. A., Hauptmann, M., van de Vijver, M. J., Koornstra, R. H., Bueno-de-Mesquita, J. M., Linn, S. C., & van 't Veer, L. J. (**2010**). The predictive value of the 70-gene signature for adjuvant chemotherapy in early breast cancer. *Breast cancer research and treatment*, *120*(3), 655–661. https://doi.org/10.1007/s10549-010-0814-2

Krejčí, D., Pehalová, L., Talábová, A., Pokorová, K., Katinová, I., Mužík, J., Dušek, L. (**2018**). Současné epidemiologické trendy novotvarů v České republice. ÚZIS. Novotvary 2018: 227. https://www.uzis.cz/res/f/008352/novotvary2018.pdf

Lange, B. M., & Conner, C. F. (**2021**). Taxanes and taxoids of the genus Taxus - A comprehensive inventory of chemical diversity. *Phytochemistry*, *190*, 112829. https://doi.org/10.1016/j.phytochem.2021.112829

Lehmann, B. D., Bauer, J. A., Chen, X., Sanders, M. E., Chakravarthy, A. B., Shyr, Y., & Pietenpol, J. A. (**2011**). Identification of human triple-negative breast cancer subtypes and preclinical models for selection of targeted therapies. *The Journal of clinical investigation*, *121*(7), 2750–2767. https://doi.org/10.1172/JCI45014

Lehmann, B. D., Jovanović, B., Chen, X., Estrada, M. V., Johnson, K. N., Shyr, Y., Moses, H. L., Sanders, M. E., & Pietenpol, J. A. (**2016**). Refinement of Triple-Negative Breast Cancer Molecular Subtypes: Implications for Neoadjuvant Chemotherapy Selection. *PloS one*, *11*(6), e0157368. https://doi.org/10.1371/journal.pone.0157368

Li, J., Jaimes, K. F., & Aller, S. G. (**2014**). Refined structures of mouse P-glycoprotein. *Protein science : a publication of the Protein Society*, *23*(1), 34–46. https://doi.org/10.1002/pro.2387

Li, G., Li, D., Wang, T., & He, S. (**2021**). Pyrimidine Biosynthetic Enzyme CAD: Its Function, Regulation, and Diagnostic Potential. *International journal of molecular sciences*, *22*(19), 10253. https://doi.org/10.3390/ijms221910253

Lindström, L. S., Karlsson, E., Wilking, U. M., Johansson, U., Hartman, J., Lidbrink, E. K., Hatschek, T., Skoog, L., & Bergh, J. (**2012**). Clinically used breast cancer markers such as estrogen receptor, progesterone receptor, and human epidermal growth factor receptor 2 are unstable throughout tumor progression. *Journal of clinical oncology: official journal of the American Society of Clinical Oncology*, *30*(21), 2601–2608. https://doi.org/10.1200/JCO.2011.37.2482

Lips, E. H., Kumar, T., Megalios, A., Visser, L. L., Sheinman, M., Fortunato, A., Shah, V., Hoogstraat, M., Sei, E., Mallo, D., Roman-Escorza, M., Ahmed, A. A., Xu, M., van den Belt-Dusebout, A. W., Brugman, W., Casasent, A. K., Clements, K., Davies, H. R., Fu, L., Grigoriadis, A., … Sawyer, E. J. (**2022**). Genomic analysis defines clonal relationships of ductal carcinoma in situ and recurrent invasive breast cancer. *Nature genetics*, *54*(6), 850–860. https://doi.org/10.1038/s41588-022-01082-3

Liscovitch, M., & Ravid, D. (**2007**). A case study in misidentification of cancer cell lines: MCF-7/AdrR cells (re-designated NCI/ADR-RES) are derived from OVCAR-8 human ovarian carcinoma cells. *Cancer letters*, *245*(1-2), 350–352. https://doi.org/10.1016/j.canlet.2006.01.013

Löwe, J., Li, H., Downing, K. H., & Nogales, E. (**2001**). Refined structure of alpha beta-tubulin at 3.5 A resolution. *Journal of molecular biology*, *313*(5), 1045–1057. https://doi.org/10.1006/jmbi.2001.5077

Lüönd, F., Tiede, S., & Christofori, G. (**2021**). Breast cancer as an example of tumour heterogeneity and tumour cell plasticity during malignant progression. *British journal of cancer*, *125*(2), 164–175. https://doi.org/10.1038/s41416-021-01328-7

Maheshwari, P., Garg, S., Kumar, A. (**2008**). Taxoids: Biosynthesis and *in vitro* production. *Biotechnology and Molecular Biology Reviews, 3* (4): 071-087.

Maloney, S. M., Hoover, C. A., Morejon-Lasso, L. V., & Prosperi, J. R. (**2020**). Mechanisms of Taxane Resistance. *Cancers*, *12*(11), 3323. https://doi.org/10.3390/cancers12113323

Martin M. (**2006**). Docetaxel, doxorubicin and cyclophosphamide (the TAC regimen): an effective adjuvant treatment for operable breast cancer. *Women's health (London, England)*, *2*(4), 527–537. https://doi.org/10.2217/17455057.2.4.527

Matsuo, H., Takada, T., Ichida, K., Nakamura, T., Nakayama, A., Ikebuchi, Y., Ito, K., Kusanagi, Y., Chiba, T., Tadokoro, S., Takada, Y., Oikawa, Y., Inoue, H., Suzuki, K., Okada, R., Nishiyama, J., Domoto, H., Watanabe, S., Fujita, M., Morimoto, Y., … Shinomiya, N. (**2009**). Common defects of ABCG2, a high-capacity urate exporter, cause gout: a function-based genetic analysis in a Japanese population. *Science translational medicine*, *1*(5), 5ra11. https://doi.org/10.1126/scitranslmed.3000237

McCart Reed, A. E., Kutasovic, J. R., Lakhani, S. R., & Simpson, P. T. (**2015**). Invasive lobular carcinoma of the breast: morphology, biomarkers and 'omics. *Breast cancer research : BCR*, *17*(1), 12. https://doi.org/10.1186/s13058-015-0519-x

McClintock B. (**1941**). The Stability of Broken Ends of Chromosomes in Zea Mays. *Genetics*, *26*(2), 234–282. https://doi.org/10.1093/genetics/26.2.234

McCorkle, J. R., Gorski, J. W., Liu, J., Riggs, M. B., McDowell, A. B., Lin, N., Wang, C., Ueland, F. R., & Kolesar, J. M. (**2021**). Lapatinib and poziotinib overcome ABCB1-mediated paclitaxel resistance in ovarian cancer. *PloS one*, *16*(8), e0254205. https://doi.org/10.1371/journal.pone.0254205

McGrogan, B. T., Gilmartin, B., Carney, D. N., & McCann, A. (**2008**). Taxanes, microtubules and chemoresistant breast cancer. *Biochimica et biophysica acta*, *1785*(2), 96–132. https://doi.org/10.1016/j.bbcan.2007.10.004

Metovic, J., Bragoni, A., Osella-Abate, S., Borella, F., Benedetto, C., Gualano, M. R., Olivero, E., Scaioli, G., Siliquini, R., Ferrando, P. M., Bertero, L., Sapino, A., Cassoni, P., & Castellano, I. (**2021**). Clinical Relevance of Tubular Breast Carcinoma: Large Retrospective Study and Meta-Analysis. *Frontiers in oncology*, *11*, 653388. https://doi.org/10.3389/fonc.2021.653388

Mitchison, T., & Kirschner, M. (**1984**). Microtubule assembly nucleated by isolated centrosomes. *Nature*, *312*(5991), 232–237. https://doi.org/10.1038/312232a0

Mo, C. H., Ackbarkhan, Z., Gu, Y. Y., Chen, G., Pang, Y. Y., Dang, Y. W., & Feng, Z. B. (**2017**). Invasive cribriform carcinoma of the breast: a clinicopathological analysis of 12 cases with review of literature. *International journal of clinical and experimental pathology*, *10*(9), 9917–9924.

Němcová-Fürstová, V., Kopperová, D., Balušíková, K., Ehrlichová, M., Brynychová, V., Václavíková, R., Daniel, P., Souček, P., & Kovář, J. (**2016**). Characterization of acquired paclitaxel resistance of breast cancer cells and involvement of ABC transporters. *Toxicology and applied pharmacology*, *310*, 215–228. https://doi.org/10.1016/j.taap.2016.09.020

Nies, A. T., & Keppler, D. (**2007**). The apical conjugate efflux pump ABCC2 (MRP2). *Pflugers Archiv : European journal of physiology*, *453*(5), 643–659. https://doi.org/10.1007/s00424-006-0109-y

Njiaju, U. O., Gamazon, E. R., Gorsic, L. K., Delaney, S. M., Wheeler, H. E., Im, H. K., & Dolan, M. E. (**2012**). Whole-genome studies identify solute carrier transporters in cellular susceptibility to paclitaxel. *Pharmacogenetics and genomics*, *22*(7), 498–507. https://doi.org/10.1097/FPC.0b013e328352f436

Nogales, E., & Zhang, R. (**2016**). Visualizing microtubule structural transitions and interactions with associated proteins. *Current opinion in structural biology*, *37*, 90–96. https://doi.org/10.1016/j.sbi.2015.12.009

Nosol, K., Romane, K., Irobalieva, R. N., Alam, A., Kowal, J., Fujita, N., & Locher, K. P. (**2020**). Cryo-EM structures reveal distinct mechanisms of inhibition of the human multidrug transporter ABCB1. *Proceedings of the National Academy of Sciences of the United States of America*, *117*(42), 26245–26253. https://doi.org/10.1073/pnas.2010264117

O'Brien, C., Cavet, G., Pandita, A., Hu, X., Haydu, L., Mohan, S., Toy, K., Rivers, C. S., Modrusan, Z., Amler, L. C., & Lackner, M. R. (**2008**). Functional genomics identifies ABCC3 as a mediator of taxane resistance in HER2-amplified breast cancer. *Cancer research*, *68*(13), 5380–5389. https://doi.org/10.1158/0008-5472.CAN-08-0234

Ojima, I., Habus, I., Zhao, M., Zucco, M., Park, Y. H., Sun, C.M., Brigaud, T. (**1992**). New and efficient approaches to the semisynthesis of taxol and its C-13 side chain analogs by means of β-lactam synthon method, *Tetrahedron, 48*(34), 6985-7012. https://doi.org/10.1016/S0040-4020(01)91210-4

Ojima, I., Duclos, O., Kuduk, S.D., Sun, C.M., Slater, J.C., Lavelle, F., Veith, J.M., Bernacki, R.J. (**1994a**). Synthesis and biological activity of 3′-alkyl- and 3′-alkenyl-3′-dephenyldocetaxels. *Bioorganic & Medicinal Chemistry Letters, 4*(21), 2631-2634. https://doi.org/10.1016/S0960-894X(01)80298-5.

Ojima, I., Duclos, O., Zucco, M., Bissery, M. C., Combeau, C., Vrignaud, P., Riou, J. F., & Lavelle, F. (**1994b**). Synthesis and structure-activity relationships of new antitumor taxoids. Effects of cyclohexyl substitution at the C-3' and/or C-2 of taxotere (docetaxel). *Journal of medicinal chemistry*, *37*(16), 2602–2608. https://doi.org/10.1021/jm00042a013

Ojima, I., Slater, J. C., Michaud, E., Kuduk, S. D., Bounaud, P. Y., Vrignaud, P., Bissery, M. C., Veith, J. M., Pera, P., & Bernacki, R. J. (**1996**). Syntheses and structure-activity relationships of the second-generation antitumor taxoids: exceptional activity against drug-resistant cancer cells. *Journal of medicinal chemistry*, *39*(20), 3889–3896. https://doi.org/10.1021/jm9604080

Ojima, I., Wang, T., Miller, M. L., Lin, S., Borella, C. P., Geng, X., Pera, P., & Bernacki, R. J. (**1999**). Synthesis and structure-activity relationships of new second-generation taxoids. *Bioorganic & medicinal chemistry letters*, *9*(24), 3423–3428. https://doi.org/10.1016/s0960-894x(99)00629-0

Ojima, I., Chen, J., Sun, L., Borella, C. P., Wang, T., Miller, M. L., Lin, S., Geng, X., Kuznetsova, L., Qu, C., Gallager, D., Zhao, X., Zanardi, I., Xia, S., Horwitz, S. B., Mallen-St Clair, J., Guerriero, J. L., Bar-Sagi, D., Veith, J. M., Pera, P., … Bernacki, R. J. (**2008**). Design, synthesis, and biological evaluation of new-generation taxoids. *Journal of medicinal chemistry*, *51*(11), 3203–3221. https://doi.org/10.1021/jm800086e

Ojima, I., Kamath, A. and Seitz, J.D. (**2014**). Taxol, Taxoids, and Related Taxanes. In Natural Products in Medicinal Chemistry, S. Hanessian (Ed.). https://doi.org/10.1002/9783527676545.ch04

Ojima, I., Lichtenthal, B., Lee, S., Wang, C., & Wang, X. (**2016**). Taxane anticancer agents: a patent perspective. *Expert opinion on therapeutic patents*, *26*(1), 1–20. https://doi.org/10.1517/13543776.2016.1111872

Ojima, I., Wang, X., Jing, Y., & Wang, C. (**2018**). Quest for Efficacious Next-Generation Taxoid Anticancer Agents and Their Tumor-Targeted Delivery. *Journal of natural products*, *81*(3), 703–721. https://doi.org/10.1021/acs.jnatprod.7b01012

Orr, G. A., Verdier-Pinard, P., McDaid, H., & Horwitz, S. B. (**2003**). Mechanisms of Taxol resistance related to microtubules. *Oncogene*, *22*(47), 7280–7295. https://doi.org/10.1038/sj.onc.1206934

Paik, S., Tang, G., Shak, S., Kim, C., Baker, J., Kim, W., Cronin, M., Baehner, F. L., Watson, D., Bryant, J., Costantino, J. P., Geyer, C. E., Jr, Wickerham, D. L., & Wolmark, N. (**2006**). Gene expression and benefit of chemotherapy in women

with node-negative, estrogen receptor-positive breast cancer. *Journal of clinical oncology : official journal of the American Society of Clinical Oncology*, *24*(23), 3726–3734. https://doi.org/10.1200/JCO.2005.04.7985

Parker, J. S., Mullins, M., Cheang, M. C., Leung, S., Voduc, D., Vickery, T., Davies, S., Fauron, C., He, X., Hu, Z., Quackenbush, J. F., Stijleman, I. J., Palazzo, J., Marron, J. S., Nobel, A. B., Mardis, E., Nielsen, T. O., Ellis, M. J., Perou, C. M., & Bernard, P. S. (**2009**). Supervised risk predictor of breast cancer based on intrinsic subtypes. *Journal of clinical oncology : official journal of the American Society of Clinical Oncology*, *27*(8), 1160–1167. https://doi.org/10.1200/JCO.2008.18.1370

Parker, A. L., Teo, W. S., McCarroll, J. A., & Kavallaris, M. (**2017**). An Emerging Role for Tubulin Isotypes in Modulating Cancer Biology and Chemotherapy Resistance. *International journal of molecular sciences*, *18*(7), 1434. https://doi.org/10.3390/ijms18071434

Pavlikova, N., Bartonova, I., Dincakova, L., Halada, P., & Kovar, J. (**2014**). Differentially expressed proteins in human breast cancer cells sensitive and resistant to paclitaxel. *International journal of oncology*, *45*(2), 822–830. https://doi.org/10.3892/ijo.2014.2484

Pavlíková, N., Bartoňová, I., Balušíková, K., Kopperova, D., Halada, P., & Kovář, J. (**2015**). Differentially expressed proteins in human MCF-7 breast cancer cells sensitive and resistant to paclitaxel. *Experimental cell research*, *333*(1), 1–10. https://doi.org/10.1016/j.yexcr.2014.12.005

Pereira, B., Chin, S. F., Rueda, O. M., Vollan, H. K., Provenzano, E., Bardwell, H. A., Pugh, M., Jones, L., Russell, R., Sammut, S. J., Tsui, D. W., Liu, B., Dawson, S. J., Abraham, J., Northen, H., Peden, J. F., Mukherjee, A., Turashvili, G., Green, A. R., McKinney, S., … Caldas, C. (**2016**). The somatic mutation profiles of 2,433 breast cancers refines their genomic and transcriptomic landscapes. *Nature communications*, *7*, 11479. https://doi.org/10.1038/ncomms11479

Perou, C. M., Sørlie, T., Eisen, M. B., van de Rijn, M., Jeffrey, S. S., Rees, C. A., Pollack, J. R., Ross, D. T., Johnsen, H., Akslen, L. A., Fluge, O., Pergamenschikov, A., Williams, C., Zhu, S. X., Lønning, P. E., Børresen-Dale, A. L., Brown, P. O., & Botstein, D. (**2000**). Molecular portraits of human breast tumours. *Nature*, *406*(6797), 747–752. https://doi.org/10.1038/35021093

Piehler, A. P., Hellum, M., Wenzel, J. J., Kaminski, E., Haug, K. B., Kierulf, P., & Kaminski, W. E. (**2008**). The human ABC transporter pseudogene family: Evidence for transcription and gene-pseudogene interference. *BMC genomics*, *9*, 165. https://doi.org/10.1186/1471-2164-9-165

Pizzagalli, M. D., Bensimon, A., & Superti-Furga, G. (**2021**). A guide to plasma membrane solute carrier proteins. *The FEBS journal*, *288*(9), 2784–2835. https://doi.org/10.1111/febs.15531

Rao, S., Horwitz, S. B., & Ringel, I. (**1992**). Direct photoaffinity labeling of tubulin with taxol. *Journal of the National Cancer Institute*, *84*(10), 785–788. https://doi.org/10.1093/jnci/84.10.785

Rao, S., Krauss, N. E., Heerding, J. M., Swindell, C. S., Ringel, I., Orr, G. A., & Horwitz, S. B. (**1994**). 3'-(p-azidobenzamido)taxol photolabels the N-terminal 31 amino acids of beta-tubulin. *The Journal of biological chemistry*, *269*(5), 3132–3134.

Rao, S., Orr, G. A., Chaudhary, A. G., Kingston, D. G., & Horwitz, S. B. (**1995**). Characterization of the taxol binding site on the microtubule. 2-(m-Azidobenzoyl)taxol photolabels a peptide (amino acids 217-231) of beta-tubulin. *The Journal of biological chemistry*, *270*(35), 20235–20238. https://doi.org/10.1074/jbc.270.35.20235

Razavi, P., Chang, M. T., Xu, G., Bandlamudi, C., Ross, D. S., Vasan, N., Cai, Y., Bielski, C. M., Donoghue, M. T. A., Jonsson, P., Penson, A., Shen, R., Pareja, F., Kundra, R., Middha, S., Cheng, M. L., Zehir, A., Kandoth, C., Patel, R., Huberman, K., … Baselga, J. (**2018**). The Genomic Landscape of Endocrine-Resistant Advanced Breast Cancers. *Cancer cell*, *34*(3), 427–438.e6. https://doi.org/10.1016/j.ccell.2018.08.008

Ren, S., Zhang, M., Wang, Y., Guo, J., Wang, J., Li, Y., & Ding, N. (**2021**). Synthesis and biological evaluation of novel cabazitaxel analogues. *Bioorganic & medicinal chemistry*, *41*, 116224. https://doi.org/10.1016/j.bmc.2021.116224

Resnicoff, M., Medrano, E. E., Podhajcer, O. L., Bravo, A. I., Bover, L., & Mordoh, J. (**1987**). Subpopulations of MCF7 cells separated by Percoll gradient centrifugation: a model to analyze the heterogeneity of human breast cancer. *Proceedings of the National Academy of Sciences of the United States of America*, *84*(20), 7295–7299. https://doi.org/10.1073/pnas.84.20.7295

Robey, R. W., Pluchino, K. M., Hall, M. D., Fojo, A. T., Bates, S. E., & Gottesman, M. M. (**2018**). Revisiting the role of ABC transporters in multidrug-resistant cancer. *Nature reviews. Cancer*, *18*(7), 452–464. https://doi.org/10.1038/s41568-018-0005-8

Rowinsky, E. K., & Donehower, R. C. (**1995**). Paclitaxel (taxol). *The New England journal of medicine*, *332*(15), 1004–1014. https://doi.org/10.1056/NEJM199504133321507

Smoter, M., Bodnar, L., Duchnowska, R., Stec, R., Grala, B., & Szczylik, C. (**2011**). The role of Tau protein in resistance to paclitaxel. *Cancer chemotherapy and pharmacology*, *68*(3), 553–557. https://doi.org/10.1007/s00280-011-1696-7

Sørlie, T., Perou, C. M., Tibshirani, R., Aas, T., Geisler, S., Johnsen, H., Hastie, T., Eisen, M. B., van de Rijn, M., Jeffrey, S. S., Thorsen, T., Quist, H., Matese, J. C., Brown, P. O., Botstein, D., Lønning, P. E., & Børresen-Dale, A. L. (**2001**). Gene expression patterns of breast carcinomas distinguish tumor subclasses with

clinical implications. *Proceedings of the National Academy of Sciences of the United States of America*, *98*(19), 10869–10874. https://doi.org/10.1073/pnas.191367098

Sorlie, T., Tibshirani, R., Parker, J., Hastie, T., Marron, J. S., Nobel, A., Deng, S., Johnsen, H., Pesich, R., Geisler, S., Demeter, J., Perou, C. M., Lønning, P. E., Brown, P. O., Børresen-Dale, A. L., & Botstein, D. (**2003**). Repeated observation of breast tumor subtypes in independent gene expression data sets. *Proceedings of the National Academy of Sciences of the United States of America*, *100*(14), 8418–8423. https://doi.org/10.1073/pnas.0932692100

Sparano, J. A., Wang, M., Martino, S., Jones, V., Perez, E. A., Saphner, T., Wolff, A. C., Sledge, G. W., Jr, Wood, W. C., & Davidson, N. E. (**2008**). Weekly paclitaxel in the adjuvant treatment of breast cancer. *The New England journal of medicine*, *358*(16), 1663–1671. https://doi.org/10.1056/NEJMoa0707056

Sun, L., Simmerling, C., & Ojima, I. (**2009**). Recent advances in the study of the bioactive conformation of taxol. *ChemMedChem*, *4*(5), 719–731. https://doi.org/10.1002/cmdc.200900044

Sung, H., Ferlay, J., Siegel, R. L., Laversanne, M., Soerjomataram, I., Jemal, A., & Bray, F. (**2021**). Global Cancer Statistics 2020: GLOBOCAN Estimates of Incidence and Mortality Worldwide for 36 Cancers in 185 Countries. *CA: a cancer journal for clinicians*, *71*(3), 209–249. https://doi.org/10.3322/caac.21660

Tabata H. (**2004**). Paclitaxel production by plant-cell-culture technology. *Advances in biochemical engineering/biotechnology*, *87*, 1–23. https://doi.org/10.1007/b13538

Tait, S. W., & Green, D. R. (**2013**). Mitochondrial regulation of cell death. *Cold Spring Harbor perspectives in biology*, *5*(9), a008706. https://doi.org/10.1101/cshperspect.a008706

Taylor, N. M. I., Manolaridis, I., Jackson, S. M., Kowal, J., Stahlberg, H., & Locher, K. P. (**2017**). Structure of the human multidrug transporter ABCG2. *Nature*, *546*(7659), 504–509. https://doi.org/10.1038/nature22345

Thomas, C., & Tampé, R. (**2020**). Structural and Mechanistic Principles of ABC Transporters. *Annual review of biochemistry*, *89*, 605–636. https://doi.org/10.1146/annurev-biochem-011520-105201

Tian, Q., Zhang, J., Tan, T. M., Chan, E., Duan, W., Chan, S. Y., Boelsterli, U. A., Ho, P. C., Yang, H., Bian, J. S., Huang, M., Zhu, Y. Z., Xiong, W., Li, X., & Zhou, S. (**2005**). Human multidrug resistance associated protein 4 confers resistance to camptothecins. *Pharmaceutical research*, *22*(11), 1837–1853. https://doi.org/10.1007/s11095-005-7595-z

Tinti, C., Yang, C., Seo, H., Conti, B., Kim, C., Joh, T. H., & Kim, K. S. (**1997**). Structure/function relationship of the cAMP response element in tyrosine hydro-

xylase gene transcription. *The Journal of biological chemistry*, *272*(31), 19158–19164. https://doi.org/10.1074/jbc.272.31.19158

Toyoda, Y., Takada, T., & Suzuki, H. (**2019**). Inhibitors of Human ABCG2: From Technical Background to Recent Updates With Clinical Implications. *Frontiers in pharmacology*, *10*, 208. https://doi.org/10.3389/fphar.2019.00208

Turashvili, G., & Brogi, E. (**2017**). Tumor Heterogeneity in Breast Cancer. *Frontiers in medicine*, *4*, 227. https://doi.org/10.3389/fmed.2017.00227

Verras, G. I., Tchabashvili, L., Mulita, F., Grypari, I. M., Sourouni, S., Panagodimou, E., & Argentou, M. I. (**2022**). Micropapillary Breast Carcinoma: From Molecular Pathogenesis to Prognosis. *Breast cancer (Dove Medical Press)*, *14*, 41–61. https://doi.org/10.2147/BCTT.S346301

Villanueva, C., Bazan, F., Kim, S., Demarchi, M., Chaigneau, L., Thiery-Vuillemin, A., Nguyen, T., Cals, L., Dobi, E., & Pivot, X. (**2011**). Cabazitaxel: a novel microtubule inhibitor. *Drugs*, *71*(10), 1251–1258. https://doi.org/10.2165/11591390-000000000-00000

Vranic, S., Feldman, R., & Gatalica, Z. (**2017**). Apocrine carcinoma of the breast: A brief update on the molecular features and targetable biomarkers. *Bosnian journal of basic medical sciences*, *17*(1), 9–11. https://doi.org/10.17305/bjbms.2016.1811

Vrignaud, P., Semiond, D., Benning, V., Beys, E., Bouchard, H., & Gupta, S. (**2014**). Preclinical profile of cabazitaxel. *Drug design, development and therapy*, *8*, 1851–1867. https://doi.org/10.2147/DDDT.S64940

Vogelstein, B., Papadopoulos, N., Velculescu, V. E., Zhou, S., Diaz, L. A., Jr, & Kinzler, K. W. (**2013**). Cancer genome landscapes. *Science (New York, N.Y.)*, *339*(6127), 1546–1558. https://doi.org/10.1126/science.1235122

Wang, C., Wang, X., Sun, Y., Taouil, A. K., Yan, S., Botchkina, G. I., & Ojima, I. (**2020**). Design, synthesis and SAR study of 3rd-generation taxoids bearing 3-CH_3, 3-CF_3O and 3-CHF_2O groups at the C2-benzoate position. *Bioorganic chemistry*, *95*, 103523. https://doi.org/10.1016/j.bioorg.2019.103523

Wani, M. C., Taylor, H. L., Wall, M. E., Coggon, P., & McPhail, A. T. (**1971**). Plant antitumor agents. VI. The isolation and structure of taxol, a novel antileukemic and antitumor agent from Taxus brevifolia. *Journal of the American Chemical Society*, *93*(9), 2325–2327. https://doi.org/10.1021/ja00738a045

Wani, M. C., & Horwitz, S. B. (**2014**). Nature as a remarkable chemist: a personal story of the discovery and development of Taxol. *Anti-cancer drugs*, *25*(5), 482–487. https://doi.org/10.1097/CAD.0000000000000063

Wang, J., Li, J., Yang, J., Zhang, L., Gao, S., Jiao, F., Yi, M., & Xu, J. (**2017**). MicroRNA-138-5p regulates neural stem cell proliferation and differentiation

in vitro by targeting TRIP6 expression. *Molecular medicine reports*, *16*(5), 7261–7266. https://doi.org/10.3892/mmr.2017.7504

Wilson, N., Ironside, A., Diana, A., & Oikonomidou, O. (**2021**). Lobular Breast Cancer: A Review. *Frontiers in oncology*, *10*, 591399. https://doi.org/10.3389/fonc.2020.591399

WHO Classification of Tumours Editorial Board. Breast Tumours. 5th ed. Lyon, France: International Agency for Research on Cancer; **2021**. *WHO Classification of Tumours*; vol 2.

Wraith J. E. (**2001**). Ornithine carbamoyltransferase deficiency. *Archives of disease in childhood*, *84*(1), 84–88. https://doi.org/10.1136/adc.84.1.84

Woodward, O. M., Köttgen, A., Coresh, J., Boerwinkle, E., Guggino, W. B., & Köttgen, M. (**2009**). Identification of a urate transporter, ABCG2, with a common functional polymorphism causing gout. *Proceedings of the National Academy of Sciences of the United States of America*, *106*(25), 10338–10342. https://doi.org/10.1073/pnas.0901249106

Yang, X. H., Sladek, T. L., Liu, X., Butler, B. R., Froelich, C. J., & Thor, A. D. (**2001**). Reconstitution of caspase 3 sensitizes MCF-7 breast cancer cells to doxorubicin- and etoposide-induced apoptosis. *Cancer research*, *61*(1), 348–354.

Yang, J., Ju, J., Guo, L., Ji, B., Shi, S., Yang, Z., Gao, S., Yuan, X., Tian, G., Liang, Y., & Yuan, P. (**2021**). Prediction of HER2-positive breast cancer recurrence and metastasis risk from histopathological images and clinical information via multimodal deep learning. *Computational and structural biotechnology journal*, *20*, 333–342. https://doi.org/10.1016/j.csbj.2021.12.028

Yardley, D. A., Hart, L. L., Ward, P. J., Wright, G. L., Shastry, M., Finney, L., DeBusk, L. M., & Hainsworth, J. D. (**2018**). Cabazitaxel Plus Lapatinib as Therapy for $HER2^+$ Metastatic Breast Cancer With Intracranial Metastases: Results of a Dose-finding Study. *Clinical breast cancer*, *18*(5), e781–e787. https://doi.org/10.1016/j.clbc.2018.03.004

Zhao, X., Jiang, C., Xu, R., Liu, Q., Liu, G., & Zhang, Y. (**2020**). TRIP6 enhances stemness property of breast cancer cells through activation of Wnt/β-catenin. *Cancer cell international*, *20*, 51. https://doi.org/10.1186/s12935-020-1136-z

Zheng, X., Wang, C., Xing, Y., Chen, S., Meng, T., You, H., Ojima, I., & Dong, Y. (**2017**). SB-T-121205, a next-generation taxane, enhances apoptosis and inhibits migration/invasion in MCF-7/PTX cells. *International journal of oncology*, *50*(3), 893–902. https://doi.org/10.3892/ijo.2017.3871

8. PUBLICATIONS UNRELATED TO PHD THESIS

Seborova, K., Kloudova-Spalenkova, A., Koucka, K., Holy, P., Ehrlichova, M., Wang, C., Ojima, I., Voleska, I., **Daniel, P.,** Balusikova, K., Jelinek, M., Kovar, J., Rob, L., Hruda, M., Mrhalova, M., Soucek, P., & Vaclavikova, R. (2021). The Role of TRIP6, ABCC3 and CPS1 Expression in Resistance of Ovarian Cancer to Taxanes. *International journal of molecular sciences*, *23*(1), 73. https://doi.org/10.3390/ijms23010073

Pavlíková, N., **Daniel, P.,** Šrámek, J., Jelínek, M., Šrámková, V., Němcová, V., Balušíková, K., Halada, P., & Kovář, J. (**2019**). Upregulation of vitamin D-binding protein is associated with changes in insulin production in pancreatic beta-cells exposed to p,p'-DDT and p,p'-DDE. *Scientific reports*, *9*(1), 18026. https://doi.org/10.1038/s41598-019-54579-z

Šrámek, J., Němcová-Fürstová, V., Balušíková, K., **Daniel, P.,** Jelínek, M., James, R. F., & Kovář, J. (**2016**). p38 MAPK Is Activated but Does Not Play a Key Role during Apoptosis Induction by Saturated Fatty Acid in Human Pancreatic β-Cells. *International journal of molecular sciences*, *17*(2), 159. https://doi.org/10.3390/ijms17020159